One-carbon metabolism in acetogenic and sulfate-reducing bacteria

Michael Visser

Thesis committee

Promotor
Prof. Dr Alfons J.M. Stams
Personal chair at the Laboratory of Microbiology
Wageningen University

Other members
Prof. Dr Harold L. Drake, University of Bayreuth, Germany
Prof. Dr Sacco C. de Vries, Wageningen University
Prof. Dr Wilfred R. Hagen, Delft University of Technology
Dr Wilfred F.M. Röling, VU University Amsterdam

This research was conducted under the auspices of the Graduate School for Socio-Economic and Natural Sciences of the Environment (SENSE)

One-carbon metabolism in acetogenic and sulfate-reducing bacteria

Michael Visser

Thesis

Submitted in fulfilment of the requirements for the degree of doctor
at Wageningen University
by the authority of the Rector Magnificus
Prof. Dr M.J. Kropff,
in the presence of the
Thesis Committee appointed by the Academic Board
to be defended in public
on Wednesday 14 January 2015
at 4 p.m. in the Aula.

Michael Visser
One-carbon metabolism in acetogenic and sulfate-reducing bacteria
210 pages.

PhD thesis, Wageningen University, Wageningen, NL (2014)
With references, with summaries in Dutch and English

ISBN 978-94-6257-173-0

Table of Contents

Chapter 1

General introduction and thesis outline

1.1 One-carbon compounds: their occurrence and importance in nature

The earth is an exceptional planet that harbors a wide diversity of life. In order to sustain life the six major building blocks of life, hydrogen, carbon, nitrogen, sulfur, oxygen, and phosphorous, are constantly recycled. The cycling is driven by geophysical processes and the combined metabolisms of all life forms. Carbon is cycled through all earth's major carbon reservoirs, including the atmosphere, land, oceans and other aquatic environments. The global distribution of carbon transpires through carbon dioxide (CO_2) in the atmosphere. CO_2 is removed from the atmosphere by photosynthesis, performed by plants, algae and cyanobacteria, and CO_2 fixation performed by chemolithotrophs. The organisms involved are able to generate organic matter from these carbon fixing reactions. Fixed carbon is eventually degraded by various organisms. Microorganisms play a major part in this, degrading organic matter eventually into CO_2 and methane. Subsequently, CO_2 returns to the start of the carbon cycle (Figure 1.1) [1].

Like CO_2 and methane, other C-1 compounds also play an important role in the carbon cycle. C-1 compounds are compounds that have only one carbon atom. Other examples of C-1 compounds are carbon monoxide (CO), formate, methylamine, and methanol. CO_2 is the highest oxidative state of carbon while methane is the highest reduced form of carbon. The oxidative state of other C-1 compounds can be found in table 1.1. C-1 compounds are present in different environments widely spread on earth because they are naturally and industrially produced (Figure 1.1). CO, for example, is produced by burning activities, volcanoes and hydrothermal vents, plants, animals, bacteria, photochemical and thermochemical degradation of organic matter in soils, marine sediments and aquatic systems [2-8]. Methanol is present in soils, oceans and even the atmosphere [9-12]. The majority of methanol is a product of pectin and lignin degradation (part of the cell membrane of plant cells) by both aerobic and anaerobic bacteria [13, 14].

One carbon compounds are excellent substrates for microbial growth. They can be used by a large variety of microorganisms, both aerobic and anaerobic. During my PhD I have predominantly worked with anaerobic CO, formate and methanol degradation. The biochemical reactions that can be performed by the anaerobic C-1 degrading microorganisms are presented in table 1.2. These reactions are catalyzed by enzyme systems, which, including the genes encoding the enzymes, form the basis of my research.

Table 1.1: Examples of compounds with one carbon atom and their characteristics.

C1 compound	Molecular formula	Molecular mass (g/mol)	Carbon oxidation state
Carbon dioxide	CO_2	44	+4
Formate	$CHOO^-$	45	+2
Carbon monoxide	CO	28	+2
Methylamine	CH_3NH_2	31	-2
Methanol	CH_3OH	32	-2
Methane	CH_4	16	-4

Table 1.2: Microbial anaerobic CO, formate and methanol degradation. Calculated from Thauer, et al. [15].

Methanogenic reactions

Reaction	ΔG° (kJ/reaction)
$4\ CHOO^- + H_2O + H^+ \rightarrow CH_4 + 3\ HCO_3$	-132
$4\ CO + 5\ H_2O \rightarrow CH_4 + 3\ HCO_3^- + 3H^+$	-195.6
$4\ CH_3OH \rightarrow 3\ CH_4 + HCO_3^- + H_2O + H^+$	-316
$HCO_3^- + 4H_2 + H^+ \rightarrow CH_4 + 3\ H_2O$	-135.6

Acetate and hydrogen producing reactions

Reaction	ΔG° (kJ/reaction)
$CHOO^- + H_2O \rightarrow HCO_3^- + H_2$	+1.3
$4\ CO + 4\ H_2O \rightarrow CH_3COO^- + 2\ HCO_3^- + 3\ H^+$	-112.8
$CO + 2\ H_2O \rightarrow HCO_3^- + H_2 + H^+$	-15
$CO + H_2O \rightarrow CHOO^- + H^+$	-16.4
$4\ CH_3OH + 2\ HCO_3^- \rightarrow 3\ CH_3COO^- + 4H_2O$	-220
$CH_3OH + 2\ H_2O \rightarrow 3\ H_2 + HCO_3^- + H^+$	+23.5
$CH_3OH + 2\ HCO_3^- \rightarrow 3\ CHOO^- + H_2O + H^+$	+19
$2\ HCO_3^- + 4\ H_2 + H^+ \rightarrow CH_3COO^-\ 4\ H_2O$	-104.6
$HCO_3^- + H_2 \rightarrow CHOO^- + H_2O$	-1.3

Coupled to nitrate and sulfate reduction

Reaction	ΔG° (kJ/reaction)
$4\ CHOO^- + 2\ H_2O + NO_3^- + 2H^+ \rightarrow 4\ HCO_3^- + NH_4^+$	-594.4
$5\ CHOO^- + 2\ NO_3^- + 2\ H^+ \rightarrow 5\ HCO_3^- + N_2 + H_2O$	-1114
$4\ CHOO^- + SO_4^{2-} + H^+ \rightarrow 4\ HCO3^- + HS^-$	-146.7
$4\ CO + NO_3^- + H^+ \rightarrow NH_4^+$	-659.6
$5\ CO + 2\ NO_3^- + H^+ \rightarrow N_2 + 4\ H_2O$	-1180.5
$4\ CO + SO_4^{2-} \rightarrow HS^- + 2\ H_2O$	-211.9
$4\ CH_3OH + 2\ H_2O + 3\ NO_3^- + 2\ H^+ \rightarrow 4\ HCO_3^- + 3\ NH_4^+$	-1798.8
$5\ CH_3OH + 6\ NO_3^- + H^+ \rightarrow 5\ HCO_3^- + 3\ N_2 + 8\ H_2O$	-3244
$4\ CH_3OH + 3\ SO_4^{2-} \rightarrow 4\ HCO^{3-} + 3\ HS^- + H^+ + 4\ H_2O$	-361.7

1.2 Anaerobic CO, formate and methanol utilizing microorganisms

C-1 compounds are present in different environments widely spread on earth. This is also true for CO, formate and methanol in many anaerobic environments. Therefore, the ability to grow with these compounds is also widespread among anaerobes, including many members of acetogens, sulfate reducing bacteria and archaea.

Multiple genera of acetogenic bacteria contain species that degrade both formate and methanol, including *Acetoanaerobium*, *Acetobacterium*, *Butyribacterium*, *Clostridium*, *Eubacterium*, *Moorella*, *Sporomusa*, and *Thermoacetogenium*. In sulfate-reducing bacteria the ability to grow with formate

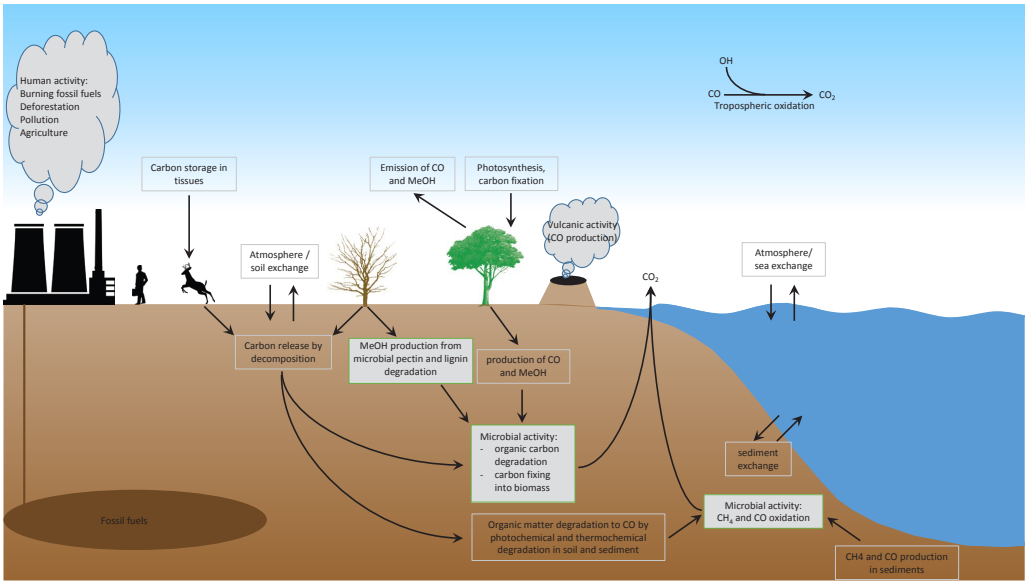

Figure 1.1: Schematic overview of the global carbon cycle. The microbial activity presented involves aerobic and anaerobic microorganisms [1-14].

and methanol is less frequent. Formate can be used as a sole carbon and energy source by multiple sulfate-reducing bacteria that completely oxidize their substrates to CO_2. However, some sulfate-reducing bacteria can also grow with formate, but need a small amount of acetate as an additional carbon source. Methanol is not a common substrate among sulfate-reducing bacteria but can be degraded by some species of *Desulfosporosinus*, *Desulfobacterium*, *Desulfotomaculum* and *Desulfovibrio* [123-135].

In archaea formate and methanol are degraded by many methanogenic strains. Members of the orders *Methanobacteriales*, *Methanococcales*, *Methanomicrobiales* and *Methanopyrales* grow with H_2/CO_2 as substrates, but many of the species can also oxidize formate to form methane. Most *Methanosarcina* species can utilize both H_2/CO_2 and methyl compounds, like methanol, but not formate. Members of the genera *Methanolobus*, *Methanococcoides* and *Methanohalophilus* grow exclusively with methyl compounds.

Growth with CO depends strongly on the concentration of CO. Many acetogenic genera, including *Acetobacterium*, *Butyribacterium*, *Clostridium*, *Eubacterium*, *Moorella*, and *Sporomusa*, contain species that can utilize CO as a sole carbon and energy source when it is present in less than 100%. However, the amount of acetogenic species that can grow with 100% CO is significantly less. CO utilizers in sulfate-reducing bacteria and archaea are less common. Moreover, species that can grow with 100% CO are even more uncommon. Isolated anaerobic species that can grow with 100% CO are *Thermincola carboxydophila* [17], *Thermincola ferriacetica* [17], *Carboxydocella sporoproducens* [44], *Carboxydocella thermautotrophica* [48], *Desulfotomaculum carboxydivorans* [41], *Moorella thermoacetica* strain *AMP* [206], *Moorella stamsii* [40], *Carboxydothermus hydrogenoformans* [74], *Carboxydothermus siderophilus* [43], *Caldanaerobacter subterraneus* subsp. *pacificus* [17], *Thermosinus carboxydivorans* [40], *Thermolithobacter carboxydivorans* [45], *Carboxydobrachium pacificum* [46].

1.3 Carbon monoxide

Carbon monoxide (CO) is a colorless and odorless gas, which is toxic for humans and animals, and also to many microorganisms. The toxicity of CO to microbes is due to its binding to metal-containing redox enzymes, which can result in the interruption of electron transport chains [17]. Interestingly, CO is an intermediate of the acetyl-CoA pathway (Figure 1.2), which is used by several anaerobes to degrade compounds to acetate or to fix CO_2 [18-20]. The pathway contains two branches, a methyl branch and a carbonyl branch. In the methyl branch five enzymes catalyze the reduction of CO_2 by six electrons to generate methyl tetrahydrofolate (CH_3-THF). Subsequently, the CH_3 is transferred via a corrinoid iron-sulfur protein (CFeSP) to the binding site of the carbon monoxide dehydrogenase/acetyl-CoA synthase (CODH/ACS) enzyme complex. The carbonyl branch is created by the reduction of CO_2 to CO, catalyzed by the CODH of the CODH/ACS complex. CO is introduced to the acetyl-CoA synthase, which catalyzes the generation of acetyl-CoA from CO, CH_3 and CoA [21]. The reverse reactions of this pathway are used by several organisms to degrade acetate [22].

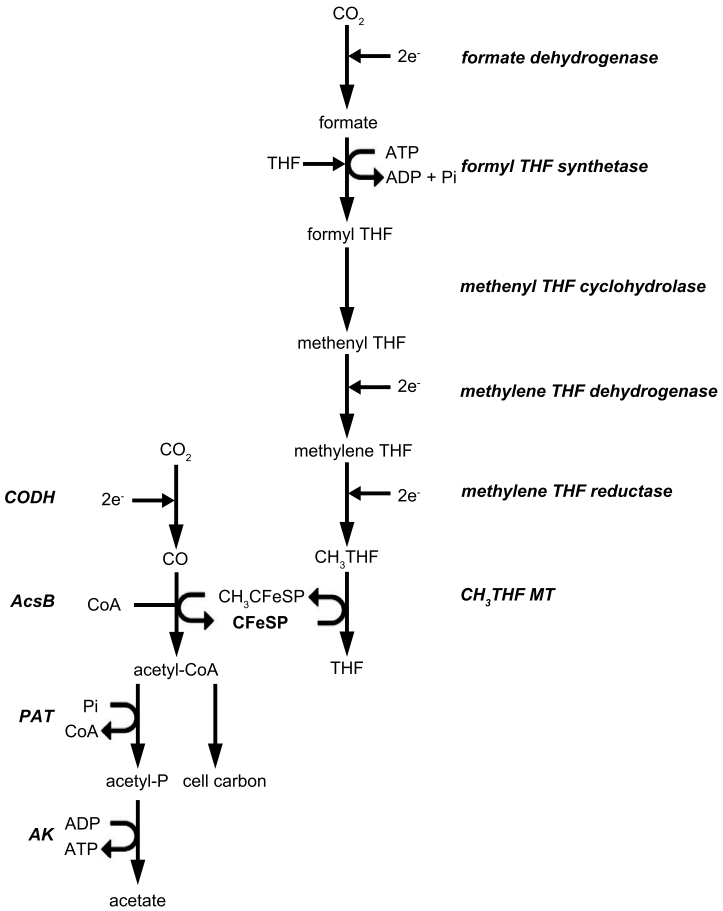

Figure 1.2: Acetyl-CoA pathway. Enzymes in this figure are in bold italic. Abbreviations: CODH, carbon-monoxide dehydrogenase; AcsB, acetyl-CoA synthase; AK, acetate kinase; CFeSP, iron-sulfur protein; CH3, methyl; PAT, phosphate acetyltransferase; THF, tetrahydrofolate; MT, methyltransferase.

Additional to CO as an intermediate product, both aerobic as anaerobic microbes can use CO as a sole carbon and energy source [23]. They do so by coupling CO oxidation to oxygen reduction [24], nitrate reduction [25], sulfate reduction [26, 27], hydrogenogenesis [28], acetogenesis [29] and methanogenesis [30, 31]. The enzyme involved in aerobic and anaerobic CO oxidation is called CO dehydrogenase (CODH). The genes that code for the aerobic CODH are designated *cox* genes and the gene encoding the catalytic subunit of the anaerobic CODH is the *cooS* gene. Metagenomic and *cooS* sequencing studies [11, 32-35] showed that the *cooS* gene can be found in many phylogenetically different microorganisms that inhabit different environments, which suggests the global importance and distribution of anaerobic microbial CO utilization.

1.3.1 Carbon monoxide dehydrogenase

Anaerobic CO oxidation is catalyzed by a nickel containing CODH in a wide diversity of prokaryotes and is an important process within the global carbon cycle. The anaerobic CODH catalyzes the following reaction:

$$CO + H_2O \rightarrow CO_2 + 2H^+ + 2e^-$$

The electrons generated by the oxidation of CO can be coupled to reduction reactions like CO_2 reduction to CH_4 [31, 36] and acetate [31, 37], sulfate reduction [38], fumarate reduction [39], metal reduction [40], or the production of hydrogen [40-48]. This leads to different end products in different microorganisms due to different CODH complexes. Acetate production from CO degradation for example involves the same bifunctional CODH complex also involved in the acetyl-CoA pathway. It contains domains catalyzing both the oxidation of CO to CO_2 (CODH) and the formation of acetyl-CoA (acetyl-CoA Synthase) [49]. In hydrogen producing CO utilizers a different CODH complex is involved. This complex contains both CODH subunits and hydrogenase subunits.

1.3.2 CODH and ECH complex

Extensive studies were done on the phototrophs *Rhodocyclus gelatinosus* and *Rhodospirillum rubrum* and the methanogen *Methanosarcina barkeri* in relation to their CO metabolism [31, 50-70]. These microorganisms were described to grow with CO as the sole carbon and energy source [53, 54, 67]. Due to an energy converting hydrogenase (ECH) hydrogen is produced during growth with CO and protons are translocated, creating a proton gradient across the cell membrane. The ECH of *Rhodospirillum rubrum* and *Methanosarcina barkeri* were purified and characterized [64, 69, 70]. The CODH/ECH complex is membrane bound and cytoplasmic oriented [71]. The electrons generated by the CODH catalytic subunit are transported to the ECH via a $4[Fe_4\text{-}S_4]$ cluster containing protein, encoded by *cooF* [51, 56, 59, 72]. A similar system was described in *Carboxydothermus hydrogenoformans* [73]. This organism can also couple hydrogen production to CO oxidation. Moreover, it was the first organism to have its genome sequenced, which revealed multiple CODH complexes, including a CODH/ECH complex (Figure 1.3) [74].

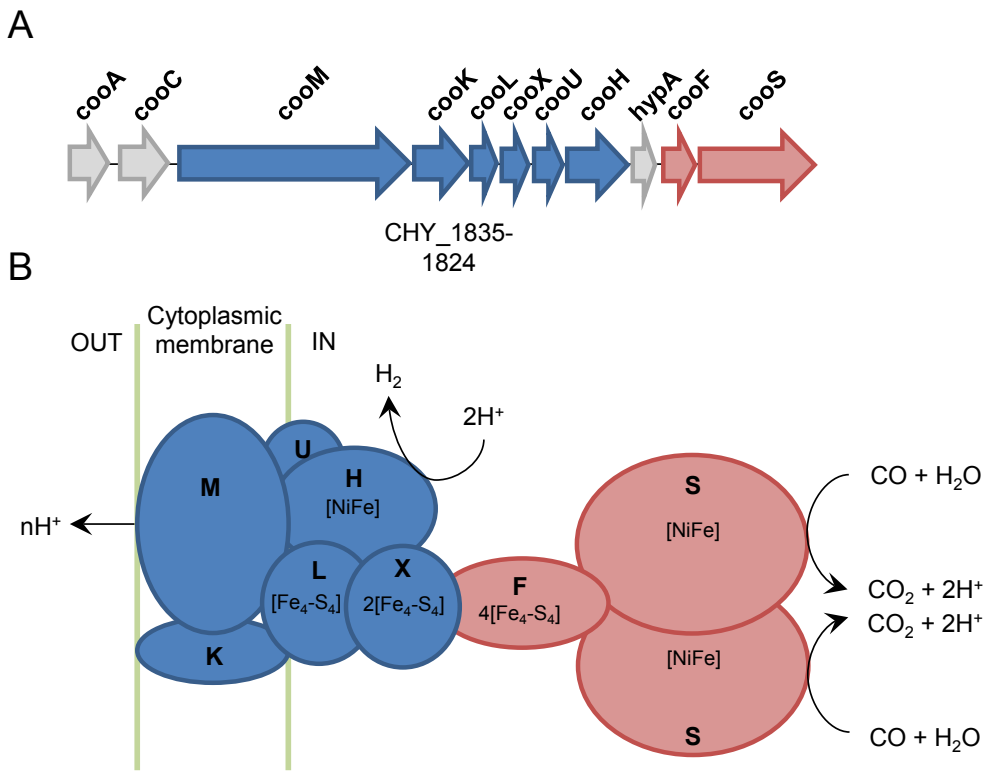

Figure 1.3: CODH-ECH (CODH I) complex in Carboxydothermus hydrogenoformans. The operon (A) contains the CODH genes (red) and the ECH genes (blue). The cooC and the hypA gene encode proteins involved in the nickel insertion into the CODH catalytic subunit (cooS) and the hydrogenase catalytic subunit (cooH), respectively [60,63,75]. The cooA gene is the CO-sensing transcriptional activator [50,76]. B shows the membrane bound complex as it was proposed by Hedderich [72]. The letters in the subunits and the color coding are similar as shown in A. Moreover, predicted iron-sulfur clusters and metal-binding sites are indicated.

1.3.4 Different carbon monoxide dehydrogenase complexes

The genome of the hydrogenogenic carboxydotroph *Carboxydothermus hydrogenoformans* revealed five genes coding for the CODH catalytic subunit (*cooS*) and neighbor genes that were thought to form five CODH complexes, CODH I-V [74,77]. These authors assigned functions to four of the five complexes: energy conservation (CODH I), NADPH generation (CODH II), carbon fixation (CODH III), and oxidative stress (CODH IV). The fifth *cooS* does not have any neighbor genes with obvious roles in CO-related processes.

Recently, the regulation of the CODH/ECH (CODH I) and CODH/ACS (CODH III) operons, by two CO-sensing transcriptional activators *cooA-I and cooA-II,* were studied in *C. hydrogenoformans* [78]. The *cooA-II* is a bifunctional regulator capable of regulating both the CODH I and CODH III operon. In contrast *cooA-I* only regulates the CODH/ECH operon. Moreover, *cooA-II* can bind CO in lower concentration compared to *cooA-I*. This suggests that the multiple *cooA* genes support

an efficient use of CO applied at different concentrations. In CO limiting conditions the *cooA-II* regulation leads to expression of both the CODH I as the CODH III complex. When CO concentrations increase the CODH I complex is induced due to additional regulation by *cooA-I* [78]. More CO utilizing bacteria have multiple CODH complexes encoded in their genome. The function of these complexes is not always known. This is also true for how they are regulated. Additional to *C. hydrogenoformans* more microorganisms have two *cooA* genes [78], which suggests that also in those microorganisms regulation of the complexes could be CO-concentration dependent. In *Methanosarcina acetivorans* C2A however, transcriptional regulation of two CODH/ACS complexes was suggested to involve a *cooS* gene that lacked other CODH neighbor genes. Since direct transcriptional regulation is unlikely, it was suggested it could be part of a catabolite responsive signal transduction pathway [79]. It is clear that more research is necessary to better understand the regulation and the function of different CODH complexes.

Parshina and co-workers [42] described the first sulfate-reducing bacterium that can grow with 100% CO and forms H_2 and CO_2 as products; *Desulfotomaculum carboxydivorans* strain CO-1-SRB. In general, sulfate reducers are sensitive to CO [80], but some known thermophilic *Desulfotomaculum* species can grow well at relatively high CO concentrations [38]. Chapter 2 describes the genome of *D. carboxydivorans* and *D. nigrificans*. Two closely related species that differ in their CO metabolism.

1.4 Methanol

Methanol is an important compound, not only in nature as part of the carbon cycle, but also for human activity. Methanol is used frequently in industry as a building block for chemicals [81] and it is proposed as a substitute for fossil fuels [82]. Methanol can also be used to improve biodegradation processes. Studies indicated that the presence of methanol accelerated the biodegradation of pollutants in industrial wastewater by mixed bacterial consortia, e.g. n-hexane[84] and dichloromethane [85]. Moreover, several studies showed that the addition of methanol enhances dechlorination of hexachlorocyclohexane, a toxic and carcinogenic pollutant that can be found in different environments worldwide [83,214,215]. In these studies methanol showed better results than other electron donors. Furthermore, the addition of methanol can be used in the treatment of nitrate, phosphorous and sulfate rich wastewater [86-91,216]. For wastewaters with low volatile fatty acids content, an external carbon addition is necessary. As methanol is a cheap compound it will not increase the treatment costs significantly. Moreover, pharmaceutical wastewater can have high concentrations of methanol [84] and can therefore be used as a methanol source, treating both wastewaters simultaneously. The importance of methanol degrading microorganisms in these application purposes makes it essential to study their methanol metabolism.

Methanol degradation is performed by aerobic and anaerobic microorganisms that degrade methanol via the use of different pathways. The most common pathways described for methanol metabolism involve a methanol dehydrogenase, predominantly used by aerobes and facultative anaerobes, and a methanol methyltransferase system. The latter is mainly used by anaerobes, including methanogens and acetogens. The methanol metabolism in sulfate-reducing bacteria has been poorly studied. It is not clear which methanol-degrading pathway they use. This section describes the different enzymes involved in methanol metabolism.

1.4.1 Methanol dehydrogenase

The use of a methanol dehydrogenase (MDH) to grow with methanol as a sole carbon and

energy source is mainly found in aerobes and facultative anaerobes. These bacteria use the MDH to oxidize methanol to formaldehyde. Many different MDHs have been found. The main difference is between Gram-positive and Gram-negative methanol utilizers. The Gram-positive bacteria use NAD(P) dependent MDHs that are present in their cytoplasm [14], while the Gram-negative bacteria use a pyrroloquinoline quinone (PQQ) dependent MDH that resides in their periplasm[92]. The periplasmic PQQ-dependent MDH uses a cytochrome c to transport electrons. Methanol is oxidized by the reduction of the PQQ cofactor. Subsequently, the $PQQH_2$ is oxidized by transferring two electrons, one at the time, to cytochrome c [102]. There are different types of MDHs that use PQQ as a cofactor, the so called MxaFI-MDH, MDH2, and XoxF-MDH. The MxaFI-MDH is more extensively studied. The crystal structure of the MxaFI-MDH has been described for *Methylobacterium extorquens* [93-96,207], *Methylophilus* species [97-100], *Paracoccus denitrificans* [208], *Hyphomicrobium denitrificans* [209], and *Methylophaga aminisulfidivorans* [210], which revealed the $\alpha_2\beta_2$ tetramer structure with two 66 kDa α subunits (*mxaF*) and two β subunits (*mxaI*) of 8.5 kDa. Each α subunit contains a PQQ cofactor and a Ca^{2+} ion [101]. Recently, the crystal structure of the XoxF-MDH has been described for *Methylacidiphilum fumariolicum* and showed the presence of a lanthanide at the catalytic site [211]. A recent review describes the phylogenetic relationship, the similarities and the differences of the PQQ-dependent MDHs [212].
In Gram-positive bacteria a PQQ independent MDH is involved in methanol oxidation. These MDHs are NAD(P) dependent and have more similarity to NAD(P) dependent alcohol dehydrogenases (ADH) than the PQQ dependent MDH. From the three families of NAD(P) dependent ADHs the MDHs described in Gram-positive bacteria are part of the ADH III family. Three NAD(P) dependent MDHs have been described [14]. The MDH of the Gram-positive *Bacillus methanolicus* C1 contains ten identical subunits and each subunit contains one zinc, one or two magnesium ions, and a tightly bound NAD(H). In addition to this NAD(H) cofactor the MDH requires exogenous NAD as coenzyme. The cofactor NAD acts as an electron acceptor during methanol oxidation, while coenzyme NAD is responsible for the re-oxidation of the cofactor [103-107]. An ADH was found in *Amycolatopsis methanolica* and *Mycobacterium gastri* that consists of three components, of which component 1 has been identified as a methanol N,N'-dimethyl-4-nitrosoaniline oxidoreductase (MNO). The MNO component catalyzes the oxidation of methanol [108-110]. In *A. methanolica* another MDH is present that oxidizes methanol in the presence of an artificial electron acceptor DCPIP [111]. However, not much is known about this MDH.

1.4.2 Methanol methyltransferase system

Methanogens and homoacetogenic bacteria use a methanol methyltransferase system to utilize methanol. This system uses two methyltransferases to transfer the methyl group from methanol to coenzyme M (CoM) in methanogens, and to tetrahydrofolate (THF) in homoacetogens.
The conversion of methanol to methane via CoM is extensively studied in *Methanosarcina barkeri*. The two methyltransferases, also called MT_1 and MT_2, were purified and characterized [112-115]. Van der Meijden and co-workers showed that MT_1 consists of two subunits in an $\alpha_2\beta$ structure. These two subunits were designated MtaB and MtaC [116]. MtaB catalyzes the cleavage of the C-O bond of methanol and the transfer of the CH_3 group to a corrinoid bound to MtaC. The MT_2, consists of only one subunit (MtaA), which catalyzes the transfer of the CH_3 bound to MtaC to CoM [112, 114, 117]. Part of the created CH_3-CoM is oxidized to CO_2 in order to generate electrons for methane production (Figure 1.4A).

In the homoacetogens *Sporomusa ovata* and *Moorella thermoacetica* the synthesis of a corrinoid protein is induced during growth with methanol [118-120], suggesting its importance in methanol metabolism. Das and co-workers [120] showed that in *M. thermoacetica* the methanol metabolism resembled that of the methanogenic archaea, consisting of three homologous subunits of MtaA, B and C. The genes coding for the *M. thermoacetica* MtaB and MtaC are positioned next to each other in the genome and are simultaneously transcribed [120, 121]. During methanol metabolism in *S. ovata* the methyl group was transferred to THF [122]. However, the MtaA protein was never described in *S. ovata*. Chapter 3 describes the methanol metabolism in *Sporomusa* strain An4 a strain closely related to *S. ovata*.

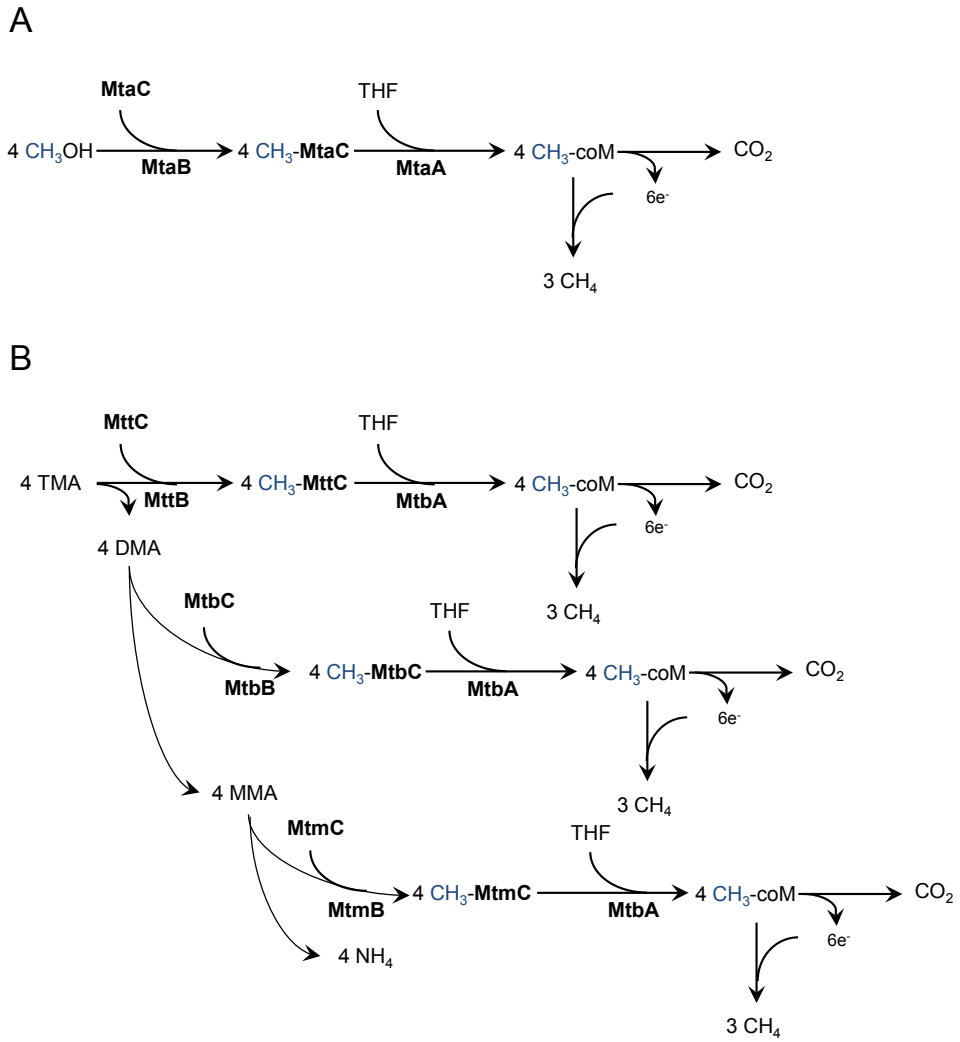

Figure 1.4: Methyltransferase systems described in Methanocarsina barkeri for the conversion of methanol (A) and trimethylamine (TMA), dimethylamine (DMA) and monomethylamine (MMA) (B) into methane.

1.4.3 Tri-,di-, mono-methylamine methyltransferases

A similar methyltransferase system as described for methanol metabolism has been described for the methylamine compounds, trimethylamine (TMA), dimethylamine (DMA), and (mono-) methylamine (MMA) in *Methanosarcina barkeri*. The proteins involved are the TMA, DMA and MMA specific methyltransferases (MttB, MtbB and MtmB, respectively) and their corrinoid proteins (MttC, MtbC and MtmC, respectively) [136-140]. There is one methyltransferase (MtbA) involved in the transfer of the CH_3 group bound to the corrinoid protein to CoM in the degradation of all three amine compounds (Figure 1.4B) [141]. The methyltransferase systems of TMA, DMA, MMA, and methanol are very similar, but are substrate specific. Kratzer et al. [142] monitored transcript levels of the *mta*, *mtt*, *mtb* and *mtm* genes in *Methanosarcina mazei* during growth with either TMA or methanol. The results indicated increased amounts of mRNA of the *mtt*, *mtb* and *mtm* genes during TMA degradation and increased mRNA levels from the MtaBC1, MtaBC2, and MtaBC3 genes in methanol-grown cells. Moreover, the substrate specificity of the mttB, mtbB and mtmB for TMA, DMA and MMA, respectively was described in *Methanosarcina barkeri* [136-138]. The substrate specificity and the different methyltransferase systems in general in the homoacetogen *Sporomusa* strain An4 will be discussed in Chapter 3.

1.4.4 Methanol metabolism in sulfate-reducing bacteria

In sulfate-reducing bacteria the methanol metabolism has not been extensively studied. It is not clear whether sulfate-reducing bacteria also use a methyltransferase system or if they use a MDH. Sulfate-reducing bacteria described to be able to utilize methanol are: *Desulfosporosinus orientis* [123], *Desulfobacterium catecholicum* [124], *Desulfobacterium aniline* [125], *Desulfovibrio carbinolicus* [126], *Desulfovibrio alcoholivorans* [127], and nine *Desulfotomaculum* strains [128-133]. Recently, the genomes of *Desulfosporosinus orientis* [134]and *Desulfotomaculum reducens* [135] have become available. This enables a first look at the methanol metabolism of these strains. The genome of *Desulfosporosinus orientis* contains both methanol methyltransferase and multiple alcohol dehydrogenase genes, while the genome of *Desulfotomaculum reducens* lacks methanol methyltransferase genes. The genome of *Desulfotomaculum kuznetsovii* was also sequenced. A description of the genome can be found in Chapter 4 and a proteome analysis was performed to assess the methanol metabolism of *D. kuznetsovii* (Chapter 5).

1.5 Formate

Formate is an important compound involved in several anaerobic processes, for example the acetyl-CoA pathway, and many fermentation reactions. In the acetyl-CoA pathway formate functions as an intermediate. It is generated by the reduction of CO_2 in the first reaction of the methyl branch (Figure 1.2). In fermentation reactions like, sugar fermentation, citrate fermentation and oxalate fermentation formate can be end product or an intermediate [143-146]. The fermentation of glucose by *Escherichia coli,* for example, uses a pyruvate formate-lyase to convert pyruvate to acetyl-CoA and formate [217]. Subsequently, the formate is converted to hydrogen and CO_2 by a formate hydrogen lyase [218].

Additionally, formate is an excellent substrate for growth in many microorganisms. Enzymes involved in formate utilization, for example the formate dehydrogenase (FDH), can be found in many microbes [147, 148], indicating the widespread occurrence in nature. Moreover, formate is besides hydrogen involved in interspecies electron transfer in microbial communities. The best

studied and generally accepted electron carrier in syntrophic interaction is hydrogen. However, already in the late eighties the first evidence was presented for the involvement of formate in interspecies electron transfer [149, 150], and the importance of formate as an electron carrier has become more apparent over the years [151-155].

Syntrophy is the cooperative growth between two microorganisms that degrade a substance neither can degrade alone, for example by the removal of inhibiting products by the partner organism. In anaerobic environments the syntrophic interaction between bacteria and methanogens is important [156, 157]. Although studies have shed some light on how these microorganisms can cooperate, it is still important to assess what makes it possible for some bacteria to grow syntrophically while others cannot and how important the role of formate is in this process. In Chapter 6 the importance of formate as interspecies electron transfer during syntrophic butyrate and propionate degradation is discussed.

1.5.1 Interspecies electron transfer

Methanogens cannot utilize complex organic compounds but use acetate, H_2/CO_2, and formate as their main substrates [158]. Therefore, bacteria are essential to form these methanogenic substrates from organic compounds. However, the production of these substrates by bacteria, when using compounds like propionate and butyrate, is thermodynamically only feasible when the concentrations of the products are kept at a low concentration by the methanogens. This is called interspecies electron transfer. Interspecies hydrogen transfer is the most studied and commonly accepted form of electron carrier. However, the importance of the C-1 compound formate as an electron carrier has become more apparent [156]. The redox potential of the proton / hydrogen couple (-414 mV) is slightly higher than the redox potential of the CO_2 / formate couple (-432 mV) and several studies on syntrophic propionate and butyrate growth showed better syntrophic growth with methanogens that can grow on both hydrogen and formate compared to sole hydrogen consumers [159-163]. The preference of hydrogen or formate in syntrophic fatty acid degrading communities has not been clear thus far, but a syntrophic relationship in which both hydrogen and formate can be transferred would be more flexible than when only hydrogen is transferred [164].

1.5.2 Reverse electron transfer

Although in propionate and butyrate oxidation the overall reaction is exergonic in syntrophic production of hydrogen or formate, two individual reactions in the pathways remain endergonic. These are the oxidation of succinate to fumarate in the propionate metabolism and the conversion of butyryl-CoA to crotonyl-CoA in the butyrate metabolism. However, syntrophic bacteria can still perform these endergonic reactions thanks to a mechanism called reverse electron transfer. Reverse electron transfer enables investment of a fraction of ATP or ion gradient in order to perform the endergonic reaction [167, 168]. Multiple reverse electron transfer mechanisms have been described over the years and their importance in syntrophic communities was shown [155, 163, 165, 166]. In syntrophic propionate metabolism the endergonic succinate oxidation to fumarate is performed by a cytoplasmic oriented membrane-bound succinate dehydrogenase that was described to couple the reaction via a menaquinone loop to formate formation by a periplasmic oriented membrane bound formate dehydrogenase (Figure 1.5A) [155, 169]. During these reactions

two protons from the membrane potential are invested. A similar system was recently described for the conversion of butyryl-CoA to crotonyl-CoA in *Syntrophomonas wolfei*. The cytoplasmic butyryl-CoA dehydrogenase transfers its electrons via an etfAB complex and a membrane bound DUF224 protein to a menaquinone cycle and further via a b-type cytochrome to an extracytoplasmic oriented membrane bound formate dehydrogenase. To couple these reactions *S. wolfei* would need a small investment of energy [163]. In addition to reverse electron transfer there are other enzyme complex systems that seem to play an important role in syntrophy, called bifurcating enzyme complexes and Rnf-complexes.

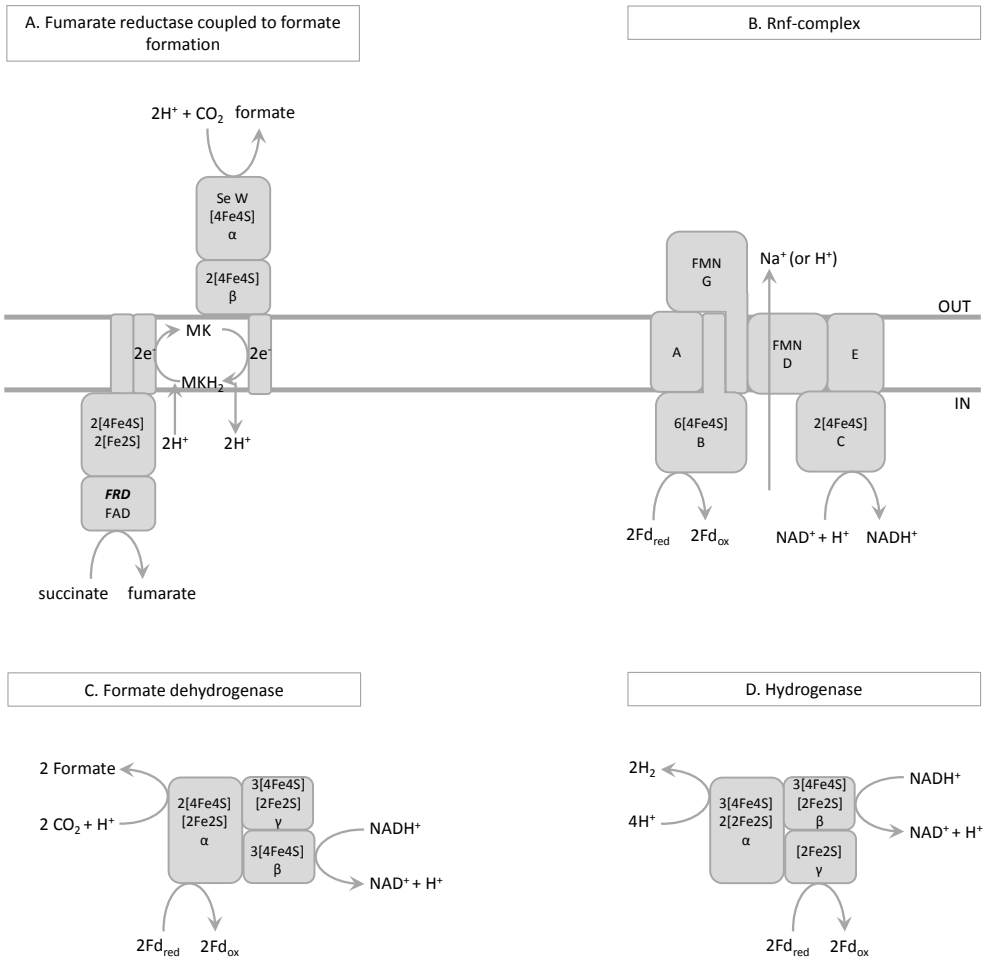

Figure 1.5: Enzyme complexes involved in reverse electron transport and energy conservation: a fumarate reductase coupled to formate formation (A), the Rnf complex (B), a bifurcating/confurcating formate dehydrogenase (C), and a bifurcating/confurcating hydrogenase (D). Predicted iron-sulfur clusters, other metal-binding sites and cofactors are indicated. Moreover, α-, β-, and γ-subunits are depicted. Abbreviations: FAD, flavin adenine dinucleotide; Fd, ferredoxin; FMN, flavin mononucleotide; MK, menaquinone.

1.5.3 Energy conserving enzyme complexes

Rnf-complexes are membrane bound electron transport complexes. The rnf genes were first described in *Rhodobacter capulatus* [170] and later in several other microorganisms [170-181]. In *Acetobacterium woodii* the Rnf complex consists of six different subunits, RnfCDGEAB [182] and is the first Rnf complex biochemically shown to transfer its electrons from reduced ferredoxin to NAD^+ [182]. This electron transport is coupled to sodium translocation over the membrane creating a membrane potential (Figure 1.5B) [183]. In *Clostridium ljungdahlii* the electron transport is coupled to proton translocation [184]. Many syntrophic metabolizers have rnf genes encoded in their genome, which leads to the suggestion that they have an important role in syntrophic lifestyle [185]. During syntrophic interaction the Rnf complex would function in the opposite direction, functioning as a reverse electron transport complex [176, 186]. It was confirmed for *A. woodii* that its Rnf complex can perform both reactions [183]. Hess et al. used an ATP hydrolysis to create a sodium gradient in membrane vesicles. Subsequently, the sodium content in the vesicles dropped after the addition of NADH in the presence of oxidized ferredoxin [183].

Bifurcating enzyme complexes catalyze three redox reactions to conserve energy. Described bifurcation (and the reversed reaction termed confurcation) enzyme complexes are the butyryl-CoA / electron transfer flavoprotein complex of *Clostridium kluyveri* [175], the [FeFe]-hydrogenase complex of *Thermotoga maritima* and *Acetobacterium woodii* ([187, 188], Figure 1.5D), and the formate dehydrogenase complex in *Clostridium acidurici* ([189], Figure 1.5C). Recently, a genome comparison analysis of syntrophic bacteria was performed. This analysis indicated that many syntrophs contained confurcating hydrogenases and FDHs in their genome, suggesting their importance in syntrophy [185].

Many of these enzyme complexes described above are coupled to hydrogen or formate formation and therefore support the importance of interspecies hydrogen and formate electron transfer in syntrophy.

1.5.4 Syntrophic growth with C1 substrates

1.5.4.1 Syntrophic anaerobic oxidation of methane

The most studied, but still poorly understood, syntrophically degraded C-1 compound is methane, in a process called anaerobic oxidation of methane (AOM). Ocean sediments produce large amounts of methane each year but nearly nothing reaches the atmosphere, because most of it is consumed by anaerobic microorganisms. AOM coupled to sulfate, iron, manganese and nitrate reduction have been demonstrated [190-192]. The microorganisms responsible for AOM are anaerobic methanotrophic archaea (ANME) that presumably use similar enzymes as the ones that catalyze CO_2 reduction to CH_4 in methanogens but in reverse [192]. Until now no isolation has been established of either the ANME or the bacteria involved in the syntrophic interaction. However, several studies have identified multiple ANME groups [193-196] and several bacteria present in AOM consortia [195-204], predominantly in AOM coupled to sulfate reduction since this is the most studied AOM interaction. How AOM is coupled to sulfate reduction remains unresolved, since no intermediate has of yet been described.

1.5.4.2 Syntrophic formate and methanol degradation

Formate can be degraded by syntrophic communities [205]. Formate oxidation coupled to hydrogen

production is exergonic when formate oxidation is coupled to methane production (Table 1.2). For the syntrophic formate oxidizer and the methanogen to share the energy generated in such a manner that both organisms gain enough to grow, low hydrogen concentrations are essential. Syntrophic formate degradation was described for *Desulfovibrio* sp. strain G11 and *Moorella thermoacetica* strain AMP. It is hypothesized that an extra-cytoplasmic formate dehydrogenase is coupled to a membrane integrated, cytoplasmic oriented hydrogenase, which generates a proton motive force that drives ATP synthesis [205]. To what extend and in what types of anaerobic microbial environments syntrophic formate degradation can compete with formate degradation by methanogens is unknown.

Moorella thermoacetica strain AMP can also grow syntrophically with methanol. When cobalt and vitamin B12 are omitted from the medium strain AMP can only grow with methanol in syntrophic association with *Methanothermobacter thermautotrophicus* strain NJ1. In this co-culture methane, and nearly no acetate, was formed as end-product [206]. How syntrophic methanol degradation can be coupled to methane production is not extensively studied. Hydrogen and formate could both function as interspecies electron carriers, since the production of hydrogen and formate from methanol oxidation are endergonic reactions that can turn exergonic when coupled to methane production (Table 1.2).

1.6 Outline of the thesis

One carbon compounds have a 'simple' molecular structure but it is evident that they play an important role in nature and society. Moreover, there are many different anaerobes that can grow with C-1 compounds. The research described in this thesis aims to get a better understanding of the metabolism of one-carbon compounds by anaerobic microbial communities. The proteins involved, and the genes encoding these proteins, in the metabolism of C-1 degraders in pure-culture and in syntrophic interactions form the basis of this thesis. This was established by performing genome sequencing and analysis studies together with proteomic analysis in acetogenic and sulfate reducing bacteria.

CO metabolism was studied in two-sulfate reducing *Desulfotomaculum* species, *D. nigrificans* and *D. carboxydivorans* by means of a genome comparison (Chapter 2). They can both degrade CO but their CO metabolism is different. *D. nigrificans* can grow with 20% CO coupled to sulfate reduction and *D. carboxydivorans* can grow with 100% CO with and without sulfate. Moreover, hydrogen is produced during CO degradation by *D. carboxydivorans*. Chapter 2 describes the differences and similarities between the two genomes and the CO metabolism.

Chapters 3 to 5 describe the methanol metabolism in an acetogenic bacterium and a sulfate-reducing bacterium. The physiology of the acetogenic bacterium, *Sporomusa* strain An4, is studied by combining genome and proteome analysis (Chapter 3). Strain An4 was grown under five different conditions for comparative proteomics, including growth with H_2 and CO_2, methanol, methanol and nitrate, betaine, and fructose. The genomic and proteomic results allow for a better understanding of the physiology of strain An4 and its methanol metabolism. The methanol metabolism of the sulfate-reducer *Desulfotomaculum kuznetsovii* was studied in Chapter 4 by searching the genome for genes that could be involved in the degradation of methanol. Subsequently, a proteomic analysis was performed to assess which proteins are produced during growth with methanol (Chapter 5).

The genome of *D. kuznetsovii* is also compared to the genome of *Pelotomaculum thermopropionicum*

(Chapter 4). In contrast to *D. kuznetsovii*, *P. thermopropionicum* is known for its ability to grow with propionate and ethanol in syntrophic association with methanogens. *D. kuznetsovii* couples propionate and ethanol degradation to sulfate reduction, but cannot grow in syntrophic association with methanogens in the absence of sulfate. Moreover, *P. thermopropionicum* cannot reduce sulfate. The genome comparison was aimed to compare two relatively closely related species that differed in their syntrophic capacity to find genes that could be specific for a syntrophic lifestyle. This concept was extrapolated in Chapter 6, by including more genome sequences of bacteria that can and bacteria that cannot grow with butyrate and propionate in syntrophic association with methanogens. This chapter describes the importance of formate as an electron carrier in syntrophic butyrate and propionate degradation and tries to identify key genes in syntrophy.

Finally, the results of the work presented in this thesis and the future perspectives are discussed in Chapter 7.

1.7 References

1. Falkowski, P.G., Fenchel, T. & Delong, E.F. The microbial engines that drive Earth's biogeochemical cycles. *Science* **320**, 1034-9 (2008).
2. Conrad, R. & Seiler, W. Characteristics of abiological carbon monoxide formation from soil organic matter, humic acids, and phenolic compounds. *Environmental Science & Technology* **19**, 1165-9 (1985).
3. Kieber, D.J., McDaniel, J. & Mopper, K. Photochemical source of biological substrates in sea water: implications for carbon cycling. *Nature* **341**, 637–639 (1989).
4. King, D.P. & Crosby, H. Impact of plant roots on soil CO cycling and soil atmosphere CO exchange. *Global Change Biology* **8**, 1085-93 (2002).
5. Lilley, M.D., de Angelis, M.A. & Gordon, L.I. CH_4, H_2, CO and N_2O in submarine hydrothermal vent waters. *Nature* **300**, 48–9 (1982).
6. Miller, W.L. & Zepp, R.G. Photochemical production of dissolved inorganic carbon from terrestrial organic matter: significance to the oceanic organic carbon cycle. . *Geophysical Research Letters* **22**, 417–20 (1995).
7. Valentine, R.L. Formation of Carbon Monoxide from the Photodegradation of Terrestrial Dissolved Organic Carbon. *Environmental Science & Technology* **27**, 409-12 (1993).
8. Zuo, Y. & Jones, R.D. Formation of carbon monoxide by photolysis of dissolved marine organic material and its significance in the carbon cycling of the oceans. *Naturwissenschaften* **82**, 472–474 (1995).
9. Schade, G.W. & Goldstein, A.H. Seasonal measurements of acetone and methanol: Abundances and implications for atmospheric budgets. *Global Biogeochemical Cycles* **20** (2006).
10. Williams, J., Holzinger, R., Gros, V., Xu, X., Atlas, E., Wallace, D. W. R. Measurements of organic species in air and seawater from the tropical Atlantic. *Geophysical Research Letters* **31** (2004).
11. Williamson, S.J. Rusch, D.B., Yooseph, S., Halpern, A.L., Heidelberg, K.B., Glass, J.I., Andrews-Pfannkoch, C., Fadrosh, D., Miller, C.S., Sutton, G., Frazier, M., Venter, J.C. The sorcerer II global ocean sampling expedition: metagenomic characterization of viruses within aquatic microbial samples. *PLoS One* **3**, e1456 (2008).
12. Dixon, J.L., Beale, R. & Nightingale, P.D. Microbial methanol uptake in northeast Atlantic waters. *Isme Journal* **5**, 704-16 (2011).
13. Schink, B. & Zeikus, J.G. Microbial methanol formation - a major end product of pectin metabolism. *Current Microbiology* **4**, 387-9 (1980).
14. Hektor, H.J., Kloosterman, H. & Dijkhuizen, L. Nicotinoprotein methanol dehydrogenase enzymes in Gram-positive methylotrophic bacteria. *Journal of Molecular Catalysis B-Enzymatic* **8**, 103-9 (2000).
15. Thauer, R.K., Jungermann, K. & Decker, K. Energy conservation in chemotrophic anaerobic bacteria. *Bacteriological Reviews* **41**, 80-100 (1977).

16. Ragsdale, S.W. & Pierce, E. Acetogenesis and the Wood-Ljungdahl pathway of CO_2 fixation. *Biochimica et Biophysica Acta* **1784**, 1873-98 (2008).
17. Techtmann, S.M., Colman, A.S. & Robb, F.T. 'That which does not kill us only makes us stronger': the role of carbon monoxide in thermophilic microbial consortia. *Environmental Microbiology* **11**, 1027-37 (2009).
18. Diekert, G. & Wohlfarth, G. Metabolism of homocetogens. *Antonie Van Leeuwenhoek* **66**, 209-21 (1994).
19. Ragsdale, S.W. Nickel and the carbon cycle. *Journal of Inorganic Biochemistry* **101**, 1657-66 (2007).
20. Ragsdale, S.W. Enzymology of the Wood-Ljungdahl pathway of acetogenesis. *Annals of the New York Academy of Sciences* **1125**, 129-36 (2008).
21. Lindahl, P.A. Acetyl-coenzyme A synthase: the case for a Ni(p)(0)-based mechanism of catalysis. *Journal of biological inorganic chemistry : JBIC : a publication of the Society of Biological Inorganic Chemistry* **9**, 516-24 (2004).
22. Goevert, D. & Conrad, R. Carbon isotope fractionation by sulfate-reducing bacteria using different pathways for the oxidation of acetate. *Environmental Science & Technology* **42**, 7813-7 (2008).
23. Wood, H.G. Life with CO or CO_2 and H_2 as a source of carbon and energy. *FASEB Journal : official publication of the Federation of American Societies for Experimental Biology* **5**, 156-63 (1991).
24. Meyer, O., Jacobitz, S. & Kruger, B. Biochemistry and physiology of aerobic carbon monoxide utilizing bacteria. *Fems Microbiology Letters* **39**, 161-79 (1986).
25. King, G.M. & Weber, C.F. Distribution, diversity and ecology of aerobic CO-oxidizing bacteria. *Nature Reviews Microbiology* **5**, 107-18 (2007).
26. Rabus, R., Hansen, T.A. & Widdel, F. Dissimilatory sulfate- and sulfur-reducing prokaryotes. *Prokaryotes* **2**, 659–768 (2006).
27. Muyzer, G. & Stams, A.J. The ecology and biotechnology of sulphate-reducing bacteria. *Nature Reviews Microbiology* **6**, 441-54 (2008).
28. Henstra, A.M., Sipma, J., Rinzema, A. & Stams, A.J. Microbiology of synthesis gas fermentation for biofuel production. *Current Opinion in Biotechnology* **18**, 200-6 (2007).
29. Drake, H.L. et al. Acetogenic bacteria: what are the in situ consequences of their diverse metabolic versatilities? *Biofactors* **6**, 13-24 (1997).
30. Deppenmeier, U. & Muller, V. Life close to the thermodynamic limit: how methanogenic archaea conserve energy. *Results and problems in cell differentiation* **45**, 123-52 (2008).
31. Oelgeschlager, E. & Rother, M. Carbon monoxide-dependent energy metabolism in anaerobic bacteria and archaea. *Archives of Microbiology* **190**, 257-69 (2008).
32. Martin-Cuadrado, A.B., Ghai, R., Gonzaga, A. & Rodriguez-Valera, F. CO dehydrogenase genes found in metagenomic fosmid clones from the deep mediterranean sea. *Applied Environmental Microbiology* **75**, 7436-44 (2009).
33. Tringe, S.G. et al. Comparative metagenomics of microbial communities. *Science* **308**, 554-7 (2005).
34. Tyson, G.W. et al. Community structure and metabolism through reconstruction of microbial genomes from the environment. *Nature* **428**, 37-43 (2004).
35. Matson, E.G., Gora, K.G. & Leadbetter, J.R. Anaerobic carbon monoxide dehydrogenase diversity in the homoacetogenic hindgut microbial communities of lower termites and the wood roach. *PLoS One* **6**, e19316 (2011).
36. Oelgeschlager, E. & Rother, M. Influence of carbon monoxide on metabolite formation in *Methanosarcina acetivorans*. *Fems Microbiology Letters* **292**, 254-60 (2009).
37. Drake, H.L. & Daniel, S.L. Physiology of the thermophilic acetogen *Moorella thermoacetica*. *Research in Microbiology* **155**, 422-36 (2004).
38. Parshina, S.N. et al. Carbon monoxide conversion by thermophilic sulfate-reducing bacteria in pure culture and in co-culture with *Carboxydothermus hydrogenoformans*. *Applied Microbiology and Biotechnology* **68**, 390-6 (2005).
39. Henstra, A.M. & Stams, A.J. Novel physiological features of *Carboxydothermus hydrogenoformans* and *Thermoterrabacterium ferrireducens*. *Applied and Environmental Microbiology* **70**, 7236-40 (2004).
40. Sokolova, T.G. et al. *Thermosinus carboxydivorans* gen. nov., sp. nov., a new anaerobic, thermophilic, carbon-monoxide-oxidizing, hydrogenogenic bacterium from a hot pool of Yellowstone National Park. *International Journal of Systematic*

and Evolutionary Microbiology **54**, 2353-9 (2004).

41. Alves, J.I., van Gelder, A.H., Alves, M.M., Sousa, D.Z. & Plugge, C.M. *Moorella stamsii* sp. nov., a new anaerobic thermophilic hydrogenogenic carboxydotroph isolated from digester sludge. *International Journal of Systematic and Evolutionary Microbiology* **63**, 4072-6 (2013).
42. Parshina, S.N. et al. *Desulfotomaculum carboxydivorans* sp. nov., a novel sulfate-reducing bacterium capable of growth at 100% CO. *International Journal of Systematic and Evolutionary Microbiology* **55**, 2159-65 (2005).
43. Slepova, T.V., Sokolova, T.G., Kolganova, T.V., Tourova, T.P. & Bonch-Osmolovskaya, E.A. *Carboxydothermus siderophilus* sp. nov., a thermophilic, hydrogenogenic, carboxydotrophic, dissimilatory Fe(III)-reducing bacterium from a Kamchatka hot spring. *International Journal of Systematic and Evolutionary Microbiology* **59**, 213-7 (2009).
44. Slepova, T.V. et al. *Carboxydocella sporoproducens* sp. nov., a novel anaerobic CO-utilizing/H_2-producing thermophilic bacterium from a Kamchatka hot spring. *International Journal of Systematic and Evolutionary Microbiology* **56**, 797-800 (2006).
45. Sokolova, T. et al. Novel chemolithotrophic, thermophilic, anaerobic bacteria *Thermolithobacter ferrireducens* gen. nov., sp. nov. and *Thermolithobacter carboxydivorans* sp. nov. *Extremophiles* **11**, 145-57 (2007).
46. Sokolova, T.G. et al. *Carboxydobrachium pacificum* gen. nov., sp. nov., a new anaerobic, thermophilic, CO-utilizing marine bacterium from Okinawa Trough. *International Journal of Systematic and Evolutionary Microbiology* **51**, 141-9 (2001).
47. Sokolova, T.G. et al. The first evidence of anaerobic CO oxidation coupled with H_2 production by a hyperthermophilic archaeon isolated from a deep-sea hydrothermal vent. *Extremophiles* **8**, 317-23 (2004).
48. Sokolova, T.G. et al. *Carboxydocella thermautotrophica* gen. nov., sp. nov., a novel anaerobic, CO-utilizing thermophile from a Kamchatkan hot spring. *International Journal of Systematic and Evolutionary Microbiology* **52**, 1961-7 (2002).
49. Ragsdale, S.W. & Kumar, M. Nickel-containing carbon monoxide dehydrogenase/acetyl-CoA synthase. *Chemical Reviews* **96**, 2515-40 (1996).
50. Bonam, D., Lehman, L., Roberts, G.P. & Ludden, P.W. Regulation of carbon monoxide dehydrogenase and hydrogenase in *Rhodospirillum rubrum*: effects of CO and oxygen on synthesis and activity. *Journal of Bacteriology* **171**, 3102-7 (1989).
51. Bonam, D. & Ludden, P.W. Purification and characterization of carbon monoxide dehydrogenase, a nickel, zinc, iron-sulfur protein, from *Rhodospirillum rubrum*. *The Journal of Biological Chemistry* **262**, 2980-7 (1987).
52. Bonam, D., McKenna, M.C., Stephens, P.J. & Ludden, P.W. Nickel-deficient carbon monoxide dehydrogenase from *Rhodospirillum rubrum*: in vivo and in vitro activation by exogenous nickel. *Proceedings of the National Academy of Sciences of the United States of America* **85**, 31-5 (1988).
53. Bonam, D., Murrell, S.A. & Ludden, P.W. Carbon monoxide dehydrogenase from *Rhodospirillum rubrum*. *Journal of Bacteriology* **159**, 693-9 (1984).
54. Daniels, L., Fuchs, G., Thauer, R.K. & Zeikus, J.G. Carbon monoxide oxidation by methanogenic bacteria. *Journal of Bacteriology* **132**, 118-26 (1977).
55. Drennan, C.L., Heo, J., Sintchak, M.D., Schreiter, E. & Ludden, P.W. Life on carbon monoxide: X-ray structure of *Rhodospirillum rubrum* Ni-Fe-S carbon monoxide dehydrogenase. *Proceedings of the National Academy of Sciences of the United States of America* **98**, 11973-8 (2001).
56. Ensign, S.A., Bonam, D. & Ludden, P.W. Nickel is required for the transfer of electrons from carbon monoxide to the iron-sulfur center(s) of carbon monoxide dehydrogenase from *Rhodospirillum rubrum*. *Biochemistry* **28**, 4968-73 (1989).
57. Ensign, S.A., Campbell, M.J. & Ludden, P.W. Activation of the nickel-deficient carbon monoxide dehydrogenase from *Rhodospirillum rubrum*: kinetic characterization and reductant requirement. *Biochemistry* **29**, 2162-8 (1990).
58. Ensign, S.A., Hyman, M.R. & Ludden, P.W. Nickel-specific, slow-binding inhibition of carbon monoxide dehydrogenase from *Rhodospirillum rubrum* by cyanide. *Biochemistry* **28**, 4973-9 (1989).
59. Ensign, S.A. & Ludden, P.W. Characterization of the CO oxidation/H_2 evolution system of *Rhodospirillum rubrum*. Role of a 22-kDa iron-sulfur protein in mediating electron transfer between carbon monoxide dehydrogenase and

hydrogenase. *The Journal of Biological Chemistry* **266**, 18395-403 (1991).

60. Jeon, W.B., Cheng, J. & Ludden, P.W. Purification and characterization of membrane-associated CooC protein and its functional role in the insertion of nickel into carbon monoxide dehydrogenase from *Rhodospirillum rubrum*. *The Journal of Biological Chemistry* **276**, 38602-9 (2001).
61. Jeon, W.B., Singer, S.W., Ludden, P.W. & Rubio, L.M. New insights into the mechanism of nickel insertion into carbon monoxide dehydrogenase: analysis of *Rhodospirillum rubrum* carbon monoxide dehydrogenase variants with substituted ligands to the [Fe3S4] portion of the active-site C-cluster. *Journal of Biological Inorganic Chemistry : JBIC : a publication of the Society of Biological Inorganic Chemistry* **10**, 903-12 (2005).
62. Kerby, R.L. et al. Genetic and physiological characterization of the *Rhodospirillum rubrum* carbon monoxide dehydrogenase system. *Journal of Bacteriology* **174**, 5284-94 (1992).
63. Kerby, R.L., Ludden, P.W. & Roberts, G.P. In vivo nickel insertion into the carbon monoxide dehydrogenase of *Rhodospirillum rubrum*: molecular and physiological characterization of cooCTJ. *Journal of Bacteriology* **179**, 2259-66 (1997).
64. Meuer, J., Bartoschek, S., Koch, J., Kunkel, A. & Hedderich, R. Purification and catalytic properties of Ech hydrogenase from *Methanosarcina barkeri*. *European journal of biochemistry / FEBS* **265**, 325-35 (1999).
65. Stephens, P.J., McKenna, M.C., Ensign, S.A., Bonam, D. & Ludden, P.W. Identification of a Ni- and Fe-containing cluster in *Rhodospirillum rubrum* carbon monoxide dehydrogenase. *The Journal of Biological Chemistry* **264**, 16347-50 (1989).
66. Tan, G.O. et al. On the structure of the nickel/iron/sulfur center of the carbon monoxide dehydrogenase from *Rhodospirillum rubrum*: an x-ray absorption spectroscopy study. *Proceedings of the National Academy of Sciences of the United States of America* **89**, 4427-31 (1992).
67. Uffen, R.L. Anaerobic growth of a *Rhodopseudomonas* species in dark with carbon-monoxide as sole carbon and energy substrate. *Proceedings of the National Academy of Sciences of the United States of America* **73**, 3298-302 (1976).
68. Ferry, J.G. CO Dehydrogenase. *Annual Review of Microbiology* **49**, 305-33 (1995).
69. Fox, J.D., He, Y.P., Shelver, D., Roberts, G.P. & Ludden, P.W. Characterization of the region encoding the CO-induced hydrogenase of *Rhodospirillum rubrum*. *Journal of Bacteriology* **178**, 6200-8 (1996).
70. Fox, J.D., Kerby, R.L., Roberts, G.P. & Ludden, P.W. Characterization of the CO-induced, CO-tolerant hydrogenase from *Rhodospirillum rubrum* and the gene encoding the large subunit of the enzyme. *Journal of Bacteriology* **178**, 1515-24 (1996).
71. Wakim, B.T. & Uffen, R.L. Membrane association of the carbon monoxide oxidation system in *Rhodopseudomonas gelatinosa*. *Journal of Bacteriology* **153**, 571-3 (1983).
72. Hedderich, R. Energy-converting [NiFe] hydrogenases from archaea and extremophiles: ancestors of complex I. *Journal of Bioenergetics and Biomembranes* **36**, 65-75 (2004).
73. Soboh, B., Linder, D. & Hedderich, R. Purification and catalytic properties of a CO-oxidizing:H2-evolving enzyme complex from *Carboxydothermus hydrogenoformans*. *European Journal of Biochemistry / FEBS* **269**, 5712-21 (2002).
74. Wu, M. et al. Life in hot carbon monoxide: the complete genome sequence of *Carboxydothermus hydrogenoformans* Z-2901. *PLoS Genetics* **1**, e65 (2005).
75. Kaluarachchi, H., Chung, K.C.C. & Zamble, D.B. Microbial nickel proteins. *Natural Product Reports* **27**, 681-94 (2010).
76. Aono, S. Biochemical and biophysical properties of the CO-sensing transcriptional activator CooA. *Accounts of Chemical Research* **36**, 825-31 (2003).
77. Svetlitchnyi, V., Peschel, C., Acker, G. & Meyer, O. Two membrane-associated NiFeS-carbon monoxide dehydrogenases from the anaerobic carbon-monoxide-utilizing eubacterium *Carboxydothermus hydrogenoformans*. *Journal of Bacteriology* **183**, 5134-44 (2001).
78. Techtmann, S.M. et al. Regulation of multiple carbon monoxide consumption pathways in anaerobic bacteria. *Frontiers in Microbiology* **2**, 147 (2011).
79. Matschiavelli, N., Oelgeschlager, E., Cocchiararo, B., Finke, J. & Rother, M. Function and regulation of isoforms of carbon monoxide dehydrogenase/acetyl coenzyme A synthase in *Methanosarcina acetivorans*. *Journal of Bacteriology* **194**, 5377-87 (2012).

80. Davidova, M.N., Tarasova, N.B., Mukhitova, F.K. & Karpilova, I.U. Carbon monoxide in metabolism of anaerobic bacteria. *Canadian Journal of Microbiology* **40**, 417-25 (1994).
81. Schrader, J. et al. Methanol-based industrial biotechnology: current status and future perspectives of methylotrophic bacteria. *Trends in Biotechnology* **27**, 107-15 (2009).
82. Goeppert, A., Czaun, M., Jones, J.P., Surya Prakash, G.K. & Olah, G.A. Recycling of carbon dioxide to methanol and derived products - closing the loop. *Chemical Society Reviews* (2014).
83. Cui, Z., Meng, F., Hong, J., Li, X. & Ren, X. Effects of electron donors on the microbial reductive dechlorination of hexachlorocyclohexane and on the environment. *Journal of Bioscience and Bioengineering* **113**, 765-70 (2012).
84. Priya, V.S. & Philip, L. Biodegradation of dichloromethane along with other VOCs from pharmaceutical wastewater. *Applied Biochemistry and Biotechnology* **169**, 1197-218 (2013).
85. Zehraoui, A., Hassan, A.A. & Sorial, G.A. Effect of methanol on the biofiltration of n-hexane. *Journal of Hazardous Materials* **219**, 176-82 (2012).
86. Cho, E. & Molof, A.H. Effect of sequentially combining methanol and acetic acid on the performance of biological nitrogen and phosphorus removal. *Journal of Environmental Management* **73**, 183-7 (2004).
87. Glombitza, F. Treatment of acid lignite mine flooding water by means of microbial sulfate reduction. *Waste Management* **21**, 197-203 (2001).
88. Pan, Y.T., Ni, B.J., Bond, P.L., Ye, L. & Yuan, Z.G. Electron competition among nitrogen oxides reduction during methanol-utilizing denitrification in wastewater treatment. *Water Research* **47**, 3273-81 (2013).
89. Paulo, P.L., Vallero, M.V., Trevino, R.H., Lettinga, G. & Lens, P.N. Thermophilic (55 degrees C) conversion of methanol in methanogenic-UASB reactors: influence of sulphate on methanol degradation and competition. *Journal of Biotechnology* **111**, 79-88 (2004).
90. Taya, C., Guerrero, J., Vanneste, G., Guisasola, A. & Baeza, J.A. Methanol-driven enhanced biological phosphorus removal with a syntrophic consortium. *Biotechnology and Bioengineering* **110**, 391-400 (2013).
91. Zhang, Y., Liss, S.N. & Allen, D.G. The effects of methanol on the biofiltration of dimethyl sulfide in inorganic biofilters. *Biotechnology and Bioengineering* **95**, 734-43 (2006).
92. Anthony, C. & Williams, P. The structure and mechanism of methanol dehydrogenase. *Biochimica et Biophysica Acta* **1647**, 18-23 (2003).
93. Afolabi, P.R. et al. Site-directed mutagenesis and X-ray crystallography of the PQQ-containing quinoprotein methanol dehydrogenase and its electron acceptor, cytochrome c(L). *Biochemistry* **40**, 9799-809 (2001).
94. Anthony, C. & Ghosh, M. The structure and function of the PQQ-containing quinoprotein dehydrogenases. *Progress in Biophysics and Molecular Biology* **69**, 1-21 (1998).
95. Ghosh, M., Anthony, C., Harlos, K., Goodwin, M.G. & Blake, C. The refined structure of the quinoprotein methanol dehydrogenase from *Methylobacterium extorquens* at 1.94 A. *Structure* **3**, 177-87 (1995).
96. Ghosh, M., Harlos, K., Blake, C.C., Richardson, I. & Anthony, C. Crystallization and preliminary crystallographic investigation of methanol dehydrogenase from *Methylobacterium extorquens* AM1. *Journal of Molecular Biology* **228**, 302-5 (1992).
97. Xia, Z.X. et al. The three-dimensional structures of methanol dehydrogenase from two methylotrophic bacteria at 2.6-A resolution. *The Journal of Biological Chemistry* **267**, 22289-97 (1992).
98. Xia, Z.X. et al. Determination of the gene sequence and the three-dimensional structure at 2.4 angstrom resolution of methanol dehydrogenase from *Methylophilus* W3A1. *Journal of Molecular Biology* **259**, 480-501 (1996).
99. Xia, Z.X. et al. Detailed active site configuration of a new crystal form of methanol dehydrogenase from *Methylophilus* W3A1 at 1.9 A resolution. *Biochemistry* **38**, 1214-20 (1999).
100. Zheng, Y.J., Xia, Z., Chen, Z., Mathews, F.S. & Bruice, T.C. Catalytic mechanism of quinoprotein methanol dehydrogenase: A theoretical and x-ray crystallographic investigation. *Proceedings of the National Academy of Sciences of the United States of America* **98**, 432-4 (2001).
101. Anthony, C., Ghosh, M. & Blake, C.C.F. The structure and function of methanol dehydrogenase and related quinoproteins containing pyrrolo-quinoline quinone. *Biochemical Journal* **304**, 665-74 (1994).

102. Anthony, C. The c-type cytochromes of methylotrophic bacteria. *Biochimica et Biophysica Acta* **1099**, 1-15 (1992).
103. de Vries, G.E., Arfman, N., Terpstra, P. & Dijkhuizen, L. Cloning, expression, and sequence analysis of the *Bacillus methanolicus* C1 methanol dehydrogenase gene. *Journal of Bacteriology* **174**, 5346-53 (1992).
104. Arfman, N. et al. Properties of an NAD(H)-containing methanol dehydrogenase and its activator protein from *Bacillus methanolicus*. *European journal of biochemistry / FEBS* **244**, 426-33 (1997).
105. Hektor, H.J., Kloosterman, H. & Dijkhuizen, L. Identification of a magnesium-dependent NAD(P)(H)-binding domain in the nicotinoprotein methanol dehydrogenase from *Bacillus methanolicus*. *The Journal of Biological Chemistry* **277**, 46966-73 (2002).
106. Krog, A. et al. Methylotrophic *Bacillus methanolicus* encodes two chromosomal and one plasmid born NAD+ dependent methanol dehydrogenase paralogs with different catalytic and biochemical properties. *PLoS One* **8**, e59188 (2013).
107. Muller, J.E. et al. Proteomic analysis of the thermophilic methylotroph *Bacillus methanolicus* MGA3. *Proteomics* **14**, 725-37 (2014).
108. Bystrykh, L.V. et al. Formaldehyde dismutase activities in gram-positive bacteria oxidizing methanol. *Journal of General Microbiology* **139**, 1979-85 (1993).
109. Bystrykh, L.V. et al. Electron microscopic analysis and structural characterization of novel NADP(H)-containing methanol: N,N'-dimethyl-4-nitrosoaniline oxidoreductases from the gram-positive methylotrophic bacteria *Amycolatopsis methanolica* and *Mycobacterium gastri* MB19. *Journal of Bacteriology* **175**, 1814-22 (1993).
110. Bystrykh, L.V., Govorukhina, N.I., Dijkhuizen, L. & Duine, J.A. Tetrazolium-dye-linked alcohol dehydrogenase of the methylotrophic actinomycete *Amycolatopsis methanolica* is a three-component complex. *European Journal of Biochemistry* **247**, 280-7 (1997).
111. Duine, J.A., Frank, J. & Berkhout, M.P. NAD-dependent, PQQ-containing methanol dehydrogenase: a bacterial dehydrogenase in a multienzyme complex. *FEBS letters* **168**, 217-21 (1984).
112. van der Meijden, P. et al. Methyltransferases involved in methanol conversion by *Methanosarcina barkeri*. *Archives of Microbiology* **134**, 238-42 (1983).
113. van der Meijden, P. et al. Activation and inactivation of methanol: 2-mercaptoethanesulfonic acid methyltransferase from *Methanosarcina barkeri*. *Journal of Bacteriology* **153**, 6-11 (1983).
114. van der Meijden, P., te Brommelstroet, B.W., Poirot, C.M., van der Drift, C. & Vogels, G.D. Purification and properties of methanol:5-hydroxybenzimidazolylcobamide methyltransferase from *Methanosarcina barkeri*. *Journal of Bacteriology* **160**, 629-35 (1984).
115. van der Meijden, P., van der Lest, C., van der Drift, C. & Vogels, G.D. Reductive activation of methanol: 5-hydroxybenzimidazolylcobamide methyltransferase of *Methanosarcina barkeri*. *Biochemical and Biophysical Research Communications* **118**, 760-6 (1984).
116. Sauer, K., Harms, U. & Thauer, R.K. Methanol:coenzyme M methyltransferase from *Methanosarcina barkeri*. Purification, properties and encoding genes of the corrinoid protein MT1. *European journal of biochemistry / FEBS* **243**, 670-7 (1997).
117. Harms, U. & Thauer, R.K. Methylcobalamin: coenzyme M methyltransferase isoenzymes MtaA and MtbA from Methanosarcina barkeri. Cloning, sequencing and differential transcription of the encoding genes, and functional overexpression of the mtaA gene in Escherichia coli. *Eur J Biochem* **235**, 653-9 (1996).
118. Stupperich, E., Aulkemeyer, P. & Eckerskorn, C. Purification and characterization of a methanol-induced cobamide-containing protein from *Sporomusa ovata*. *Archives of Microbiology* **158**, 370-3 (1992).
119. Zhou, W. et al. Isolation, crystallization and preliminary X-ray analysis of a methanol-induced corrinoid protein from *Moorella thermoacetica*. *Acta Crystallographica. Section F, Structural Biology and Crystallization Communications* **61**, 537-40 (2005).
120. Das, A. et al. Characterization of a corrinoid protein involved in the C1 metabolism of strict anaerobic bacterium Moorella thermoacetica. *Proteins* **67**, 167-76 (2007).
121. Pierce, E. et al. The complete genome sequence of *Moorella thermoacetica* (f. *Clostridium thermoaceticum*). *Environmental*

Microbiology **10**, 2550-73 (2008).

122. Stupperich, E. & Konle, R. Corrinoid-Dependent Methyl Transfer Reactions Are Involved in Methanol and 3,4-Dimethoxybenzoate Metabolism by Sporomusa ovata. *Appl Environ Microbiol* **59**, 3110-6 (1993).
123. Klemps, R., Cypionka, H., Widdel, F. & Pfennig, N. Growth with hydrogen, and further physiological-characteristics of *Desulfotomaculum* species. *Archives of Microbiology* **143**, 203-8 (1985).
124. Szewzyk, R. & Pfennig, N. Complete oxidation of catechol by the strictly anaerobic sulfate-reducing *Desulfobacterium catecholicum* sp.nov. *Archives of Microbiology* **147**, 163-8 (1987).
125. Schnell, S., Bak, F. & Pfennig, N. Anaerobic degradation of aniline and dihydroxybenzenes by newly isolated sulfate-reducing bacteria and description of *Desulfobacterium anilini*. *Archives of Microbiology* **152**, 556-63 (1989).
126. Nanninga, H.J. & Gottschal, J.C. Properties of *Desulfovibrio carbinolicus* sp. nov. and other sulfate-reducing bacteria Isolated from an anaerobic-purification plant. *Applied and Environmental Microbiology* **53**, 802-9 (1987).
127. Qatibi, A.I., Niviere, V. & Garcia, J.L. *Desulfovibrio alcoholovorans* sp.nov, a sulfate-reducing bacterium able to grow on glycerol, 1,2-propanediol and 1,3-propanediol. *Archives of Microbiology* **155**, 143-8 (1991).
128. Fardeau, M.L. et al. Isolation and characterization of a thermophilic sulfate-reducing bacterium, *Desulfotomaculum thermosapovorans* sp. nov. *International Journal of Systematic Bacteriology* **45**, 218-21 (1995).
129. Goorissen, H.P., Boschker, H.T., Stams, A.J. & Hansen, T.A. Isolation of thermophilic *Desulfotomaculum* strains with methanol and sulfite from solfataric mud pools, and characterization of *Desulfotomaculum solfataricum* sp. nov. *International Journal of Systematic and Evolutionary Microbiology* **53**, 1223-9 (2003).
130. Liu, Y.T. et al. Description of two new thermophilic *Desulfotomaculum* spp., *Desulfotomaculum putei* sp. nov, from a deep terrestrial subsurface, and *Desulfotomaculum luciae* sp. nov, from a hot spring. *International Journal of Systematic Bacteriology* **47**, 615-21 (1997).
131. Nazina, T.N., Ivanova, A.E., Kanchaveli, L.P. & Rozanova, E.P. A new sporeforming thermophilic methylotrophic sulfate-reducing bacterium, *Desulfotomaculum kuznetsovii* sp. nov. *Mikrobiologiya* **57**, 823–7 (1988).
132. Tebo, B.M. & Obraztsova, A.Y. Sulfate-reducing bacterium grows with Cr(VI), U(VI), Mn(IV), and Fe(III) as electron acceptors. *Fems Microbiology Letters* **162**, 193-8 (1998).
133. Balk, M. et al. Methanol utilizing *Desulfotomaculum* species utilizes hydrogen in a methanol-fed sulfate-reducing bioreactor. *Applied Microbiology and Biotechnology* **73**, 1203-11 (2007).
134. Pester, M. et al. Complete genome sequences of *Desulfosporosinus orientis* DSM765T, *Desulfosporosinus youngiae* DSM17734T, *Desulfosporosinus meridiei* DSM13257T, and *Desulfosporosinus acidiphilus* DSM22704T. *Journal of Bacteriology* **194**, 6300-1 (2012).
135. Junier, P. et al. The genome of the Gram-positive metal- and sulfate-reducing bacterium *Desulfotomaculum reducens* strain MI-1. *Environmental Microbiology* **12**, 2738-54 (2010).
136. Burke, S.A. & Krzycki, J.A. Reconstitution of monomethylamine:Coenzyme M methyl transfer with a corrinoid protein and two methyltransferases purified from *Methanosarcina barkeri*. *The Journal of Biological Chemistry* **272**, 16570-7 (1997).
137. Burke, S.A., Lo, S.L. & Krzycki, J.A. Clustered genes encoding the methyltransferases of methanogenesis from monomethylamine. *Journal of Bacteriology* **180**, 3432-40 (1998).
138. Ferguson, D.J., Jr., Gorlatova, N., Grahame, D.A. & Krzycki, J.A. Reconstitution of dimethylamine:coenzyme M methyl transfer with a discrete corrinoid protein and two methyltransferases purified from *Methanosarcina barkeri*. *The Journal of Biological Chemistry* **275**, 29053-60 (2000).
139. Wassenaar, R.W., Keltjens, J.T., van der Drift, C. & Vogels, G.D. Purification and characterization of dimethylamine:5-hydroxybenzimidazolyl-cobamide methyltransferase from *Methanosarcina barkeri* Fusaro. *European Journal of Biochemistry / FEBS* **253**, 692-7 (1998).
140. Paul, L., Ferguson, D.J., Jr. & Krzycki, J.A. The trimethylamine methyltransferase gene and multiple dimethylamine methyltransferase genes of *Methanosarcina barkeri* contain in-frame and read-through amber codons. *Journal of Biotechnology* **182**, 2520-9 (2000).
141. Ferguson, D.J., Jr., Krzycki, J.A. & Grahame, D.A. Specific roles of methylcobamide:coenzyme M methyltransferase

isozymes in metabolism of methanol and methylamines in *Methanosarcina barkeri*. *The Journal of Biological Chemistry* **271**, 5189-94 (1996).

142. Kratzer, C., Carini, P., Hovey, R. & Deppenmeier, U. Transcriptional profiling of methyltransferase genes during growth of *Methanosarcina mazei* on trimethylamine. *Journal of Bacteriology* **191**, 5108-15 (2009).
143. Anantharam, V., Allison, M.J. & Maloney, P.C. Oxalate:formate exchange. The basis for energy coupling in *Oxalobacter*. *The Journal of Biological Chemistry* **264**, 7244-50 (1989).
144. Miller, T.L. & Wolin, M.J. Formation of hydrogen and formate by *Ruminococcus albus*. *Journal of Bacteriology* **116**, 836-46 (1973).
145. Palframan, R.J., Gibson, G.R. & Rastall, R.A. Carbohydrate preferences of *Bifidobacterium* species isolated from the human gut. *Current Issues in Intestinal Microbiology* **4**, 71-5 (2003).
146. Starrenburg, M.J. & Hugenholtz, J. Citrate fermentation by *Lactococcus* and *Leuconostoc* spp. *Applied and Environmental Microbiology* **57**, 3535-40 (1991).
147. Ferry, J.G. Formate dehydrogenase. *FEMS Microbiol Rev* **7**, 377-82 (1990).
148. Jormakka, M., Byrne, B. & Iwata, S. Formate dehydrogenase-a versatile enzyme in changing environments. *Current Opinion in Structural Biology* **13**, 418-23 (2003).
149. Thiele, J.H. & Zeikus, J.G. Control of interspecies electron flow during anaerobic digestion: significance of formate transfer versus hydrogen transfer during syntrophic methanogenesis in flocs. *Applied and Environmental Microbiology* **54**, 20-9 (1988).
150. Boone, D.R., Johnson, R.L. & Liu, Y. Diffusion of the interspecies electron carriers $H(_2)$ and formate in methanogenic ecosystems and its implications in the measurement of $K(_m)$ for $H(_2)$ or formate uptake. *Applied and Environmental Microbiology* **55**, 1735-41 (1989).
151. de Bok, F.A. et al. Two W-containing formate dehydrogenases (CO_2-reductases) involved in syntrophic propionate oxidation by *Syntrophobacter fumaroxidans*. *European Journal of Biochemistry / FEBS* **270**, 2476-85 (2003).
152. Dong, X., Plugge, C.M. & Stams, A.J. Anaerobic degradation of propionate by a mesophilic acetogenic bacterium in coculture and triculture with different methanogens. *Appl Environ Microbiol* **60**, 2834-8 (1994).
153. Dong, X. & Stams, A.J. Evidence for H_2 and formate formation during syntrophic butyrate and propionate degradation. *Anaerobe* **1**, 35-9 (1995).
154. Kosaka, T. et al. The genome of *Pelotomaculum thermopropionicum* reveals niche-associated evolution in anaerobic microbiota. *Genome Research* **18**, 442-8 (2008).
155. Worm, P., Stams, A.J., Cheng, X. & Plugge, C.M. Growth- and substrate-dependent transcription of formate dehydrogenase and hydrogenase coding genes in *Syntrophobacter fumaroxidans* and *Methanospirillum hungatei*. *Microbiology* **157**, 280-9 (2011).
156. Stams, A.J. & Plugge, C.M. Electron transfer in syntrophic communities of anaerobic bacteria and archaea. *Nature Reviews Microbiology* **7**, 568-77 (2009).
157. Ferry, J.G. & Lessner, D.J. Methanogenesis in marine sediments. *Annals of the New York Academy of Sciences* **1125**, 147-57 (2008).
158. Liu, Y. & Whitman, W.B. Metabolic, phylogenetic, and ecological diversity of the methanogenic archaea. *Annals of the New York Academy of Sciences* **1125**, 171-89 (2008).
159. de Bok, F.A., Luijten, M.L. & Stams, A.J. Biochemical evidence for formate transfer in syntrophic propionate-oxidizing cocultures of *Syntrophobacter fumaroxidans* and *Methanospirillum hungatei*. *Applied and Environmental Microbiology* **68**, 4247-52 (2002).
160. Dong, X., Plugge, C.M. & Stams, A.J. Anaerobic degradation of propionate by a mesophilic acetogenic bacterium in coculture and triculture with different methanogens. *Applied and Environmental Microbiology* **60**, 2834-8 (1994).
161. Mcinerney, M.J., Bryant, M.P., Hespell, R.B. & Costerton, J.W. *Syntrophomonas wolfei* gen.nov sp.nov, an anaerobic, syntrophic, fatty-acid oxidizing bacterium. *Applied Environmental Microbiology* **41**, 1029-39 (1981).
162. Plugge, C.M., Balk, M. & Stams, A.J.M. *Desulfotomaculum thermobenzoicum* subsp. *thermosyntrophicum* subsp. nov., a thermophilic, syntrophic, propionate-oxidizing, spore-forming bacterium. *International Journal of Systematic and*

Evolutionary Microbiology **52**, 391-9 (2002).

163. Schmidt, A., Muller, N., Schink, B. & Schleheck, D. A proteomic view at the biochemistry of syntrophic butyrate oxidation in *Syntrophomonas wolfei*. *PLoS One* **8** (2013).
164. Sieber, J.R., Le, H.M. & McInerney, M.J. The importance of hydrogen and formate transfer for syntrophic fatty, aromatic and alicyclic metabolism. *Environmental Microbiology* **16**, 177-88 (2014).
165. Friedrich, M. & Schink, B. Hydrogen formation from glycolate driven by reversed electron transport in membrane vesicles of a syntrophic glycolate-oxidizing bacterium. *European journal of biochemistry / FEBS* **217**, 233-40 (1993).
166. Wallrabenstein, C. & Schink, B. Evidence of reversed electron-transport in syntrophic butyrate or benzoate oxidation by *Syntrophomonas wolfei* and *Syntrophus buswellii*. *Archives of Microbiology* **162**, 136-42 (1994).
167. Kröger, A. et al. Fumarate respiration of *Wolinella succinogenes*: enzymology, energetics and coupling mechanism. *Biochimica et Biophysica Acta* **1553**, 23-38 (2002).
168. McInerney, M.J., Sieber, J.R. & Gunsalus, R.P. Syntrophy in anaerobic global carbon cycles. *Current opinion in biotechnology* **20**, 623-32 (2009).
169. Van Kuijk, B.L.M., Schlosser, E. & Stams, A.J.M. Investigation of the fumarate metabolism of the syntrophic propionate-oxidizing bacterium strain MPOB. *Archives of Microbiology* **169**, 346-52 (1998).
170. Schmehl, M. et al. Identification of a new class of nitrogen fixation genes in *Rhodobacter capsulatus*: a putative membrane complex involved in electron transport to nitrogenase. *Molecular & General Genetics : MGG* **241**, 602-15 (1993).
171. Boiangiu, C.D. et al. Sodium ion pumps and hydrogen production in glutamate fermenting anaerobic bacteria. *Journal of Molecular Microbiology and Biotechnology* **10**, 105-19 (2005).
172. Bruggemann, H. et al. The genome sequence of *Clostridium tetani*, the causative agent of tetanus disease. *Proceedings of the National Academy of Sciences of the United States of America* **100**, 1316-21 (2003).
173. Curatti, L., Brown, C.S., Ludden, P.W. & Rubio, L.M. Genes required for rapid expression of nitrogenase activity in *Azotobacter vinelandii*. *Proceedings of the National Academy of Sciences of the United States of America* **102**, 6291-6 (2005).
174. Imkamp, F., Biegel, E., Jayamani, E., Buckel, W. & Muller, V. Dissection of the caffeate respiratory chain in the acetogen *Acetobacterium woodii*: identification of an Rnf-type NADH dehydrogenase as a potential coupling site. *Journal of Bacteriology* **189**, 8145-53 (2007).
175. Li, F. et al. Coupled ferredoxin and crotonyl coenzyme A (CoA) reduction with NADH catalyzed by the butyryl-CoA dehydrogenase/Etf complex from *Clostridium kluyveri*. *Journal of Bacteriology* **190**, 843-50 (2008).
176. McInerney, M.J. et al. The genome of *Syntrophus aciditrophicus*: life at the thermodynamic limit of microbial growth. *Proceedings of the National Academy of Sciences of the United States of America* **104**, 7600-5 (2007).
177. Muller, N., Worm, P., Schink, B., Stams, A.J. & Plugge, C.M. Syntrophic butyrate and propionate oxidation processes: from genomes to reaction mechanisms. *Environ Microbiol Rep* **2**, 489-99 (2010).
178. Kube, M. et al. Analysis of the complete genomes of *Acholeplasma brassicae*, *A. palmae* and *A. laidlawii* and their comparison to the obligate parasites from '*Candidatus Phytoplasma*'. *Journal of Molecular Microbiology and Biotechnology* **24**, 19-36 (2014).
179. Li, Q. et al. Electron transport in the pathway of acetate conversion to methane in the marine archaeon *Methanosarcina acetivorans*. *Journal of Bacteriology* **188**, 702-10 (2006).
180. Sorokin, D.Y. et al. Genome analysis of *Chitinivibrio alkaliphilus* gen. nov., sp. nov., a novel extremely haloalkaliphilic anaerobic chitinolytic bacterium from the candidate phylum Termite Group 3. *Environmental Microbiology* **16**, 1549-65 (2014).
181. Kopke, M. et al. *Clostridium ljungdahlii* represents a microbial production platform based on syngas. *Proceedings of the National Academy of Sciences of the United States of America* **107**, 13087-92 (2010).
182. Biegel, E., Schmidt, S. & Muller, V. Genetic, immunological and biochemical evidence for a Rnf complex in the acetogen *Acetobacterium woodii*. *Environmental Microbiology* **11**, 1438-43 (2009).
183. Hess, V., Schuchmann, K. & Muller, V. The ferredoxin:NAD+ oxidoreductase (Rnf) from the acetogen *Acetobacterium*

woodii requires Na+ and is reversibly coupled to the membrane potential. *The Journal of Biological Chemistry* **288**, 31496-502 (2013).

184. Tremblay, P.L., Zhang, T., Dar, S.A., Leang, C. & Lovley, D.R. The Rnf complex of *Clostridium ljungdahlii* is a proton-translocating ferredoxin:NAD+ oxidoreductase essential for autotrophic growth. *MBio* **4**, e00406-12 (2012).
185. Sieber, J.R., McInerney, M.J. & Gunsalus, R.P. Genomic insights into syntrophy: The paradigm for anaerobic metabolic cooperation. *Annual Review of Microbiology* **66**, 429-52 (2012).
186. Meyer, B. et al. The energy-conserving electron transfer system used by *Desulfovibrio alaskensis* strain G20 during pyruvate fermentation involves reduction of endogenously formed fumarate and cytoplasmic and membrane-bound complexes, Hdr-Flox and Rnf. *Environmental Microbiology* (2014).
187. Schut, G.J. & Adams, M.W. The iron-hydrogenase of *Thermotoga maritima* utilizes ferredoxin and NADH synergistically: a new perspective on anaerobic hydrogen production. *Journal of Bacteriology* **191**, 4451-7 (2009).
188. Schuchmann, K. & Muller, V. A bacterial electron-bifurcating hydrogenase. *The Journal of Biological Chemistry* **287**, 31165-71 (2012).
189. Wang, S., Huang, H., Kahnt, J. & Thauer, R.K. *Clostridium acidurici* electron-bifurcating formate dehydrogenase. *Applied and Environmental Microbiology* **79**, 6176-9 (2013).
190. Beal, E.J., House, C.H. & Orphan, V.J. Manganese- and iron-dependent marine methane oxidation. *Science* **325**, 184-7 (2009).
191. Haroon, M.F. et al. Anaerobic oxidation of methane coupled to nitrate reduction in a novel archaeal lineage. *Nature* **500**, 567-70 (2013).
192. Thauer, R.K. Anaerobic oxidation of methane with sulfate: on the reversibility of the reactions that are catalyzed by enzymes also involved in methanogenesis from CO2. *Current Opinion in Microbiology* **14**, 292-9 (2011).
193. Hu, S., Zeng, R.J., Keller, J., Lant, P.A. & Yuan, Z. Effect of nitrate and nitrite on the selection of microorganisms in the denitrifying anaerobic methane oxidation process. *Environmental Microbiology Reports* **3**, 315-9 (2011).
194. Lloyd, K.G., Lapham, L. & Teske, A. An anaerobic methane-oxidizing community of ANME-1b archaea in hypersaline Gulf of Mexico sediments. *Applied and Environmental Microbiology* **72**, 7218-30 (2006).
195. Orphan, V.J. et al. Comparative analysis of methane-oxidizing archaea and sulfate-reducing bacteria in anoxic marine sediments. *Applied and Environmental Microbiology* **67**, 1922-34 (2001).
196. Orphan, V.J., House, C.H., Hinrichs, K.U., McKeegan, K.D. & DeLong, E.F. Methane-consuming archaea revealed by directly coupled isotopic and phylogenetic analysis. *Science* **293**, 484-7 (2001).
197. Boetius, A. et al. A marine microbial consortium apparently mediating anaerobic oxidation of methane. *Nature* **407**, 623-6 (2000).
198. Holler, T. et al. Thermophilic anaerobic oxidation of methane by marine microbial consortia. *The ISME journal* **5**, 1946-56 (2011).
199. Kleindienst, S., Ramette, A., Amann, R. & Knittel, K. Distribution and in situ abundance of sulfate-reducing bacteria in diverse marine hydrocarbon seep sediments. *Environmental Microbiology* **14**, 2689-710 (2012).
200. Knittel, K. et al. Activity, distribution, and diversity of sulfate reducers and other bacteria in sediments above gas hydrate (Cascadia margin, Oregon). *Geomicrobiology Journal* **20**, 269-94 (2003).
201. Losekann, T. et al. Diversity and abundance of aerobic and anaerobic methane oxidizers at the Haakon Mosby mud volcano, Barents Sea. *Applied Environmental Microbiology* **73**, 3348-62 (2007).
202. Michaelis, W. et al. Microbial reefs in the Black Sea fueled by anaerobic oxidation of methane. *Science* **297**, 1013-5 (2002).
203. Pernthaler, A. et al. Diverse syntrophic partnerships from deep-sea methane vents revealed by direct cell capture and metagenomics. *Proceedings of the National Academy of Sciences of the United States of America* **105**, 7052-7 (2008).
204. Schreiber, L., Holler, T., Knittel, K., Meyerdierks, A. & Amann, R. Identification of the dominant sulfate-reducing bacterial partner of anaerobic methanotrophs of the ANME-2 clade. *Environ Microbiol* **12**, 2327-40 (2010).
205. Dolfing, J., Jiang, B., Henstra, A.M., Stams, A.J. & Plugge, C.M. Syntrophic growth on formate: a new microbial niche in anoxic environments. *Applied and Environmental Microbiology* **74**, 6126-31 (2008).

206. Jiang, B. et al. Atypical one-carbon metabolism of an acetogenic and hydrogenogenic *Moorella thermoacetica* strain AMP. *Archives of Microbiology* **191**, 123-31 (2009).
207. Williams P.A., Coates L., Mohammed F., Gill R., Erskine P.T., Coker A., Wood S.P., Anthony C., Cooper J.B. The atomic resolution structure of methanol dehydrogenase from *Methylobacterium extorquens*. *Acta Crystallographica Section D: Biological Crystallography* **61**, 75–9 (2005).
208. Xia Z.X., Dai W.W., He Y.N., White S.A., Mathews F.S., Davidson V.L. X-ray structure of methanol dehydrogenase from *Paracoccus denitrificans* and molecular modeling of its interactions with cytochromec-551i. *Journal of Biological Inorganic Chemestry* **8**(8), 843–54 (2003).
209. Nojiri M., Hira D., Yamaguchi K., Okajima T., Tanizawa K., Suzuki S. Crystal structures of cytochrome c_L and methanol dehydrogenase from *Hyphomicrobium denitrificans*: structural and mechanistic insights into interactions between the two proteins. *Biochemistry* **45**(11), 3481–92 (2006).
210. Choi J.M., Kim H.G., Kim J.S., Youn H.S., Eom S.H., Yu S.L., Kim S.W., Lee S.H. Purification, crystallization and preliminary X-ray crystallographic analysis of a methanol dehydrogenase from the marine bacterium *Methylophaga aminisulfidivorans* MP(T). *Acta Crystallographica Section F: Structural Biology Communications* **67**, 513–6 (2011).
211. Pol A., Barends T.R.M., Dietl A., Khadem A.F., Eygensteyn J., Jetten M.S.M., Op den Camp H.J.M. Rare earth metals are essential for methanotrophic life in volcanic mudpots. *Environmental Microbiology* **16**, 255–264 (2014).
212. Keltjens, J.T., Pol, A., Reimann, J., Op den Camp, H.J.M. PPQ-dependent methanol dehydrogenase: rare-earth elements make a difference. *Applied Microbiology and Biotechnology* **98**, 6163-81 (2014).
213. Bhatt, P., Kumar, M. S., Mudliar, S., and Chakrabarti, T.: Enhanced biodegradation of hexachlorocyclohexane in upflow anaerobic sludge blanket reactor using methanol as an electron donor. *Bioresource Technology* **99**, 2594-2602 (2008)
214. Middeldorp, P.J., van Doesburg, W., Schraa, G., Stams, A.J.M. Reductive dechlorination of hexachlorocyclohexane (HCH) isomers in soil under anaerobic conditions. *Biodegradation* **16**(3),283-90 (2005).
215. Bhatt, P., Kumar, M.S., Mudliar, S., Chakrabarti, T. Enhanced biodegradation of hexachlorocyclohexane in upflow anaerobic sludge blanket reactor using methanol as an electron donor. *Bioresource Technology* **99**(7), 2594-602 (2007)
216. Liamleam, W., Annachhatre, A.P. Electron donors for biological sulfate reduction *Biotechnology Advances* **25** (5), 452–63 (2007).
217. Knappe, J., Sawers G. A radical-chemical route to acetyl-CoA: the anaerobically induced pyruvate formate-lyase system of *Escherichia coli*. *FEMS Microbiology Review* **6**(4), 383-98 (1990).
218. Bagramyan, K., Trchounian, A. Structural and functional features of formate hydrogen lyase, an enzyme of mixed-acid fermentation from *Escherichia coli*. *Biochemistry (Moscow)* **68**(11), 1159-70 (2003).

Chapter 2

Genome analyses of the carboxydotrophic sulfate-reducers *Desulfotomaculum nigrificans* and *Desulfotomaculum carboxydivorans* and reclassification of *Desulfotomaculum carboxydivorans* as a later synonym of *Desulfotomaculum nigrificans*

Michael Visser, Sofiya N. Parshina, Joana I. Alves, Diana Z. Sousa, Inês A. C. Pereira, Gerard Muyzer, Jan Kuever, Alexander V. Lebedinsky, Jasper J. Koehorst, Petra Worm, Caroline M. Plugge, Peter J. Schaap, Lynne A. Goodwin, Alla Lapidus, Nikos C. Kyrpides, Janine C. Detter, Tanja Woyke, Patrick Chain, Karen W. Davenport, Stefan Spring, Manfred Rohde, Hans Peter Klenk, Alfons J.M. Stams

Standards in Genomic Sciences (2014) 9:655-675

2.1 Abstract

Desulfotomaculum nigrificans and *D. carboxydivorans* are moderately thermophilic members of the polyphyletic spore-forming genus *Desulfotomaculum* in the family *Peptococcaceae*. They are phylogenetically very closely related and belong to 'subgroup a' of the *Desulfotomaculum* cluster 1. *D. nigrificans* and *D. carboxydivorans* have a similar growth substrate spectrum; they can grow with glucose and fructose as electron donors in the presence of sulfate. Additionally, both species are able to ferment fructose, although fermentation of glucose is only reported for *D. carboxydivorans*. *D. nigrificans* is able to grow with 20% carbon monoxide (CO) coupled to sulfate reduction, while D. carboxydivorans can grow at 100% CO with and without sulfate. Hydrogen is produced during growth with CO by *D. carboxydivorans*. Here we present a summary of the features of *D. nigrificans* and *D. carboxydivorans* together with the description of the complete genome sequencing and annotation of both strains. Moreover, we compared the genomes of both strains to reveal their differences. This comparison led us to propose a reclassification of *D. carboxydivorans* as a later heterotypic synonym of *D. nigrificans*.

2.2 Introduction

In 1965, the genus *Desulfotomaculum* was created for sulfate-reducing bacteria that form heat-resistant spores [1]. One of the first species that was included in this new genus was *D. nigrificans* Delft 74, which was originally described as "*Clostridium nigrificans*" by Werkman and Weaver (1927) [2]. Later, Starkey (1938) renamed it to "Sporovibrio desulfuricans" [3] before it was finally renamed as D. nigrificans [1]. *D. nigrificans* is a moderate thermophile that typically grows with fructose and glucose coupled to sulfate reduction [1-4]; without sulfate, only growth with fructose was observed. Utilizing sugars is rare among *Desulfotomaculum* species. Additionally, *D. nigrificans* was described to be able to grow with a number of other substrates including lactate, ethanol, alanine, formate, and carbon monoxide (20%) coupled to sulfate reduction [5, 6].

Another moderately thermophilic *Desulfotomaculum* species that can grow with glucose and CO is *D. carboxydivorans* CO-1-SRB [6]. *D. carboxydivorans* was isolated from sludge in an anaerobic bioreactor treating paper mill wastewater [6] and was described to be the first sulfate-reducing bacterium able to grow at 100% CO. *D. carboxydivorans* converted CO in the presence and absence of sulfate and produced hydrogen during CO conversion. *D. carboxydivorans* can also grow with glucose. In contrast to *D. nigrificans*, *D. carboxydivorans* degrades glucose both with and without sulfate.

Phylogenetically, *D. carboxydivorans* is most closely related to *D. nigrificans*. However, *D. nigrificans* is not able to produce hydrogen from CO. Therefore, by comparing the genomes of these strains, the physiological differences might be explained. Here we present a summary of the features of *D. nigrificans* and *D. carboxydivorans*, together with the description of the complete genome sequencing and annotation of both strains. Moreover, we compared the genomes of both strains to reveal differences between these phylogenetically very closely related strains. This comparison led us to propose to that *D. carboxydivorans* is a later heterotypic synonym of *D. nigrificans*.

2.3 Classification and features

Comparison of the 16S rRNA gene sequences of *D. carboxydivorans* CO-1-SRB DSM 14880 and *D. nigrificans* DSM 574 revealed that the two bacteria are highly related (99% sequence similarity). Both strains are part of the *Desulfotomaculum* cluster 1 subgroup a, together with *D. aeronauticum*,

D. putei, *D. hydrothermale*, "*D. reducens*" and *D. ruminis* (Figure 2.1).

D. nigrificans and *D. carboxydivorans* are Gram-positive, sulfate-reducing, rod shaped bacteria with rounded ends (0.3-0.5 µm thick and 3-6 µm long [1]; 0.5-1.5 µm thick and 5-15 µm long [6], respectively (Figure 2.2 and Figure 2.3). They have a similar temperature range for growth and can both grow optimally at 55°C. Additional similarities can be found in the substrates used for growth. Both *D. nigrificans* and *D. carboxydivorans* can grow with fructose, glucose and alanine. These substrates are incompletely oxidized to acetate, coupled to sulfate reduction. Other suitable electron acceptors in addition to sulfate are thiosulfate and sulfite. Neither nitrate nor elemental sulfur are used as electron acceptors.

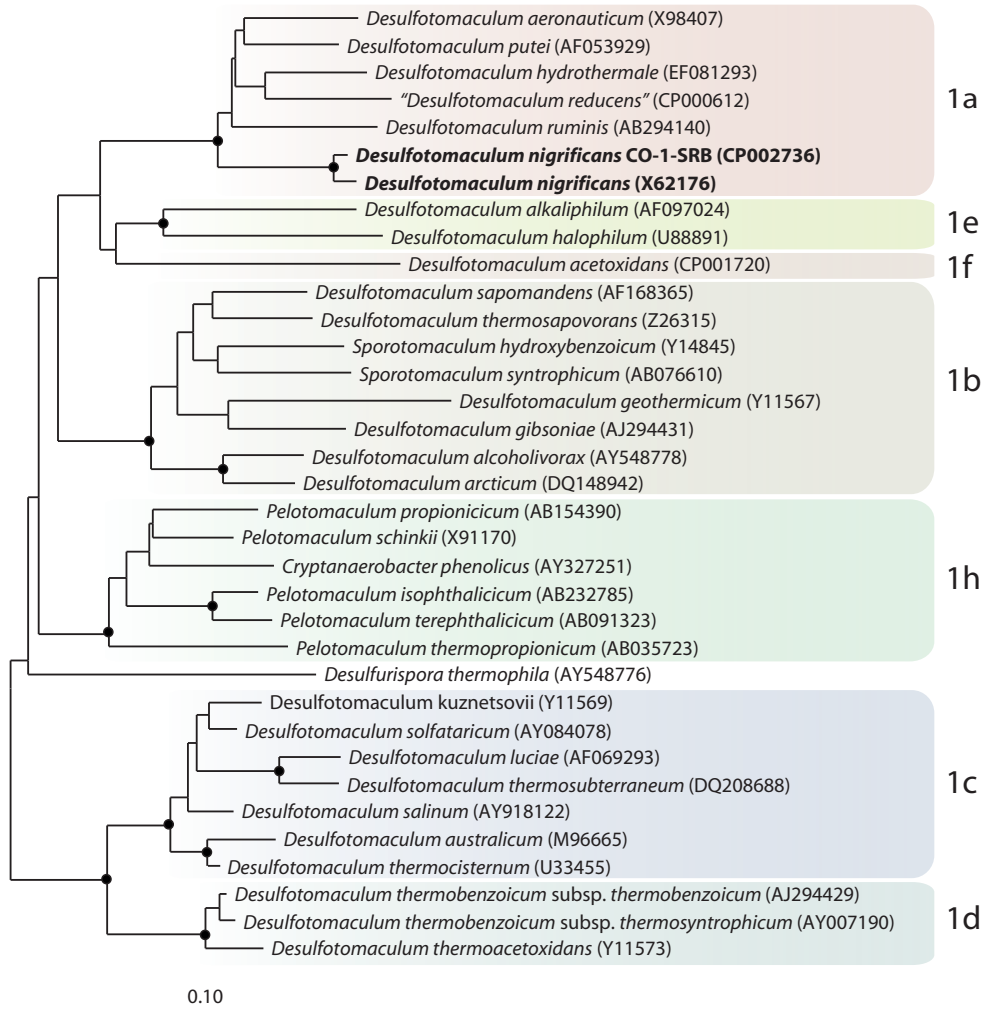

Figure 2.1: Neighbor joining tree based on 16S rRNA sequences showing the phylogenetic affiliation of Desulfotomaculum and related species divided in the subgroups of Desulfotomaculum cluster 1. DSM 574 and DSM 14880 are in bold type. The sequences of different Thermotogales were used as outgroup, but were pruned from the tree. Closed circles represent bootstrap values between 75 and 100%. The scale bar represents 10% sequence divergence.

In the absence of an electron acceptor, *D. nigrificans* is able to grow by fermentation of fructose and pyruvate [7]. Additionally, *D. nigrificans* has been reported to grow with lactate and ethanol in syntrophic interaction with *Methanobacterium thermoautotrophicum* [5]. Syntrophic growth of *D. carboxydivorans* has never been tested. *D. carboxydivorans* is able to grow in the absence of an electron acceptor with CO (100%), pyruvate, lactate, glucose and fructose [6]. The cellular fatty acid patterns of the two strains were analyzed by Parshina et al. [6] and Krishnamurthi et al. [8]. Both fatty acid patterns are similar and the dominating fatty acids were identified as 16:0, iso 15:0, iso 17:0, anteiso 15:0, 18:0 and iso 16:0. Collins and Weddel [9] analyzed the respiratory lipoquinone content of *D. nigrificans* DSM 574 and found MK7 as the predominant isoprenoid quinone. A summary of the classification and general features of *D. nigrificans* and *D. carboxydivorans* is presented in Table 2.1 and 2.2, respectively.

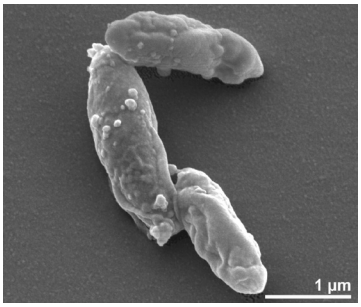

Figure 2.2: Scanning electron microscopic photograph of DSM 574

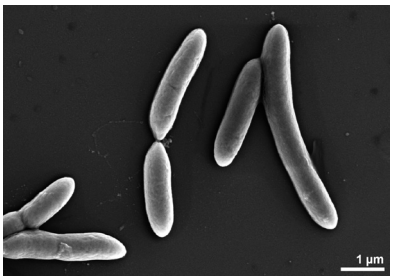

Figure 2.3: Scanning electron microscopic photograph of DSM 14880

Table 2.1: Classification and general features of D. nigrificans DSM 574 according to the MIGS recommendations [10].

MIGS ID	Property	Term	Evidence code[a]
	Current classification	Domain *Bacteria* Phylum *Firmicutes* Class *Clostridia* Order *Clostridiales* Family *Peptococcaceae* Genus *Desulfotomaculum* Species *Desulfotomaculum nigrificans* Type strain Delft 74	TAS [11] TAS [12-14] TAS [15, 16] TAS [17, 18] TAS [18, 19] TAS [1, 18] TAS [1, 18]
	Gram stain	negative, with a Gram-positive cell wall structure	
	Cell shape	rods, rounded ends, sometimes paired	TAS [1]
	Motility	Slight tumbling, peritrichous flagella	TAS [1]
	Sporulation	oval, terminal or subterminal, slightly swelling the cell	TAS [1]
	Temperature range	30-70 °C	TAS [1]
	Optimum temperature	55 °C	TAS [1]
	Carbon source	glucose and other carbohydrates	TAS [1, 4, 5]
	Energy source	heterotrophic	TAS [1, 4, 5]
	Electron acceptor	sulfate, thiosulfate and sulfite.	TAS [4]
MIGS-6	Habitat	soils, compost heaps, thermal spring water, spoiled foods.	TAS [1]
MIGS-6.3	Salinity	not reported	
MIGS-22	Oxygen	obligate anaerobic	TAS [1]
MIGS-15	Biotic relationship	free living	TAS [1]
MIGS-14	Pathogenicity	none	TAS [1]
MIGS-4	Geographic location	Delft, The Netherlands	
MIGS-5	Sample collection time		
MIGS-4.1	Latitude	52.011	
MIGS-4.2	Longitude	4.360	
MIGS-4.3	Depth	not reported	

Evidence codes - TAS: Traceable Author Statement (i.e., a direct report exists in the literature); NAS: Non-traceable Author Statement (i.e., not directly observed for the living, isolated sample, but based on a generally accepted property for the species, or anecdotal evidence). Evidence codes are from the Gene Ontology project [20].

Table 2.2: Classification and general features of D. carboxydivorans DSM 14880 according to the MIGS recommendations [10].

MIGS ID	Property	Term	Evidence code[a]
	Current classification	Domain *Bacteria* Phylum *Firmicutes* Class *Clostridia* Order *Clostridiales* Family *Peptococcaceae* Genus *Desulfotomaculum* Species *Desulfotomaculum carboxydivorans* Type strain CO-1-SRB	TAS [11] TAS [12-14] TAS [15, 16] TAS [17, 18] TAS [18, 19] TAS [18, 19] TAS [18, 19]
	Gram stain	negative, with a Gram-positive cell wall structure	TAS [6]
	Cell shape	rods, rounded ends, sometimes paired.	TAS [6]
	Motility	twisting and tumbling motion	TAS [6]
	Sporulation	oval, terminal or subterminal	TAS [6]
	Temperature range	30-68°C	TAS [6]
	Optimum temperature	55°C	TAS [6]
	Carbon source	100% CO, with and without sulfate	TAS [6]
	Energy source	hydrogenogenic and heterotrophic growth	TAS [6]
	Electron acceptor	sulfate, thiosulfate and sulfite.	TAS [6]
MIGS-6	Habitat	Paper mill waste water sludge	
MIGS-6.3	Salinity	0-17 g NaCl l^{-1}	TAS [6]
MIGS-22	Oxygen	obligate anaerobe	TAS [6]
MIGS-15	Biotic relationship	free living	TAS [6]
MIGS-14	Pathogenicity	none	
MIGS-4	Geographic location	Eerbeek, the Netherlands	TAS [6]
MIGS-5	Sample collection time	1999	TAS [6]
MIGS-4.1	Latitude	52.104217	TAS [6]
MIGS-4.2	Longitude	6.060133	TAS [6]
MIGS-4.3	Depth	not reported	

Evidence codes - TAS: Traceable Author Statement (i.e., a direct report exists in the literature); NAS: Non-traceable Author Statement (i.e., not directly observed for the living, isolated sample, but based on a generally accepted property for the species, or anecdotal evidence). Evidence codes are from the Gene Ontology project [20].

2.4 Genome sequencing and annotation

2.4.1 Genome project history

D. nigrificans and *D. carboxydivorans* were selected for sequencing in the DOE Joint Genome Institute Community Sequencing Program 2009, proposal 300132_795700 'Exploring the genetic and physiological diversity of *Desulfotomaculum* species'. They are important for their position in subgroup a of the *Desulfotomaculum* cluster 1. Sequencing the complete genome of the two strains was proposed as it would allow the study of the genetic and physiological diversity within subgroup a. Furthermore, a comparison of the two genomes should reveal the genes involved in CO metabolism and the H_2 production in *D. carboxydivorans*. The genome projects of *D. nigrificans* and *D. carboxydivorans* are listed in the Genome OnLine Database (GOLD) [21] as project Gi03933 and Gc01783, respectively. The two complete genome sequences were deposited in Genbank. Sequencing, finishing and annotation of the two genomes were performed by the DOE Joint Genome Institute (JGI). A summary of the project information of *D. nigrificans* and *D. carboxydivorans* is shown in Table 2.3.

2.4.2 Growth conditions and DNA isolation

D. nigrificans and *D. carboxydivorans* were grown anaerobically at 55°C in bicarbonate buffered medium with lactate and sulfate as substrates [6]. DNA of cell pellets was isolated using the standard DOE-JGI CTAB method recommended by the DOE Joint Genome Institute (JGI, Walnut Creek, CA, USA). Cells were resuspended in TE (10 mM tris; 1 mM EDTA, pH 8.0). Subsequently, cells were lysed using lysozyme and proteinase K, and DNA was extracted and purified using CTAB and phenol:chloroform:isoamylalcohol extractions. After precipitation in 2-propanol and washing in 70% ethanol, the DNA was resuspended in TE containing RNase. Following a quality and quantity check using agarose gel electrophoresis in the presence of ethidium bromide, and spectrophotometric measurement using a NanoDrop ND-1000 spectrophotometer (NanoDrop® Technologies, Wilmington, DE, USA).

Table 2.3: Genome sequencing project information of DSM 574 and DSM 14880.

MIGS ID	Property	**Term** (for DSM 574)	**Term** (for DSM 14880)
MIGS-31	Finishing quality	Permanent draft	Finished
MIGS-28	Libraries used	Three genomic libraries: 454 standard library, 454 PE libraries (7kb insert size), one Illumina library	Four genomic libraries: one 454 pyrosequence standard library, two 454 PE libraries (4kb and 11 kb insert size), one Illumina library
MIGS-29	Sequencing platforms	Illumina GAii, 454 GS FLX Titanium	Illumina GAii, 454 GS FLX Titanium
MIGS-31.2	Fold coverage	462.8 × Illumina; 35.2 × pyrosequence	116.8 × Illumina; 50.6 × pyrosequence
MIGS-30	Assemblers	Newbler version 2.3-PreRelease-June 30,2009, VELVET version 1.0.13, phrap version SPS - 4.24	Newbler version 2.3-PreRelease-June 30, 2009, VELVET version 1.0.13, phrap version SPS - 4.24

MIGS-32	Gene calling method	Prodigal 1.4, GenePRIMP	Prodigal 1.4, GenePRIMP
	INSDC ID	AEVP00000000	CP002736.1
	Genome Database release	December 10, 2010	August 13, 2012
	Genbank Date of Release	February 17, 2011	May 23, 2011
MIGS-13	GOLD ID NCBI project ID Source material identifier	Gi03933 46699 DSM 574^T	Gc01783 50757 DSM 14880^T
	Project relevance	Obtain insight into the phylogenetic and physiological diversity of *Desulfotomaculum* species.	Obtain insight into the phylogenetic and physiological diversity of *Desulfotomaculum* species, and hydrogenogenic CO conversion.

2.5 Genome sequencing and assembly

The genome of *D nigrificans* strain Delft 74 (DSM 574) was sequenced using a combination of Illumina and 454 sequencing platforms. All general aspects of library construction and sequencing can be found at the JGI website [22]. Pyrosequencing reads were assembled using the Newbler assembler (Roche). The initial Newbler assembly consisting of 75 contigs in two scaffolds was converted into a phrap [23] assembly by making fake reads from the consensus, to collect the read pairs in the 454 paired end library. Illumina GAii sequencing data (3,053.3 Mb) was assembled with Velvet [24] and the consensus sequences were shredded into 1.5 kb overlapped fake reads and assembled together with the 454 data. The 454 draft assembly was based on 127.9 Mb 454 draft data and all of the 454 paired end data. Newbler parameters are -consed -a 50 -l 350 -g -m -ml 21. The Phred/Phrap/Consed software package [23] was used for sequence assembly and quality assessment in the subsequent finishing process. After the shotgun stage, reads were assembled with parallel phrap (High Performance Software, LLC). Whenever possible mis-assemblies were corrected with gapResolution [22], Dupfinisher [25], or sequencing cloned bridging PCR fragments with subcloning. Some gaps between contigs were closed by editing in Consed, by PCR and by Bubble PCR primer walks (J.-F. Chang, unpublished). Some miss-assembly is still possible in the current assembly that consists in seven contigs and one scaffold. A total of 268 additional reactions and one shatter library were necessary to close gaps and to raise the quality of the final contigs. Illumina reads were also used to correct potential base errors and increase consensus quality using a software Polisher developed at JGI [26]. The error rate of the final genome sequence is less than 1 in 100,000. Together, the combination of the Illumina and 454 sequencing platforms provided 498.0× coverage of the genome. The final assembly contained 332,256 pyrosequence and 37,872,777 Illumina reads.

The same protocol applied to the *D. carboxydivorans* strain CO-1-SRB (DSM 14880) genome allowed to produce finished assembly without gaps. Illumina GAii sequencing data (334.0Mb) was assembled with Velvet 0.7.63 and the 454 draft assembly was based on 138.8 MB of sequence.

A total of 290 additional reactions were necessary to close some gaps and to raise the quality of the final contigs. Illumina reads were also used to correct potential base errors and increase consensus quality using a software Polisher developed at JGI [26]. The error rate of the final genome sequence is less than 1 in 100,000. Together, the combination of the Illumina and 454 sequencing platforms provided 167.4× coverage of the genome. The final assembly contained 543,495 pyrosequence and 9,254,176 Illumina reads

2.6 Genome annotation

Genes were identified using Prodigal [27] as part of the DOE-JGI genome annotation pipeline [28], followed by a round of manual curation using the JGI GenePRIMP pipeline [29]. The predicted CDSs were translated and used to search the National Center for Biotechnology Information (NCBI) nonredundant database, UniProt, TIGR-Fam, Pfam, PRIAM, KEGG, COG, and InterPro databases. Additional gene prediction analysis and functional annotation was performed within the Integrated Microbial Genomes - Expert Review (IMG-ER) platform [30].

Table 2.4: Genome statistics of DSM 574 (A) and DSM 14880 (B).

Attribute	A. Genome (total)		B. Genome (total)	
	Value	% of total	Value	% of total
Genome size (bp)	3,052,787	100	2,892,255	100.00
DNA coding region (bp)	2,595,629	85.02	2457154	84.96
DNA G+C content (bp)	1,412,511	46.28	1,348,537	46.63
Total genes	3,112	100	2,844	100
RNA genes	98	3.15	97	3.41
Protein-coding genes	3,014	96.85	2,747	96.59
Genes in paralog clusters	1,542	49.55	1,363	47.93
Genes assigned to COGs	2,340	75.19	2,174	76.44
Pseudo genes	137	4.40	88	3.09
Genes with signal peptides	582	18.70	504	17.72
Genes with transmembrane helices	721	23.17	647	22.75

2.7 Genome properties

The genome of *D. nigrificans* and *D. carboxydivorans* consists of one chromosome of 3,052,787 and 2,892,255 nucleotides with a GC content of 46.28 and 46.63%, respectively (Table 2.4). Of the 3,112 genes in the genome of *D. nigrificans*, 98 are RNA genes of which 6 16S rRNA genes. A total of 2,340 genes of the 3,014 protein coding genes are assigned to COG functional categories. The distribution of these genes into COG functional categories is presented in Table 2.5. The distribution of the 2,174 COG assigned genes of *D. carboxydivorans* into COG functional categories is also presented in Table 2.5. Of the 2,844 predicted genes in the *D. carboxydivorans* genome, 2,747 are protein coding genes and 97 RNA genes, of which 8 are 16S rRNA genes. Both strains have sets of multiple 16S rRNA genes. Within the sets and among the sets most of the genes are 99.5-99.9% identical. Each strain has one differently deviating 16S rRNA gene, the

difference probably originating from differential gene loss. In addition, 3.09% of the total genes of *D. carboxydivorans* are identified as pseudo genes. More genome statistics of *D. nigrificans* and *D. carboxydivorans* are displayed in Table 2.4.

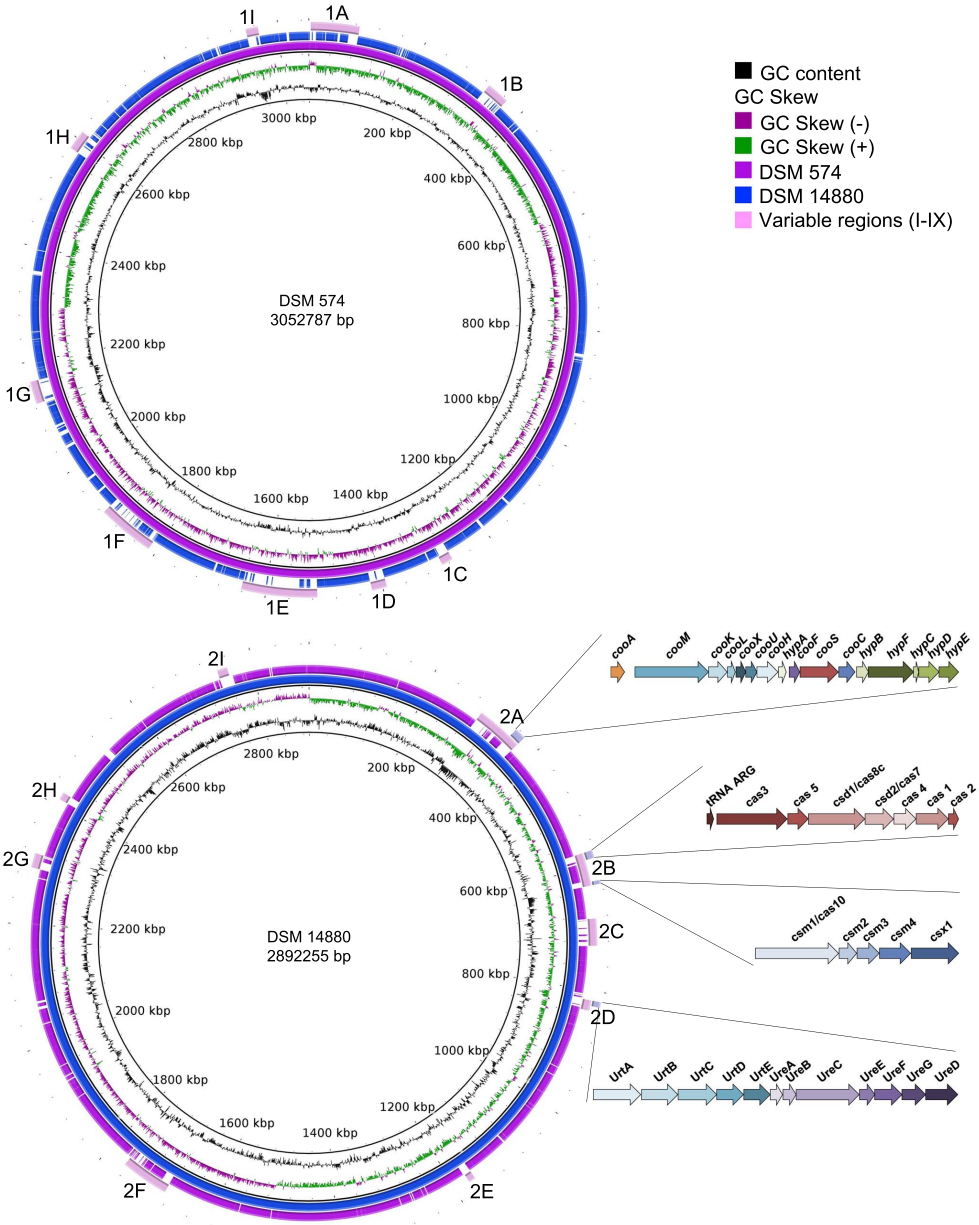

Figure 2.4: Graphical map of the DSM 574 (upper) and DSM 14880 (lower) chromosome. In both maps one genome was compared to the other. When genes were not similar or present in the other genome it resulted in gaps. The indicated variable regions with their function can also be found in Table 6 and the supplementary data S1.

Table 2.5: Number of DSM 574 and DSM 14880 genes associated with the general COG functional categories.

Code	Description	DSM 574		DSM 14880	
		Value	%age[a]	Value	%age[a]
J	Translation	153	5.97	152	3.39
A	RNA processing and modification	1	0.04	0	0.00
K	Transcription	153	5.97	139	5.85
L	Replication, recombination and repair	210	8.20	172	7.23
B	Chromatin structure and dynamics	1	0.04	1	0.04
D	Cell cycle control, mitosis and meiosis	45	1.76	45	1.89
Y	Nuclear structure	0	0.00	0	0.00
V	Defense mechanisms	22	0.86	22	0.93
T	Signal transduction mechanisms	171	6.71	148	6.22
M	Cell wall/membrane biogenesis	132	5.15	126	5.3
N	Cell motility	70	2.73	68	2.86
Z	Cytoskeleton	0	0.00	0	0.00
W	Extracellular structures	0	0.00	0	0.00
U	Intracellular trafficking and secretion	65	2.54	64	2.69
O	Posttranslational modification, protein turnover, chaperones	83	3.24	85	3.57
C	Energy production and conversion	217	8.47	211	8.87
G	Carbohydrate transport and metabolism	125	4.88	98	4.12
E	Amino acid transport and metabolism	224	8.74	216	9.08
F	Nucleotide transport and metabolism	62	2.42	60	2.52
H	Coenzyme transport and metabolism	134	5.23	133	5.59
I	Lipid transport and metabolism	40	1.56	36	1.51
P	Inorganic ion transport and metabolism	104	4.06	101	4.25
Q	Secondary metabolites biosynthesis, transport and catabolism	29	1.13	27	1.14
R	General function prediction only	261	10.19	250	10.51
S	Function unknown	241	9.41	224	9.42
-	Not in COGs	772	24.81	670	23.56

a) The total is based on the total number of protein coding genes in the annotated genome.

Table 2.6: Description of genes present in the variable regions depicted in Figure 2.4.

Variable region	Functions
1A	Transposases, recombinases, transport proteins, isomerases, histidine kinase and threonine dehydrogenase
1B	Transposases, recombinases, resolvase and alcohol dehydrogenase
1C	Helicases, DNA-methylation, endonuclease and recombinase
1D	TRAP transporter, Threonine dehydrogenase, 2 keto-4-petnenoate hydratase, sugar kinase, aldolase, glycerol dehydrogenase and mannonate dehydratase
1E	Pilus assembly, proteases and hypothetical proteins dominate this variable region
1F	Protease, DNA methylase, RNA polymerase, recombinase, cytochrome c biogenesis, Fe^{2+} transport system and many hypothetical proteins
1G	Transposase, secretory protein secB, nucleotide sugar dehydrogenase, glycosyltransferase, sugar epimerase, O-antigen ligase and copper amine oxidase
1H	Pyruvate ferredoxin oxidoreductase, transport proteins, sugar phosphate permease, threonine dehydrogenase, transposase, DNA methylase and endonuclease
1I	Growth inhibitor protein, terminase, phage portal protein, secretory protein, recombinase and many hypothetical proteins
2A	Endonuclease, DNA methylase, transposase, ATP binding protein, ATPase, threonine kinase, pyridoxamine 5'phosphate oxidase, ferric reductase, many hypothetical proteins and the CODH-ECH complex
2B	CRISPR-Cas
2C	DNA-helicases, -methyltransferase, and -replication protein, restriction protein and many hypothetical proteins
2D	Urea metabolism
2E	Mainly transport proteins and agmatinase
2F	Alpha ribazole phosphatase, metal dependent phosphohydrolase, phenylacetate-CoA ligase, methyltransferase, amine oxidase, aldehyde dehydrogenase, transposase, phage tail component and many hypothetical proteins
2G	Pilus associated proteins
2H	Recombinase, integrase, AAA ATPase, restriction modification system, deoxyribonuclease
2I	Many transferase proteins

2.8 Insights into the genomes

2.8.1 Incomplete oxidation of organic compounds

D. nigrificans and *D. carboxydivorans* oxidize organic substrates such as lactate, pyruvate, ethanol and sugars incompletely to acetate. Both genomes have gene copies that are predicted to encode L-lactate dehydrogenases (DesniDRAFT_1264, 2906; Desca_0533) and D-lactate dehydrogenase (DesniDRAFT_0054, 1145, 1691; Desca_0863, 2222), which are involved in the oxidation of lactate to pyruvate. For incomplete oxidation of pyruvate to acetate via acetyl-CoA *D. nigrificans* and *D. carboxydivorans* have genes encoding a putative pyruvate dehydrogenase (DesniDRAFT_1250, 2504, 1245 and Desca_0770, 0146, 0775, respectively) and subsequently an acetyl-CoA synthetase (DesniDRAFT_2242 and Desca_0484, respectively). Although the two strains cannot grow with succinate, fumarate and malate as electron donors, genes to metabolize these compounds are present in both genomes. *D. nigrificans* and *D. carboxydivorans* have genes putatively coding for a fumarate reductase (DesniDRAFT_0617-15 and Desca_1387-89), fumarate hydratase (DesniDRAFT_0612-13 and Desca_1391-92), malate dehydrogenase (DesniDRAFT_0618 and Desca_1386), and a pyruvate carboxylase (DesniDRAFT_1477-78 and Desca_2116-17) that might be involved in the oxidation of succinate, fumarate and malate to pyruvate. For growth on ethanol, both genomes contain alcohol dehydrogenases (DesniDRAFT_0051, 0320, 0326, 0367, 1219, 2126, 2174, 2779; Desca_0375, 0418, 1671, 1913, 1943, 2553, 2558) and acetaldehyde dehydrogenases (DesniDRAFT_0038; Desca_1928).

For sulfate reducers to oxidize acetate to CO_2, either the complete tricarboxylic acid (TCA) cycle or acetyl-CoA pathway has to be present [31]. Since *D. nigrificans* and *D. carboxydivorans* cannot grow with acetate, it was expected neither strain would possess a complete TCA cycle; which was verified by a lack of the putative genes that code for ATP-dependent citrate synthase, aconitase, and isocitrate dehydrogenase. All genes coding for the acetyl-CoA pathway are present in both genomes, except for the genes encoding the acetyl-CoA synthase subunit and the FeS-protein large and small subunit. Probably the gene coding for the acetyl-CoA synthetase is also involved in the acetyl-CoA production from acetate and coenzyme A.

2.8.2 Sugar metabolism

D. nigrificans and *D. carboxydivorans* are able to utilize glucose and fructose as electron donors in the presence of sulfate. Additionally, both species are able to ferment fructose, although fermentation of glucose is only reported for *D. carboxydivorans* [5,6]. The capability of utilizing sugars for growth is unusual among *Desulfotomaculum* species. The other *Desulfotomaculum* species that belong to cluster I, sub group a, *D. ruminis*, *D. aeronauticum*, *D. putei* and *D. hydrothermale* (with the exception of "*D. reducens*"), are not able to grow with glucose or fructose [32-34]. Glucose metabolism in *D. nigrificans* was studied before [4]. Akagi and Jackson showed that the majority of the glucose was degraded by the Embden-Meyerhof-Parnas pathway and in several instances the glucose followed the Entner-Doudoroff pathway [4]. The Embden-Meyerhof-Parnas pathway and the pentose phosphate pathway are predicted to be complete in the genome of *D. nigrificans* and *D. carboxydivorans*. However, genes coding for the 6-phosphogluconate dehydratase and the 2-keto-3-deoxy-6-phosphogluconate aldolase, the two characteristic enzymes of the Entner-Doudoroff pathway, were not found in the genome of *D. nigrificans* and *D. carboxydivorans*. A phosphotransferase system (PTS) for glucose-specific transport was not found in either genome. Such a system is present in the genome of the glucose-utilizer *D. reducens* (Dred_0332).

Genes coding for the fructose-specific PTS are present in an operon structure in *D. nigrificans* (DesniDRAFT_2286 and 2291) and *D. carboxydivorans* (Desca_2698 and 2703). This system is likely involved in fructose uptake and its subsequent phosphorylation to fructose-1-phosphate. The fructose-1-phosphate thus formed can be further phosphorylated by 1-phosphofructokinase to fructose-1,6-bisphosphate (DesniDRAFT_2290 and Desca_2702).
Unlike *D. nigrificans* and *D. carboxydivorans*, *D. ruminis* and *D. kuznetsovii* are not able to grow with glucose or fructose. However, they have the genes that code for all the enzymes involved in the Embden-Meyerhof-Parnas pathway present in their genome. What is missing in their genome is the PTS for fructose-specific transport. This suggests that the absence of this PTS system prevents the use of fructose for growth.

2.8.3 Growth on one-carbon substrates

D. nigrificans and *D. carboxydivorans* can grow with formate plus sulfate in the presence of yeast extract and acetate as a carbon source. Since the genomes lack a complete acetyl-CoA pathway, *D. nigrificans* and *D. carboxydivorans* are not able to produce acetyl-CoA from formate and need an additional carbon source. The two genomes have similar genes that putatively code for three formate dehydrogenases (FDHs). The first FDH consists of an alpha subunit (DesniDRAFT_0989, Desca_1018), which is located next to a hydrogenase (DesniDRAFT_0990, Desca_1017) and a flavoprotein (DesniDRAFT_0988 and Desca_1019). The flavoprotein has one predicted transmembrane helix. Therefore, these genes might code for one intracellular membrane associated FDH. The second FDH gene cluster (DesniDRAFT_1389-1392, Desca_2053-2055) putatively codes for a confurcating cytoplasmic FDH. The third is predicted to code for an extracellular FDH (DesniDRAFT_1396-1397, Desca_2059-2060) associated with the membrane by a proposed 10 transmembrane helixes containing protein (DesniDRAFT_1395, Desca_2058). BLAST results and orthologous BLAST analysis [35] indicate that this transmembrane helix protein is orthologous to cytochrome b. Therefore, electron transport from this FDH might go through cytochrome b.
D. nigrificans and *D. carboxydivorans* are able to grow with CO in the presence of yeast extract. However, *D. nigrificans* grows with up to 20% of CO coupled to sulfate reduction, while *D. carboxydivorans* can grow with 100% CO with and without sulfate. These physiological differences should also be visible in the genome for the genes involved with carbon monoxide dehydrogenase (CODH). Figure 5 shows the organization of the CODH catalytic subunit (*cooS*) and neighboring genes in *D. nigrificans* and *D. carboxydivorans*. *D. nigrificans* has two *cooS* genes in the genome (DesniDRAFT_0854 and 1323) while *D. carboxydivorans* has three (Desca_0349, 1148, 1990). The organization of the *cooS* and neighboring genes in *D. nigrificans* is similar to that of two of the *cooS* and neighboring genes in *D. carboxydivorans*. However, one *cooS* gene cluster in the *D. carboxydivorans* genome cannot be found in the genome of *D. nigrificans*. The genes in this cluster are similar to genes described to be involved in the H_2 production from CO oxidation [36-39]. *Carboxydothermus hydrogenoformans* was the first bacterium described to have multiple *cooS* genes, one of which is united in a cluster with hydrogenase genes [39]. The hydrogenase module of this gene cluster represents a membrane-bound energy-converting hydrogenase (ECH) capable of energizing the membrane by proton translocation. Among sequenced *Desulfotomaculum* species, only *D. carboxydivorans, D. acetoxidans*, and *D. ruminis* possess putative genes coding for ECHs. However, in the latter two genomes, ECH encoding genes do not cluster with *cooS* genes.

Earlier analysis showed that clustering of cooS genes and ECH genes is a characteristic feature of hydrogenogenic carboxydotrophs [40]. The presence of the putative ECH-cooS gene cluster in *D. carboxydivorans* explains its ability to grow hydrogenogenically with CO.

In *D. nigrificans* there are no CODH involved genes in close proximity of the *cooS* genes, apart from one *cooC* gene (DesniDRAFT_0855). Apparently, this is sufficient for *D. nigrificans* to grow with 20% of CO coupled to sulfate reduction. However, *D. ruminis*, another *Desulfotomaculum* species in cluster 1a (Figure 2.1) of which the genome was recently described [41], also has the *cooS* gene (Desru_0859) downstream of a transcriptional regulator (Desru_0858) and upstream of the *cooC* gene (Desru_0860) but that bacterium is not able to grow on CO and sulfate. The reason for this is not yet clear.
A cluster of nitrogenase genes (Dtox_1023 to 1030) has been described in the genome of *Desulfotomaculum acetoxidans* [42]. In the genomes of *D. nigrificans* and *D. carboxydivorans* very similar gene clusters occur (DesniDRAFT_0869-0858 and Desca_1134-1144). Notably, in both cases there are *cooS* genes in the vicinity (DesniDRAFT_0854 and Desca_1148). They are located on another DNA strand and are convergently directed. Since the low-potential carbon monoxide

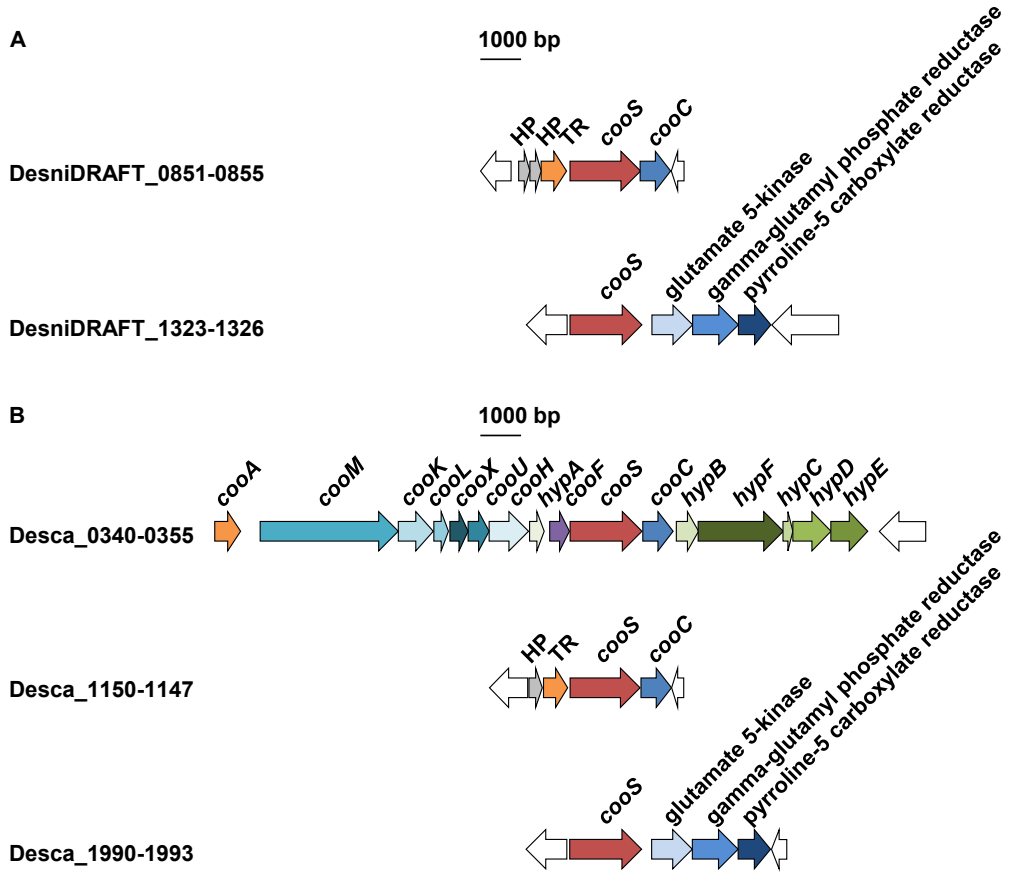

Figure 2.5: Organization of cooS and neighboring genes in DSM 574 (A) and DSM 14880 (B). Abbreviations: HP, hypothetical protein; TR, transcriptional regulator.

seems to be a good electron donor for nitrogen fixation, this proximity might be more than mere coincidence. This would suggest that small amounts of CO could be oxidized by *D. nigrificans* in the absence of sulfate. *D. ruminis* also has a similar gene cluster (Desru_3454-3445). However, in contrast to the genomes of *D. nigrificans* and *D. carboxydivorans* no cooS gene is nearby in the genome of *D. ruminis*.

Methyltransferase genes as present in *D. kuznetsovii* that might point to possible growth with methanol or methylated amines were not found in the genomes of *D. nigrificans* and *D. carboxydivorans*. These two strains accordingly, do not grow with methanol. Growth on methylated amines was never tested, but the genome suggests there is no growth possible with these compounds.

2.8.4 Hydrogen metabolism

D. nigrificans and *D. carboxydivorans* have a similar hydrogenase composition that is dominated by [FeFe] hydrogenases, as observed in other *Desulfotomaculum* spp. Each of the two bacteria has 9 [FeFe] hydrogenases, divided in the following groups: Three copies of trimeric bifurcating hydrogenases (DesniDRAFT_0775-0777, DesniDRAFT_0770-0772 and DesniDRAFT_1331-1333; Desca_1224-1226, Desca_1230-1232 and Desca_1996-1998); two copies of a monomeric hydrogenase (DesniDRAFT_0646 and DesniDRAFT_0308; Desca_1356 and Desca_1680); one HsfB-type hydrogenase encoding a PAS-sensing domain that is likely involved in sensing and regulation (DesniDRAFT_0986 and Desca_1021); one hydrogenase that is part of a 5-gene operon also encoding one membrane protein and two flavin-dependent oxidoreductases (DesniDRAFT_1073-1077 and Desca_0931-0935); and finally two copies of a membrane-associated hydrogenase (DesniDRAFT_1068-1070 and DesniDRAFT_2001-2003; Desca_0940-0938 and Desca_2453-2455). The catalytic subunit (DesniDRAFT_1068, 2001 and Desca_0940, 2453) of this hydrogenase contains a tat signal motif, which suggests that the hydrogenase complex is positioned extracellular. Moreover, the membrane associated subunit is a 10 transmembrane helix containing protein that is orthologous to cytochrome b. This is similar to the extracellular FDH.

The high number of hydrogenases in the genomes of the two bacteria indicates a high metabolic flexibility. This is important for changing growth strategies, from, for example, sulfate respiration to syntrophic growth. A syntrophic co-culture of *D. nigrificans* and *Methanobacterium thermoautotrophicum* on lactate and ethanol was described [5]. Syntrophic consortia are able to grow from very small free energy changes due to their ability to overcome thermodynamically difficult reactions. Reverse electron transfer is an essential part of this. The genes coding for the bifurcating hydrogenases and the confurcating formate dehydrogenase in the *D. nigrificans* genome are therefore likely candidates to be involved in syntrophic growth on lactate and ethanol.

A membrane-associated ECH is present only in *D. carboxydivorans*, as mentioned above, and no other [NiFe] hydrogenases are present. Other membrane associated complexes found in the genome of *D. nigrificans* and *D. carboxydivorans* are complex I (DesniDRAFT_0902-0892 and Desca_1110-1120) and a H^+-pumping membrane-bound pyrophosphatase (DesniDRAFT_2060 and Desca_2506).

2.8.5 Electron acceptor metabolism

The genes for the assimilatory sulfate reduction are organized in an identical way in *D. nigrificans*

and *D. carboxydivorans*. ATP-sulfurylase (DesniDRAFT_1837, Desca_2237) is followed by adenosine-5´-phosphosulfate (APS) reductase (DesniDRAFT_1836-1835, Desca_2378-2377), and the QmoAB complex (DesniDRAFT_1834-1833, Desca_ 2376-2375). A qmoC gene is absent but seems to be substituted by heterodisulfide reductases (Hdr) CB (DesniDRAFT _1838-1839, Desca_ 2381-2380). This organization is also found in *D. ruminis* and *D. reducens*. The position

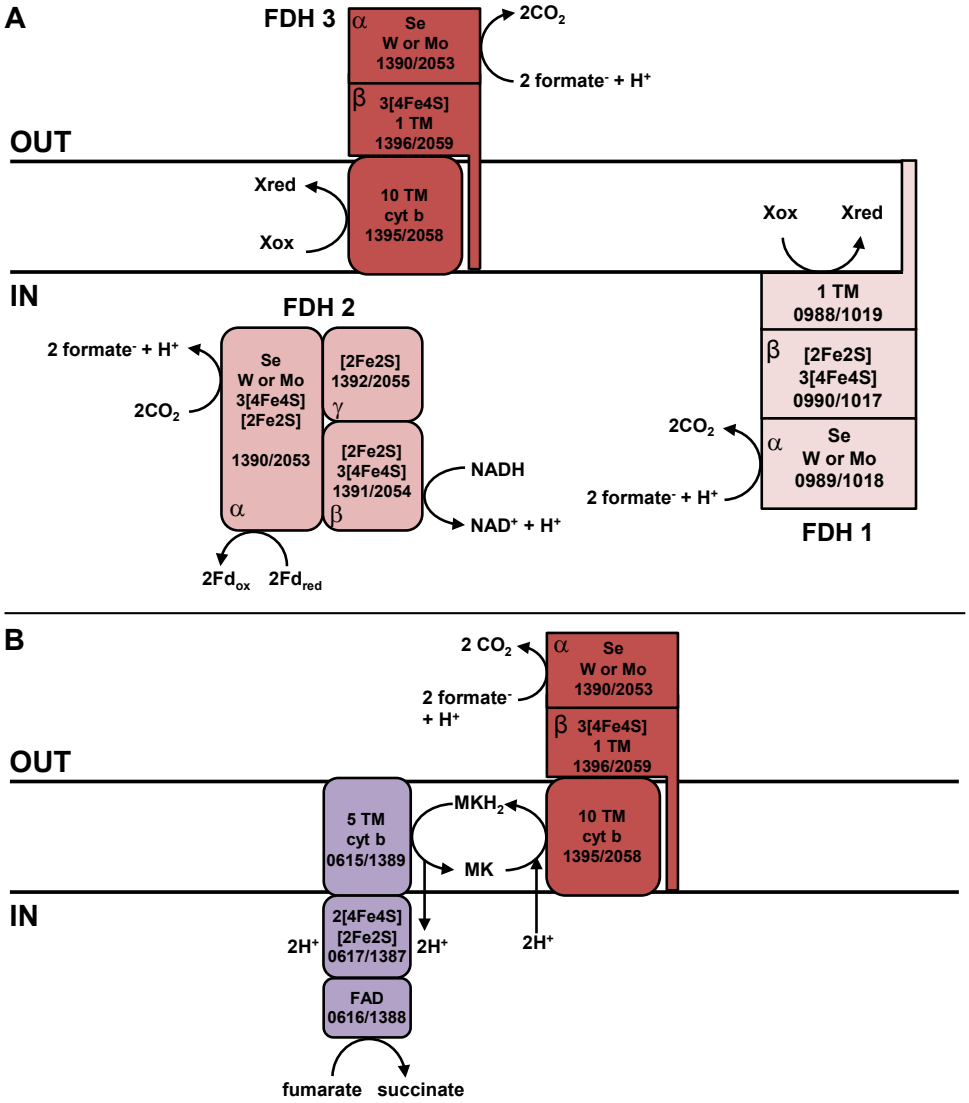

Figure 2.6: Schematic representation of putative formate dehydrogenases in the genome of DSM 574 and DSM 14880 (A). Including the hypothesized electron interaction of the putative extracellular membrane bound formate dehydrogenase with the putative fumarate reductase (B). The electron acceptor fumarate is reduced to succinate by using formate as an electron donor. Gene locus tag numbers and α-, β-, and γ-subunits are depicted. Moreover, predicted iron-sulfur clusters and other metal-binding sites are indicated.

of the HdrCB is switched to the other side in *D. acetoxidans*, *D. gibsoniae*, *D. alcoholicoviorans*, *Desulfurispora thermophila*, and *Desulfarculus baarsii* (which owns a Gram-positive aprBA [43]). In contrast to these organisms, *D. kuznetsovii*, *Ammonifex degensii*, *Desulfovirgula thermocuniculi*, and Gram-negative sulfate-reducing bacteria which possess a Gram-positive aprBA [43] like *Desulfomonile tiedjei* and *Syntrophobacter fumaroxidans* have a complete qmoABC complex (for *D. kuznetsovii*: Desku_ 1075, Desku_1076, Desku_1078).

The genes for the dissimilatory sulfite reductase found and their organization are identical to all other six *Desulfotomaculum* genomes published so far and most other Gram-positive sulfate-reducing bacteria. The dsrAB genes (DesniDRAFT_2256-2255, Desca_2666-2665) are linked to a dsrD gene (DesniDRAFT_2254, Desca_2664). Both organisms also contain a truncated DsrMK complex [44] (DesniDRAFT_2267-2268, Desca_2678-2679) which is linked to a dsrC gene (DesniDRAFT_2266, Desca_2677) as it was found in *D. ruminis* [41]. This truncated DsrMK is generally found in Gram-positive sulfate-reducing bacteria and not restricted to members of the genus *Desulfotomaculum*.

D. nigrificans and *D. carboxydivorans* lack nitrate reduction genes for reduction of nitrate to N_2. Nitrate reductase, nitric-oxide forming nitrite reductase, nitric-oxide reductase and nitrous-oxide reductase are all absent in both genomes. However, a nitrite/sulphite reductase (DesniDRAFT_1001, 2506; Desca_0162, 1181) and an ammonia forming nitrite reductase (DesniDRAFT_0204; Desca_2313) are present in the genome of *D. nigrificans* and *D. carboxydivorans*. No taurine degradation pathway was detected in the genome of either strain, but it was described for the closely related *D. ruminis* [41]

2.8.6 Fumarate reductases

Using fumarate as an electron acceptor for growth of *D. nigrificans* and *D. carboxydivorans* has not been tested yet. However, a fumarate reductase is present in the genomes of the two bacteria. The three genes encode for a FAD containing catalytic subunit (DesniDRAFT_0617; Desca_1387), an iron sulfur containing subunit (DesniDRAFT_0616; Desca_1388), and a membrane associated cytochrome b (DesniDRAFT_0615 and Desca_1389). This cytochrome b protein might perform an electron interaction with the cytochrome b of the extracellular FDH (Figure 2.6, panel B). This interaction could occur as described in *Wolinella succinogenes,* where fumarate can be used as an electron acceptor for growth on formate [45].

2.8.7 Comparative genomics

Distinct genes in *Desulfotomaculum carboxydivorans* and *D. nigrificans*

To reveal genomic differences between these two very closely related species, a bidirectional BLAST of the protein coding genes was performed. BLAST analyses were performed using standard settings and best hits were filtered for 70% sequence coverage and 40% identity (supplementary data S1 [46]). A total of 2,529 homologous genes was found (Figure 2.7). The distinct genes were screened for operon structure and function, revealing genes involved in CRISPR, urea metabolism and hydrogenogenic CO metabolism in *D. carboxydivorans*.

CRISPR genes in *D. carboxydivorans* were found to have low sequence coverage and or identity with genes in the *D. nigrificans* genome (Figure 2.3). These genes involved two CRISPR-Cas systems, which we classified as an I-C subtype (Desca_0534-0540) and a III-A subtype (Desca_0572-0576). *D. nigrificans* has one CRISPR-Cas system subtype, I-A (DesniDRAFT_2444-2452), which is also

present in *D. carboxydivorans* (Desca_0726-0734). The presence of multiple CRISPR-Cas systems and the occurrence of the different subtypes in one strain has been described previously [47,48] and shows that the co-occurrence of subtype I-A with I-C and III-A is a common feature. However, it also shows that *D. carboxydivorans* is part of the 2% of bacteria that have a III-A subtype without a III-B subtype.

The genome of *D. carboxydivorans* also contains genes coding for an urease (Desca_0743-0749) and urea transport (Desca_0738-0742) (Figure 2.3). Urease catalyzes the reaction of urea to CO_2 and ammonia. Urea is very common in the environment and is a nitrogen source for many bacteria [49]. The genome of *D. nigrificans* lacks the genes coding for an urease, which indicates that *D. nigrificans* is relatively more restricted regarding its nitrogen source. Other interesting genes that are present in the *D. carboxydivorans* genome and not in the *D. nigrificans* genome are genes involved in the carbon monoxide dehydrogenase (CODH) and hydrogenase as described above.

2.8.8 Taxonomic conclusions

The overall similarity of the genome sequences of the type strains of *D. nigrificans* and *D. carboxydivorans* was estimated by using the Genome-To-Genome Distance Calculator (GGDC) as described previously [51]. This program calculates DNA-DNA similarity values by comparing the genomes to obtain high-scoring segment pairs (HSPs) and inferring distances from a set of three formulas (1, HSP length/total length; 2, identities/HSP length; 3, identities/total length). According to the GGDC the average estimated DNA-DNA similarity value between the two type strains is 86.5 ± 5.5% and thus clearly above 70%, which is the widely accepted threshold value for assigning strains to the same species [52]. The high similarity of the genome sequences of both type strains was further supported by the average nucleotide identity of shared genes

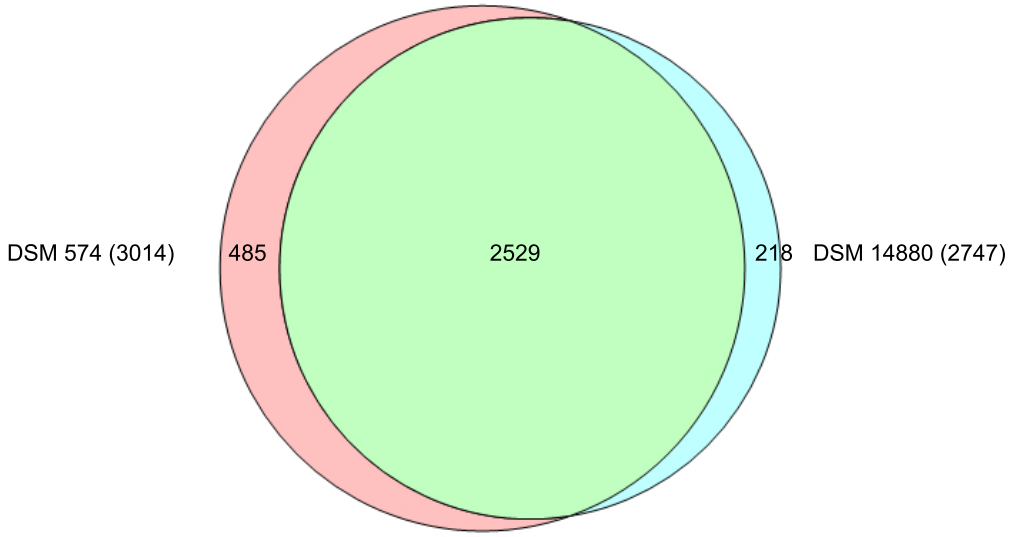

Figure 2.7: Venn diagram showing a comparison of the protein coding genes of DSM 574 and DSM 14880. The number of overlapping protein coding genes is given inside the areas of the circles and the total number of derived protein sequences used for each strain is shown in parentheses. The figure was created using the program Venn diagram plotter available from the Pacific Northwest National Laboratory Software Distribution Center [50].

(ANI), which proved to be above 99%. This ANI value is much higher than the 95 to 96% value shown to correspond to the 70% DNA-DNA hybridization level [53]. Moreover, the two strains have almost identical 16S rRNA gene sequences (>99%) and a high number of shared genes (Figure 2.7). It should be mentioned that the previously reported and deposited rRNA gene sequence of *D. nigrificans* DSM 574 contained a lot ambiguities and some missing nucleotides, which are counted as mismatches by BLAST. Therefore, we reanalyzed the rRNA gene sequences of *D. nigrificans* deposited in the NCIMB culture collections and confirmed the identity of the rRNA gene sequence found in the genome of DSM 574. We propose that the species should be united under one name. According to the rules of priority as given by the Bacteriological Code [54] the name *D. nigrificans* should be used for the unified taxon, with *D. carboxydivorans* as a later heterotypic synonym.

2.8.9 Emended description of Desulfotomaculum nigrificans (Werkman and Weaver 1927) Campbell and Postgate 1965

The description is as given by Campbell and Postgate [1] and Parshina et al. [6] with the following modifications.

The cells are Gram-positive, rod-shaped with rounded ends, 0.3-1.5 x 2-15 µm, single or sometimes paired. Motility with tumbling or twisting movements conferred by peritrichous flagella. Terminal or subterminal oval endospores that are slightly swelling the cells. Thermophilic and neutrophilic with a temperature optimum of 55°C. NaCl is not required for growth. The following substrates are utilized, coupled to the reduction of sulfate to sulfide: DL-lactate, pyruvate, ethanol, L-alanine, D-fructose, and D-glucose. Acetate and methanol are not utilized. Substrates are incompletely oxidized to acetate. In the presence of 0.5 g/l yeast extract, lithoheterotrophic growth is possible, such as growth on H_2 and CO_2 with sulfate or growth on 20% CO with sulfate for *D. nigrificans* strain Delft 74 and growth on 100% CO with or without sulfate for strain CO-1-SRB. Suitable electron acceptors with lactate as substrate are sulfate, sulfite and thiosulfate, but not elemental sulfur or nitrate. Fermentation of pyruvate and fructose; strain CO-1-SRB is also able to ferment DL-lactate, glucose and CO. The prevalent respiratory lipoquinone is MK7 with only small amounts of MK6. The dominating cytochromes are of type *b*. Major cellular fatty acids are 16:0, iso 15:0, iso 17:0, anteiso 15:0, 18:0 and iso 16:0. The DNA G+C content is around 46 mol%. The type strain is Delft 74 (=NCIMB 8395 = DSM 574 = ATCC 19998 = NBRC 13698).

2.9 Acknowledgements

We would like to gratefully acknowledge the help of Christine Munk and Megan Lu for finishing the genome sequence (both at JGI). The work conducted by the U.S. Department of Energy Joint Genome Institute is supported by the Office of Science of the U.S. Department of Energy under Contract No. DE-AC02-05CH11231, and was also supported by grants CW-TOP 700.55.343 and ALW 819.02.014 of the Netherlands Science Foundation (NWO) and grant 323009 of the European Research Council.

2.10 References

1. Campbell, L.L. & Postgate, J.R. Classification of the spore-forming sulfate-reducing bacteria. *Bacteriology Reviews* **29**, 359-63 (1965).
2. Werkman, C.H. & Weaver, H.J. Studies in the bacteriology of sulphur stinker spoilage of canned sweet corn. *Oiwa*

State Collage Journal **2**, 57-67 (1927).

3. Starkey, R.L. A study of spore formation and other morphological characteristics of *Vibrio desulfuricans*. *Archiv für Mikrobiologie* **9**, 368-404 (1938).
4. Akagi, J.M. & Jackson, G. Degradation of glucose by proliferating cells of *Desulfotomaculum nigrificans*. *Applied Microbiology* **15**, 1427-30 (1967).
5. Klemps, R., Cypionka, H., Widdel, F. & Norbert, P. Growth with hydrogen, and further physiological characteristics of *Desulfotomaculum* species. *Archieves of Microbiology* **143**, 203-8 (1985).
6. Parshina, S.N. et al. *Desulfotomaculum carboxydivorans* sp. nov., a novel sulfate-reducing bacterium capable of growth at 100% CO. *International Journal of Systematic and Evolutionary Microbiology* **55**, 2159-65 (2005).
7. Postgate, J.R. Sulfate-free growth of *Clostridium nigrificans*. *Journal of Bacteriology* **85**, 1450-1 (1963).
8. Krishnamurthi, S. et al. *Desulfotomaculum defluvii* sp. nov., a sulfate-reducing bacterium isolated from the subsurface environment of a landfill. *International Journal of Systematic and Evolutionary Microbiology* **63**, 2290-5 (2012).
9. Collins, M. & Weddel, F. Respiratory quinones of sulphate-reducing and sulphur-reducing bacteria: a systematic investigation *Systematic and Applied Microbiology* **8**, 8-18 (1986).
10. 1Field, D. et al. The minimum information about a genome sequence (MIGS) specification. *Nature Biotechnology* **26**, 541-547 (2008).
11. Woese, C.R., Kandler, O. & Wheelis, M.L. Towards a natural system of organisms: proposal for the domains Archaea, Bacteria, and Eucarya. *Proc Natl Acad Sci U S A* **87**, 4576-9 (1990).
12. Garrity, G.M. & Holt, J.G. in Bergey's manual of systematic bacteriology (eds. Garrity, G.M., Boone, D.R. & Castenholz, R.W.) 119-169 (Springer, New York, 2001).
13. Gibbons, N.E. & Murray, R.G.E. Proposal concerning the higher taxa of bacteria. *International Journal of Systematic Biotechnology* **28**, 1-6 (1978).
14. Murray, R.G.E. in Bergey's manual of systematic bacteriology (ed. Holt, J.G.) 31-34 (The Williams and Wilkins Co., Baltimore, 1984).
15. Euzeby, J. List of new names and new combinations previously effectively, but not validly, published. *Int J Syst Evol Microbiol* **60**, 1009-10 (2010).
16. Rainey, F.A. in Bergey's manual of systematic bacteriology (eds. De Vos, P. et al.) 736 (Springer, New York, 2009).
17. Prévot, A.R. Dictionnaire des Bactéries Pathogènes (eds. Hauderoy, P. et al.) (Masson et Cie, Paris, 1953).
18. Skerman, V.B.D., Mcgowan, V. & Sneath, P.H.A. Approved Lists of Bacterial Names. *Int J Syst Bacteriol* **30**, 225-420 (1980).
19. Rogosa, M. *Peptococcaceae*, a new family to include the Gram-positive, anaerobic cocci of the genera *Peptococcus*, *Peptostreptococcus* and *Ruminococcus*. *International Journal of Systematic Bacteriology*, 234-7 (1971).
20. Ashburner, M. et al. Gene ontology: tool for the unification of biology. The Gene Ontology Consortium. *Nature Genetics* **25**, 25-9 (2000).
21. Pagani, I. et al. The Genomes OnLine Database (GOLD) v.4: status of genomic and metagenomic projects and their associated metadata. *Nucleic Acids Research* **40**, D571-9 (2012).
22. JGI website. http://www.jgi.doe.gov/.
23. The Phred/Phrap/Consed software package. http://www.phrap.com.
24. Zerbino, D.R. & Birney, E. Velvet: algorithms for de novo short read assembly using de Bruijn graphs. *Genome Research* **18**, 821-9 (2008).
25. Han, C. & Chain, P. in international conference on bioinformatics & computational biology (eds. H.R., A. & H., V.) 141-6 (CSREA Press, 2006).
26. Lapidus, A. et al. (AGBT, Marco Island, FL, 2008).
27. Hyatt, D. et al. Prodigal: prokaryotic gene recognition and translation initiation site identification. *BMC Bioinformatics* **11**, 119 (2010).
28. Mavromatis, K. et al. The DOE-JGI Standard operating procedure for the annotations of microbial genomes. *Standards in Genomic Sciences* **1**, 63-7 (2009).

29. Pati, A. et al. GenePRIMP: a gene prediction improvement pipeline for prokaryotic genomes. *Nature Methods* **7**, 455-7 (2010).
30. Markowitz, V.M. et al. IMG ER: a system for microbial genome annotation expert review and curation. *Bioinformatics* **25**, 2271-8 (2009).
31. Goevert, D. & Conrad, R. Carbon isotope fractionation by sulfate-reducing bacteria using different pathways for the oxidation of acetate. *Environmental Science & Technology* **42**, 7813-7 (2008).
32. Hagenauer, A., Hippe, H. & Rainey, F.A. *Desulfotomaculum aeronauticum* sp. nov., a Sporeforming, Thiosulfate-Reducing Bacterium from Corroded Aluminium Alloy in an Aircraft. *Systematic and Applied Microbiology* **20**, 65-71 (1997).
33. Haouari, O. et al. *Desulfotomaculum hydrothermale* sp. nov., a thermophilic sulfate-reducing bacterium isolated from a terrestrial Tunisian hot spring. *International Journal of Systematic and Evolutionary Microbiology* **58**, 2529-35 (2008).
34. Liu, Y. et al. Description of two new thermophilic *Desulfotomaculum* spp., *Desulfotomaculum putei* sp. nov., from a deep terrestrial subsurface, and *Desulfotomaculum luciae* sp. nov., from a hot spring. *International Journal of Systematic Bacteriology* **47**, 615-21 (1997).
35. Zhou, Y. & Landweber, L.F. BLASTO: a tool for searching orthologous groups. *Nucleic Acids Research* **35**, W678-82 (2007).
36. Fox, J.D., He, Y., Shelver, D., Roberts, G.P. & Ludden, P.W. Characterization of the region encoding the CO-induced hydrogenase of *Rhodospirillum rubrum*. *Journal of Bacteriology* **178**, 6200-8 (1996).
37. Hedderich, R. Energy-converting [NiFe] hydrogenases from archaea and extremophiles: ancestors of complex I. *Journal of Bioenergetics and Biomembranes* **36**, 65-75 (2004).
38. Meuer, J., Bartoschek, S., Koch, J., Kunkel, A. & Hedderich, R. Purification and catalytic properties of Ech hydrogenase from *Methanosarcina barkeri*. *European journal of biochemistry / FEBS* **265**, 325-35 (1999).
39. Wu, M. et al. Life in hot carbon monoxide: the complete genome sequence of *Carboxydothermus hydrogenoformans* Z-2901. *PLoS Genet* **1**, e65 (2005).
40. Sokolova, T.G. et al. Diversity and ecophysiological features of thermophilic carboxydotrophic anaerobes. *FEMS Microbiology Ecology* **68**, 131-41 (2009).
41. Spring, S. et al. Complete genome sequence of the sulfate-reducing firmicute *Desulfotomaculum ruminis* type strain (DL(T)). *Standards in Genomic Sciences* **7**, 304-19 (2012).
42. Spring, S. et al. Complete genome sequence of *Desulfotomaculum acetoxidans* type strain (5575). *Standards in Genomic Sciences* **1**, 242-53 (2009).
43. Meyer, B. & Kuever, J. Phylogeny of the alpha and beta subunits of the dissimilatory adenosine-5'-phosphosulfate (APS) reductase from sulfate-reducing prokaryotes--origin and evolution of the dissimilatory sulfate-reduction pathway. *Microbiology* **153**, 2026-44 (2007).
44. Junier, P. et al. The genome of the Gram-positive metal- and sulfate-reducing bacterium *Desulfotomaculum reducens* strain MI-1. *Environmental Microbiology* **12**, 2738-54 (2010).
45. Kroger, A. et al. Fumarate respiration of *Wolinella succinogenes*: enzymology, energetics and coupling mechanism. *Biochimica et Biophysica Acta* **1553**, 23-38 (2002).
46. Visser, M., Parshina, S.N., Alves, J.I., Sousa, D.Z., Pereira, I.A., Muyzer, G., Kuever, J., Lebedinsky, A.V., Koehorst, J.J., Worm, P., Plugge, C.M., Schaap, P., Goodwin, L., Lapidus, A., Kyrpides, N.C., Detter, J.C., Woyke, T., Chain, P., Davenport, K.W., Spring, S., Rohde, M., Klenk, H.P., Stams, A.J.M. Genome analyses of the carboxydotrophic sulfate-reducers *Desulfotomaculum nigrificans* and *Desulfotomaculum carboxydivorans* and reclassification of *Desulfotomaculum carboxydivorans* as a later synonym of *Desulfotomaculum nigrificans*. *Standards in Genomic Sciences* **9**, 655-675 (2014)..
47. Makarova, K.S. et al. Evolution and classification of the CRISPR-Cas systems. *Nature Reviews. Microbiology* **9**, 467-77 (2011).
48. Staals, R.H.J. & Brouns, S.J.J. in CRISPR-Cas Systems (eds. Barrangou, R. & van der Oost, J.) 145-96 (Springer, 2012).
49. Mobley, H.L. & Hausinger, R.P. Microbial ureases: significance, regulation, and molecular characterization. *Microbiological Reviews* **53**, 85-108 (1989).
50. Venn diagram plotter available from the Pacific Northwest National Laboratory Software Distribution Center:

http://omics.pnl.gov.

51. Auch, A.F., von Jan, M., Klenk, H.P. & Goker, M. Digital DNA-DNA hybridization for microbial species delineation by means of genome-to-genome sequence comparison. *Standards in Genomic Sciences* **2**, 117-34 (2010).
52. Wayne, L.G. et al. Report of the ad-hoc-committee on reconciliation of approaches to bacterial systematics. *International Journal of Systematic Bacteriology* **37**, 463-4 (1987).
53. Richter, M. & Rossello-Mora, R. Shifting the genomic gold standard for the prokaryotic species definition. *Proceedings of the National Academy of Sciences of the United States of America* **106**, 19126-31 (2009).
54. Lapage, S.P. et al. International Code of Nomenclature of Bacteria: Bacteriological Code, 1990 Revision (Washington (DC), 1992).

Chapter 3

Genome and proteome analysis reveals novel insight of the one-carbon metabolism of the acetogen *Sporomusa* strain An4

Michael Visser, Mervin Pieterse, Martijn W. Pinkse, Bart Nijsse, Willem M. de Vos, Peter J. Schaap and Alfons J. M. Stams

In preparation for publication

3.1 Abstract

The *Sporomusa* genus comprises anaerobic spore-forming acetogenic bacteria with a Gram-negative cell wall. The characteristic substrates for *Sporomusa* species are one-carbon substrates and N-methylated compounds. In the degradation of these compounds different methyltransferases are involved. In addition, *Sporomusa* species can grow autotrophically with H_2 and CO_2, and use a variety of sugars for acetogenic growth. In order to gain a better understanding of the physiology of *Sporomusa*, a genome analysis of *Sporomusa* strain An4 was combined with a differential proteome analysis of cells grown under five different conditions. These conditions were: acetogenic growth with H_2 and CO_2, methanol, betaine, and fructose; and respiratory growth with methanol and nitrate. In addition, the genome of strain An4 was compared to the recently sequenced genome of *Sporomusa ovata*. The comparison indicated that *Sporomusa* strain An4 is a *S. ovata* strain. The proteome analysis showed a high abundance of many methyltransferases, predominantly trimethylamine methyltransferases, during growth with betaine. However, trimethylamine is one of the main end products of betaine degradation in *Sporomusa* strain An4. Why growth with betaine leads to the synthesis of many methyltransferases cannot be concluded from this study.

During growth with methanol three methyltransferase gene products were highly abundant. These included the two methanol methyltransferase subunits MtaB and MtaC. However, instead of a MtaA another methyltransferase was produced, a methyltetrahydrofolate methyltransferase. This suggests its involvement in the methanol metabolism. Therefore, we propose a novel methanol metabolism in *Sporomusa* strain An4 that uses a methyltetrahydrofolate methyltransferase instead of a MtaA.

3.2 Introduction

The genus *Sporomusa* was described in 1984 [1]. It is a genus of motile spore-forming acetogenic bacteria with a Gram-negative cell wall. Currently, the genus *Sporomusa* consists of 9 validated species. *Sporomusa* strains have been isolated from soils and sediments [1-4], from wastewater [1,5] and from the gut and faeces of animals [1,6-8]. The characteristic substrates for *Sporomusa* species are one-carbon substrates, such as methanol, and N-methylated compounds such as betaine. In addition, they can grow autotrophically with H_2 and CO_2, and use a variety of sugars for anaerobic acetogenic growth. Like other acetogenic bacteria they employ the acetyl-CoA pathway for energy conservation and CO_2 fixation [9,10].

Sporomusa strain An4 was isolated from an underground gas storage in Russia with methanol and perchlorate as substrates. Besides perchlorate, the strain was also able to use nitrate as electron acceptor. Unfortunately, in course of this study the strain lost its ability to use perchlorate as electron acceptor. The ability to respire with inorganic electron acceptors is not very common among *Sporomusa* species; only *Sporomusa ovata* and *Sporomusa* strain An4 have been described to reduce nitrate to ammonium [1,11]. *Sporomusa* strain An4 is, according to phylogenetic analysis based on 16S rRNA gene sequences, closely related to *Sporomusa* strain DR5 and *S. ovata* (99% and 98% sequence similarity, respectively) [11].

Sporomusa strains are known to produce atypical corrinoids. More than 90% of the corrinoids in *Sporomusa ovata* consist of two synthesized coenzyme B_{12} analogues, *p*-cresolyl cobamide and phenolyl cobamide [12-14]. Some other studies provided insight into the transfer of the methyl group from methylated substrates. For *S. ovata* the involvement of a cobamide-containing protein in the

formation of methyl-tetrahydrofolate (CH_3-THF) was shown [15]. The synthesis of this protein was induced when *S. ovata* was grown on methanol. The cobamide-containing methyltransferase of *S. ovata* was purified and characterized [16,17]. Moreover, it was shown that different methyltransferases are involved in degradation of different methylated-substrates [15] and cytochromes appeared to be essential for autotrophic growth and methyl group oxidation [18]. These and other studies [19,20] provided some insight into the physiology of *Sporomusa.*

The lack of genome information hampered further understanding of the ecophysiology of *Sporomusa* species. Only recently genomic information became available for *Sporomusa* species [21]. Here we describe a genomic comparison, between the recently sequenced *Sporomusa ovata* and *Sporomusa* strain An4, and a proteogenomic approach to get insight into the catabolic pathways of the metabolism of *Sporomusa* strain An4. Five different growth conditions were selected; acetogenic growth with H_2 and CO_2, methanol, betaine, and fructose; and respiratory growth with methanol and nitrate. Functional genome analysis was combined with differential proteome analysis of cells grown with the different substrates.

3.3 Experimental procedures

3.3.1 Source of inoculum and culture medium

Sporomusa strain An4 (=DSM 21435, =JSM 15643) was isolated from a water sample of an underground gas storage in Russia [11]. The strain was enriched and isolated with methanol and perchlorate in a basal bicarbonate buffered medium described by Stams et al. [40]. The same medium but with the addition of 0.1 g L^{-1} yeast extract was used in this study. The electron donors were added in 20 mM concentrations and electron acceptors in 10 mM concentrations, from concentrated stock solutions (sterilized by autoclaving). Cultivation of strain An4 was done at a neutral pH and at 30°C in 117 ml glass serum vials with butyl rubber stoppers and aluminium crimp seals. The vials contained 50 ml basal medium and a gas phase of 1.7 bar N_2/CO_2 (80%/20%, v/v). However, when hydrogen was the electron donor the gas phase was 1.7 bar H_2/CO_2 (80%/20%, v/v). In all experiments the inoculum size was 10%(v/v).

3.3.2 Experimental design

To obtain insight into the physiology of *Sporomusa* strain An4 a combined genome and proteome analysis was performed. First, growth of strain An4 was studied in five conditions with following substrates: 1) hydrogen and carbon dioxide (H_2 and CO_2), 2) methanol, 3) methanol and nitrate, 4) betaine and 5) fructose. Subsequently, DNA was isolated from methanol-grown cells. For protein extraction strain An4 was grown in all five conditions. Cells were adapted to the different growth conditions by transferring three times. Subsequently, 1.2 liter bottles containing 500 ml medium were inoculated. Protein extraction of all growth conditions was performed at late exponential phase.

3.3.3 Analytical methods

Substrate concentrations were tested using high pressure liquid chromatography. The substrates methanol, betaine, and fructose and the product acetate were analysed using a MetaCarb 67H 5 x 300 mm column (Varian, Middelburg, the Netherlands) connected to a SpectraSYSTEM RI-150 detector (Thermo electron corporation, Waltham, Massachusetts, USA). The 5 mM H_2SO_4 mobile phase had a flow of 0.8 ml min^{-1}. The temperature was controlled at 30°C during the analysis.

Crotonate was used as an internal standard.
Nitrate was measured using an ED 40 electrochemical detector (Dionex, Breda, The Netherlands) after separation on an Ionpac AS9-SC 4 x 50 mm column (Dionex, Breda, The Netherlands). Potassium fluoride (2 mM) was used as internal standard. The analysis was conducted at a temperature of 35°C with a flow rate of 1.2 ml min^{-1}. The mobile phase used consisted of 1.29 g L^{-1} Na_2CO_3¬ 10 H2O and 0.12 g L^{-1} $NaHCO_3$.
Hydrogen gas samples were analysed by gas chromatography with a Shimadzu GC-14B (Shimadzu, Kyoto, Japan) equipped with a packed column (Molsieve 13X, 60-80 mesh, 2 m length, 3 mm internal diameter; Varian, Middelburg, The Netherlands) and a thermal conductivity detector set at 70 mA. The injector temperature and the oven temperature were both 100°C. The detector temperature was 150°C. Argon was used as the carrier gas at a flow rate of 30 ml min^{-1}.
Growth was measured using the optical density at 600 nm (OD_{600}). Uninoculated medium served as a reference.

3.3.4 DNA isolation, genome sequencing and genome annotation.

Genomic DNA from *Sporomusa* strain An4 was isolated using the standard DOE Joint Genome Institute (JGI) CTAB method. Sequencing the genome of strain An4 was done by using the 454 pyrosequencing technique and additional mate-pair sequencing [41]. Shot-gun sequencing was performed to a redundancy of 44x (539893 reads). The assembly of these reads was performed using the Newbler Assembler software (454 Life Sciences) resulting in 163 contigs of more than 500 bp. The additional Illumina mate-pair reads were used to extend the contigs and to create scaffolds by using SSPACE Basic v2.0 [42] with an insert from PicardTools. Gaps were filled with the mate-pair reads by using SSPACE GapFilling v1.11 [43]. The final assembly was improved with Pilon v1.4 using both 454 and mate-pair reads, which resulted in 16 scaffolds of more than 42 kbp. Scaffolds were reordered according to the *Sporomusa ovata* draft genome. The 16 scaffolds were submitted to RAST server service [22] for automatic annotation yielding 5280 protein encoding genes.

3.3.5 Genome comparison

The genome of *Sporomusa* strain An4 was compared to the genome of *Sporomusa ovata* by comparing their functional domain profiles, which were obtained with InterProScan 5 (version 5RC7, 27th January 2014). Differences are discussed in the text. The average nucleotide identity of shared genes (ANI) was used to determine if strain An4 is a *S. ovata* or a novel *Sporomusa* species.
Comparison of selected *Sporomusa* strain An4 genes and putative proteins to other microorganisms than *S. ovata* was performed by BLAST analysis. Nucleotide sequences were compared to genes in the NCBI nucleotide collection database. The comparison was optimized for highly similar sequences. Amino acid sequences of selected strain An4 proteins were compared to proteins for homology, using the NCBI non-redundant protein sequence database, with default settings. For alignment only amino acid sequences were used when the genome of the microorganism was fully sequenced. Additionally, the sequences required a minimum coverage of 80% and for alignment purposes the minimum identity was either 40% or 50%. Alignment was performed using MUSCLE [46].
To identify cofactor binding motifs, transmembrane helices, and twin-arginine translocation motifs

in the N-terminus we used Pfam 27.0 (March 2013) [45], TMHMM Server v. 2.0 [48] and the TatP 1.0 Server [49], respectively. Sequences with similarity to iron-only or [FeFe]-hydrogenases, were manually analysed for the presence of conserved H-cluster residues [50]. RNA loop predictions with Mfold version 3.2. was used to predict incorporation of selenocysteine [51,52]. We compared the predicted RNA loop in the 50-100 bp region downstream of the UGA-codon with the consensus loop described [53].

3.3.6 Protein extraction

For the preparation of protein samples 500 ml of each growth condition was centrifuged. The pellets were resuspended in SDT-lysis buffer (100mM Tris/HCl pH 7.6 + 4% SDS + 0.1M dithiothreitol) separately and sonificated to disrupt the bacterial cell wall. Unbroken cells and debris were removed by centrifugation at 13.000 rpm for ten minutes. Protein concentration in the protein samples were measured by using Bradford reagent (Sigma Aldrich, St. Louis, USA) using bovine serum albumin as a standard.

3.3.7 Proteome analysis

For each growth condition an equal amount of total protein was separated by SDS-PAGE on a 10 well PAGE® Novex 4-12% Bis-Tris gel (Invitrogen) and ran using MES-SDS as running buffer for 30 min at a constant voltage of 200 V. The gel was stained with Coomassie Blue (Colloidal Blue Staining Kit, Invitrogen) after which entire gel lanes were cut into 25 equal slides using a gridcutter (Gelcompany, SA, USA). Gel pieces were reduced with dithiotreitol (10 mM, 30 min, room temperature), alkylated with iodoacetamide (20 mM, 60 min, room temperature in the dark) and digested with trypsin overnight at 37°C. After digestion, formic acid and DMSO were added (both 5% v/v) to increase peptide recovery. Protein digests were analyzed on a reversed phase nano-LC coupled to a LTQ Orbitrap Velos (Thermo Fisher Scientific, Bremen, Germany). An Agilent 1200 series HPLC system was equipped with in–house packed trapping column (100 µm ID and 20 mm length) and analytical column (50 µm ID and 250 mm length) filled with Reprosil Pur 120 C18-AQ (Dr. Maisch, Ammerbuch-Entringen, Germany) essentially as described by Meiring et al. [44]. Trapping was performed at 5 µl/min for 10 minutes in solvent A (0.1 M acetic acid), and elution was achieved with a gradient from 0 to 40% solvent B (0.1 M acetic acid in 8:2 v/v acetonitrile:water) for 40 minutes. The LTQ Orbitrap Velos was operated in data dependent mode automatically switching between MS and MS/MS. Survey full scan MS spectra were acquired from *m/z* 400 to 1500 in the Orbitrap with a resolution of 30,000 at *m/z* 400 after accumulation to a target value of 1e6 in the linear ion trap. The ten most intense, multiply charged ions at a threshold of above 1000 were fragmented in the linear ion trap using collision-induced dissociation (CID) at a target value of 1e4. All raw data files were processed into peaklists using Proteome Discoverer 1.1.

For each condition approximately 80,000 to 100,000 MS/MS spectra were obtained from trypsin-digested protein mixtures of cell free extracts. The MS/MS spectra were submitted to a local implementation of the OMSSA search engine [25] and searched against a peptide database derived from the predicted proteins of the *Sporomusa* strain An4 draft genome RAST annotation. The following search parameters were used: a precursor ion tolerance of 0.03 Da, fragment ion tolerance of 0.5 Da, a miss cleavage allowance of up to and including 2. Cysteines were considered to be carboxyamidomethylated, oxidation of methionine and deamination of

glutamine and aspargine were treated as variable modifications. The set E-value threshold was determined iteratively from the false discovery rate (FDR) and was set to 0.01. With this setting an FDR of < 2% was obtained for all samples. The FDR was calculated from top hit spectral matches to peptides in the reversed database as described by Elias and Gygi [45]. The proteome analysis resulted in the identification of 2280 different proteins (with at least 2 unique peptides identified). Spectral counting [26] was used to study protein abundance. Higher counts lower the chance of false positives, making it more reliable that the protein is produced. 788 predicted proteins showed >9 counts and are listed in the supplementary data (Supplementary file S1). Proteins that possibly play an important role under different growth conditions are discussed in more detail in the text.

3.3.8 Enzyme activity assays

Enzyme activities were analysed spectrofotometrically by measuring the color change of methyl viologen (MV) at 578 nm, due to reduction or oxidation. Glass cuvettes were anaerobically prepared by flushing with N_2. Except for the CODH assay, where the glass cuvette was flushed with CO. The CODH assay mixture contained 50 mM 3-(N-morpholino)propanesulfonic acid-KOH (pH 7), 1 mM MV and 0.1 mM dithiotreitol (DTT). The FDH assay mixture contained Tris-HCL (pH 8), 1 mM MV, 0.1 mM DTT and 10 mM formate. In the CODH and FDH assay the absorbance increased.

The nitrate and nitrite reductase assay mixture both contained 50 mM Tris-HCl (pH 7.5), 0.5 mM MV, a small amount of dithionite solution to reach a starting absorbance of approximately 1.5, and 4 mM nitrate or 0.25 mM nitrite, respectively.

3.4 Results

Whole genome shotgun sequencing combined with mate-pair sequencing of *Sporomusa* strain An4 resulted in 4.9 Mbp assembled sequence data with an average scaffold size of 308 kbp. The draft genome was automatically annotated using RAST [22]. 5280 protein-encoding genes were identified. To study the physiology of *Sporomusa* strain An4 genome analysis was combined with differential proteomics.

Shotgun proteomics was applied to study the differential expression of proteins involved in growth with different substrates: H_2 and CO_2, methanol, methanol and nitrate, betaine, and fructose. Adapted cultures were harvested for protein extraction when they were at late exponential phase. Equal amounts of total protein were used for proteome analysis. For each condition approximately 80,000 to 100,000 MS/MS spectra were obtained. Omssa [25] was used to obtain Peptide Spectrum Matches (PSM) with an efficiency of 43.6% and a FDR of <2%. Spectral counting [26] was used to study protein abundance.

3.4.1. Genome comparison

The genome of *Sporomusa* strain An4 was compared to the recently sequenced *Sporomusa ovata*. The two genomes showed high similarity by the average nucleotide identity of shared genes (ANI), which proved to be above 99%. This ANI value is much higher than the 95 to 96% value shown to correspond to the 70% DNA-DNA hybridization level [54]. This indicates that *Sporomusa* strain An4 is a *S. ovata* strain. Aditionally, a functional domain analysis was performed to show differences between the two *Sporomusa* genomes. The genome of the *S. ovata* type strain

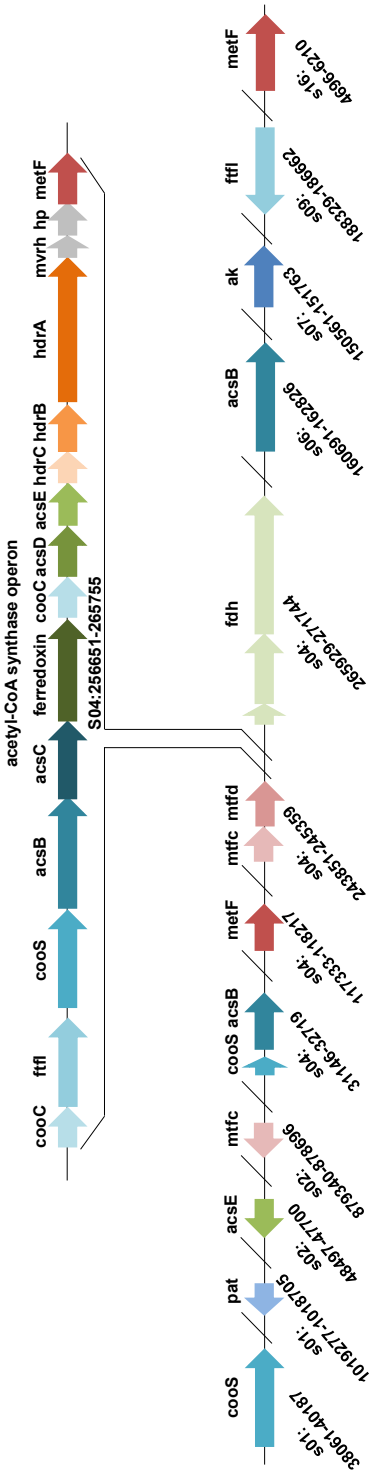

Figure 3.1: Relative position of the acetyl-CoA synthase operon and genes involved in the acetyl-CoA pathway outside the operon. Scaffold and base pair numbers are located below the genes. Abbreviations are acsE: CH_3-THF methyltransferase, ak: acetate kinase, fdh: formate dehydrogenase, ftfl: formate-THF ligase, hdr: heterodisulfide reductase, hp: hypothetical protein, mtfc: methenyl-THF cyclohydrolase, mtfd: methylene-THF dehydrogenase, mvrh: methyl-viologen-reducing hydrogenase, pat: phosphate acetyltransferase.

contained six genes that could not be found in the genome of strain An4. These included genes encoding two transposases, a protein of unknown function, an isopentenyl-diphosphate delta-isomerase and a toxin-antitoxin protein. The genome of strain An4 contained two genes that could not be found in the genome of *S. ovata*. These genes encoded a multicopper oxidase and a peptidase. The function of these proteins in strain An4 is currently not known.

3.4.2 Central acetogenesis metabolism, the acetyl-CoA pathway

All genes coding for enzymes involved in the acetyl-CoA pathway are present in the genome of *Sporomusa* strain An4 (Figure 3.1). Many of these genes are situated in close proximity with each other in scaffold 4, such as a methenyl-THF cyclohydrolase, methylene-THF dehydrogenase, the acetyl-CoA synthase operon and formate dehydrogenase (FDH) genes. The genes coding for the acetate kinase and the phosphate acetyltransferase are in separate scaffolds. The genome of strain An4 contains several genes that code for the same enzymes involved in the acetyl-CoA pathway, including formate-THF ligase (s04:246990-248750, s09:188329-186662), methenyl-THF cyclohydrolase (s02:879340-878696, s04:243851-244483), methylene-THF reductase (metF, s04:117333-118217, s04:264802-265755, s16:4696-6210), acetyl-CoA synthase catalytic subunit (acsB, s04:31610-32719, s04:250966-253092 and s06:160691-162826), and carbon monoxide dehydrogenase (CODH) catalytic subunit (cooS, s01:38061-40187, s04:31146-31481, s04:248953-250890). The proteomic analysis shows peptide abundance of the proteins involved in the acetyl-CoA pathway (Table 3.1), which indicates the synthesis of these proteins.

3.4.3 Growth with one-carbon substrates

One carbon substrates are characteristic growth substrates of *Sporomusa* species, including strain An4. Genes putatively coding for enzymes involved in one carbon-metabolism can be found in the genome of strain An4. Growth with CO for example involves genes coding for a CODH. As mentioned above the genome of strain An4 contains three genes that putatively code for the CODH catalytic subunit. One is part of the acetyl-CoA synthase operon (s04:248953-250890), one is situated up- and down-stream of genes coding for hypothetical proteins (s01:38061-40187), and one that is only 336 bp long is situated downstream of a small (1110 bp) *acsB* (s04:31146-31481). Only the *cooS* that is part of the acetyl-CoA synthase operon is expressed when *Sporomusa* strain An4 grows at the selected growth conditions (Table 3.1).

Sporomusa strain An4 can also grow with formate but formate can also be an intermediate of the acetyl-CoA pathway. The genome of strain An4 contains four putative FDHs. Two dimeric cytoplasmic FDHs (s02:691908-691925, s14:45413-48330), one dimeric periplasmic FDH (s02:705272-705302), the small subunit contains a tat motif, which indicates transport of the FDH complex into the periplasm. One trimeric cytoplasmic FDH (s04:265929-271744) that contains a predicted ferredoxin and NADH binding site, suggesting possible confurcating function. The latter FDH genes are situated upstream of the acetyl-CoA synthase operon (Figure 3.1) and the product of these FDH genes were measured in high abundance in the proteome analysis of all growth conditions (Table 3.1).

Table 3.1: Proteomic data of proteins involved in the acetyl-CoA pathway of Sporomusa strain An4. The table shows the predicted function of the proteins, the reference to the genome, and their related peptide abundance in the five different growth conditions: hydrogen and carbon dioxide (H_2 CO_2), methanol (MeOH), methanol and nitrate (NO_3^-), betaine (B), and fructose (F). The proteins that are part of the acetyl-CoA synthase operon and a formate dehydrogenase are boxed. Abbreviations are similar as used in Figure 3.1.

Function	Reference to genome	H_2 CO_2	MeOH	NO_3^-	B	F
Phosphate acetyltransferase	s01:1019277-1018705	31	29	16	25	42
acsB	s04:31610-32719	246	270	99	99	117
MetF	s04:117333-118217	5	6	4	2	7
Methenyl-THF cyclohydrolase	s04:243851-244483	102	118	41	51	86
Methylene-THF dehydrogenase	s04:244496-245359	79	128	40	67	100
Acetyl-CoA synthase operon						
cooC I	s04:256651-257406	28	57	10	43	77
formate-THF ligase	s04:246990-248750	2053	1769	971	944	1337
CooS	s04:248953-250890	718	619	232	278	353
acsB	s04:250966-253092	564	713	252	226	307
acsC	s04:253218-254561	673	779	635	476	819
ferredoxin	s04:254634-256604	130	153	77	50	71
cooC II	s04:256651-257406	28	57	10	43	77
acsD	s04:257428-258396	312	284	173	208	323
acsE (CH_3-THF methyltransferase)	s04:258478-259269	170	196	94	139	209
heterodisulfide reductase, C subunit	s04:259305-259895	30	38	31	14	42
heterodisulfide reductase, B subunit	s04:259892-260755	59	59	19	26	40
heterodisulfide reductase, A subunit	s04:260877-263705	291	312	181	116	210
methyl-viologen-reducing hydrogenase, delta subunit	s04:263708-264115	36	36	6	21	38
Zinc-finger protein	s04:264137-264805	64	81	46	34	76
MetF	s04:264802-265755	112	120	53	63	107
Formate dehydrogenase						
FDH gamma subunit	s04:265929-266465	35	36	40	24	52
FDH beta subunit	s04:266455-268209	235	224	186	148	275
FDH alpha subunit	s04:268226-271744	756	751	574	501	749
acsB	s06:160691-162826	137	146	76	53	93
acetate kinase	s07:150561-151763	160	175	116	193	195
formate-THF ligase	s09:188329-186662	311	364	1275	983	191
MetF	s16:4696-6210	6	10	14	7	2

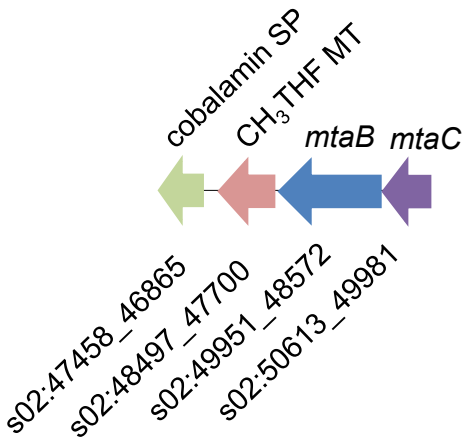

Figure 3.2: Methyltransferase genes, mtaB and mtaC, predicted to be involved in methanol-specific methyl transfer of Sporomusa strain An4. Including a CH_3-THF methyltransferase (CH_3-THF MT) and a cobalamin synthesis protein (cobalamin SP) upstream.

The genome of strain An4 contains a gene coding for a methyltransferase that is predicted to be methanol specific (s02:49951-48572). The amino acid sequence of this putative methyltransferase (MT) was used for BLAST analysis to find homologs. BLAST results showed 99% coverage and 62% amino acid identity with the methanol: corrinoid MT, MtaB, of *M. thermoacetica* (data not shown). Another MT gene (s02:50613-49951) is situated downstream of the methanol MT in the genome of *Sporomusa* strain An4. This gene is homologous to the MT MtaC of *M. thermoacetica*, with 98% coverage and 45% amino acid identity (data not shown). Situated upstream of the *mtaB* homolog is a CH_3-THF MT gene (s02:48497-47700) and a gene coding for a cobalamin synthesis protein (s02:47458-46865, Figure 3.2).

In *Moorella thermoacetica* the two genes *mtaB* and *mtaC* are known to code for two subunits of a methanol specific MT. Together with another MT, encoded by the *mtaA* gene, methyl transfer from methanol to THF is performed. Six possible *mtaA* genes can be found in the genome of *Sporomusa* strain An4. BLAST analysis showed that these six genes had a variety between 93% to 97% coverage and 24% to 31% identity with *MtaA* in *M. thermoacetica* (data not shown).

The proteome analysis revealed that the products of the two MT genes, *mtaB* and *mtaC,* had a high protein abundance in strain An4 when grown with methanol (Table 3.2). This strongly indicates that the products of these genes are produced. However, none of the six possible *mtaA* homologs showed any abundance in the proteome results of the methanol and the methanol with nitrate growth condition (Supplementary file S1). Moreover, the gene product of the CH_3-THF MT (s02:48497-47700) gene upstream of the *mtaB* showed high abundace in the methanol and the methanol with nitrate growth condition, suggesting its involvement in methanol metabolism. The MtaC protein is a cobalamin binding protein. Production of cobalamin biosynthesis and transport proteins by strain An4 was suggested by the proteome data (Supplementary file S1). More genes coding for MTs that function in a similar manner as the methanol MTs can be found in the genome of strain An4. These include genes putatively coding for tri-, di- and mono-methylamine (TMA, DMA and MMA, respectively) MTs, which could apart from being involved in the utilization of methylamines also be part of methyl group oxidation in the betaine metabolism.

Table 3.2: Proteomic data of proteins involved in methanol metabolism in Sporomusa strain An4. The table shows the predicted function of the proteins, the reference to the genome, and their related peptide abundance in the five different growth conditions: hydrogen and carbon dioxide (H_2 CO_2), methanol (MeOH), methanol and nitrate (NO_3^-), betaine (B), and fructose (F).

Function	Reference to genome	H_2 CO_2	MeOH	NO_3^-	B	F
CH_3-THF MT	s02:48497-47700	5	317	110	0	2
MtaB	s02:49951-48572	49	996	848	21	26
MtaC	s02:50613-49951	35	631	527	9	20

3.4.4 Betaine metabolism

Betaine was described to be utilized via reduction to trimethylamine and acetyl phosphate in *Sporomusa* species. The electrons required for this reaction can be generated via the oxidation of methyl groups [1,23]. The genome of *Sporomusa* strain An4 contains genes putatively coding for the glycine/sarcosine/betaine reductase components A, B and C. The substrate specificity of the three different reductases of *Eubacterium acidaminophilum* was described to be dependent on the strict specificity of the three different B components [24]. B components consist of an alpha and a beta subunit in an $\alpha_2\beta_2$ structure. Subunits GrdEB are described to be glycine specific, GrdGF sarcosine specific, and GrdIH betaine specific [24]. We aligned the amino acid sequence of the B components of *E. acidaminophilum* with those of *Sporomusa* strain An4 and constructed a Neighbor-Joining Tree (Supplementary file S2). The genome of An4 encodes two B components with an alpha and beta subunit. The two subunits of one B component (s02:956398-955076 and s02:955063-953744) cluster together with the GrdI and GrdH of *E. acidaminophilum*, suggesting specificity for betaine. The other two genes of strain An4 (s02:984589-983303 and s02:983278-981968), however, did not cluster clearly, leaving the substrate specificity indistinct.

The proteome results indicate the production of the glycine/sarcosine/betaine reductase components A, B and C by strain An4. This included both above described substrate specific B components, suggesting the production of a betaine reductase and a sarcosine or glycine reductase by strain An4. Additionally, a thioredoxin involved in these reductase catalysed reactions was also detected in the proteome analysis (Table 3.3).

The putative A component and beta subunit of the B components in strain An4 are selenocysteine containing proteins. Selenocysteine incorporation into a protein requires the presence of a selenocysteine incorporation system. Genes encoding such a system are present in the genome of strain An4. Additionally, the proteins involved in this system are produced by strain An4 (Table 3.3).

Many MTs showed high abundance during growth of strain An4 with betaine. These MTs were predominantly TMA MTs. Two other MTs showed high abundance in the betaine growth condition, tetrahydromethanopterin S-MT subunit H (s02:1027341-1026421) and a CH_3THF MT (s02:987110-986313), suggesting that they could be involved in the betaine metabolism of *Sporomusa* strain An4.

Table 3.3: Proteomic data of proteins involved in betaine metabolism and the selenocysteine incorporation system in Sporomusa strain An4. The table shows the predicted function of the proteins, the reference to the genome, and their related peptide abundance in the five different growth conditions: hydrogen and carbon dioxide (H_2 CO_2), methanol (MeOH), methanol and nitrate (NO_3^-), betaine (B), and fructose (F).

Function	Reference to genome	H_2 CO_2	MeOH	NO_3^-	B	F
MttA/MtbA/MtmA	s01:223800-222931	0	0	0	6	0
MttB	s01:235381-233915	12	2	48	159	7
MttB	s01:236881-235415	9	0	18	177	4
MttC	s01:237546-236914	9	1	30	140	4
Betaine reductase component B beta subunit	s02:955063-953744	20	97	34	634	33
Betaine reductase component B alpha subunit	s02:956398-955076	29	95	41	749	46
L-seryl-tRNA(Sec) selenium transferase	s02:957810-956425	0	0	4	9	0
Glycine/sarcosine/betaine reductase component C chain 2	s02:959004-957838	5	17	4	218	18
Glycine/sarcosine/betaine reductase component C chain 1	s02:960547-959009	21	85	48	612	46
Selenocysteine-specific translation elongation factor	s02:964433-962559	0	0	0	15	0
Selenide,water dikinase	s02:965472-964441	0	0	0	10	0
Glycine betaine transporter OpuD	s02:967011-965521	0	0	0	5	0
Glycine/sarcosine/betaine reductase protein A	s02:967496-967011	0	0	1	6	0
Glycine/sarcosine/betaine reductase component C chain 2	s02:969321-968155	1	3	9	67	5
Glycine/sarcosine/betaine reductase component C chain 1	s02:970864-969326	37	52	23	282	12
Thioredoxin	s02:971933-971616	7	2	0	64	2
MttB	s02:979643-978258	32	0	78	505	11
MttB	s02:981223-979757	37	7	108	474	25
MttC	s02:981887-981255	13	2	44	239	4
Glycine/sarcosine reductase component B beta subunit	s02:983278-981968	12	0	48	337	13
Glycine/sarcosine reductase component B alpha subunit	s02:984589-983303	5	0	11	105	0
5-CH_3THF homocysteine MT	s02:987110-986313	5	0	3	160	4
MttC	s02:1019796-1019149	0	0	0	8	0
MttA/MtbA/MtmA	s02:1020874-1019798	0	0	0	18	0
MttC	s02:1024844-1024197	0	1	0	229	11
MttB	s02:1026315-1024885	2	0	3	701	24
N5-CH_3-tetrahydromethanopterin coM MT subunit H	s02:1027341-1026421	3	8	4	539	11
MttB	s03:82561-81161	0	0	0	11	0

3.4.5 Hydrogen metabolism

The genome of *Sporomusa* strain An4 contains four [FeFe] hydrogenases and three [NiFe] hydrogenases, divided in the following groups: One trimeric NADH binding (possible bifurcating) [FeFe] hydrogenase (s02:952536-948975); One trimeric membrane associated [FeFe] hydrogenase (s02:218844-216550), with a cytochrome b as the membrane associated subunit; Two single [FeFe] hydrogenases, one is predicted to be cytoplasmic (s01:660545-659154) and the other membrane associated (s04:173095-175008); One dimeric membrane linked [NiFe] hydrogenase (s02:868100- 865482); One dimeric cytoplasmic [NiFe] hydrogenase (s01:852958-855286); One trimeric periplasmic membrane associated hydrogenase (s04:378765-382552). The small subunit (s04:378765-379895) of this hydrogenase contains a tat signal motif, which suggests transport of the complex to the periplasm. Moreover, the membrane associated subunit is a putative 4 transmembrane helix containing cytochrome b. The proteome results showed protein abundance of the NiFe hydrogenase (s04:378765-382552) and NADH binding [FeFe] hydrogenase (s02:952536-948975) in all five growth conditions (Supplementary data S1). No other hydrogenases were detected in the proteome.

Table 3.4: Proteomic data of proteins involved in the fructose metabolism in Sporomusa strain An4. The table shows the predicted function of the proteins, the reference to the genome, and their related peptide abundance in the five different growth conditions: hydrogen and carbon dioxide (H_2 CO_2), methanol (MeOH), methanol and nitrate (NO_3^-), betaine (B), and fructose (F).

Function	Reference to genome	H_2 CO_2	MeOH	NO_3^-	B	F
Pyruvate kinase	s01:263433-263185	0	0	0	0	0
Fructose-bisphosphate aldolase	s01:453162-454010	4	21	0	15	9
Fructose-bisphosphate aldolase	s01:586052-585123	18	38	14	21	67
Pyruvate kinase	s01:768932-770686	12	32	19	20	19
Enolase	s02:168899-167613	40	53	88	84	85
phosphoglycerate mutase	s02:170488-168947	2	3	5	2	6
Triosephosphate isomerase	s02:171258-170506	7	12	11	10	12
Phosphoglycerate kinase	s02:172467-171280	13	9	10	16	25
NAD-dependent glyceraldehyde-3-phosphate dehydrogenase	s02:173554-172547	64	75	97	77	121
Phosphoenolpyruvate-protein phosphotransferase of PTS system	s03:92519-90783	11	24	33	25	262
PTS system, fructose-specific IIA component	s03:93272-92820	1	7	1	4	28
PTS system, fructose-specific IIB and IIC component	s03:94704-93331	2	6	2	1	24
1-phosphofructokinase	s03:95679-94741	0	0	0	0	9
Transcriptional repressor of the fructose operon	s03:96462-95692	0	1	0	0	16
Pyruvate,phosphate dikinase	s14:90011-92668	218	267	275	292	1147

3.4.6 Fructose metabolism

Sporomusa strain An4 was described, like *S. ovata*, to grow with fructose, but not with glucose [11]. The genome of *Sporomusa* strain An4 contains all genes required for the fermentation of fructose-6-phosphate to pyruvate and eventually acetate. Additionally, the phosphotransferase system (PTS) necessary to transport fructose into the bacterial cell and simultaneously phosphorylate the sugar, to fructose-6-phosphate, is also encoded in the genome of strain An4. Moreover, all proteins necessary for fructose degradation were detected in the proteome analysis (Table 3.4).

3.4.7 Electron acceptor metabolism

Sporomusa strain An4, like *Sporomusa ovata*, reduces nitrate via nitrite to ammonium [11]. In the genome of strain An4 genes involved in nitrate reduction and nitrite reduction were identified (Figure 3.3). The *napGHCA* genes, are positioned next to each other. Additionally, a *nrfH* (s06:206354-206827) and *nrfA* (s06:206820-208109) gene are near the napGHCA cluster. Between the *napGHCA* cluster and the *nrfHA* nitrite reduction genes are cytochrome c biosynthesis genes, *ccmA* (s06:200761-201282), *ccmB* (s06:201254-201931), *ccmC* (s06:201946-202620), *ccmE* (s06:202620-202982), and a *ccmF* gene (s06:202990-205176). Moreover, a hydroxylamine reductase gene (s06:208981-210624) is upstream the *nrfH* and *nrfA* genes.

Another gene known to be involved in cytochrome c biosynthesis, *ccdA* gene, is also present in the genome of strain An4 (s04:361456-362160). In addition, gene copies of the *ccmA* (s01:189649-189035, s09:89626-89012) *ccmB* (s01:188958-188383, s09:89037-88360), *ccmC* (s01:188374-187715, s09:88351-87692), *ccmE* (s01:187718-187347, s09:87695-87324), *ccmF* (s09:87327-85135), *nrfH* (s09:85098-84625), *nrfA* (s09:84632-83349), and hydroxylamine reductase (s09:81617-83281) are present in the genome.

Nitrate reductase, nitrite reductase, hydroxylamine reductase and cytochrome c biosynthesis proteins are all detected in the proteome analysis (Table 3.5). However, these proteins are mainly encoded by the genes illustrated in figure 3.3. Nearly none of the gene copy products showed protein abundance.

As mentioned the ability of strain An4 to reduce (per)chlorate was lost. Typical genes involved in perchlorate reduction were not found in the genome.

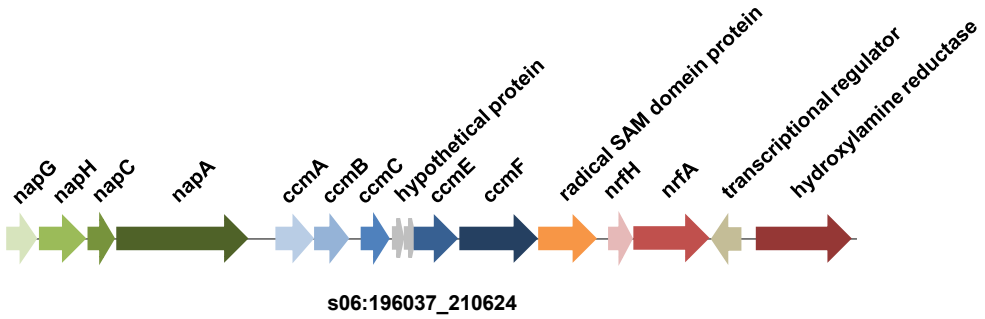

Figure 3.3: Relative location of nitrate reduction genes, nitrite reduction genes, c type cytochrome biosynthesis genes and neighbouring genes in the Sporomusa strain An4 draft genome.

Table 3.5: Proteomic data of proteins involved in nitrate reduction, nitrite reduction and the biosynthesis of cytochrome c in Sporomusa strain An4. The table shows the predicted function of the proteins, the reference to the genome, and their related peptide abundance in the five different growth conditions: hydrogen and carbon dioxide (H_2 CO_2), methanol (MeOH), methanol and nitrate (NO_3^-), betaine (B), and fructose (F).

Function	Reference to genome	H_2 CO_2	MeOH	NO_3^-	B	F
NapG	s06:196037-196582	2	5	29	10	0
NapH	s06:196582-197379	0	0	9	0	0
NapA	s06:197916-200177	0	0	170	0	0
CcmA	s06:200761-201282	0	0	5	0	0
CcmC	s06:201946-202620	0	0	5	0	0
CcmF	s06:202990-205176	0	0	37	0	0
Heme biosynthesis protein	s06:205231-206214	0	0	10	0	0
NrfH	s06:206354-206827	0	0	24	0	0
NrfA	s06:206820-208109	5	1	177	3	2
Hydroxylamine reductase	s06:208981-210624	10	18	76	11	9
Hydroxylamine reductase	s09:81617-83281	0	5	1	0	0
NrfA	s09:84632-83349	4	6	2	3	2

Table 3.6 Enzyme activity (in U/mg) measured from cell free extracts of Sporomusa strain An4 cells grown with H_2 and CO_2, methanol (MeOH), and methanol and nitrate (NO_3^-). Enzymes measured included carbon monoxide dehydrogenase (CODH), formate dehydrogenase (FDH), nitrate reductase (NO_3^- reductase) and nitrite reductase (NO_2^- reductase). The activity values are averages of biological replicates (n3). Standard deviation (SD) between replicates are included. Moreover, reference to the proteome/genome is given and the proteome data values are included in parentheses.

Enzyme name	Reference to proteome/ genome	H_2 CO_2	SD	MeOH	SD	NO3-	SD
CODH	CooS/ s04:248953-250890	1.47 (718)	0.2	1.37 (619)	0.15	0.45 (232)	0.06
FDH	FDH alpha subunit/ s04:268226-271744	2.44 (756)	0.18	2.2 (751)	0.2	1.86 (574)	0.15
NO_3^- reductase	NapA/ s06:197916-200177	0.55 (0)	0.11	0.77 (0)	0.13	5.88 (170)	0.18
NO_2^- reductase	NrfA/ s06:206820-208109	0.37 (5)	0.15	0.51 (1)	0.07	8.1 (177)	0.2

3.4.8 Enzyme activity measurements

Additional enzyme activity measurements were performed on some of the key enzymes to relate the abundances of proteins determined by proteomics to protein function. The enzymes measured are: carbon monoxide dehydrogenase, formate dehydrogenase, nitrate reductase and nitrite reductase. Enzymes were measured from the cell free extract from cells grown with H_2 and CO_2, methanol, and methanol and nitrate. Activities were measured in all three growth

conditions, which indicates that the proteins are produced. Moreover, the nitrate reductase and the nitrite reductase activities are higher in cell free extracts of cells grown with methanol and nitrate.

3.5 Discussion

By combining genome and proteome analysis, physiological information about *Sporomusa* strain An4 was obtained. Strain An4 was isolated with methanol and perchlorate, but unfortunately, the strain had lost its ability to use perchlorate as electron acceptor before we could analyse the proteins involved. Moreover, the genome comparison with *Sporomusa ovata* did not result in candidate genes that could be involved in the perchlorate reduction of strain An4. Clark et al. describes that chlorate reduction genes are flanked by insertion sequences and suggests that it is a highly mobile metabolism [55]. In *Alicycliphilus denitrificans* strain BC the chlorate reduction genes are located on a plasmid [56]. Apparently, *Sporomusa* strain An4 lost genes involved in perchlorate reduction before the start of our experiments. The deposited DSM strain cannot reduce (per) chlorate any more either.

The genome comparison between *Sporomusa ovata* and *Sporomusa* strain An4 showed only a few differences. The function of these proteins and why they are present in strain An4 and not in *S. ovata* cannot be concluded from our analysis. Furthermore, the comparison showed an ANI value that was higher than the 95 to 96% value that corresponds to the 70% DNA-DNA hybridization level. Therefore, we can conclude that *Sporomusa* strain An4 is a *Sporomusa ovata* strain.

The proteome analysis was performed without biological replicates. Therefore, growth conditions cannot be well compared when changes in protein levels occur, but the proteome data indicate whether a protein is abundantly produced at a certain growth condition. Higher protein abundance lowers the chance of false positives, making it more reliable that a protein is produced. In addition, four enzyme activities were measured to support that protein abundance in the proteome data corresponds to protein production.

The proteome results indicate the production of proteins involved in cobalamin synthesis and transport. Cobalamin is essential for growth with methanol due to the production of the cobalamin binding MtaC, which is involved in methanol metabolism. However, this was partly expected from previous experiments with *Sporomusa ovata.* Stupperich et al. [16] showed that a cobalamin binding methanol specific MT was expressed by *S. ovata* and they hypothesized that the enzyme was involved in the cleavage of the C-O bond of methanol, the transfer of the CH_3 of methanol metabolism or both. Later, the CH_3-group from methanol was found to be transferred to THF, creating CH_3-THF and an entrance into the acetyl-CoA pathway [15]. CH_3 transfer of methanol in the close relative *Moorella thermoacetica* was shown to be due to three enzyme subunits that are homologs of the methanogenic methanol:coenzyme M MT system [27,28]. This system is composed of two MTs [29,30]. Methanol: 5-hydroxybenzimidazolylcobamide MT is the first MT and consists of two subunits, MtaB and MtaC [31]. MtaB catalyzes the transfer of the CH_3 group from methanol to a corrinoid bound to MtaC. The second MT consists of only one subunit (MtaA), which catalyzes the transfer of the CH_3 bound to MtaC to coenzyme M [29,30,32,33]. In *Moorella thermoacetica* the CH_3 is transferred to THF by the MtaA homolog [28].

We found three MT gene products that have high abundance when grown with methanol and with methanol and nitrate. Two of these MT genes have high similarity to the *mtaB* and *mtaC* of *Moorella thermoacetica*. However, no putative *mtaA* gene product was abundant when strain

An4 was grown with methanol or methanol and nitrate. Instead the gene product of a putative CH_3-THF MT gene, situated upstream of the *mtaB*, showed a high abundance. This suggests its involvement in the methanol metabolism. Therefore, we propose a novel methanol metabolism without the involvement of a MtaA homolog. Instead of MtaA, the CH_3-THF MT transfers the CH_3 group bound to MtaC to THF (Figure 3.4B).

The FDH upstream of the acetyl-CoA synthase operon is the only FDH with peptide counts in all five growth conditions. This together with the proximity of the FDH to the acetyl-CoA synthase operon suggests that this FDH is generally involved in the acetyl-CoA pathway. The other FDHs present in the genome might be involved in other growth conditions, for example in growth with formate as a substrate.

In the proteome nearly all the proteins involved in the reduction of nitrate are present when nitrate was added as electron acceptor. NapA is the periplasmic nitrate reductase which obtains its electrons from the cytoplasmic membrane quinol pool by electron transport of either NapC or NapGH. Both NapC and NapGH are quinol dehydrogenases. They can be present in microorganisms separately or together [34-38]. Although *napC* was present in the genome, its

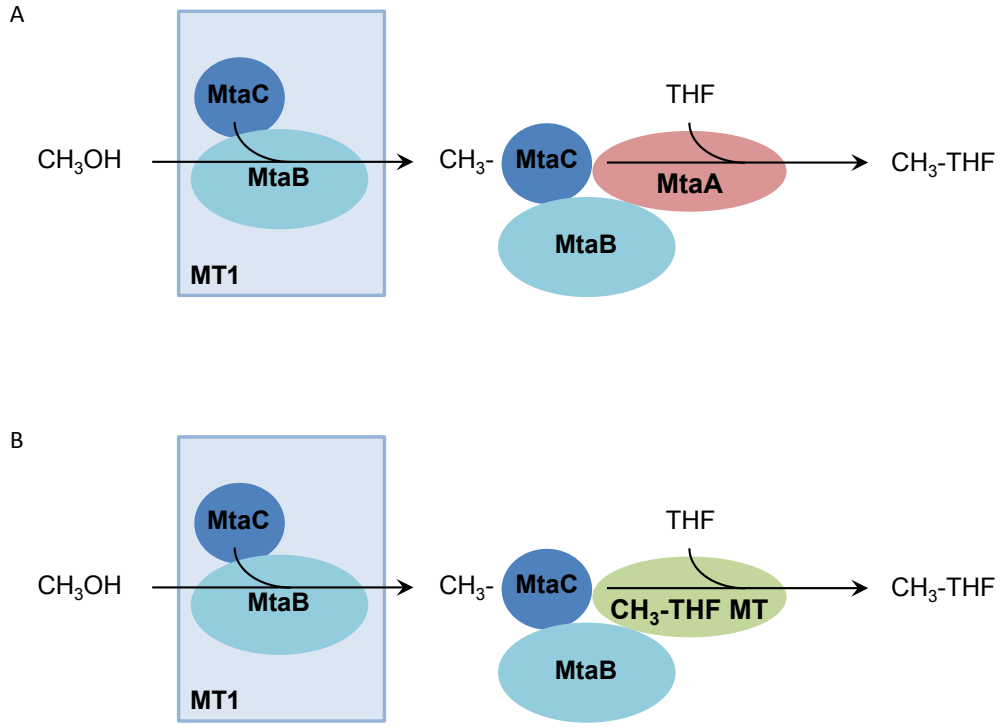

Figure 3.4: Methanol metabolism of Moorella thermoacetica (A) and proposed methanol metabolism in Sporomusa strain An4 (B). The AcsB subunit of methanol methyltransferase one (MT1) cleaves the C-O bond of methanol and transfers the CH_3 to the MtaC subunit. Subsequently, in M. thermoacetica MtaA catalyses the transfer of the CH_3 group to THF (A). In Sporomusa strain An4 the CH_3-THF MT catalyses the transfer of the CH_3 group to THF, creating CH_3-THF (B).

product was not found in the proteomics data. This could mean that either strain An4 only uses the NapGH quinol dehydrogenase complex to transport electrons to nitrate reductase NapA, or the quinol dehydrogenase NapC was not detected, since it is a membrane protein. Membrane proteins like NapC can be difficult to extract and hence difficult to detect compared to periplasmic and cytoplasmic proteins.
In nitrate reduction c-type cytochromes are important for the translocation of electrons. The biosynthesis of c-type cytochromes, also called the Ccm system, consists of up to ten components. These components are CcmA to CcmI and CcdA or DsbD [39]. In *Sporomusa* strain An4 *ccmA*, *ccmB*, *ccmC, ccmE* and *ccmF* can be found in the genome near the nitrate reduction genes. A *ccdA* gene is also present in the An4 genome, but only CcmA, CcmC and CcmF protein levels were detected. CcmB, CcmE and CcdA are membrane proteins and therefore might not be detected.

High abundance of betaine reductase was found when *Sporomusa* strain An4 was grown with betaine. Additionally, high enzyme levels were found for another reductase, a glycine or sarcosine reductase (s02:984589-981968). Since *Sporomusa* strain An4 can grow with both sarcosine and glycine [11] it is not immediately clear which substrate specificity this enzyme has.
Sporomusa ovata can only utilize sarcosine, not glycine, and produces methylamine, acetate and CO_2, which suggests the involvement of a reductive cleavage reaction. Moreover, Möller et al. [1] also suggested that during growth with betaine a small amount of betaine was demethylated to N,N dimethyl-glycine in *Sporomusa* species. Subsequently, this N,N dimethyl-glycine was presumably demethylated further to sarcosine. This, together with the fact that the genome comparison between the two *Sporomusa* strains did not indicate that strain An4 uses a different reaction for sarcosine utilization, leads us to think that strain An4 uses a sarcosine reductase for betaine degradation and not a glycine reductase.
The proteome analysis shows high abundance of many MTs, predominantly TMA MTs, during growth with betaine. However, TMA is one of the main end products of betaine degradation in *Sporomusa* species, including strain An4 (data not shown). The betaine reductase requires electrons that can be generated via the oxidation of methyl groups [1,23]. The TMA MTs, the DMA MT, and the MMA MT might be involved in the oxidation of small amounts of TMA to NH_4. However, this does not explain the many TMA MT enzymes that are produced during growth with betaine.
Two other MTs, tetrahydromethanopterin S-MT subunit H and a CH_3THF MT, also showed high abundance in the proteomics results during growth with betaine. The gene coding for the tetrahydromethanopterin S-MT subunit H is also present in the genome of *Sporomusa ovata,* but is designated as a methyltransferase 2. MtaA, MtmA, MtbA and MttA MTs are also methyltransferase 2 enzymes. The tetrahydromethanopterin S-MT subunit H could, therefore, be involved in the methyl transfer from a corrinoid bound TMA MT to THF; or maybe the MTs that have high abundance in strain An4 during growth with betaine are somehow involved in demethylation of betaine to sarcosine. Clearly, growth with betaine leads to the production of many MTs in *Sporomusa* strain An4.

This study improved our understanding of the pathways involved in the different growth conditions. Moreover, it revealed novel insights on the methanol metabolism of *Sporomusa* strain An4.

3.6 Acknowledgements

Our research is funded by grants of the division of Chemical Sciences (CW-TOP 700.55.343) and Earth and Life Sciences (ALW 819.02.014) of the Netherlands Organisation for Scientific Research (NWO), and of The Netherlands Proteomics Centre embedded in the Netherlands Genomics Initiative.

3.7 References

1. Möller, B., OBmer, R., Howard, B.H.,Gottsehalk, G., Hippe, H. *Sporomusa*, a new genus of gram-negative anaerobic bacteria including *Sporomusa sphaeroides* spec. nov. and *Sporomusa ovata* spec. nov. *Archives of Microbiology* **139**(4), 388-96 (1984).
2. Dehning, I., Stieb, M., Schink, B. *Sporomusa malonica* sp. nov., a homoacetogenic bacterium growing by decarboxylation of malonate or succinate. *Archives of Microbiology* **151**(5), 421-6 (1989).
3. Hermann, M., Popoff, M.R., Sebald, M. *Sporomusa paucivorans* sp. nov., a methylotrophic bacterium that forms acetic acid from hydrogen and carbon dioxide. *International Journal of Systemic Bacteriology* **37**, 93-101 (1987).
4. Sass, H., Wieringa, E., Cypionka, H., Babenzien, H.D., Overmann, J. High genetic and physiological diversity of sulfate-reducing bacteria isolated from an oligotrophic lake sediment. *Archives of Microbiology* **170**(4), 243-51 (1998).
5. Ollivier, B., Cordruwiseh, R., Lombardo, A., Garcia, J.L. Isolation and characterization of *Sporomusa acidovorans* sp. nov., a methylotrophic homoacetogenic bacterium *Archives of Microbiology* **142**(3), 307-10 (1989).
6. Boga, H.I., Ludwig, W., Brune, A. *Sporomusa aerivorans* sp. nov., an oxygen-reducing homoacetogenic bacterium from the gut of a soil-feeding termite. *International Journal of Systematic and Evolutionary Microbiology* **53**(5), 1397-1404 (2003).
7. Breznak, J.A. and Switzer, J.M.Acetate Synthesis from $H(_2)$ plus $CO(_2)$ by Termite Gut Microbes. *Applied Environmental Microbiolology* **52**(4), 623-30 (1986).
8. Breznak, J.A., Switzer, J.M., Seitz, H.J. *Sporomusa termitida* sp. nov., an H_2/CO_2-utilizing acetogen isolated from termites. *Archieves of Microbiology* **150**(3), 282-8 (1988).
9. Drake, H.L., Daniel, S.L., Küsel, K., Matthies, C., Kuhner, C., Braus-Stromeyer, S. Acetogenic bacteria: what are the in situ consequences of their diverse metabolic versatilities? *Biofactors* **6**(1), 13-24 (1997).
10. Drake, H.L., A.S. Göβner, and S.L. Daniel, Old acetogens, new light. Annals of the *New York Academy of Sciences* 2008. p. 100-128 (2008).
11. Balk, M., Mehboob, F., van Gelder A.H., Rijpstra, I.C., Sinninghe Damsté, J.S., Stams A.J.M. (Per)chlorate reduction by an acetogenic bacterium, *Sporomusa* sp., isolated from an underground gas storage. *Applied Microbiology and Biotechnology* **88**(2), 595-603 (2010).
12. Stupperich, E., Eisinger, H.J., Albracht, S.P., Evidence for a super-reduced cobamide as the major corrinoid fraction in vivo and a histidine residue as a cobalt ligand of the p-cresolyl cobamide in the acetogenic bacterium *Sporomusa ovata*. *European journal of biochemistry / FEBS*, **193**(1), 105-9 (1990).
13. Stupperich, E., Eisinger, H.J., Krautler, B. Diversity of corrinoids in acetogenic bacteria. P-cresolylcobamide from *Sporomusa ovata*, 5-methoxy-6-methylbenzimidazolylcobamide from *Clostridium formicoaceticum* and vitamin B12 from *Acetobacterium woodii*. *European journal of biochemistry / FEBS* **172**(2), 459-64 (1988).
14. Stupperich, E., Eisinger, H.J., Krautler, B. Identification of phenolyl cobamide from the homoacetogenic bacterium *Sporomusa ovata*. *European journal of biochemistry / FEBS* **186**(3), 657-61 (1989).
15. Stupperich, E. and Konle, R. Corrinoid-dependent methyl transfer reactions are involved in methanol and 3,4-Dimethoxybenzoate Metabolism by *Sporomusa ovata*. Applied Environmental Microbiolpgy, **59**(9): p. 3110-6 (1993).
16. Stupperich, E., Aulkemeyer, P., Eckerskorn, C. Purification and characterization of a methanol-induced cobamide-containing protein from *Sporomusa ovata*. *Archieves of Microbiology* **158**(5), 370-3 (1992).
17. Wagner, U.G., Stupperich, E., Aulkemeyer, P., Kratky, C. Crystallization and preliminary X-ray diffraction studies of a corrinoid protein from *Sporomusa ovata*. *Journal of Molecular Biology* **236**(1), 388-9 (1994).

18. Kamlage, B. and Blaut, M. Isolation of a cytochrome-deficient mutant strain of *Sporomusa sphaeroides* not capable of oxidizing methyl groups. *Journal of Bacteriology* **175**(10), 3043-50 (1993).
19. Dobrindt, U. and Blaut, M. Purification and characterization of a membrane-bound hydrogenase from *Sporomusa sphaeroides* involved in energy-transducing electron transport. *Archieves of Microbiology* **165**(2), 141-7 (1996).
20. Wagner, U.G., Stupperich, E., Kratky, C. Structure of the molybdate/tungstate binding protein mop from *Sporomusa ovata*. *Structure* **8**(11), 1127-36 (2000).
21. Poehlein, A., Gottschalk, G., Daniel, R. First Insights into the genome of the Gram-negative, endospore-forming organism *Sporomusa ovata* strain H1 DSM 2662. *Genome Announcement* **1**(5) 2013.
22. Aziz, R.K., Bartels, D., Best, A.A., DeJongh, M., Disz, T., Edwards, R.A., Formsma, K., Gerdes, S., Glass, E.M., Kubal, M., Meyer, F., Olsen, G.J., Olson, R., Osterman, A.L., Overbeek, R.A., McNeil, L.K., Paarmann, D., Paczian, T., Parrello, B., Pusch, G.D., Reich, C., Stevens, R., Vassieva, O., Vonstein, V., Wilke, A., Zagnitko, O. The RAST Server: rapid annotations using subsystems technology. *BMC genomics* **9**, 75 (2008).
23. Andreesen, J.R. Glycine metabolism in anaerobes *Antonie van Leeuwenhoek* **66**, 223-37 (1994).
24. Meyer, M., Granderath, K., Andreesen, J.R., Purification and characterization of protein P, of betaine reductase and its relationship to the corresponding proteins glycine reductase and sarcosine reductase from *Eubacterium acidaminophilum*. *European Journal of Biochemestry* **234**, 184-91 (1995).
25. Geer, L.Y., Markey, S.P., Kowalak, J.A., Wagner, L., Xu, M., Maynard, D.M., Yang, X., Shi, W., Bryant, S.H. *Journal of Proteome Research* **3**(5), 958-64 (2004).
26. Liu, H., Sadygov, R.G., Yates J.R., A Model for Random Sampling and Estimation of Relative Protein Abundance in Shotgun Proteomics. *Analytical Chemistry* **76**, 4193-201 (2004).
27. Das, A., Fu, Z.Q., Tempel, W., Liu, Z.J., Chang, J., Chen, L., Lee, D., Zhou, W., Xu, H., Shaw, N., Rose, J.P., Ljungdahl, L.G., Wang, B.C. Characterization of a corrinoid protein involved in the C1 metabolism of strict anaerobic bacterium *Moorella thermoacetica. Proteins* **67**(1), 167-76 (2007).
28. Pierce, E., et al., The complete genome sequence of *Moorella thermoacetica (f. Clostridium thermoaceticum). Environmental Microbiology* **10**(10), 2550-73 (2008).
29. van der Meijden, P., Heythuysen, H.J., Pouwels, A., Houwen, F., van der Drift, C., Vogels, G.D. Methyltransferases involved in methanol conversion by *Methanosarcina barkeri. Archives of Microbiology* **134**, 238-42 (1983).
30. van der Meijden, P., te Brömmelstroet, B.W., Poirot, C.M., van der Drift, C., Vogels, G.D. Purification and properties of methanol:5-hydroxybenzimidazolylcobamide methyltransferase from *Methanosarcina barkeri. Journal of Bacteriology* **160**(2), 629-35 (1984).
31. Sauer, K., Harms, U., Thauer, R.K. Methanol:coenzyme M methyltransferase from *Methanosarcina barkeri.* Purification, properties and encoding genes of the corrinoid protein MT1. *European Journal of Biochemestry* **243**(3), 670-7 (1997).
32. Harms, U. and Thauer, R.K. Methylcobalamin: coenzyme M methyltransferase isoenzymes MtaA and MtbA from *Methanosarcina barkeri.* Cloning, sequencing and differential transcription of the encoding genes, and functional overexpression of the mtaA gene in *Escherichia coli. European Journal of Biochemestry* **235**(3), 653-9 (1996).
33. LeClerc, G.M. and Grahame, D.A. Methylcobamide:coenzyme M methyltransferase isozymes from *Methanosarcina barkeri.* Physicochemical characterization, cloning, sequence analysis, and heterologous gene expression. *European Journal of Biochemestry* **271**(31), 18725-31 (1996).
34. Brondijk, T.H., Fiegen, D., Richardson, D.J., Cole, J.A. Roles of NapF, NapG and NapH, subunits of the *Escherichia coli* periplasmic nitrate reductase, in ubiquinol oxidation. *Molecular Microbiology* **44**(1), 245-55 (2002).
35. Brondijk, T.H., Nilavongse, A., Filenko, N., Richardson, D.J., Cole, J.A. NapGH components of the periplasmic nitrate reductase of *Escherichia coli* K-12: location, topology and physiological roles in quinol oxidation and redox balancing. *Biochemestry Journal* **379**(1), 47-55 (2004).
36. Kern, M. and Simon, J. Characterization of the NapGH quinol dehydrogenase complex involved in *Wolinella succinogenes* nitrate respiration. *Molecular Microbiology* **69**(5), 1137-52 (2008).
37. Kern, M. and J. Simon, Periplasmic nitrate reduction in *Wolinella succinogenes:* cytoplasmic NapF facilitates NapA maturation and requires the menaquinol dehydrogenase NapH for membrane attachment. *Microbiology* **155**(8),

2784-94 (2009).

38. Simpson, P.J., Richardson, D.J., Codd, R. The periplasmic nitrate reductase in *Shewanella:* the resolution, distribution and functional implications of two NAP isoforms, NapEDABC and NapDAGHB. *Microbiology* **156**(2), 302-12 (2010).
39. Sanders, C., Turkarslan, S., Lee, D.W., Daldal, F. Cytochrome c biogenesis: the Ccm system. *Trends in Microbiology* **18**(6), 266-74 (2010).
40. Stams, A.J., Van Dijk, J.B., Dijkema, C., Plugge, C.M. Growth of syntrophic propionate-oxidizing bacteria with fumarate in the absence of methanogenic bacteria. *Applied Environmental Microbiology* **59**(4), 1114-9 (1993).
41. Droege, M. and Hill, B. The Genome Sequencer FLX System-longer reads, more applications, straight forward bioinformatics and more complete data sets. *Journal of Biotechnology* **136**(1-2), 3-10 (2008).
42. Boetzer, M., Henkel, C.V., Jansen, H.J., Butler, D., Pirovano, W. Scaffolding preassembled contigs using SSPACE. *Bioinformatics* **27**, 578 –579 (2011).
43. Boetzer, M., Pirovano, W. Toward almost closed genomes with GapFiller. Genome Biology **13**, R56 (2012).
44. Meiring, H.D., van der Heeft, E., ten Hove, G.J. Nanoscale LC-MS(n): technical design and applications to peptide and protein analysis. *Journal of Separation Science* **25**(9), 557-68 (2002).
45. Elias, J.E. and Gygi, S.P. Target-decoy search strategy for increased confidence in large-scale protein identifications by mass spectrometry. *Nature Methods* **4**, 207-14 (2007) .
46. Edgar, R.C. MUSCLE: multiple sequence alignment with high accuracy and high throughput. *Nucleic Acids Research* **32**, 1792-7 (2004).
47. Punta, M., Coggill, P.C., Eberhardt, R.Y., Mistry, J., Tate, J., Boursnell, C., Pang, N., Forslund, K., Ceric, G., Clements, J., Heger, A., Holm, L., Sonnhammer, E.L.L., Eddy, S.R., Bateman, A., Finn, R.D. The Pfam protein families database. *Nucleic Acids Research* **40**, D290-D301 (2012).
48. Moller, S., Croning, M.D.R., Apweiler, R. Evaluation of methods for the prediction of membrane spanning regions. *Bioinformatics* **17**, 646-53 (2001).
49. Bendtsen, J.D., Nielsen, H., Widdick, D., Palmer, T., Brunak, S. Prediction of twin-arginine signal peptides BMC. *Bioinformatics* **6**, (2005).
50. Vignais, P.M., Billoud, B. Occurrence, classification, and biological function of hydrogenases: an overview. *Chemical Reviews* **107**, 4206-72 (2007).
51. Mathews, D.H., Sabina, J., Zuker, M., Turner, D.H. Expanded sequence dependence of thermodynamic parameters improves prediction of RNA secondary structure *Journal of Molecular Biology* **288**, 911-40 (1999).
52. Zuker, M. Mfold web server for nucleic acid folding and hybridization prediction *Nucleic Acids Research* **31**, 3406-15 (2003).
53. Zhang, Y. & Gladyshev, V.N. An algorithm for identification of bacterial selenocysteine insertion sequence elements and selenoprotein genes. *Bioinformatics* **21**, 2580-9 (2005).
54. Richter, M. & Rossello-Mora, R. Shifting the genomic gold standard for the prokaryotic species definition. *Proceedings of the National Academy of Sciences of the United States of America* **106**, 19126-31 (2009).
55. Clark, I.C., Melnyk, R.A., Engelbrektson, A., Coates, J.D., Structure and evolution of chlorate reduction composite transposons. *MBio* **6**,4(4) e00379-13 (2013).
56. Oosterkamp, M.J., Veuskens, T., Plugge, C.M., Langenhoff, A.A., Gerritse, J., van Berkel, W.J., Pieper, D.H., Junca, H., Goodwin, L.A., Daligault, H.E., Bruce, D.C., Detter, J.C., Tapia, R., Han, C.S., Land, M.L., Hauser, L.J., Smidt, H., Stams, A.J.M. Genome sequences of *Alicycliphilus denitrificans* strains BC and K601T. *Journal of Bacteriology* **193**(18): 5028-9 (2011).

Chapter 4

Genome analysis of *Desulfotomaculum kuznetsovii* strain 17^T reveals a physiological similarity with *Pelotomaculum thermopropionicum* strain SI^T

Michael Visser, Petra Worm, Gerard Muyzer, Inês A.C. Pereira, Peter J. Schaap, Caroline M. Plugge, Jan Kuever, Sofiya N. Parshina, Tamara N. Nazina, Anna E. Ivanova, Rizlan Bernier-Latmani, Lynne A. Goodwin, Nikos C. Kyrpides, Tanja Woyke, Patrick Chain, Karen W. Davenport, Stefan Spring, Hans-Peter Klenk, Alfons J.M. Stams

Standards in Genomic Sciences (2013) 8:69-87

4.1 Abstract

Desulfotomaculum kuznetsovii is a moderately thermophilic member of the polyphyletic sporeforming genus *Desulfotomaculum* in the family *Peptococcaceae*. This species is of interest because it originates from deep subsurface thermal mineral water at a depth of about 3000 m. *D. kuznetsovii* is a rather versatile bacterium as it can grow with a large variety of organic substrates, including short-chain and long-chain fatty acids, which are degraded completely to carbon dioxide coupled to the reduction of sulfate. It can grow methylotrophically with methanol and sulfate and autotrophically with H_2 + CO_2 and sulfate. For growth it does not require any vitamins. Here, we describe the features of *D. kuznetsovii* together with the genome sequence and annotation. The chromosome has 3,601,386 bp organized in one contig. A total of 3567 candidate protein encoding genes and 58 RNA genes were identified. Genes of the acetyl-CoA pathway, possibly involved in heterotrophic growth with acetate and methanol, and in CO_2 fixation during autotrophic growth are present. Genomic comparison revealed that D. kuznetsovii shows a high similarity with *Pelotomaculum thermopropionicum*. Genes involved in propionate metabolism of these two strains show a strong similarity. However, main differences are found in genes involved in the electron acceptor metabolism.

4.2 Introduction

Desulfotomaculum kuznetsovii strain 17^T (VKM B-1805; DSM 6115) is a moderately thermophilic sulfate reducing bacterium isolated from deep subsurface thermal mineral water [1]. It grows with a wide range of substrates, including organic acids, such as long-chain fatty acids, short-chain fatty acids (butyrate, propionate, acetate), lactate, pyruvate, fumarate and succinate as well as ethanol and methanol. These substrates are degraded to CO_2 coupled to sulfate reduction. The strain is also able to grow autotrophically with H_2, CO_2 and sulfate and to ferment pyruvate and fumarate. For growth, *D. kuznetsovii* has no vitamin requirement.

Desulfotomaculum is a genus of Gram-positive, spore forming anaerobes that is phylogenetically and physiologically very diverse. The genus is poorly studied physiologically, while its members are known to play an important role in the carbon and sulfur cycle in a variety of often adverse environments. The genus is divided phylogenetically into different subgroups [2,3]. To get a thorough understanding of the evolutionary relationship of the different *Desulfotomaculum* subgroups and the physiology of the individual species, it is important to have genome sequence information. Here, we present a summary of the features of *D. kuznetsovii* strain 17^T, together with the description of the complete genomic sequencing and annotation. Moreover, we describe a physiological and genomic comparison of *D. kuznetsovii* strain 17^T and *Pelotomaculum thermopropionicum strain* SI^T, because phylogenetically *P. thermopropionicum* is the closest related organism with a validly published name that has a completely sequenced genome. However, the two strains have different physiological traits. For example, *P. thermopropionicum* is not able to grow by sulfate reduction, but is able to grow in syntrophy with methanogens. *D. kuznetsovii* lacks this ability. By comparing the genomes of the two bacteria we were able to identify the main similarities and differences.

4.3 Classification and features

D. kuznetsovii is a member of the phylum Firmicutes. Phylogenetic analysis of the 16S rRNA genes of *D. kuznetsovii* shows that it clusters in *Desulfotomaculum* cluster 1. This cluster not only contains *Desulfotomaculum* species, but also members of the genera *Sporotomaculum*, *Cryptanaerobacter*

and *Pelotomaculum*. *D. kuznetsovii* is part of subgroup 1c together with *D. solfataricum*, *D. luciae*, *D. thermosubterraneum*, *D. salinum*, *D. australicum*, and *D. thermocisternum*, while *Pelotomaculum* species belong to subgroup 1h (Figure 4.1) [3].

D. kuznetsovii cells are rod shaped (1.0-1.4 x 3.5-5 µm) with rounded ends and peritrichous flagella (Figure 4.2). Spores of *D. kuznetsovii* are spherical (1.3 µm in diameter) and centrally located causing swelling of the cells. *D. kuznetsovii* grows between 50 and 85°C, but the optimal growth temperature is 60-65°C. The substrates *D. kuznetsovii* can grow with are completely oxidized to CO_2. Suitable electron acceptors are sulfate, thiosulfate and sulfite. *D. kuznetsovii* is also able to grow by fermentation of pyruvate and fumarate. A summary of the classification and general features of *D. kuznetsovii* is presented in Table 4.1 [1].

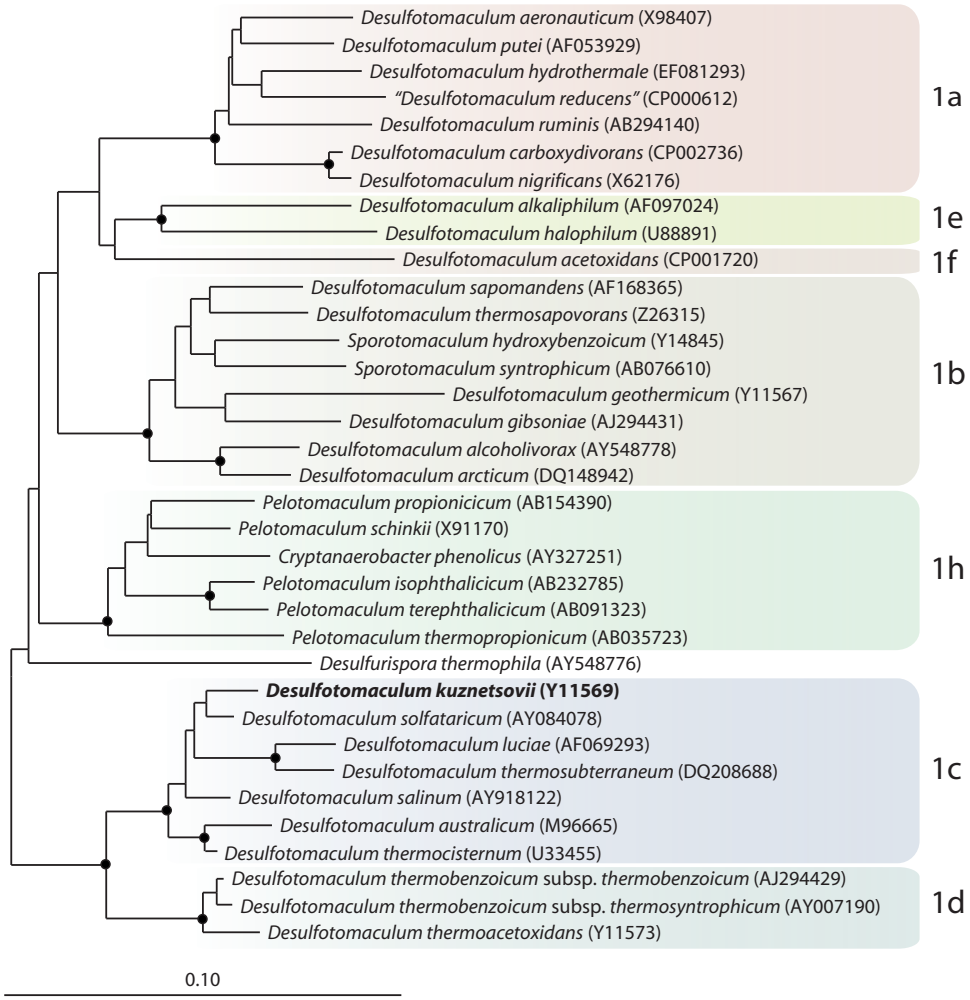

Figure 4.1: Neighbor joining tree based on 16S rRNA sequences showing the phylogenetic affiliation of Desulfotomaculum and related species divided in the subgroups of Desulfotomaculum cluster 1. D. kuznetsovii is printed in bold type. The sequences of different Thermotogales were used as outgroup, but were pruned from the tree. Closed circles represent bootstrap values between 75 and 100%. The scale bar represents 10% sequence difference.

Table 4.1: Classification and general features of D. kuznetsovii DSM 6115 according to the MIGS recommendations [4].

MIGS ID	Property	Term	Evidence code[a]
	Current classification	Domain *Bacteria*	TAS [5]
		Phylum *Firmicutes*	TAS [6-8]
		Class *Clostridia*	TAS [9, 10]
		Order *Clostridiales*	TAS [11, 12]
		Family *Peptococcaceae*	TAS [12, 13]
		Genus *Desulfotomaculum*	TAS [12-14]
		Species *Desulfotomaculum kuznetsovii*	TAS [1,16]
		Type strain 17	
	Gram stain	Positive	TAS [1]
	Cell shape	Rods	TAS [1]
	Motility	peritrichous flagella	TAS [1]
	Sporulation	oval, terminal or subterminal, slightly swelling the cell.	TAS [1]
	Temperature range	50-85°C	TAS [1]
	Optimum temperature	60-65°C	TAS [1]
	Carbon source	CO_2 (autotrophic) and organic substrates (heterotrophic)	TAS [1]
	Energy source	Sulfate-dependent growth and fermentative growth with pyruvate and fumarate.	TAS [1]
	Electron acceptor	Sulfate, thiosulfate and sulfite.	TAS [1]
MIGS-6	Habitat	Geothermal groundwater, sediment and hot solfataric fields.	TAS [1, 15, 16]
MIGS-6.3	Salinity	2-3% NaCl	TAS [1]
MIGS-22	Oxygen	Obligate anaerobes	TAS [1]
MIGS-15	Biotic relationship	Free living	TAS [1]
MIGS-14	Pathogenicity	None	
MIGS-4	Geographic location	Sukhumi, Georgia	TAS [1]
MIGS-5	Sample collection time	1987 or before	TAS [1]
MIGS-4.1	Latitude	43.009	TAS [1]
MIGS-4.2	Longitude	40.989	TAS [1]
MIGS-4.3	Depth	2800-3250 m	TAS [1]

Evidence codes - TAS: Traceable Author Statement (i.e., a direct report exists in the literature); NAS: Non-traceable Author Statement (i.e., not directly observed for the living, isolated sample, but based on a generally accepted property for the species, or anecdotal evidence). Evidence codes are from the Gene Ontology project [17].

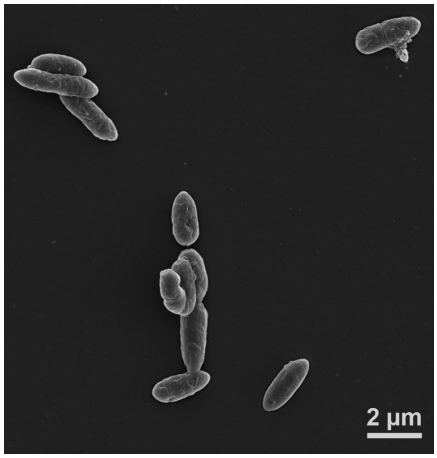

Figure 4.2: Scanning electron microscopic photograph of D. kuznetsovii.

4.4 Genome sequencing and annotation

Genome project history

D. kuznetsovii was selected for sequencing in the DOE Joint Genome Institute Community Sequencing Program 2009, proposal 300132_795700 'Exploring the genetic and physiological diversity of *Desulfotomaculum* species', because of its phylogenetic position in one of the *Desulfotomaculum* subgroups, its important role in bioremediation, and its ability to use propionate, acetate and methanol for growth. The genome project is listed in the Genome OnLine Database (GOLD) [18] as project Gc01781, and the complete genome sequence was deposited in Genbank. Sequencing, finishing and annotation of the *D. kuznetsovii* genome were performed by the DOE Joint Genome Institute (JGI). A summary of the project information is shown in Table 4.2.

4.5 Growth conditions and DNA isolation

D. kuznetsovii was grown anaerobically at 60°C in bicarbonate buffered medium with propionate and sulfate as substrates [1]. DNA of cell pellets was isolated using the standard DOE-JGI CTAB method recommended by the DOE Joint Genome Institute (JGI, Walnut Creek, CA, USA). In short, cells were resuspended in TE (10 mM tris; 1 mM EDTA, pH 8.0). Subsequently, cells were lysed using lysozyme and proteinase K, and DNA was extracted and purified using CTAB and phenol:chloroform:isoamylalcohol extractions. After precipitation in 2-propanol and washing in 70% ethanol, the DNA was resuspended in TE containing RNase. Followed by a quality and quantity check using agarose gel electrophoresis in the presence of ethidium bromide, and spectrophotometric measurement using a NanoDrop ND-1000 spectrophotometer (NanoDrop® Technologies, Wilmington, DE, USA).

4.6 Genome sequencing and assembly

The genome was sequenced using a combination of Illumina and 454 sequencing platforms. All general aspects of library construction and sequencing can be found at the JGI website [19]. Pyrosequencing reads were assembled using the Newbler assembler (Roche). The initial Newbler assembly consisting of 81 contigs in five scaffolds was converted into a phrap [20] assembly by making fake reads from the consensus, to collect the read pairs in the 454 paired end library. Illumina

GAii sequencing data (570.2 Mb) was assembled with Velvet [21] and the consensus sequences were shredded into 1.5 kb overlapped fake reads and assembled together with the 454 data. The 454 draft assembly was based on 134.6 Mb 454 draft data and all of the 454 paired end data. Newbler parameters are -consed -a 50 -l 350 -g -m -ml 20. The Phred/Phrap/Consed software package [20] was used for sequence assembly and quality assessment in the subsequent finishing process. After the shotgun stage, reads were assembled with parallel phrap (High Performance Software, LLC). Possible mis-assemblies were corrected with gapResolution [19], Dupfinisher [22], or sequencing cloned bridging PCR fragments with subcloning. Gaps between contigs were closed by editing in Consed, by PCR and by Bubble PCR primer walks (J.F. Chang, unpublished). A total of 400 additional reactions and one shatter library were necessary to close gaps and to raise the quality of the finished sequence. Illumina reads were also used to correct potential base errors and increase consensus quality using a software Polisher developed at JGI [23]. The error rate of the completed genome sequence is less than 1 in 100,000. Together, the combination of the Illumina and 454 sequencing platforms provided 188.8 x coverage of the genome. The final assembly contained 323,815 pyrosequence and 15,594,144 Illumina reads.

4.7 Genome annotation

Genes were identified using Prodigal [24] as part of the Oak Ridge National Laboratory genome annotation pipeline, followed by a round of manual curation using the JGI GenePRIMP pipeline [25]. The predicted CDSs were translated and used to search the National Center for Biotechnology Information (NCBI) nonredundant database, UniProt, TIGR-Fam, Pfam, PRIAM, KEGG, COG, and InterPro databases. Additional gene prediction analysis and functional annotation was performed within the Integrated Microbial Genomes - Expert Review (IMG-ER) platform [26].

Table 4.2: Genome sequencing project information.

MIGS ID	Property	Term
MIGS-31	Finishing quality	Finished
MIGS-28	Libraries used	Four genomic libraries: one Illumina shotgun library, one 454 standard library, two paired end 454 libraries
MIGS-29	Sequencing platforms	Illumina GAii, 454 Titanium
MIGS-31.2	Fold coverage	158.2 × illumina; 30.6 × pyrosequencing
MIGS-30	Assemblers	VELVET, version 0.7.63; Newbler, version 2.3. phrap version SPS - 4.24
MIGS-32	Gene calling method	Prodigal 1.4, GenePRIMP
	INSDC ID	CP002770.1
	Genome Database release	July 20, 2012
	Genbank Date of Release	May 24, 2011
MIGS-13	GOLD ID NCBI project ID Source material identifier	Gc01781 48313 DSM 6115^T
	Project relevance	Obtain insight into the phylogenetic and physiological diversity of *Desulfotomaculum* species, and bioremediation.

4.8 Genome properties and genome comparison with other strains

The genome of *D. kuznetsovii* consists of a circular chromosome of 3,601,386 bp with 54.88% GC content (Table 4.3 and Figure 4.3). 4.66% of the total number of genes was identified as pseudo genes. Of the 3.625 genes predicted, 3,567 are protein-coding genes of which 2,560 are assigned to COG functional categories. The distribution of these genes into COG functional categories is presented in Table 4.4.

The genome of *D. kuznetsovii* has 58 RNA genes of which three are 16S rRNA genes. This is one more than the previously described rrnA and rrnB [27]. These two rRNA genes contained two large inserts, one at the variable 5'terminal region and one at the variable 3'terminal region. The main differences between the two rRNA genes were found in these inserts. These inserts were hypothesized to be involved in the operation of ribosomes at high temperatures. However, more research is needed to assess the function of these inserts. All three rRNA genes of *D. kuznetsovii* have a size of approximately 1,700 nucleotides. This suggests that the third rRNA gene might also contain inserts. Alignment of the 16S rRNA genes confirmed the presence of inserts in all three 16S rRNA genes (data not shown).
BLAST analysis [28, 29] of the genes of *D. kuznetsovii* against genes in the KEGG Sequence Similarity DataBase revealed similarity with other *Desulfotomaculum* strains (Table 4.5), *D. acetoxidans*, *D. carboxydivorans*, "*D. reducens*" and *D. ruminis*, but interestingly also with non-*Desulfotomaculum* strains. *D. kuznetsovii* contains 873 genes with high similarity to genes of *Pelotomaculum thermopropionicum*, which is more than to any of the sequenced *Desulfotomaculum* species. Moreover, we identified the conserved proteins of *D. kuznetsovii* across three related fully sequenced species (Table 4.6). The bidirectional best blast hits showed that despite the smaller genome of *P. thermopropionicum* it contained more homologous predicted proteins with *D. kuznetsovii* (1406) compared to *D. acetoxidans* (1309) and "*D. reducens*" (1330). This suggests a strong physiological similarity between *D. kuznetsovii* and *P. thermopropionicum*.

Table 4.3 Genome statistics.

Attribute	Value	% of total[a]
Genome size (bp)	3,601,386	100.00
Genome coding region (bp)	3057959	84.91
Genome G+C content (bp)	1,976,601	54.88
Total genes	3,625	100.00
RNA genes	58	1.60
Protein-coding genes	3567	98.40
Genes in paralog clusters	1373	37.88
Genes assigned to COGs	2560	70.62
Pseudo genes	169	4.66
Genes with signal peptides	582	16.06
Genes with transmembrane helices	748	20.63

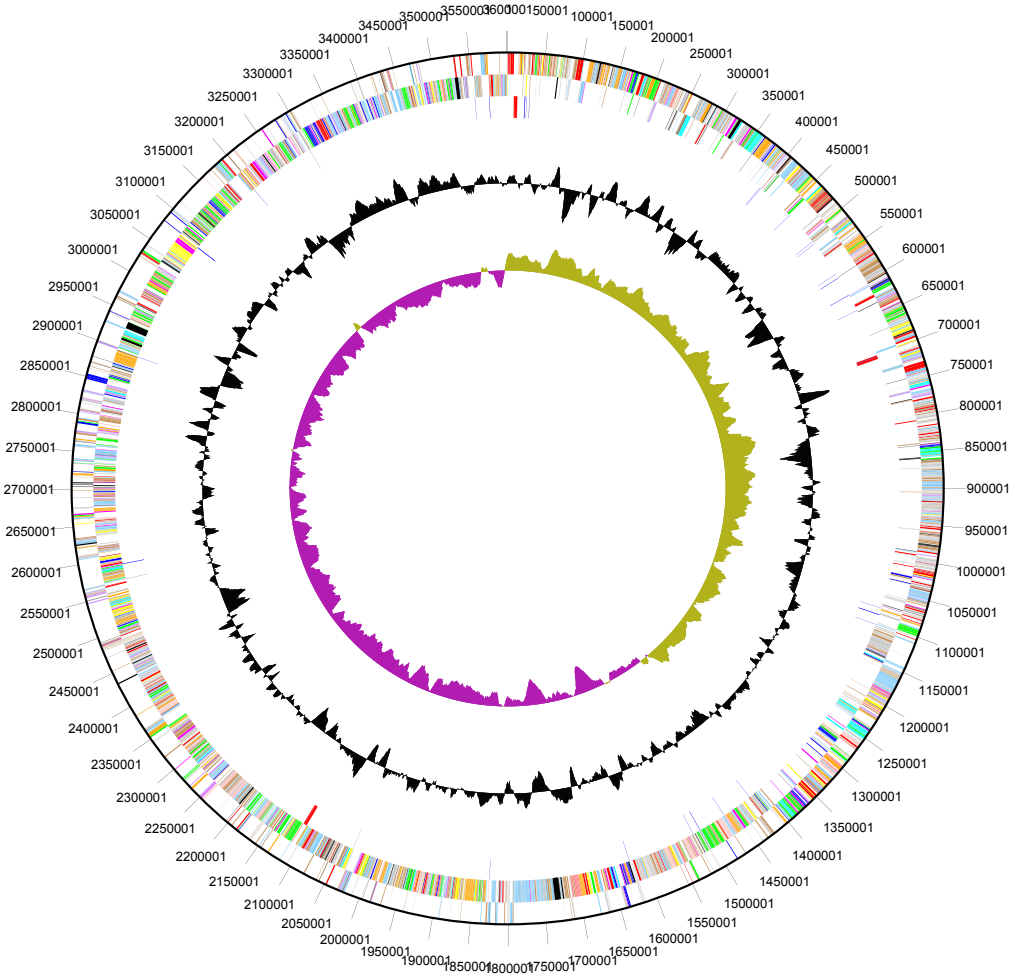

Figure 4.3: Graphical map of the chromosome of D. kuznetsovii. From outside to the centre: Genes on the forward strand (colored by COG categories), Genes on the reverse strand (colored by COG categories), RNA genes (tRNAs green, rRNAs red, other RNAs black), GC content, GC skew.

Table 4.4: Number of genes associated with the general COG functional categories.

Code	Value	**%age**[a]	Description
J	148	5.32	Translation
A	0	0.00	RNA processing and modification
K	184	6.61	Transcription
L	207	7.44	Replication, recombination and repair
B	2	0.07	Chromatin structure and dynamics
D	60	2.16	Cell cycle control, mitosis and meiosis
Y	0	0.00	Nuclear structure
V	35	1.26	Defense mechanisms
T	177	6.36	Signal transduction mechanisms
M	122	4.38	Cell wall/membrane biogenesis
N	79	2.84	Cell motility
Z	2	0.07	Cytoskeleton
W	0	0.00	Extracellular structures
U	75	2.69	Intracellular trafficking and secretion
O	81	2.91	Posttranslational modification, protein turnover, chaperones
C	261	9.38	Energy production and conversion
G	106	3.81	Carbohydrate transport and metabolism
E	197	7.08	Amino acid transport and metabolism
F	55	1.98	Nucleotide transport and metabolism
H	158	5.68	Coenzyme transport and metabolism
I	89	3.20	Lipid transport and metabolism
P	127	4.56	Inorganic ion transport and metabolism
Q	122	3.58	Secondary metabolites biosynthesis, transport and catabolism
R	331	11.89	General function prediction only
S	257	9.23	Function unknown
-	1,065	29.38	Not in COGs

Table 4.5: Taxonomic distribution of the top KEGG hits of D. kuznetsovii genes based on BLAST against KEGG database. Species that had more than 50 genes similar to D. kuznetsovii were included in this table, others were only summarized in categories.

Kingdom	Category	Species	Hits
Archaea			91
	Crenarchaeota		9
	Euryarchaeota		81
	Thaumarchaeota		1
Bacteria			2,963
	Acidobacteria		2
	Actinobacteria		16
	Alphaproteobacteria		13
	Bacteroidetes		5
	Betaproteobacteria		14
	Cyanobacteria		19
	Deinococcus-Thermus		16
	Deltaproteobacteria		62
	Epsilonproteobacteria		1
	Firmicutes		2,728
		Ammonifex degensii	170
		Carboxydothermus hydrogenoformans	58
		Desulfotomaculum acetoxidans	310
		Candidatus Desulforudis audaxviator	154
		Desulfotomaculum carboxydivorans	268
		Desulfotomaculum reducens	111
		Desulfotomaculum ruminis	132
		Moorella thermoacetica	183
		Pelotomaculum thermopropionicum	873
		Thermincola potens JR	104
	Fusobacteria		2
	Gammaproteobacteria		12
	Green nonsulfur bacteria		20
	Green sulfur bacteria		4
	Hyperthermophilic bacteria		31
	Other Proteobacteria		1
	Spirochaetes		9
	Synergistetes		6

	Verrucomicrobia		2
Eukaryotes			3
	Plants		1
	Protists		2
NULL			342
TOTAL			3,399

Table 4.6: Proteins homologous to D. kuznetsovii proteins in three related species with fully sequenced genomes†. Numbers in bolt represent the highest number of homologous proteins.

Subject DB / Input Query	*Desulfotomaculum acetoxidans*	*Desulfotomaculum kuznetsovii*	*Desulfotomaculum reducens*	*Pelotomaculum thermopropionicum*
Desulfotomaculum acetoxidans	4068	1539	1525	1486
		1309	1316	1255
Desulfotomaculum kuznetsovii	1509	3398	1518	**1645**
	1309		1330	**1406**
Desulfotomaculum reducens	1537	1571	3276	1438
	1316	1330		1211
Pelotomaculum thermopropionicum	1430	**1600**	1395	2919
	1255	**1406**	1211	

† BlastP analyses were performed using standard settings and best hits were filtered for 40% identity over an alignment length of 75 amino acids as a minimum requirement. The values show the number of predicted proteins that are homologous to the query species in each row. The number of similar proteins obtained with an unidirectional BLAST is indicated in light grey. Bidirectional best blast hits are indicated in dark grey. Proteomes were obtained from ftp.ncbi.nih.gov/Bacteria/. Accession numbers are in parenthesis: D. acetoxidans (NC_013216); D. kuznetsovii (NC_015573);"D. reducens" (NC_009253); Pelotomaculum thermopropionicum (NC_009454).

4.9 Insights into the genome

4.9.1 Involvement of the acetyl-coA pathway in growth with acetate and methanol

D. kuznetsovii oxidizes acetate completely to CO_2. The pathway of acetate degradation has not been studied yet, but sulfate reducers may employ the tricarboxylic acid (TCA) cycle or the acetyl-CoA pathway for acetate degradation, as exemplified by *Desulfobacter postgatei* and *Desulfobacca acetoxidans*, respectively [30]. Most genes predicted to code for enzymes of the TCA cycle are present in the genome of *D. kuznetsovii*, but genes with similarity to those coding for an ATP-dependent citrate synthase and isocitrate dehydrogenase are missing. This suggests that the TCA cycle is not complete and that the TCA cycle enzymes have mainly an anabolic function or a function in other catabolic pathways, such as the propionate degradation pathway. Genes

with similarity to those coding for enzymes involved in the acetyl-CoA pathway are all present in the genome of *D. kuznetsovii* (Figure 4.4), which suggests its involvement in acetate oxidation. However, there are no genes similar to those that code for acetate kinase and phosphate acetyltransferase present in the genome. The reaction from acetate to acetyl-CoA is likely performed by acetyl-CoA synthetase (Desku_1241).

D. acetoxidans is an acetate oxidizing *Desulfotomaculum* species, positioned in subgroup 1e (Figure 4.1), that also uses the acetyl-CoA pathway for acetate oxidation to CO_2 [31]. The genes involved in acetate oxidation in *D. acetoxidans* are similar to those in *D. kuznetsovii*, but there are some exceptions. The genome of *D. acetoxidans* does not contain a gene that putatively codes for acetyl-CoA synthetase, similar to *D. kuznetsovii*, but contains genes that putatively code for an acetate kinase and a phosphate acetyltransferase [32]. Additionally, putative carbon-monoxide dehydrogenase complex coding genes involved in the acetyl-CoA pathway show differences between the two *Desulfotomaculum* species. *D. kuznetsovii* lacks a ferredoxin coding gene that

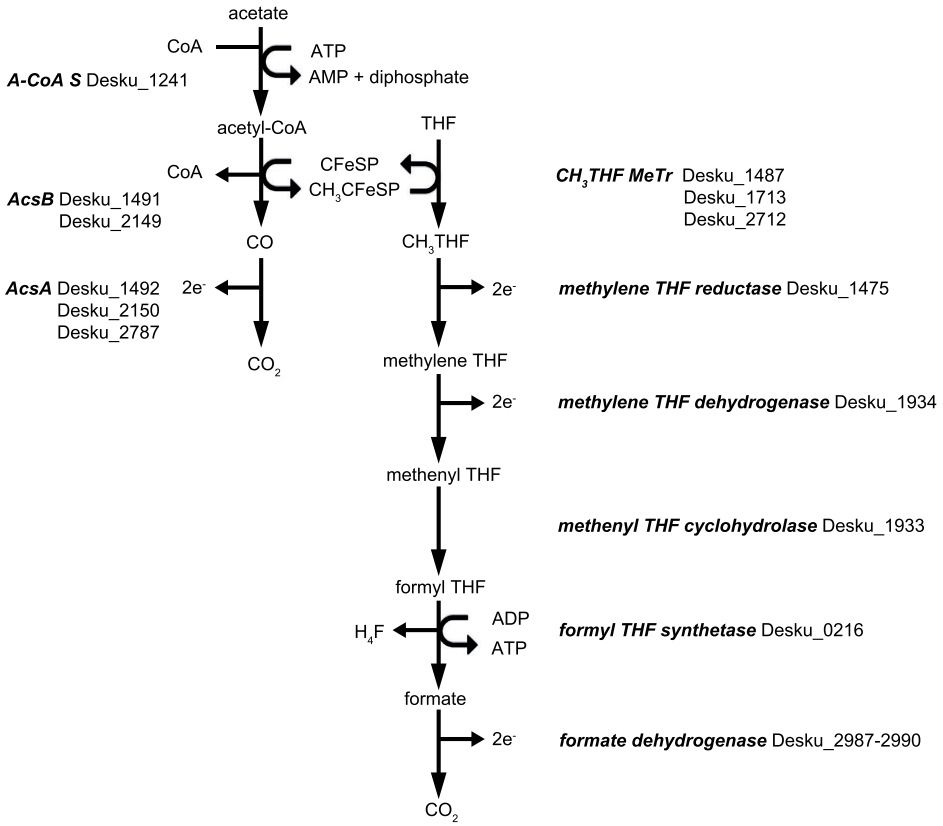

Figure 4.4: Pathway of acetate oxidation to CO2 by D. kuznetsovii. Enzymes in this figure are in bold italic and their locus tags are included. Genes with the locus tags Desku_1488 and Desku_1490 putatively code for the small subunit and the large subunit of the iron-sulfur protein, respectively. This protein is involved in transferring the methyl from acetyl-CoA to tetrahydrofolate. Abbreviations: A-CoA S, acetyl-CoA synthetase; AcsA, carbon-monoxide dehydrogenase; AcsB, acetyl-CoA synthase; CFeSP, iron-sulfur protein; CH3, methyl; THF, tetrahydrofolate; MeTr, methyltransferase.

is located between *cooC* (Desku_1493) and *acsE* (Desku_1487), which in contrast is present in the genome of *D. acetoxidans* (Dtox_1273). Moreover, three genes similar to heterodisulfide reductase encoding genes (Desku_1486-1484) are located upstream of *acsE* in *D. kuznetsovii*, which is not the case in the genome of *D. acetoxidans*.

Table 4.7: Genes in D. kuznetsovii that are annotated as enzymes involved in propionate metabolism†.

Gene symbol	Locus tag	Function	Homologous protein in *P. thermopropionicum*	
			Identity (%)	Locus tag
sdhB	Desku_0434	Succinate dehydrogenase, FeS protein	76	PTH_1018
sdhA	Desku_0435	Succinate dehydrogenase, flavoprotein	76	PTH_1017
sdhC	Desku_0436	Succinate dehydrogenase, cytochrome b	51	PTH_1016
citE	Desku_1348	Citrate lyase	57	PTH_1335
sdhA	Desku_1353	Succinate dehydrogenase, flavoprotein	83	PTH_1491
sdhB	Desku_1354	Succinate dehydrogenase, FeS protein	75	PTH_1490
mmcB	Desku_1358	Fumarase, N-terminal domain	73	PTH_1356
mmcC	Desku_1359	Fumarase, C-terminal domain	77	PTH_1357
mmcD2	Desku_1361	Succinyl-CoA synthetase, alpha subunit	78	PTH_1359
mmcE	Desku_1362	Methylmalonyl-CoA mutase, N-terminal domain	77	PTH_1361
mmcF	Desku_1363	Methylmalonyl-CoA mutase, C-terminal domain	82	PTH_1362
mmcG	Desku_1364	Methylmalonyl-CoA epimerase	86	PTH_1363
mmcH	Desku_1365	Methylmalonyl-CoA decarboxylase, alpha subunit	75	PTH_1364
mmcI	Desku_1366	Methylmalonyl-CoA decarboxylase, epsilon subunit	82	PTH_1365
mmcJ	Desku_1367	Methylmalonyl-CoA decarboxylase, gamma subunit	56	PTH_1366
mmcK	Desku_1368	Malate dehydrogenase	75	PTH_1367
mmcL	Desku_1369	Transcarboxylase 5S subunit	66	PTH_1368
pykF	Desku_1651	Pyruvate kinase	73	PTH_2214
ppsA	Desku_2615	Pyruvate phosphate dikinase	78	PTH_0903
citE	Desku_2747	Citrate lyase	56	PTH_1335

†Corresponding homologs in P. thermopropionicum are included.

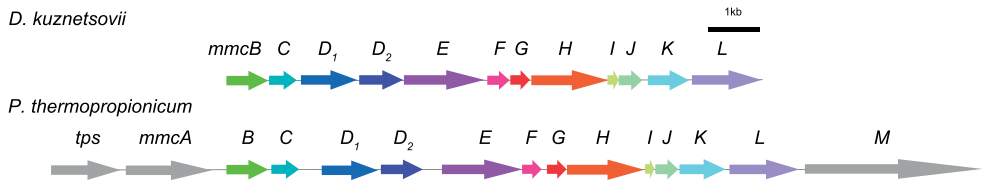

Figure 4.5: Gene organization of the mmc cluster in D. kuznetsovii and P. thermopropionicum. Names of the genes can be found in table 4.7, except for tps, which is a transposase gene.

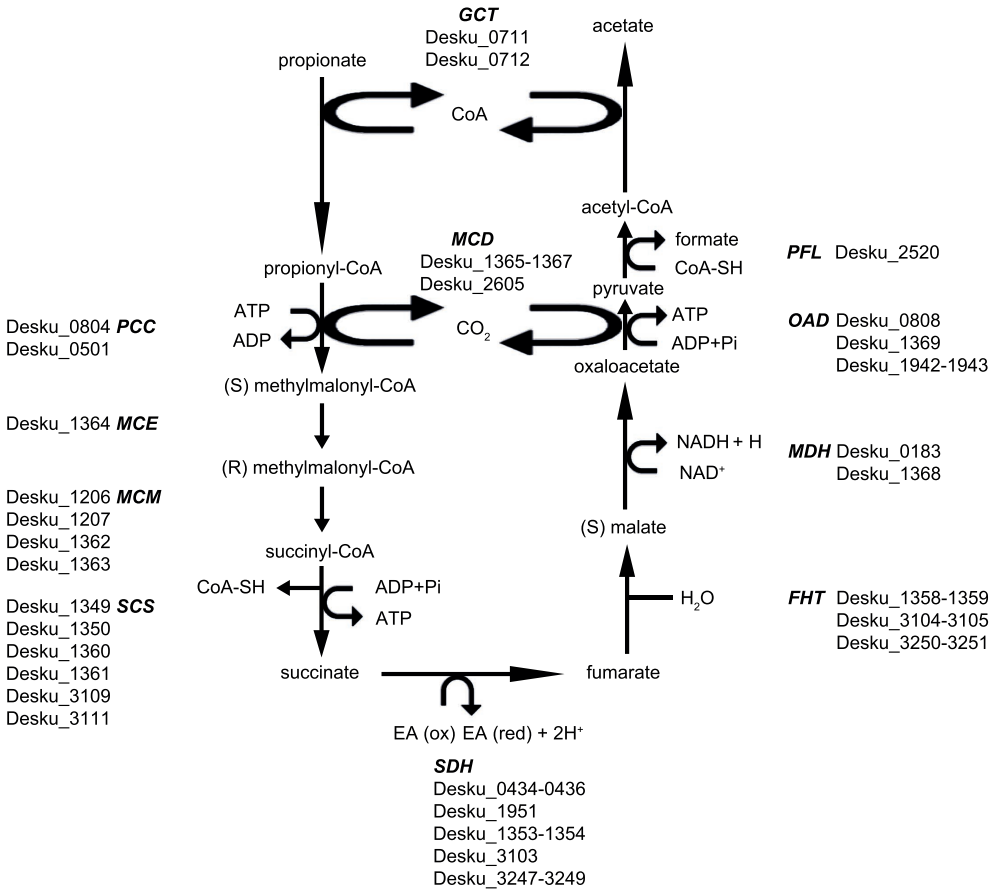

Figure 4.6: Propionate degradation pathway in D. kuznetsovii based on genomic data. Enzymes are depicted in bold italic. Next to these enzymes are the possible encoding genes, and their locus tags. GCT, Glutaconate CoA-transferase; MCD, Methylmalonyl-CoA decarboxylase; PCC, Propionyl-CoA carboxylase; MCE, Methylmalonyl-CoA epimerase; MCM, Methylmalonyl-CoA mutase; SCS, Succinyl-CoA synthetase; SDH, Succinate dehydrogenase; FHT, Fumarase; MDH, Malate dehydrogenase; OAD, Oxaloacetate decarboxylase; PFL, Pyruvate formate lyase.

4.9.2 Methanol metabolism

Growth of *D. kuznetsovii* with methanol and sulfate was studied [33]. In that study the activity of methyltransferase, an enzyme that is involved in methanol metabolism in methanogens and acetogens [34, 35], could not be assessed, while low activities of an alcohol dehydrogenase could be measured. An alcohol dehydrogenase with a molecular mass of 42 kDa was partially purified and showed activity with methanol [33]. The genome of *D. kuznetsovii* contains several alcohol dehydrogenase genes (Desku_0165, 0619, 0624, 0628, 2955, 3082) that each code for an enzyme with a size of approximately 42 kDa. In the genome, genes with similarity to those coding for a methanol methyltransferase *mtaA* (Desku_0050, 0055, 0060), *mtaB* (Desku_0051) and *mtaC* (Desku_0048, 0049, 0052, 0056) were also found, suggesting a methanol metabolism as described in *Moorella thermoacetica* [34]. Further studies are needed to obtain information about the diversity of the methanol-degradation pathways in *D. kuznetsovii*.

4.9.3 Comparison of D. kuznetsovii and P. thermopropionicum genomes

Genomic comparison revealed that a large number of *D. kuznetsovii* genes show similarity to genes of *Pelotomaculum thermopropionicum*, a syntrophic propionate oxidizing thermophile (Table 4.5 and 4.6). Interestingly, among them are genes that putatively code for enzymes involved in propionate metabolism (Table 4.7). Moreover, the genetic organization of the methylmalonyl-CoA (mmc) cluster in the genome of both bacteria is similar (Figure 4.5). However, *D. kuznetsovii* lacks *tps*, *mmcA* and *mmcM* in the mmc cluster. *mmcA* codes for a response regulator and *mmcM* for pyruvate ferredoxin oxidoreductase.

Based on 16S rRNA gene sequences, *D. kuznetsovii* and *P. thermopropionicum* group in cluster group c and h of the *Desulfotomaculum* cluster 1, respectively (Figure 4.1). *P. thermopropionicum* is known for its ability to grow with propionate and ethanol in syntrophic association with methanogens. It is not able to grow by sulfate respiration, despite the presence of sulfate reduction genes in the genome [36]. In contrast, *D. kuznetsovii* is able to grow with propionate (Figure 4.6) and ethanol with sulfate. However, in the absence of sulfate, it cannot grow in syntrophic association with methanogens. Therefore, differences are expected in genes coding for hydrogenases, formate dehydrogenases, and those involved in sulfate reduction.

4.9.3.1 Sulfate reduction genes

Figure 4.7 depicts the sulfate reduction pathway of the two strains. In the genome of *D. kuznetsovii* two genes (Desku_2103; Desku_3527) are annotated as phosphoadenosine phosphosulfate reductase encoding genes whose corresponding proteins might be involved in assimilatory sulfate metabolism. The *P. thermopropionicum* genome lacks these genes [37]. Instead, the *P. thermopropionicum* genome contains an adenylylsulfate kinase gene (PTH_0238). In the dissimilatory sulfate reduction pathway, the two strains both have genes that code for enzymes to reduce sulfate to H_2S. However, *P. thermopropionicum* is missing the gene that codes for an adenylylsulfate reductase beta subunit, which is present in the *D. kuznetsovii* genome (Desku_1073). Moreover, the gene labeled as a dissimilatory sulfite reductase (*dsr*) alpha and beta subunit in the *P. thermopropionicum* genome (PTH_0242) is not similar to *dsrA* or *dsrB* from *D. kuznetsovii* or any other *Desulfotomaculum* strain. However, it has high similarity to the *dsrC* gene from *D. kuznetsovii*, indicating that it is not a *dsrA* or *dsrB* gene but a *dsrC* gene (data not shown). Therefore, the inability of *P. thermopropionicum* to grow by sulfate respiration is most likely caused by the absence of an adenylylsulfate reductase

beta subunit encoding gene and the *dsrAB* genes.

4.9.3.2 Hydrogenase and formate dehydrogenase genes

Schut and Adams (2009) [38] showed that the trimeric [FeFe]-hydrogenase from *Thermotoga maritima* oxidizes NADH and ferredoxin simultaneously to produce H_2. Similar bifurcating / confurcating [FeFe]-hydrogenases and formate dehydrogenases are present in *Syntrophobacter fumaroxidans* and *P. thermopropionicum* [39]. Both generate NADH and ferredoxin during propionate degradation via the methylmalonyl-CoA pathway and might use confurcating hydrogenases and formate dehydrogenases to drive the unfavorable re-oxidation of NADH (E0'=-320mV) by the exergonic re-oxidation of ferredoxin (E0'=-398mV) to produce hydrogen (E0'= -414mV) or formate (E0'= -432mV) that are subsequently transferred to hydrogen and formate scavenging methanogens. Additionally, up-regulation of genes encoding hydrogenases and formate dehydrogenases in *P. thermopropionicum* was shown during syntrophic growth [40]. The *P. thermopropionicum* genome contains three [FeFe]-hydrogenases, one [NiFe]-hydrogenase and two formate dehydrogenases. One [FeFe]-hydrogenase (PTH_0668-0670) was shown to be down-regulated during syntrophic growth, while the other two [FeFe]-hydrogenases (PTH_1377-1379 and PTH_2010-2012) were up-regulated. The two formate dehydrogenases of *P. thermopropionicum* (I, PTH_1711-1714 and II, PTH_2645-2649) were both up-regulated during syntrophic growth [42]. According to TMHMM server v. 2.0 [41] formate dehydrogenase I of *P. thermopropionicum* has transmembrane helices. Therefore, it might play an essential role in the interspecies transfer of reducing equivalents in syntrophic growth.

The genome of *D. kuznetsovii* was screened for hydrogenase and formate dehydrogenase encoding gene clusters with BLAST analysis. Pfam search [42] was used to identify motifs in the amino acid sequences and the TMHMM Server v. 2.0 [41] was used to screen for transmembrane helices. The TatP 1.0 Server was used to screen for twin-arginine translocation (Tat) motifs in the N-terminus to predict protein localization in the cell [43]. The incorporation of selenocysteine (SeCys) was examined by RNA loop predictions with Mfold version 3.2 [44]. The predicted RNA loop in the 50-100 bp region downstream of the UGA-codon was compared with the consensus loop described earlier [45].

Compared to *P. thermopropionicum*, *D. kuznetsovii* lacks membrane associated formate dehydrogenases and hydrogenases and also lacks [NiFe]-hydrogenase. This might be an explanation why *D. kuznetsovii* cannot grow in syntrophic relation with methanogens. The genome of *D. kuznetsovii* indicates the presence of a confurcating selenocysteine-incorporated formate dehydrogenase (Desku_2987-2991), two trimeric confurcating [FeFe]-hydrogenases (Desku_2307-2309, Desku_2995-2997) and two [FeFe]-hydrogenases (Desku_0995, Desku_2934-2935) without NADH-binding sites (Figure 4.8). Several subunits of these enzymes are related to subunits of NADH dehydrogenase (complex I), including the NADH-binding proteins related to NuoF (Desku_2990, 2308 and 2996) and the electron transfer subunits related to NuoE (Desku_2991, 2935, and 2997) and to NuoG (Desku_2989). In three of the [FeFe]-hydrogenases this NuoG-like domain is fused with the catalytic subunit (Desku_2995, 2307 and 2934). Two of the multimeric hydrogenases are found next to [FeFe]-hydrogenases containing PAS-sensor domains (Desku_2932 and Desku_2994), suggesting they are involved in the regulation of the synthesis of those hydrogenases. All complexes are predicted to be cytoplasmic and not membrane bound.

Apart from a possible involvement in the acetate oxidation pathway (Figure 4.4), it remains unclear for which purpose *D. kuznetsovii* uses its confurcating formate dehydrogenase and hydrogenases because our genome analysis indicates that pyruvate oxidation during propionate degradation generates formate instead of ferredoxin (Figure 4.6).

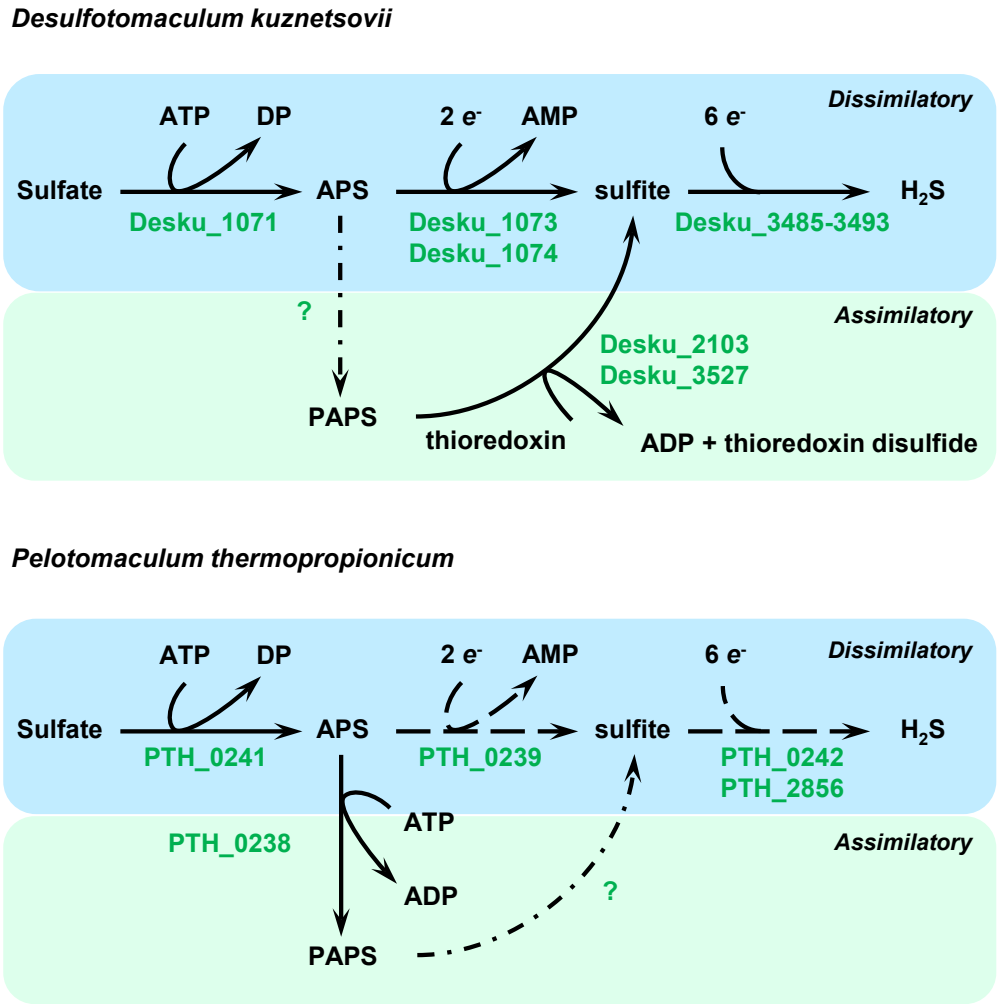

Figure 4.7: Sulfate reduction pathway of D. kuznetsovii and P. thermopropionicum. Depicted in green are genes that code for sulfate reduction enzymes that are present in the genome. Dashed arrows indicate the presence of a subunit encoding gene, but not the presence of all genes required for the enzyme. Dashed dotted arrows are used when no genes were found for the reaction. Abbreviations: APS, adenylylsulfate; DP, diphosphate; PAPS, 3'-Phosphoadenylyl-sulfate (PAPS); redA, reduced acceptor; oxA, oxidized acceptor.

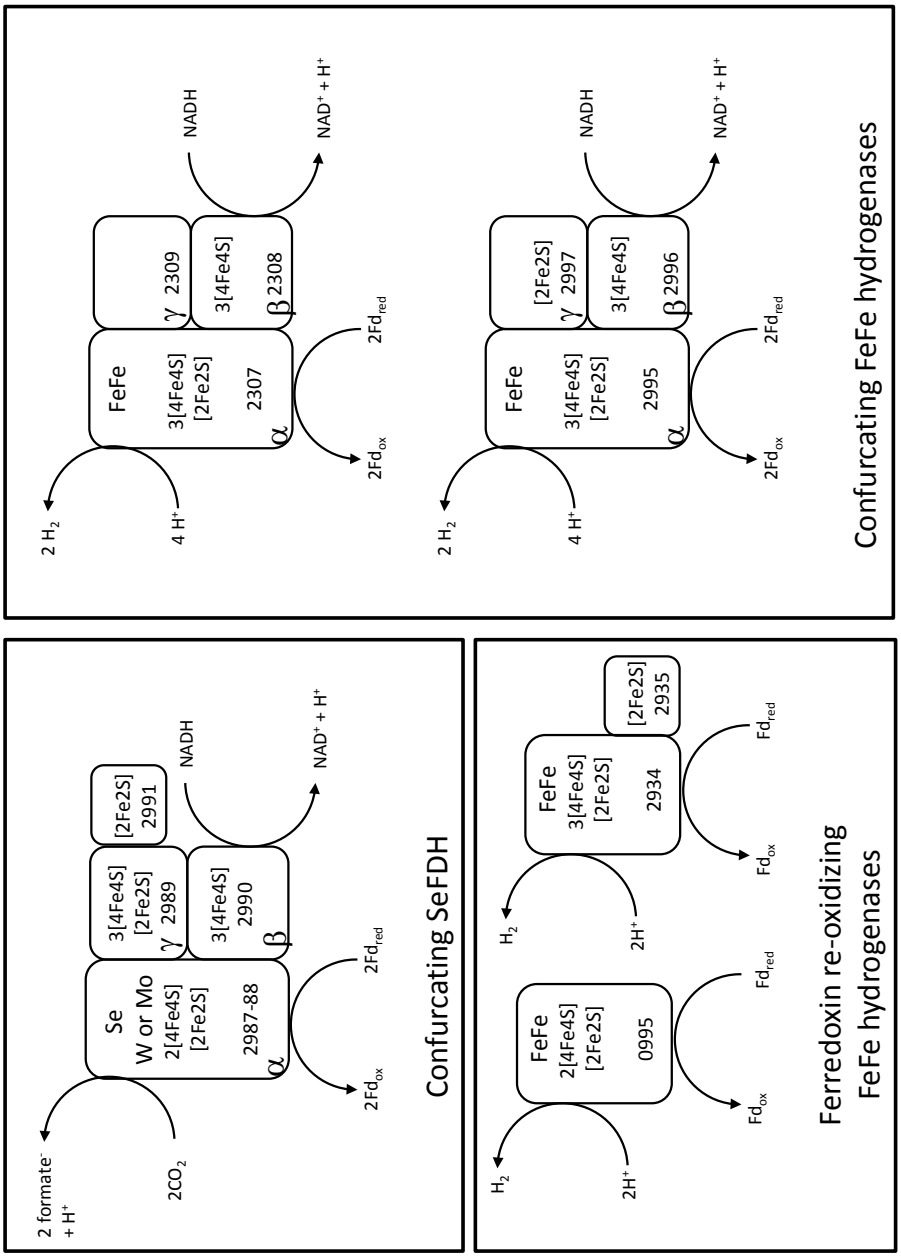

Figure 4.8: Schematic representation of a putative confurcating formate dehydrogenase, two putative confurcating [FeFe]-hydrogenases and two ferredoxin reoxidizing [FeFe]-hydrogenases in Desulfotomaculum kuznetsovii. Gene locus tag numbers and α-, β-, and γ-subunits are depicted. Moreover, predicted iron-sulfur clusters and metal-binding sites are indicated.

4.10 Vitamin synthesis

D. kuznetsovii is able to grow in medium without vitamins [1]. This indicates that *D. kuznetsovii* is able to synthesize all the vitamins that are required for its metabolism and that vitamin synthesis genes should be present in the genome. Vitamin B12 is essential for the methylmalonyl-CoA pathway and the acetyl-coA pathway. The biosynthesis of cobalamin (vitamin B12) is known to occur from uroporphyrinogen-III to adenosylcobalamin via two possible pathways, the aerobic and anaerobic pathway of the corrinoid ring [46, 47]. The *D. kuznetsovii* genome contains all genes needed for the anaerobic pathway: cysGA (Desku_1520), cysGB (Desku_1460, Desku_1523), cbiA (Desku_1765, Desku_2368), cbiBCDEFGHJLPT (Desku_2369, 1459, 1468, 1467, 1464, 1463, 1462, 1461, 1465, 2370 and 1466, respectively), cobalt reductase (Desku_2757), btuR (Desku_0004, 1209), cobS (Desku_2367) and cobU (Desku_2371). Moreover, *D. kuznetsovii* has genes to convert glutamyl tRNA to uroporphyrinogen-III, hemABCDL (Desku_1522, 1518, 1521, 1520 and 1522, respectively). The genome also contains some unassigned cobalamin synthesis genes (P47K, Desku_0046, 0053; cbiM, Desku_2905), corrinoid transport proteins (Desku_0693, 702, 2237-2239, 2902-2904, 3025-3027) and, interestingly, two cobN genes (Desku_2189, 2227), genes involved in the aerobic pathway. It is unclear why *D. kuznetsovii* has these cobN genes, since all anaerobic pathway genes are present in the genome, and it is unclear if the products of these two genes are used for cobalamin synthesis by *D. kuznetsovii*.

Other vitamin synthesis genes present in the genome of *D. kuznetsovii* are genes involved in biotin synthesis (vitamin H) (Desku_1295-1297, 2246-2247, 2317), nicotinamide (vitamin B3) synthesis (Desku_0433, 0614, 0662, 0815, 1248, 1417, 1472, 1499, 1925, 1951, 3103, 3121, 3227, 3228, 3231, 3246, 3337), thiamin (vitamin B1) synthesis (0372, 0543, 0545, 2253, 2363, 2639), riboflavin (vitamin B2) synthesis (Desku_1244-1247), and pantothenate (vitamin B5) synthesis (Desku_3262). The genes involved in coenzyme A production from pantothenate are also present in the *D. kuznetsovii* genome (Desku_1254, 1307, 3145, 3200). Moreover, genes involved in the biosynthesis of pyridoxine (vitamin B6) via the deoxyxylulose 5-phosphate (DXP) independent route were found to be in the genome (Desku_0007, 0008). These genes code for two enzymes that facilitate the conversion of glutamine to the active form of vitamin B6, pyridoxal 5'-phosphate [48].

Menaquinone (vitamin K) and ubiquinone (coenzyme Q10) biosynthesis is important because of the electron transport function in the membranes. The genes that code for the biosynthesis enzymes from polyprenyldiphosphate to menaquinone and ubiquinone are present in the *D. kuznetsovii* genome (Desku_0124, 0126, 0629, 1551-1554, 1829, 2629 and 3525), except for the genes that code for a 2-polyprenyl-6-methoxyphenol 4-monooxygenase (UbiH) and 2-polyprenyl-3-methyl-6-methoxy-1,4-benzoquinone hydroxylase (UbiF). Additionally, three genes (Desku_1548-1550) could be identified as putative menaquinone biosynthesis genes and are part of a menaquinone biosynthesis gene cluster (Desku_1548-1554). The products of those three genes could be involved in the reactions of the missing UbiH and UbiF encoding genes.

Folate (vitamin B9) biosynthesis is also of great importance for *D. kuznetsovii*, because it is an essential part of the acetyl-CoA pathway. It is involved in the transfer of one-carbon compounds and can be biosynthesized from chorismate and guanosine triphosphate (GTP) [49-52]. Both pathways use a dihydropteroate synthase to produce dihydropteroate. The genome of *D. kuznetsovii* contains the genes encoding the enzymes involved in the pathway from chorismate to dihydropteroate (Desku_0219, 2268-2269) and from GTP to dihydropteroate (Desku_0210, 0219-0221 and

1419). The gene encoding a phosphatase (Desku_0210) in the *D. kuznetsovii* genome is probably involved in the removal of phosphate groups from dihydropterine triphosphate as a substitute for an alkaline phosphatase encoding gene, which is not present in the genome. Additionally, the genome contains a bifunctional protein encoding gene (Desku_404) that is expected to be responsible for the production of dihydrofolate (DHF) and the addition of multiple glutamate moieties to DHF or tetrahydrofolate (THF). However, the *D. kuznetsovii* genome lacks the DHF reductase encoding gene, which is required to reduce DHF to THF. The DHF reductase encoding gene appears to be absent in many microorganisms [53]. Levin et al. [53] propose that in *Halobacterium salinarum* a dihydrofolate synthase and a dihydropteroate synthase domain, is able to replace the function of the DHF reductase. Additionally, the authors show that when using a BLAST search homologs of polypeptides can be found in organisms that lack a DHF reductase [53]. However, BLAST results showed no homologous protein encoding gene in the genome of *D. kuznetsovii* (data not shown). How in *D. kuznetsovii* DHF is reduced to THF can currently not be deduced from the genome sequence.

4.11 Acknowledgements

The work conducted by the U.S. Department of Energy Joint Genome Institute is supported by the Office of Science of the U.S. Department of Energy under Contract No. DE-AC02-05CH11231, and was also supported by grants CW-TOP 700.55.343 and ALW 819.02.014 of the Netherlands Science Foundation (NWO) and grant 323009 of the European Research Council.

4.12 References

1. Nazina, T.N., Ivanova, A.E., Kanchaveli, L.P. & Rozanova, E.P. A new sporeforming thermophilic methylotrophic sulfate-reducing bacterium, *Desulfotomaculum kuznetsovii* sp. nov. *Mikrobiologiya* **57**, 823–7 (1988).
2. Plugge, C.M., Zhang, W., Scholten, J.C. & Stams, A.J. Metabolic flexibility of sulfate-reducing bacteria. *Frontiers in Microbiology* **2**, 81-7 (2011).
3. Stackebrandt, E. et al. Phylogenetic analysis of the genus *Desulfotomaculum*: evidence for the misclassification of *Desulfotomaculum guttoideum* and description of *Desulfotomaculum orientis* as *Desulfosporosinus orientis* gen. nov., comb. nov. *International Journal of Systematic Bacteriology* **47**, 1134-9 (1997).
4. Field, D. et al. The minimum information about a genome sequence (MIGS) specification. *Nature Biotechnology* **26**, 541-7 (2008).
5. Woese, C.R., Kandler, O. & Wheelis, M.L. Towards a natural system of organisms: proposal for the domains Archaea, Bacteria, and Eucarya. *Proc Natl Acad Sci U S A* **87**, 4576-9 (1990).
6. Gibbons, N.E. & Murray, R.G.E. Proposal concerning the higher taxa of bacteria. *International Journal of Systematic Biotechnology* **28**, 1-6 (1978).
7. Garrity, G.M. & Holt, J.G. in Bergey's manual of systematic bacteriology (eds. Garrity, G.M., Boone, D.R. & Castenholz, R.W.) 119-169 (Springer, New York, 2001).
8. Murray, R.G.E. in Bergey's manual of systematic bacteriology (ed. Holt, J.G.) 31-34 (The Williams and Wilkins Co., Baltimore, 1984).
9. Euzeby, J. List of new names and new combinations previously effectively, but not validly, published. *Int J Syst Evol Microbiol* **60**, 1009-10 (2010).
10. Rainey, F.A. in Bergey's manual of systematic bacteriology (eds. De Vos, P. et al.) 736 (Springer, New York, 2009).
11. Prévot, A.R. Dictionnaire des Bactéries Pathogènes (eds. Hauderoy, P. et al.) (Masson et Cie, Paris, 1953).
12. Skerman, V.B.D., Mcgowan, V. & Sneath, P.H.A. Approved Lists of Bacterial Names. *Int J Syst Bacteriol* **30**, 225-420 (1980).

13. Rogosa, M. *Peptococcaceae*, a new family to include the Gram-positive, anaerobic cocci of the genera *Peptococcus*, *Peptostreptococcus* and *Ruminococcus*. *International Journal of Systematic Bacteriology*, 234-7 (1971).
14. Campbell, L.L. & Postgate, J.R. Classification of the spore-forming sulfate-reducing bacteria. *Bacteriol Rev* **29**, 359-63 (1965).
15. Goorissen, H.P., Boschker, H.T., Stams, A.J. & Hansen, T.A. Isolation of thermophilic *Desulfotomaculum* strains with methanol and sulfite from solfataric mud pools, and characterization of *Desulfotomaculum solfataricum* sp. nov. *International Journal of Systematic and Evolutionary Microbiology* **53**, 1223-9 (2003).
16. Isaksen, M.F., Bak, F. & Jorgensen, B.B. Thermophilic sulfate-reducing bacteria in cold marine sediment. *Microbiology Ecology* **14**, 1-8 (1994).
17. Ashburner, M. et al. Gene ontology: tool for the unification of biology. The Gene Ontology Consortium. *Nature Genetics* **25**, 25-9 (2000).
18. Pagani, I. et al. The Genomes OnLine Database (GOLD) v.4: status of genomic and metagenomic projects and their associated metadata. *Nucleic AcidsResearch* **40**, D571-9 (2012).
19. JGI website. http://www.jgi.doe.gov/.
20. The Phred/Phrap/Consed software package. http://www.phrap.com.
21. Zerbino, D.R. & Birney, E. Velvet: algorithms for de novo short read assembly using de Bruijn graphs. *Genome research* **18**, 821-9 (2008).
22. Han, C. & Chain, P. in International conference on bioinformatics & computational biology (eds. H.R., A. & H., V.) 141-6 (CSREA Press, 2006).
23. Lapidus, A. et al. (AGBT, Marco Island, FL, 2008).
24. Hyatt, D. et al. Prodigal: prokaryotic gene recognition and translation initiation site identification. *BMC Bioinformatics* **11**, 119 (2010).
25. Pati, A. et al. GenePRIMP: a gene prediction improvement pipeline for prokaryotic genomes. *Nature Methods* **7**, 455-7 (2010).
26. Markowitz, V.M. et al. IMG ER: a system for microbial genome annotation expert review and curation. *Bioinformatics* **25**, 2271-8 (2009).
27. Tourova, T.P., Kuznetsov, B.B., Novikova, E.V., Poltaraus, A.B. & Nazina, T.N. Heterogeneity of the nucleotide sequences of the 16 S rRNA genes of the type strain of *Desulfotomaculum kuznetsovii*. . *Mikrobiologiya* **70**, 788-95 (2001).
28. Altschul, S.F. et al. Gapped BLAST and PSI-BLAST: a new generation of protein database search programs. *Nucleic Acids Research* **25**, 3389-402 (1997).
29. Altschul, S.F. et al. Protein database searches using compositionally adjusted substitution matrices. *The FEBS Journal* **272**, 5101-9 (2005).
30. Goevert, D. & Conrad, R. Carbon isotope fractionation by sulfate-reducing bacteria using different pathways for the oxidation of acetate. *Environmental Science & Technology* **42**, 7813-7 (2008).
31. Spormann, A.M. & Thauer, R.K. Anaerobic acetate oxidation to CO_2 in *Desulfotomaculum acetoxidans*. *Archives of Microbiology* **150**, 374-80 (1988).
32. Spring, S. Lapidus ,A., Schröder, M,. Gleim, D., Sims, D., Meincke, L,. Glavina Del Rio, T., Tice, H., Copeland, A., Cheng JF, Lucas S, Chen F, Nolan M, Bruce D, Goodwin L, Pitluck S, Ivanova N, Mavromatis K, Mikhailova N, Pati A, Chen ,A., Palaniappan, K., Land, M., Hauser, L., Chang, Y.J., Jeffries, C.D., Chain, P., Saunders, E., Brettin, T., Detter, J.C., Göker, M., Bristow, J., Eisen, J.A., Markowitz, V., Hugenholtz, P., Kyrpides, N.C., Klenk, H.P., Han, C. Complete genome sequence of *Desulfotomaculum acetoxidans* type strain (5575). *Standards in Genomic Sciences* **1**, 242-53 (2009).
33. Goorissen, H.P., Stams, A.J.M. & Hansen, T.A. Methanol dissimilation in *Desulfotomaculum kuznetsovii PhD dissertation: Thermophilic methanol utilization by sulfate reducing bacteria* **Chapter 3**, 55-61 (2002).
34. Pierce, E., Xie, G., Barabote, R.D., Saunders, E., Han, C.S., Detter, J.C., Richardson, P., Brettin, T.S., Das, A., Ljungdahl, L.G., Ragsdale, S.W. The complete genome sequence of *Moorella thermoacetica* (f. *Clostridium thermoaceticum*). *Environmental Microbiology* **10**, 2550-73 (2008).
35. van der Meijden, P. et al. Methyltransferases involved in methanol conversion by *Methanosarcina barkeri*. *Archives of*

Microbiology **134**, 238-42 (1983).

36. Imachi, H. et al. *Pelotomaculum thermopropionicum* gen. nov., sp. nov., an anaerobic, thermophilic, syntrophic propionate-oxidizing bacterium. *International Journal of Systematic and Evolutionary Microbiology* **52**, 1729-35 (2002).
37. Kosaka, T. et al. The genome of *Pelotomaculum thermopropionicum* reveals niche-associated evolution in anaerobic microbiota. *Genome Research* **18**, 442-8 (2008).
38. Schut, G.J. & Adams, M.W. The iron-hydrogenase of *Thermotoga maritima* utilizes ferredoxin and NADH synergistically: a new perspective on anaerobic hydrogen production. *Journal of Bacteriology* **191**, 4451-7 (2009).
39. Müller, N., Worm, P., Schink, B., Stams, A.J.M. & Plugge, C.M. Syntrophic butyrate and propionate oxidation processes: from genomes to reaction mechanisms. *Environmental Microbiology Reports* **2**, 489-99 (2010).
40. Kato, S., Kosaka, T. & Watanabe, K. Substrate-dependent transcriptomic shifts in *Pelotomaculum thermopropionicum* grown in syntrophic co-culture with *Methanothermobacter thermautotrophicus*. *Microbial Biotechnology* **2**, 575-84 (2009).
41. DTU. (Center for biological sequence analysis: Technical University of Denmark, 2009).
42. Sanger Institute, C.U. (2009).
43. Bendtsen, J.D., Nielsen, H., Widdick, D., Palmer, T. & Brunak, S. Prediction of twin-arginine signal peptides. *BMC Bioinformatics* **6**, 167 (2005).
44. Zuker, M. Mfold web server for nucleic acid folding and hybridization prediction. *Nucleic acids research* **31**, 3406-15 (2003).
45. Zhang, Y. & Gladyshev, V.N. An algorithm for identification of bacterial selenocysteine insertion sequence elements and selenoprotein genes. *Bioinformatics* **21**, 2580-9 (2005).
46. Roessner, C.A., Santander, P.J. & Scott, A.I. Multiple biosynthetic pathways for vitamin B12: variations on a central theme. *Vitamins and Hormones* **61**, 267-97 (2001).
47. Roth, J.R., Lawrence, J.G. & Bobik, T.A. Cobalamin (coenzyme B12): synthesis and biological significance. *Annual Review of Microbiology* **50**, 137-81 (1996).
48. Fitzpatrick, T.B. et al. Two independent routes of de novo vitamin B6 biosynthesis: not that different after all. *The Biochemical Journal* **407**, 1-13 (2007).
49. Bermingham, A. & Derrick, J.P. The folic acid biosynthesis pathway in bacteria: evaluation of potential for antibacterial drug discovery. *BioEssays : News and Reviews in Molecular, Cellular and Developmental Biology* **24**, 637-48 (2002).
50. Dosselaere, F. & Vanderleyden, J. A metabolic node in action: chorismate-utilizing enzymes in microorganisms. *Critical Reviews in Microbiology* **27**, 75-131 (2001).
51. Hu, S.I., Drake, H.L. & Wood, H.G. Synthesis of acetyl coenzyme A from carbon monoxide, methyltetrahydrofolate, and coenzyme A by enzymes from *Clostridium thermoaceticum*. *Journal of Bacteriology* **149**, 440-8 (1982).
52. Stupperich, E. & Konle, R. Corrinoid-Dependent Methyl Transfer Reactions Are Involved in Methanol and 3,4-Dimethoxybenzoate Metabolism by Sporomusa ovata. *Appl Environ Microbiol* **59**, 3110-6 (1993).
53. Levin, I., Giladi, M., Altman-Price, N., Ortenberg, R. & Mevarech, M. An alternative pathway for reduced folate biosynthesis in bacteria and halophilic archaea. *Molecular Microbiology* **54**, 1307-18 (2004).

Chapter 5

Comparative proteomics reveals two methanol-degrading pathways in the sulfate-reducing bacterium *Desulfotomaculum kuznetsovii*

Michael Visser, Mervin Pieterse, Martijn W. Pinkse, and Alfons J. M. Stams

In preparation for publication

5.1 Abstract

Several phylogenetic groups of microorganisms are able to grow with methanol as a sole carbon and energy source. Aerobic methylotrophs generally oxidize methanol to formaldehyde by using a methanol dehydrogenase, while anaerobic methylotrophs such as methanogens and acetogens are known to use a methanol methyltransferase system. However, the methanol metabolism of sulfate-reducing bacteria has not been extensively studied. Previous work with the sulfate reducing bacterium *Desulfotomaculum kuznetsovii* resulted in a partially purified alcohol dehydrogenase that showed activity with methanol and ethanol. However, the genome also indicated the presence of a methanol methyltransferase system. Therefore, we used a comparative proteomics approach by using nanoLC-MS/MS to unravel the methanol metabolism of *D. kuznetsovii*. Cells were grown under four different conditions: Methanol and sulfate in presence and absence of cobalt and vitamin B12, lactate and sulfate, and ethanol and sulfate. The lactate growth condition was used as a reference. Spectral count results indicate the presence of two methanol degrading pathways in *D. kuznetsovii,* a cobalt dependent methanol methyltransferase system and a cobalt independent alcohol dehydrogenase.

5.2 Introduction

Several phylogenetic groups of microorganisms are able to grow with methanol as a sole carbon and energy source. Aerobic methylotrophs generally oxidize methanol to formaldehyde by using a methanol dehydrogenase (MDH). Multiple MDHs, such as MDHs that use pyrroloquinoline quinone (PQQ) or NAD(P) as a cofactor, have been characterized over the years [1,2]. Anaerobic methylotrophs such as methanogenic archaea and acetogenic bacteria are known to use a methanol methyltransferase (MT) system. This system involves two MT enzymes, MT_1 and MT_2. MT_1 consists of two subunits, the first (MtaB) is involved in the breaking of the C-O bond of methanol and transferring the methyl to the second subunit (MtaC). MT_2 (also MtaA) transfers the methyl from MtaC to coenzyme M in methanogens [3-6], and tetrahydrofolate in acetogens [7-9]. In sulfate-reducing bacteria (SRB) the methanol metabolism has not been extensively studied. Therefore, it is not clear whether SRB use a MT system or if they use a MDH. Several SRB can utilize methanol, such as *Desulfosporosinus orientis* [10], *Desulfobacterium catecholicum* [11], *Desulfobacterium aniline* [12], *Desulfovibrio carbinolicus* [13], *Desulfovibrio alcoholivorans* [14], and nine *Desulfotomaculum* strains [15-20] including *D. kuznetsovii.* Growth of *D. kuznetsovii* with methanol and sulfate was studied and resulted in a partially purified alcohol dehydrogenase (ADH) with a molecular mass of 42 kDa that also showed activity with methanol [21]. However, analysis of the genome of *D. kuznetsovii* revealed not only the presence of multiple alcohol dehydrogenases with the predicted size of approximately 42 kDa, but also methanol methyltransferase genes [22]. Therefore, the methanol metabolism in *D. kuznetsovii* remained unsolved.

Here, we describe the presence of two methanol metabolism systems in *D. kuznetsovii* by growing adapted cells with methanol and sulfate in the presence and absence of cobalt and vitamin B12 using a comparative proteomics approach. This is the first evidence for the occurrence of both a methanol oxidizing ADH and a MT system in a bacterium.

5.3 Material and Methods

5.3.1 Culture medium and experimental design

Desulfotomaculum kuznetsovii [19] was grown in bicarbonate buffered medium described by Stams et

al. [23]. Moreover, the acid trace element of the medium contained $CoCl_2$ and the vitamin solution contained vitamin B12, unless stated differently. The electron donors (20 mM) and sulfate (10 mM) were added from concentrated stock solutions (sterilized by autoclaving). Cultivation of *D. kuznetsovii* was performed at pH 7 and at 60° C in 117 ml glass serum bottles with butyl rubber stoppers and aluminum crimp seals. The bottles contained 50 ml basal medium and a gas phase of 1.7 bar N_2/CO_2 (80%/20%, v/v). In all experiments the inoculum size was 1% (v/v). For growth experiments and proteome analysis cultures were transferred at least 5 times to ensure full adaptation to the growth substrate.

To investigate if a methanol methyltransferase system is involved in methanol conversion, *D. kuznetsovii* was grown with methanol and sulfate in normal medium and in medium deprived from cobalt ($CoCl_2$) and vitamin B12. Growth was recorded by monitoring the optical density at 600 nm (U-1500 spectrophotometer Hitachi) and by determination of the methanol concentration using a GC (GC-2010 Shimadzu, Sil 5 CB column) daily.

Additional to the two methanol growth conditions, two other growth conditions were used for a comparative proteomics analysis. Those growth conditions were: lactate with sulfate and ethanol with sulfate.

5.3.2 Protein extraction

For the preparation of protein samples, all four conditions of 500 ml cell suspensions, including their independent duplicates, were grown until the late exponential phase and harvested by centrifugation. The pellets were resuspended separately in SDT-lysis buffer (100mM Tris/HCl pH 7.6 + 4% SDS + 0.1M dithiothreitol) and sonified (Sonifier B12, Branson Sonic Power Company, Danbury, Connecticut) to disrupt the bacterial cell wall. Unbroken cells and debris were removed by centrifugation at 13.000 rpm for ten minutes. The protein containing supernatant was used for the proteome analysis.

5.3.3 Comparative proteomics

The proteome analyses of *D. kuznetsovii* cells grown in the four growth conditions were performed using LC-MS/MS [24]. As a control of sample quality an equal amount of total protein was separated by SDS-PAGE on a 10 well SDS-PAGE 10% Bis-Tris Gel (Mini Protean System, Bio-Rad, U.S.) for 90 min at a constant voltage of 120 mV using Tris-SDS as running buffer. Label free quantitative proteomics type experiments were carried to find differentially expressed proteins under all different growth conditions studied. Equal amounts of the protein extracts were loaded onto a Novex 4-12% Bis-Tris SDS page gel (Invitrogen) and electrophoreses for 5 min at 200V constant voltage using MES-SDS as running buffer. For each lane a single band containing all proteins was cut out and treated for reduction and alkylation using 20 mM dithiotreitol and 40 mM iodoacetamide in 50 mM ammonium bicarbonate. Digestion was performed by incubating the samples overnight at 37 °C with trypsin at a 1:20 enzyme-protein ratio. Peptides were diluted with 5% formic acid and 5% DMSO and subjected to nanoLC-MS/MS using an EasyLC 1000 and an Orbitrap Q-Exactive Plus instrument (Thermofisher Scientific). Each peptide sample was auto-sampled and separated in a 25 cm analytical column (75 μm inner diameter) in-house packed with 5 μm C18 column material (Reprosil Pur-AQ, Dr. Maisch) with a 60 min gradient from 5% to 40% acetonitrile in 0.6% acetic acid. The effluent from the column was directly electrosprayed into the mass spectrometer. Full MS1 spectra were acquired in the positive ion mode from m/z

300-1200 at a resolution of 70,000 after accumulation of 3e6 ions within a maximal injection time of 250 ms. A top 20 method was used to acquire MS2 spectra at a resolution of 17,500 after accumulation of 1e5 ions within a maximal injection time of 50 ms. Parent ions were isolated with a 2,5 m/z window and fragmented with a HCD energy of 28. Only multiply charged ions were selected and the dynamic exclusion time was set to 30 seconds. Raw data were analyzed using Proteome Discoverer 1.4 (ThermoFischer Scientific) and Mascot 2.2 (matrixscience) was used as search engine. A database containing all protein entries of *D. kuznetsovii* listed in Uniprot was used to search the data. Search settings used were; 5 ppm for parent ions, 0.02 Da for fragment ions, trypsin as proteolytic agent, carbamidomethyl cysteine as fixed modification and methionine oxidation as variable modification. Scaffold 3.0 (ProteomeSoftware) was used to merge all search results. Filtering of the data was done by setting the minimum protein threshold to 99%, the minimum peptide count to 2 and the minimum peptide threshold to 95%.

The genome of *D. kuznetsovii* is publicly available (ref: NC_015573.1) and encodes 3,625 genes, from which 3567 genes are predicted to be protein-coding [22]. The raw proteome analysis resulted in the identification of 892 different proteins (with at least 2 unique peptides identified). Proteins 3 times more peptide counts in one condition compared to another are considerd proteins with increased abundance and are listed in the supplementary data (Supplementary file S1). Proteins that possibly play an important role under different growth conditions are discussed in more detail in the text.

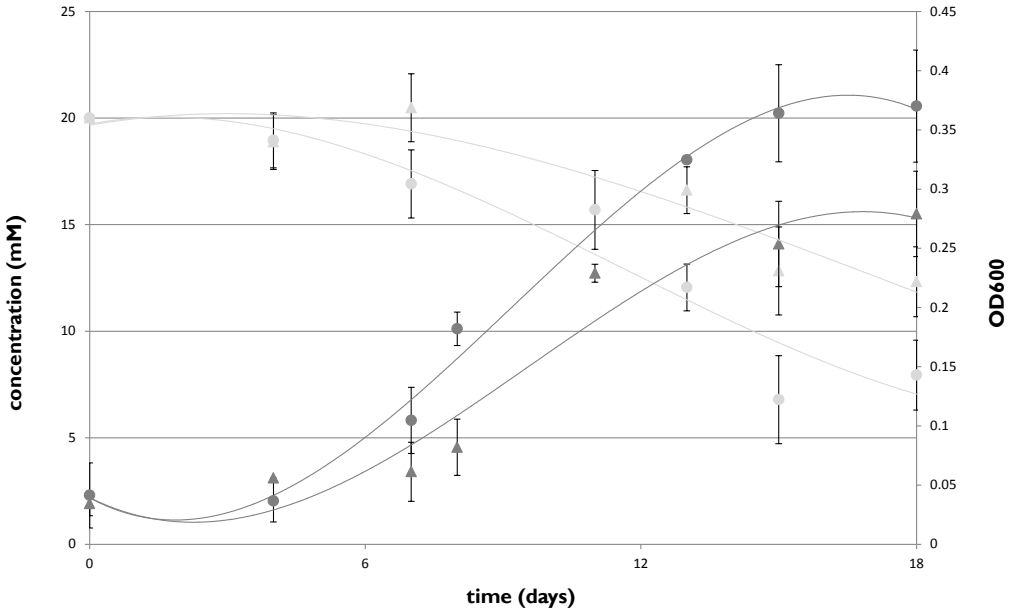

Figure 5.1: Methanol dependent growth in D. kuznetsovii with (depicted with ○) and without cobalt and vitamin B12 in the medium (depicted with Δ). Methanol concentrations and optical density values are presented in light and dark grey, respectively. Error bars indicate standard deviation values of the biological replicates (n = 3).

5.4 Results

5.4.1 Effect of cobalt and vitamin B12 on growth with methanol

The presence of genes coding for a methanol MT system in the genome of *Desulfotomaculum kuznetsovii* suggested the involvement of a vitamin B12-dependent MT system in methanol conversion, while previous analyses pointed to the involvement of an alcohol dehydrogenase [21]. To assess the involvement of either enzyme system in the methanol metabolism we assessed the effect of cobalt on growth with methanol.

D. kuznetsovii was grown with methanol and sulfate in the presence or absence of cobalt and vitamin B12. Cultures were transferred 5 times to new medium bottles before analysis, to ensure full adaptation to the growth substrate (Figure 5.1). When cobalt and vitamin B12 were omitted from the medium *D. kuznetsovii* was still able to degrade methanol but the rate of conversion decreased. This suggests the involvement of a methanol MT system in the methanol metabolism of *D. kuznetsovii*. Moreover, it indicates the presence of a second, cobalamin independent, methanol utilization system.

5.4.2 Comparative proteomics analysis

To perform the comparative proteomics analysis *D. kuznetsovii* cells were adapted to four different growth conditions: methanol and sulfate in presence and absence of cobalt and vitamin B12, lactate and sulfate, and ethanol and sulfate. The lactate growth condition was used as a reference, while the ethanol growth condition was used because Goorissen et al. [21] indicated the involvement of an alcohol dehydrogenase for growth with methanol and ethanol. Proteins 3 times more abundant in one condition compared to another are considered proteins with increased abundance.

5.4.3 Methanol metabolism

Growth of *D. kuznetsovii* with methanol in the presence of cobalt and vitamin B12 showed an increased abundance, compared to the other growth conditions, of proteins encoded by genes of one operon structure (Desku_0050-60), which were annotated as proteins involved in vitamin B12 biosynthesis and a methanol MT system (Table 5.1). Two MtaA MTs, a MtaB and MtaC are highly abundant. The increased abundance of the corrinoid binding MtaC indicates the necessity of vitamin B12 in the cell. However, no vitamin B12 transport encoding genes can be found in the genome of *D. kuznetsovii.* All genes essential for vitamin B12 synthesis, however, are present in the genome and the strain does not require vitamins for growth [22]. Hence the increased abundance of vitamin B12 biosynthesis proteins coincides with the expression of the MT system during growth with methanol.

When cobalt and vitamin B12 was omitted from the medium *D. kuznetsovii* was still able to grow with methanol. At this growth condition the abundance of the MT system and the vitamin B12 synthesis pathway were very low. The proteome results showed higher abundance of an alcohol dehydrogenase (Desku_2952) and an aldehyde ferredoxin oxidoreductase (Desku_2951) during growth with methanol with and without cobalt and vitamin B12 limitation and with ethanol (Table 5.1), which indicates the involvement of those proteins in both ethanol and methanol metabolism of *D. kuznetsovii*.

Two other alcohol dehydrogenases (Desku_0619, 3082) and four other aldehyde dehydrogenases (Desku_0621, 2946, 2983, 3081) are present in the proteome data (Supplementary file S1),

but these have no enhanced abundance in any of the growth conditions, including growth with methanol and ethanol.

Table 5.1: Proteomic data of proteins involved in the D. kuznetsovii methanol metabolism. The table shows the predicted function of the proteins, the reference to the genome (in locus tags), and their related peptide abundance in the four different growth conditions and their independent duplicates: lactate and sulfate (L), methanol and sulfate (M), methanol and sulfate in the absence of cobalt and vitamin B12 (M-cobalt-B12), and ethanol and sulfate (E).

Function	locus tag	L 1	L 2	M 1	M 2	M-cobalt -B12 1	M-cobalt -B12 2	E 1	E 2
MtaA	Desku_0050	1	0	107	125	11	6	15	15
MtaB	Desku_0051	0	1	68	77	11	1	12	14
MtaC	Desku_0052	0	0	52	60	1	1	1	2
Cobalamin synthesis protein	Desku_0053	0	0	5	7	0	0	0	0
4Fe-4S ferredoxin iron-sulfur binding protein	Desku_0054	0	0	9	7	0	0	0	0
Methionine synthase B12-binding module cap protein	Desku_0056	0	0	54	49	1	1	4	6
Ferredoxin	Desku_0057	0	0	108	98	7	4	11	14
Tetrahydromethanopterin S-MT	Desku_0058	0	0	26	35	2	2	5	5
Pyridoxamine 5'-phosphate oxidase-related FMN-binding protein	Desku_0059	0	0	89	101	2	1	2	2
MtaA	Desku_0060	0	0	62	84	3	0	7	6
Aldehyde ferredoxin oxidoreductase	Desku_2951	16	20	121	125	156	166	153	126
Alcohol dehydrogenase	Desku_2952	0	0	372	409	569	581	271	174

5.4.4 Sulfate reduction

Sulfate was added at all growth conditions and the sulfate reduction genes as described in Chapter 4 [22] were expressed at approximately equal levels.

5.4.5 Acetyl-CoA pathway and lactate metabolism

Although not at all growth conditions the acetyl-CoA pathway is involved, the proteins of the acetyl-CoA pathway were present in approximately equal abundance at all growth conditions, with the exception of two acetate-CoA ligase/acetyl-CoA synthetase proteins (ACL, Table 5.3). One ACL (Desku_2303) had an increased abundance during growth with lactate, while the other ACL (Desku_2843) had an increased abundance during growth with methanol in the absence of cobalt and vitamin B12. This suggests that the synthesis of these ACL enzymes is regulated. Interestingly, all four *D. kuznetsovii* ACL amino acid sequences are different from each other. When using the ten best BLAST hits from all four ACL enzymes in a neighbor joining tree the four *D. kuznetsovii* ACLs end up in four different clusters (Supplementary file S2).

Table 5.2: Proteomic data of proteins involved in sulfate reduction in D. kuznetsovii. The table shows the predicted function of the proteins, the reference to the genome (in locus tags), and their related peptide abundance in the four different growth conditions and their independent duplicates: lactate and sulfate (L), methanol and sulfate (M), methanol and sulfate in the absence of cobalt and vitamin B12 (M-cobalt-B12), and ethanol and sulfate (E).

Protein Description	locus tag	L 1	L 2	M 1	M 2	M-cobalt -B12 1	M-cobalt -B12 2	E 1	E 2
Sulfate adenylyltransferase	Desku_1071	123	195	196	185	186	200	176	175
Putative uncharacterized protein	Desku_1072	13	37	44	46	48	49	20	21
Adenylylsulfate reductase, beta subunit	Desku_1073	30	47	36	39	48	43	49	61
Adenylylsulfate reductase, alpha subunit	Desku_1074	197	322	267	290	313	334	329	312
Sulfur relay protein, TusE/DsrC/DsvC family	Desku_3485	33	33	14	14	18	22	21	25
Putative uncharacterized protein	Desku_3486	10	19	18	17	23	22	16	17
Sulfate reductase gamma subunit	Desku_3487	2	2	4	3	4	3	3	2
Dissimilatory sulfite reductase D	Desku_3491	2	6	2	2	6	5	5	7
Sulfite reductase, dissimilatory-type beta subunit	Desku_3492	58	100	58	58	100	102	94	90
Sulfite reductase, dissimilatory-type alpha subunit	Desku_3493	94	140	110	117	136	132	112	132

Table 5.3: Proteomic data of proteins involved in the acetyl-CoA pathway in D. kuznetsovii and proteins that had an increased abundance in growth with lactate. The table shows the predicted function of the proteins, the reference to the genome (in locus tags), and their related peptide abundance in the four different growth conditions and their independent duplicates: lactate and sulfate (L), methanol and sulfate (M), methanol and sulfate in the absence of cobalt and vitamin B12 (M-cobalt-B12), and ethanol and sulfate (E). Proteins 3 times more abundant in a growth condition are marked bolt.

Protein Description	locus tag	L 1	L 2	M 1	M 2	M-cobalt -B12 1	M-cobalt -B12 2	E 1	E 2
Formate-tetrahydrofolate ligase	Desku_0216	46	100	93	98	125	123	77	64
Acetate-CoA ligase	Desku_1241	0	0	8	5	11	12	7	6
Methylenetetrahydrofolate reductase	Desku_1475	13	30	31	27	38	47	36	34
Putative uncharacterized protein	Desku_1476	7	16	17	17	32	33	27	15
Methyl-viologen-reducing hydrogenase delta subunit	Desku_1477	4	4	4	6	13	11	11	8
Fumarate reductase/succinate dehydrogenase flavoprotein domain protein	Desku_1478	19	29	32	33	70	79	41	41

Dihydroorotate dehydrogenase, electron transfer subunit, iron-sulfur cluster binding domain protein	Desku_1480	16	24	26	22	31	41	16	18
4Fe-4S ferredoxin iron-sulfur binding domain-containing protein	Desku_1481	16	19	21	19	28	31	24	23
Coenzyme F420 hydrogenase/ dehydrogenase beta subunit domain protein	Desku_1482	14	13	19	19	26	37	11	15
Methyl-viologen-reducing hydrogenase delta subunit	Desku_1483	3	5	4	5	9	7	8	5
CoB-CoM heterodisulfide reductase	Desku_1484	14	12	9	15	16	15	12	12
Heterodisulfide reductase subunit C-like protein	Desku_1485	12	17	13	15	16	15	16	19
4Fe-4S ferredoxin iron-sulfur binding domain-containing protein	Desku_1486	25	34	26	29	45	38	36	32
acsE 5-methyltetrahydrofolate corrinoid/iron sulfur protein methyltransferase	Desku_1487	14	25	17	20	22	21	18	21
CO dehydrogenase/acetyl-CoA synthase delta subunit, TIM barrel	Desku_1488	14	24	37	24	12	13	21	30
CO dehydrogenase/acetyl-CoA synthase delta subunit, TIM barrel	Desku_1490	31	45	56	47	22	17	33	43
CO dehydrogenase/acetyl-CoA synthase complex, beta subunit	Desku_1491	53	72	98	101	131	120	83	79
Carbon-monoxide dehydrogenase, catalytic subunit	Desku_1492	13	17	7	7	12	16	7	5
Methenyl tetrahydrofolate cyclohydrolase	Desku_1933	9	19	19	24	21	22	13	14
5,10-methylene-tetrahydrofolate dehydrogenase	Desku_1934	14	20	18	19	24	25	15	17
Acetate-CoA ligase	Desku_2054	1	1	6	5	7	7	7	1
CO dehydrogenase/acetyl-CoA synthase complex, beta subunit	Desku_2149	60	74	135	127	158	155	92	81
Cluster of CO dehydrogenase/acetyl-CoA synthase complex, beta subunit	Desku_2150	71	89	149	145	174	172	110	96
Carbon-monoxide dehydrogenase, catalytic subunit	Desku_2150	48	82	141	146	175	200	110	101
Acetyl coenzyme A synthetase (ADP forming)	Desku_2303	**30**	**45**	5	3	3	5	10	12
Lactate utilization protein B/C	Desku_2393	**38**	**41**	1	0	0	0	0	0
Lactate utilization protein B/C	Desku_2394	**12**	**18**	0	0	0	0	0	0
L-lactate transport	Desku_2395	**3**	**7**	0	0	0	0	0	0
Acetyl-coenzyme A synthetase	Desku_2843	0	0	5	7	**26**	**28**	7	7

In addition to the ACL (Desku_2303), the presence of lactate induced several proteins, including a lactate dehydrogenase (Desku_3009), a lactate transporter (Desku_2395), and two hypothetical proteins annotated as lactate utilization proteins (Desku_2393-4, Table5.3). The protein encoded by Desku_2393 contains two 4Fe4S clusters and two cysteine rich domains but nothing can be concluded about the function of this protein from this analysis.

5.4.6 Hydrogenases

Genes coding for four hydrogenases were described to be present in the genome of *D. kuznetsovii* (Chapter 4 [22]). The two possible confurcating hydrogenases (Desku_2307-9; 2995-7) were synthesized during growth of *D. kuznetsovii* with different substrates (Table 5.4), while the other two predicted hydrogenases cannot be found in the proteome data. One of the produced hydrogenases (Desku_2307-9) showed increased abundance during growth with methanol in the absence of cobalt and vitamin B12, while the other hydrogenase (Desku_2995-7) showed increased abundance when *D. kuznetsovii* was grown with lactate and ethanol.
Other highly produced proteins and proteins that had an increased abundance during one or multiple growth conditions can be found in supplementary file S1.

Table 5.4: Proteomic data of predicted hydrogenases in D. kuznetsovii. The table shows the predicted function of the proteins, the reference to the genome (in locus tags), and their related peptide abundance in the four different growth conditions and their independent duplicates: lactate and sulfate (L), methanol and sulfate (M), methanol and sulfate in the absence of cobalt and vitamin B12 (M -B12), and ethanol and sulfate (E).

Protein Description	locus tag	L 1	L 2	M 1	M 2	M -B12 1	M -B12 2	E 1	E 2
Hydrogenase, Fe-only, α subunit	Desku_2307	0	3	40	39	105	121	32	4
Hydrogenase β subunit	Desku_2308	5	5	33	23	76	75	16	7
Hydrogenase γ subunit	Desku_2309	3	2	15	13	23	19	8	1
Hydrogenase, Fe-only, α subunit	Desku_2995	47	70	14	13	12	23	127	151
Hydrogenase β subunit	Desku_2996	60	86	5	8	10	16	96	101
Hydrogenase γ subunit	Desku_2997	9	9	1	1	1	2	13	17

5.5 Discussion

5.5.1 Methanol and ethanol metabolism

The results indicate that the synthesis of MtaA, MtaB and MtaC is induced together with vitamin B12 biosynthesis proteins when *D. kuznetsovii* is grown with methanol and sulfate in the presence of cobalt. The presence of cobalt plays an essential role in this regulation. Studies on cobalt limitation showed a decreased conversion rate when methanogens and acetogens were grown with methanol [26-28]. This was explained by the essential role of cobalt in corrinoid biosynthesis [29] and the production of corrinoid dependent proteins by the methanol utilizers [6, 26-28, 30]. The MtaC subunit of the methanol MT system was described to bind the corrinoid [7, 31, 32]. By depriving the environment of cobalt the methanol MT system is not functional. Therefore, we used medium without cobalt and vitamin B12 to study the MT independent methanol metabolism of *D. kuznetsovii*.

Goorissen [21] partially purified an ADH with a molecular mass of 42 kDa that showed activity with ethanol and methanol. In that study, the ADH was present during growth with ethanol and sulfate, but was more abundant during growth with methanol and sulfate. However, the ADH activity with ethanol was higher compared to methanol. Activity was measured with nicotinamide adenine dinucleotide (NAD), 2,6 dichlorophenolindophenol (DCPIP) and 3-(4,5-dimethylthiazol-2-yl)-2,4 diphenyltetrazolium bromide (MTT) as an electron acceptor, but not with NADP. The highest activity was measured with ethanol and NAD. Moreover, activity of the reverse reaction was measured when using both acetylaldehyde and formaldehyde [21].

Our results show that an ADH (Desku_2952) is induced when *D. kuznetsovii* is grown with ethanol and methanol. Moreover, when grown with methanol in the absence of cobalt and vitamin B12 approximately twice as much ADH was produced by *D. kuznetsovii* compared to ethanol-grown cells. The predicted size of the ADH is 41 kDA, which also resembles the mass of the enzyme partially purified by Goorissen [21]. Additional to the ADH (Desku_2952) the proteome results show that an aldehyde ferredoxin oxidoreductase (Desku_2951) is co-induced. The two genes are next to each other in the genome. The genome possesses one formate dehydrogenase (Desku_2987-90) of which the products have an equal abundance in all growth conditions. These results suggest that two methanol utilizing pathways are present in *D. kuznetsovii* (Figure 5.2). Other ADHs are present in the *D. kuznetsovii* genome but these do not seem to be involved in the ethanol and/or methanol degradation. However, these might be involved in the degradation of other alcohols, such as propanol and butanol.

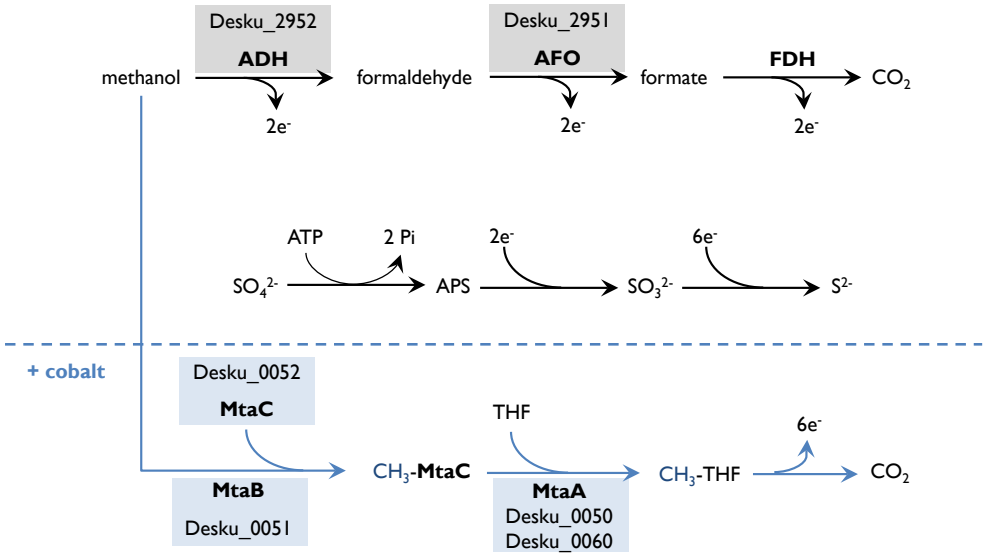

Figure 5.2: Hypothesized methanol metabolism pathways in D. kuznetsovii. Methanol is oxidized to CO_2 by an alcohol dehydrogenase (ADH), Aldehyde ferredoxin oxidoreductase (AFO) and a formate dehydrogenase (FDH). Electrons that are generated through the oxidation reactions can be used for the reduction of sulfate. When cobalt is present in the environment the second methanol oxidizing pathway is induced (indicated in blue) and part of the methanol is methylated to methyl-tetrahydrofolate (CH_3-THF). Subsequently, methyl-tetrahydrofolate is oxidized to CO_2 generating the same amount of electrons. Locus tag numbers are indicated for the boxed enzymes.

More SRB have been described to grow with methanol and sulfate, but the metabolic pathways are unknown. In recent years two genome sequences of methanol utilizing SRB were published, *Desulfotomaculum reducens* [33] and *Desulfosporosinus orientis* [34]. This enables the identification of genes possibly involved in their methanol metabolism. The genome of *D. reducens*, does not contain methanol MT genes, indicating the involvement of an ADH in methanol conversion. Multiple ADH genes can be found in the genome of *D. reducens*, including one with high similarity to the gene coding for the methanol utilizing ADH of *D. kuznetsovii.* However, this ADH is not situated next to an aldehyde ferredoxin oxidoreductase. In *Desulfosporosinus orientis* methanol MT genes and an ADH gene that is similar to the one in *D. kuznetsovii* are both present in the genome. However, this ADH is also not situated next to an aldehyde ferredoxin oxidoreductase. Further research is required to assess if the use of a similar ADH and two methanol utilizing systems, as we describe here in *D. kuznetsovii,* are also present in other SRB.

5.5.2 Possible hydrogen production from methanol and ethanol metabolism

The proteome results indicate a difference in the hydrogenases when *D. kuznetsovii* was grown with ethanol (Desku_2995-7) compared to methanol with cobalt and vitamin B12 limitation (Desku_2307-9). These possible confurcating hydrogenases could be used by *D. kuznetsovii* to produce hydrogen by coupling the endergonic oxidation of NADH with the exergonic oxidation of reduced ferredoxin. Since the results from Goorissen [21] suggest that the ADH reduces NAD^+, the NADH and reduced ferredoxin from respectively the ADH and the aldehyde ferredoxin oxidoreductase could be used by these hydrogenases. The hydrogen produced could subsequently be used to reduce sulfate as part of a hydrogen-cycling model, which was suggested by Odom and Peck [35]. However, why the ethanol and methanol with cobalt and vitamin B12 limitation growth conditions use a different hydrogenase cannot be said from this analysis.

Hydrogen production by *D. kuznetsovii* during ethanol and methanol growth suggests the possibility of syntrophic growth with a hydrogen utilizing methanogen in the absence of sulfate. However, our attempt to grow *D. kuznetsovii* with methanol in the absence of sulfate and in the presence of a hydrogen utilizing methanogen was unsuccessful (data not shown).

5.5.3 Lactate metabolism

The lactate growth condition was included as a reference. Moreover, the results show lactate specific induced proteins, like a lactate transport protein and lactate dehydrogenase. Additionally, two hypothetical proteins were induced that are located next to the lactate transport protein. Therefore, they might be involved in lactate transport into the cell. Interestingly, lactate degradation by *D. kuznetsovii* is not completely to CO_2, but incompletely to acetate. This is rather contradictory for a complete oxidizer as *D. kuznetsovii* and for the protein levels involved in the acetyl-CoA pathway, which were present in approximately equal abundance at all growth conditions, including the lactate with sulfate condition. However, why *D. kuznetsovii* oxidizes lactate incompletely to acetate, while all enzymes for complete oxidation are present, remains unclear.

The increased abundance of the Desku_2303 ACL during growth with lactate and sulfate suggests that this protein is involved in the production of acetate. Moreover, this ACL causes a strong separation in the neighbor joining tree and has poor similarity with the other three ACLs of *D. kuznetsovii.* The results indicate that the four ACL enzymes in *D. kuznetsovii* are regulated.

5.6 References

1. Anthony, C. & Williams, P. The structure and mechanism of methanol dehydrogenase. *Biochimica et Biophysica Acta* **1647**, 18-23 (2003).
2. Hektor, H.J., Kloosterman, H. & Dijkhuizen, L. Nicotinoprotein methanol dehydrogenase enzymes in Gram-positive methylotrophic bacteria. *Journal of Molecular Catalysis B-Enzymatic* **8**, 103-9 (2000).
3. Harms, U. & Thauer, R.K. Methylcobalamin: coenzyme M methyltransferase isoenzymes MtaA and MtbA from *Methanosarcina barkeri*. Cloning, sequencing and differential transcription of the encoding genes, and functional overexpression of the mtaA gene in *Escherichia coli*. *European Journal of Biochemistry / FEBS* **235**, 653-9 (1996).
4. Sauer, K., Harms, U. & Thauer, R.K. Methanol:coenzyme M methyltransferase from *Methanosarcina barkeri*. Purification, properties and encoding genes of the corrinoid protein MT1. *European journal of biochemistry / FEBS* **243**, 670-7 (1997).
5. van der Meijden, P. et al. Methyltransferases involved in methanol conversion by *Methanosarcina barkeri*. *Arch Microbiol* **134**, 238-42 (1983).
6. van der Meijden, P., te Brommelstroet, B.W., Poirot, C.M., van der Drift, C. & Vogels, G.D. Purification and properties of methanol:5-hydroxybenzimidazolylcobamide methyltransferase from *Methanosarcina barkeri*. *Journal of Bacteriology* **160**, 629-35 (1984).
7. Das, A. et al. Characterization of a corrinoid protein involved in the C1 metabolism of strict anaerobic bacterium *Moorella thermoacetica*. *Proteins* **67**, 167-76 (2007).
8. Pierce, E. et al. The complete genome sequence of *Moorella thermoacetica* (f. *Clostridium thermoaceticum*). *Environmental Microbiology* **10**, 2550-73 (2008).
9. Stupperich, E. & Konle, R. Corrinoid-Dependent Methyl Transfer Reactions Are Involved in Methanol and 3,4-Dimethoxybenzoate Metabolism by *Sporomusa ovata*. *Appl Environ Microbiol* **59**, 3110-6 (1993).
10. Klemps, R., Cypionka, H., Widdel, F. & Pfennig, N. Growth with hydrogen, and further physiological-characteristics of *Desulfotomaculum* species. *Archives of Microbiology* **143**, 203-8 (1985).
11. Szewzyk, R. & Pfennig, N. Complete oxidation of catechol by the strictly anaerobic sulfate-reducing *Desulfobacterium catecholicum* sp.nov. *Archives of Microbiology* **147**, 163-8 (1987).
12. Schnell, S., Bak, F. & Pfennig, N. Anaerobic degradation of aniline and dihydroxybenzenes by newly isolated sulfate-reducing bacteria and description of *Desulfobacterium anilini*. *Archives of Microbiology* **152**, 556-63 (1989).
13. Nanninga, H.J. & Gottschal, J.C. Properties of *Desulfovibrio carbinolicus* sp. nov. and other sulfate-reducing bacteria Isolated from an anaerobic-purification plant. *Applied and Environmental Microbiology* **53**, 802-9 (1987).
14. Qatibi, A.I., Niviere, V. & Garcia, J.L. *Desulfovibrio alcoholovorans* sp.nov, a sulfate-reducing bacterium able to grow on glycerol, 1,2-propanediol and 1,3-propanediol. *Archives of Microbiology* **155**, 143-8 (1991).
15. Balk, M., Weijma, J., Goorissen, H.P., Ronteltap, M., Hansen, T.A., Stams, A.J.M. Methanol utilizing *Desulfotomaculum* species utilizes hydrogen in a methanol-fed sulfate-reducing bioreactor. *Applied Microbiology and Biotechnology* **73**, 1203-11 (2007).
16. Fardeau, M.L. et al. Isolation and characterization of a thermophilic sulfate-reducing bacterium, *Desulfotomaculum thermosapovorans* sp. nov. *International Journal of Systematic Bacteriology* **45**, 218-21 (1995).
17. Goorissen, H.P., Boschker, H.T., Stams, A.J. & Hansen, T.A. Isolation of thermophilic *Desulfotomaculum* strains with methanol and sulfite from solfataric mud pools, and characterization of *Desulfotomaculum solfataricum* sp. nov. *International Journal of Systematic and Evolutionary Microbiology* **53**, 1223-9 (2003).
18. Liu, Y.T. et al. Description of two new thermophilic *Desulfotomaculum* spp., *Desulfotomaculum putei* sp. nov, from a deep terrestrial subsurface, and *Desulfotomaculum luciae* sp. nov, from a hot spring. *International Journal of Systematic Bacteriology* **47**, 615-21 (1997).
19. Nazina, T.N., Ivanova, A.E., Kanchaveli, L.P. & Rozanova, E.P. A new sporeforming thermophilic methylotrophic sulfate-reducing bacterium, *Desulfotomaculum kuznetsovii* sp. nov. *Mikrobiologiya* **57**, 823–7 (1988).
20. Tebo, B.M. & Obraztsova, A.Y. Sulfate-reducing bacterium grows with Cr(VI), U(VI), Mn(IV), and Fe(III) as electron acceptors. *Fems Microbiology Letters* **162**, 193-8 (1998).

21. Goorissen, H.P., Stams, A.J.M. & Hansen, T.A. in Department of Microbiology 104 (University of Groningen, Groningen, 2002).
22. Visser, M., Worm, P., Muyzer, G., Pereira, I.A., Schaap, P.J., Plugge, C.M., Kuever, J,. Parshina, S.N., Nazina, T.N,. Ivanova, A.E., Bernier-Latmani, R., Goodwin, L.A., Kyrpides, N.C,. Woyke, T., Chain, P., Davenport, K.W., Spring, S., Klenk, H.P., Stams, A.J.M. Genome analysis of *Desulfotomaculum kuznetsovii* strain 17(T) reveals a physiological similarity with *Pelotomaculum thermopropionicum* strain SI(T). *Standards in genomic sciences* **8**, 69-87 (2013).
23. Stams, A.J.M., Vandijk, J.B., Dijkema, C. & Plugge, C.M. Growth of syntrophic propionate-oxidizing bacteria with fumarate in the absence of methanogenic bacteria. *Applied Environmental Microbiology* **59**, 1114-9 (1993).
24. Lasonder, E. et al. Analysis of the *Plasmodium falciparum* proteome by high-accuracy mass spectrometry. *Nature* **419**, 537-42 (2002).
25. Sokal, A. & Rohlf, J. Introduction to biostatistics (Dover Publications, 2009).
26. Florencio, L., Field, J.A. & Lettinga, G. Importance of cobalt for individual trophic groups in an anaerobic methanol-degrading consortium. *Applied and Environmental Microbiology* **60**, 227-34 (1994).
27. Florencio, L., Jenicek, P., Field, J.A. & Lettinga, G. Effect of cobalt on the anaerobic degradation of methanol. *Journal of Fermentation and Bioengineering* **75**, 368-74 (1993).
28. Paulo, P.L., Jiang, B., Cysneiros, D., Stams, A.J. & Lettinga, G. Effect of cobalt on the anaerobic thermophilic conversion of methanol. *Biotechnol Bioeng* **85**, 434-41 (2004).
29. Stupperich, E., Eisinger, H.J. & Albracht, S.P. Evidence for a super-reduced cobamide as the major corrinoid fraction in vivo and a histidine residue as a cobalt ligand of the p-cresolyl cobamide in the acetogenic bacterium *Sporomusa ovata*. *European Journal of Biochemistry / FEBS* **193**, 105-9 (1990).
30. Stupperich, E. & Konle, R. Corrinoid-dependent methyl transfer reactions are involved in methanol and 3,4-dimethoxybenzoate metabolism by *Sporomusa ovata*. *Applied and Environmental Microbiology* **59**, 3110-6 (1993).
31. Hagemeier, C.H., Kruer, M., Thauer, R.K., Warkentin, E. & Ermler, U. Insight into the mechanism of biological methanol activation based on the crystal structure of the methanol-cobalamin methyltransferase complex. *Proceedings of the National Academy of Sciences of the United States of America* **103**, 18917-22 (2006).
32. Sauer, K. & Thauer, R.K. Methanol:coenzyme M methyltransferase from *Methanosarcina barkeri* - substitution of the corrinoid harbouring subunit MtaC by free cob(I)alamin. *European Journal of Biochemistry / FEBS* **261**, 674-81 (1999).
33. Junier, P. et al. The genome of the Gram-positive metal- and sulfate-reducing bacterium *Desulfotomaculum reducens* strain MI-1. *Environmental Microbiology* **12**, 2738-54 (2010).
34. Pester, M. et al. Complete genome sequences of *Desulfosporosinus orientis* DSM765T, *Desulfosporosinus youngiae* DSM17734T, *Desulfosporosinus meridiei* DSM13257T, and *Desulfosporosinus acidiphilus* DSM22704T. *Journal of Bacteriology* **194**, 6300-1 (2012).
35. Odom, J.M. & Peck, H.D. Hydrogen Cycling as a General Mechanism for Energy Coupling in the Sulfate-Reducing Bacteria, Desulfovibrio-Sp. *Fems Microbiology Letters* **12**, 47-50 (1981).

Chapter 6

A genomic comparison of syntrophic and non-syntrophic butyrate- and propionate-degrading bacteria points to a key role of formate in syntrophy

Michael Visser

This chapter is adapted from the review accepted in BBA - Bioenergetics Special Issue: 18th European Bioenergetics Conference (Biochim. Biophys. Acta, Volume 1837, Issue 7, July 2014).

A genomic view on syntrophic versus non-syntrophic lifestyle in anaerobic fatty acid degrading communities

Petra Worm[1],, Jasper J. Koehorst[2]**, Michael Visser[1]**, Vicente T. Sedano-Núñez[1], Peter J. Schaap[2], Caroline M. Plugge[1], Diana Z. Sousa[1,3], Alfons J.M. Stams[1,3].*

Volume 1837, Issue 12, December 2014, Pages 2004–2016

Laboratory of Microbiology, Wageningen University, Dreijenplein 10, 6703 HB Wageningen, the Netherlands
Systems and Synthetic Biology, Wageningen University, Dreijenplein 10, 6703 HB Wageningen, the Netherlands
Centre of Biological Engineering, University of Minho, 4710-057 Braga, Portugal

* Corresponding author. Tel.: +31 317 483107; Fax: +31 0317 483829; e-mail address: petra.worm@wur.nl
** Both authors contributed equally

6.1 Abstract

In sulfate-reducing and methanogenic environments complex biopolymers are hydrolyzed and degraded by fermentative micro-organisms that produce hydrogen, carbon dioxide and short chain fatty acids. Degradation of short chain fatty acids can be coupled to methanogenesis or to sulfate reduction. Here, a genome perspective why some of these micro-organisms are able to grow in syntrophy with methanogens and others are not is presented. Bacterial strains were selected based on genome availability and on their ability to grow with butyrate and propionate alone or in syntrophic association with methanogens. Systematic functional domain profiling allowed shedding light on this fundamental and ecologically important question. Extra-cytoplasmic formate dehydrogenases (InterPro domain number; IPR006443), including their maturation protein FdhE (IPR024064 and IPR006452) is a typical difference between syntrophic and non-syntrophic butyrate and propionate degraders. This also implies that formate is an important electron carrier in syntrophic butyrate and propionate degradation. Furthermore, two domains with a currently unknown function seem to be associated with the ability of syntrophic growth. One is putatively involved in capsule or biofilm production (IPR019079) and a second in cell division, shape-determination or sporulation (IPR018365). The sulfate-reducing bacteria *Desulfobacterium autotrophicum* HRM2, *Desulfomonile tiedjei* and *Desulfosporosinus meridei* were never tested for syntrophic growth, but all crucial domains were found in their genomes, which suggests their possible ability to grow in syntrophic association with methanogens. In addition, profiling domains involved in electron transfer mechanisms revealed the important role of the Rnf-complex and the formate transporter in syntrophy, and indicates that DUF224 may also have a role in electron transfer in bacteria other than *Syntrophomonas wolfei*.

6.2 Introduction

Environments with a low redox potential are abundantly present on earth, especially in the deeper zones of marine and freshwater sediments. The low redox potential is created by the depletion of oxygen and the formation of hydrogen sulfide in the anaerobic degradation of organic matter. In the decomposition of sulfur-containing organic compounds such as the amino acids (cysteine and methionine) and cofactors (biotin and thiamin) hydrogen sulfide is released. Additionally, hydrogen sulfide is formed by anaerobic microorganisms that respire with sulfate or other sulfur compounds, such as thiosulfate and elemental sulfur. This respiratory type of sulfidogenesis is quantitatively most important [1-3].

Respiratory sulfate reduction is an important process in nature, especially in marine sediments where the sulfate concentration is high (about 20 mM) [4]. In freshwater environments that are generally low in sulfate, sulfate reduction does not play an important role unless hydrogen sulfide is rapidly oxidized by sulfide-oxidizing microbes [5,6]. In sulfate-depleted anoxic environments methanogenesis is the most abundant process [7,8]. Interestingly, in marine environments methanogenesis occurs simultaneously with sulfate reduction as well, especially in zones where the available sulfate is not sufficient to degrade organic matter [9]. In both marine and freshwater environments microbes involved in sulfate-reduction and methanogenesis interact strongly with each other, and this interaction is strongly depending on the availability of sulfate. Generally, sulfate reduction is favoured over methanogenesis when sufficient sulfate is present [4,8].

In sulfate-reducing and methanogenic environments organic material is degraded in a cascade process. Complex biopolymers are first hydrolysed and degraded by fermentative microorganisms

that produce hydrogen, carbon dioxide and organic compounds, typically organic acids (butyrate, propionate, acetate and formate) as products. In sulfate-reducing environments these compounds are the common substrates for sulfate-reducing microorganisms. Phylogenetically and physiologically sulfate reducing microorganisms are very diverse [4]. Phylogenetically they occur in the bacterial and archaeal domain of life. Some sulfate reducers have the ability to grow autotrophically with H_2 and sulfate as energy substrates. Often these autotrophs are the sulfate reducers that are also able to degrade acetate completely to CO_2, employing the reversible Wood-Ljungdahl pathway for acetate degradation and acetate formation [10].

In methanogenic environments, methanogens use H_2/CO_2, formate and acetate as the main substrates [11]. Methanogenic archaea belong to different phylotypes. The ability to use acetate is restricted to archaea belonging to the order Methanosarcinales, with *Methanosarcina* and *Methanosaeta* as important genera. The ability to grow with H_2/CO_2 and formate occurs in most of the currently described orders of methanogens [11]. Higher organic compounds such as propionate and butyrate, that are typical intermediates in methanogenic environments, are not degraded by methanogens. Therefore, acetogenic bacteria are required to degrade such compounds to the methanogenic substrates acetate, formate and H_2/CO_2 [8,12]. For thermodynamic reasons such bacteria can only degrade propionate and butyrate when the products are efficiently taken away by methanogens. This is also known as interspecies electron transfer of which interspecies hydrogen transfer is the most studied and commonly accepted form of electron carrier. However, the importance of formate as an electron carrier has become more apparent the last decades. The methanogenic substrates acetate and formate can also be degraded by syntrophic communities [13,14]. Syntrophic acetate degradation especially occurs under conditions at which the activity of acetoclastic methanogens is low such as a high temperature and high levels of ammonium [13]. However, for syntrophic formate degradation it is of yet unclear to what extend and in what types of anaerobic microbial environments it can compete with formate degradation by methanogens. Though the basic concepts of sulfate reduction and methanogenesis are clear, it is not very clear how sulfate-reducing and methanogenic communities in freshwater and marine sediments are responding to changes in the sulfate availability. The metabolic flexibility of sulfate-reducing bacteria has been addressed recently [15-17]. Several sulfate reducers are able to grow acetogenically in syntrophic association with methanogens, which is for instance the case for *Syntrophobacter fumaroxidans* growing with propionate. Nevertheless, not all sulfate reducers possess the ability to switch from a sulfate-dependent lifestyle to a syntrophic lifestyle. For instance, *Desulfobulbus propionicus* is a bacterium that grows with propionate and sulfate, but it is not able to grow with propionate in syntrophy with methanogens. Similarly, the thermophilic sulfate reducer *Desulfotomaculum kuznetsovii* is able to degrade propionate with sulfate, but it is not able to grow in syntrophy with methanogens, while the phylogenetically closely related non-sulfate-reducing bacterium *Pelotomaculum thermopropionicum* grows with propionate in syntrophy with methanogens [18]. This chapter converses the importance of formate as an electron carrier in syntrophic butyrate and propionate degradation and tries to answer a fundamental and ecologically important question: "what are the key properties that make that a butyrate- or propionate-degrading bacterium is able to grow in syntrophy with methanogens or not". The availability of genome sequences of bacteria that can and bacteria that cannot grow with butyrate and propionate in syntrophic association may allow identifying key genes in syntrophy. If formate is an important electron carrier this should also become apparent from the genome comparison.

6.2 Microbial functions required for syntrophic growth

6.2.1 Functional profiling strategies

Bacterial strains were selected based on genome availability, and ability to grow with butyrate and/ or propionate syntrophically or not. Sulfate reducers that grow with butyrate and/or propionate, whose genomes are available and currently have not been tested for syntrophic growth were included in the analysis (Table 6.1). Correct codon usage of sequences coding for selenocystein-containing formate dehydrogenases and hydrogenases was verified. Functional domain profiles were obtained with InterProScan 5 (version 5RC7, 27th January 2014). To get more insight into microbial functions required for syntrophic growth, domain based functional profiles of five butyrate- or propionate-degrading syntrophs were compared with the non-syntrophs *Desulfobulbus propionicus* and *Desulfotomaculum kuznetsovii*. Domains only present in syntrophs are listed in Table 6.1. Genomes of sulfate reducers that degrade butyrate or propionate, but were never tested for syntrophy, were screened for these domains (Table 6.1). Functional domains assigned to proteins involved in electron transport were separately analyzed. Domains that were unique for each protein were selected. Genomes of butyrate- or propionate-degrading syntrophs, non-syntrophs and sulfate reducers that never have been tested for syntrophy were screened for these domains (Table 6.2). Electron transport mechanisms in butyrate- and propionate-degrading syntrophs and non-syntrophs were predicted from their genomes by using the tools described below (Figure 6.3A-G).

6.2.2 Electron transfer complexes predicted from genome analysis

Gene analysis started with automatic annotations of genomes from DOE-Joined Genome Institute [19]. NCBI-pBLAST analysis with sequences from biochemically confirmed active subunits, was used to indicate the presence of gene clusters coding for formate dehydrogenases, hydrogenases, electron transfer flavoprotein (Etf) and Rnf complexes in the genomes of *Syntrophomonas wolfei*, *Syntrophus aciditrophicus*, *Syntrophothermus lipocalidus*, *Syntrophobacter fumaroxidans*, *Pelotomaculum thermopropionicum*, *Desulfotomaculum kuznetsovii*, and *Desulfobulbus propionicus*. N-terminal amino acid sequences that corresponded to those of formate dehydrogenase 1 and -2 of *S. fumaroxidans* were used to find the gene clusters that code for these enzymes. To identify cofactor binding motifs, transmembrane helices, and twin-arginine translocation motifs in the N-terminus we used the Pfam protein families database version 27.0 (March 2013) [20], TMHMM Server v. 2.0 [21] and the TatP 1.0 Server [22] respectively. RNA loop predictions with Mfold version 3.2. was used to predict incorporation of selenocysteine [23,24]. We compared the predicted RNA loop in the 50-100 bp region downstream of the UGA-codon with the consensus loop previously described [25]. Sequences with similarity to iron-only or [FeFe]-hydrogenases, were manually analyzed for the presence of conserved H-cluster residues [26]. Bifurcation of electrons can occur via FAD, without the presence of iron-sulfur clusters [27]. When a FAD binding domain was predicted by Pfam we propose that electrons from reduced ferredoxin and NADH can confurcate. In some cases, also an NADH binding site and/or iron sulphur cluster binding motifs were found with Pfam. Cofactor binding to NADH: ubiquinone oxidoreductase subunits in bacteria as listed by Yano and co-workers [28] was predicted based on domain similarity as determined by Pfam. We predict that enzyme complexes with an NADH binding domain, iron-sulfur clusters and a domain binding Mo/W, Se or hydrogen and not necessarily flavin, might have electron confurcating functions. Iron-only hydrogenases ([Fe]-hydrogenases) do not contain Fe-S clusters nor Ni and Fe clusters, and

were initially referred to as "metal-free" hydrogenases. They are present mainly in methanogens, they belong to a phylogenetically distinct class and their function in bacteria is not clear [29].

6.2.3 Domain based genome comparison of syntrophic and non-syntrophic butyrate and/or propionate degraders

Six domains are present in the genomes of all analyzed butyrate- or propionate-degrading syntrophs and not in non-syntrophs (Table 6.1). Domain "IPR006443" is exclusively present in the extra-cytoplasmic formate dehydrogenase (FDH) alpha subunit. Domains "IPR024064 and IPR006452" both belong to FdhE. The gene *fdh*E in *Escherichia coli* is required for maturation of the membrane bound FDH-complex [30]. The fact that extra-cytoplasmic formate dehydrogenases are only present in syntrophs and not in non-syntrophs strongly indicates that extra-cytoplasmic formate production is essential for syntrophic propionate and butyrate oxidation, and thus that formate plays a major role in interspecies electron transfer. The redox potential of the couple proton / hydrogen ($E^{0'}$= -414 mV) is slightly higher than the redox potential of the couple CO_2 / formate (-432 mV). The preference in syntrophic butyrate and propionate degrading communities has not been clear thus far, but a syntrophic relationship in which both hydrogen and formate can be transferred would be more flexible than when only hydrogen is transferred [31]. Moreover, multiple studies indicate that interspecies formate transfer is of significant importance in syntrophic degradation of butyrate and propionate. For example, *Syntrophobacter fumaroxidans* and *Syntrophospora bryantii* oxidize propionate and butyrate, respectively, in syntrophy with hydrogen and formate-using methanogens such as *Methanospirillum hungatei* and *Methanobacterium formicicum*, but not with the hydrogen only-using *Methanobrevibacter arboriphilus* [32]. In analogy with this, *S. wolfei* oxidizes butyrate faster with the formate and hydrogen-using *M. hungatei* than with the hydrogen-only using *M. arboriphilus* [33]. The importance of formate transfer in *S. wolfei* co-cultures is additionally supported by the observed involvement of an extra-cytoplasmic formate dehydrogenase in the final reduction of CO_2 with electrons generated by the butyryl-CoA to crotonyl-CoA conversion [34]. Moreover, this extra-cytoplasmic formate dehydrogenase was more expressed during syntrophic growth compared to axenic growth [34].

Domain "IPR019079", named CapA, was found in genomes of all the syntrophs and was not present in the genomes of the two non-syntrophs (Table 6.1). CapA is part of a membrane bound complex that synthesizes poly-g-glutamate to form a capsule or biofilm in *Bacillus subtilis*, *B. anthracis*, *Staphylococcus epidermidis* and *Fusobacterium nucleatum* [49-51]. The presence of this domain in butyrate- and propionate-degrading bacteria may contribute to the formation of exo-polymeric substances that may facilitate syntrophic growth. Domain "IPR018365" is present in FtsW, RodA, SpoVE, that are membrane integrated proteins involved in cell division, shape-determination and sporulation in *Escherichia coli* and *Bacillus subtilis* [52-54]. What the exact function of this domain is in syntrophic butyrate and propionate degraders is unclear. The domain "IPR020539" that seems exclusively present in syntrophs in our analysis belongs to the protein Ribonuclease P which removes extra residues at the 5'- side from precursor tRNA, resulting in mature tRNA. However, what its function could be in syntrophic growth is unclear, but just coincidence cannot be excluded. As can be seen from Table 1, only one copy of this domain is present in the genome of a syntrophic bacterium, whereas for the domains involved in periplasmic formate dehydrogenases, CapA-domains and Cell cycle FtsW / RodA / SpoVE- domains, more copies are

Table 6.1. Domain based genome comparison of syntrophic and non-syntrophic butyrate and propionate degraders. Domains present in genomes of all butyrate- and propionate-degrading syntrophs and absent in those of non-syntrophs are listed and domain abundance is indicated. Syntrophs are shaded white, non-syntrophs are shaded black and sulfate reducers that were never tested for syntrophic growth are shaded grey.

		Syntrophomonas wolfei	*Syntrophus aciditrophicus*	*Syntrophothermus lipocalidus*	*Syntrophobacter fumaroxidans*	*Pelotomaculum thermopropionicum*	*Desulfotomaculum kuznetsovii*	*Desulfobulbus propionicus*	*Desulfobulbus japonicus*	*Desulfatibacillum alkenivorans*	*Desulfatirhabdium butyrativorans*	*Desulfobacterium autotrophicum* HRM2	*Desulfospira joergensenii*	*Desulfotignum balticum*	*Desulfomonile tiedjei*	*Desulfarculus baarsii*	*Desulfosporosinus meridiei*	*Desulfotalea psychrophila*	*Desulfatibacillum aliphaticivorans*	*Desulfotomaculum gibsoniae*
Growth on butyrate[¥]																				
Growth on propionate[¥]																				
Extra-cytoplasmic FDH alpha subunit	IPR006443	1	2	1	3	1	0	0	0	2	1	5	2	0	2	0	1	0	0	1
FdhE-like protein	IPR024064	4	6	2	5	3	0	0	0	0	0	4	4	0	2	1	2	0	0	2
FDH accessory protein	IPR006452	2	3	1	2	1	0	0	0	0	0	2	2	0	1	0	1	0	0	1
Capsule synthesis protein, CapA	IPR019079	2	2	4	2	1	0	0	0	0	0	4	2	0	2	0	4	4	0	2
Cell cycle, FtsW / RodA / SpoVE,	IPR018365	1	2	2	2	1	0	0	0	2	1	3	0	1	1	2	2	0	0	0
Ribonuclease P, conserved site	IPR020539	1	1	1	1	1	0	0	0	2	1	1	0	0	1	1	1	1	0	0

[¥]The ability of substrate conversion was retreived from literature [18,21,22,24-37].

Table 6.2. Profiles of functional domains involved in electron transfer mechanisms. Profiles of functional domains involved in electron transfer mechanisms are shown. Domain abundance is indicated. Syntrophic propionate and/or butyrate degraders are shaded white, non-syntrophic propionate and/or butyrate degraders are shaded black and sulfate reducers that were never tested for syntrophic growth are shaded grey. Abbreviations are explained as formate dehydrogenase (FDH); NADH: ubiquinone oxidoreductase subunit 51 kDa (NUO 51kDa); membrane-bound ferredoxin:NAD+ oxidoreductase (Rnf) complex; Butyryl-CoA dehydrogenase (Bcd); Domain of unknown function 224 (DUF224).

			Syntrophomonas wolfei	*Syntrophus aciditrophicus*	*Syntrophothermus lipocalidus*	*Syntrophobacter fumaroxidans*	*Pelotomaculum thermopropionicum*	*Desulfotomaculum kuznetsovii*	*Desulfobulbus propionicus*	*Desulfobulbus japonicus*	*Desulfatibacillum alkenivorans*	*Desulfatirhabdium butyrativorans*	*Desulfobacterium autotrophicum* HRM2	*Desulfospira joergensenii*	*Desulfotignum balticum*	*Desulfomonile tiedjei*	*Desulfarculus baarsii*	*Desulfosporosinus meridiei*	*Desulfotalea psychrophila*	*Desulfatibacillum aliphaticivorans*	*Desulfotomaculum gibsoniae*
Growth on SCFA[¥]		Butyrate																			
		Propionate																			
Protein (complex)	Subunit	InterPro number																			
Cytoplasmic FDH	Alpha	IPR027467	4	2	2	3	1	2	0	0	5	3	10	2	5	2	3	4	2	2	2
		IPR006655	2	4	0	5	2	2	2	1	9	5	9	3	4	7	1	7	4	1	6
		IPR006478	0	0	1	3	0	1	0	0	1	1	1	0	0	2	0	2	0	1	1
	NUO 51kDa	IPR019575	12	12	4	8	6	12	8	2	12	4	6	0	12	9	8	6	8	6	12
		IPR001949	8	6	3	4	3	5	4	1	6	2	3	0	6	4	4	1	2	3	4
Extra-cytopl. FDH	alpha	IPR006443	3	4	1	5	2	0	0	1	3	2	5	4	0	2	0	2	0	1	2
Formate transporter	-	IPR000292	2	1	0	1	1	0	0	0	4	0	4	0	0	0	2	2	0	2	0
		IPR024002	2	0	0	1	0	0	0	0	4	0	2	0	0	0	2	2	0	2	0

			Syntrophomonas wolfei	*Syntrophus aciditrophicus*	*Syntrophothermus lipocalidus*	*Syntrophobacter fumaroxidans*	*Pelotomaculum thermopropionicum*	*Desulfotomaculum kuznetsovii*	*Desulfobulbus propionicus*	*Desulfobulbus japonicus*	*Desulfatibacillum alkenivorans*	*Desulfatirhabdium butyrativorans*	*Desulfobacterium autotrophicum* HRM2	*Desulfospira joergensenii*	*Desulfotignum balticum*	*Desulfomonile tiedjei*	*Desulfarculus baarsii*	*Desulfosporosinus meridiei*	*Desulfotalea psychrophila*	*Desulfatibacillum aliphaticivorans*	*Desulfotomaculum gibsoniae*
FeFe-hydrogenase	Alpa	IPR004108	4	1	3	3	4	8	3	0	0	0	4	1	2	1	1	5	4	0	7
		IPR009016	5	1	3	3	5	8	3	0	0	0	6	1	2	1	1	5	6	0	7
		IPR003149	9	3	9	6	9	12	6	0	0	0	9	3	3	3	0	9	6	0	9
		IPR013352	3	1	3	2	3	4	2	0	0	0	3	1	1	1	0	3	2	0	3
NiFe-hydrogenase		IPR001501†	0	2	3	17	2	0	10	7	12	1	12	2	6	3	2	7	14	8	8
		IPR018194†	0	1	2	6	2	0	6	4	9	2	8	2	4	4	4	5	13	7	2
Rnf complex	RnfB	IPR007202	2	2	0	9	6	10	2	0	22	7	30	10	10	14	13	6	4	4	13
		IPR010207	0	1	0	1	0	0	0	0	1	0	5	1	0	1	0	0	2	1	0
	RnfC	IPR026902	0	1	0	1	0	0	0	1	4	0	2	2	1	1	1	3	6	1	0
		IPR010208	0	2	0	2	0	0	0	0	0	0	4	0	0	2	2	0	4	0	0
	RnfD	IPR004338	0	1	0	1	0	0	0	0	2	1	4	1	2	1	1	0	4	0	0
		IPR011303	0	1	0	1	0	0	0	0	2	1	2	1	1	1	1	0	2	0	0
	RnfG	IPR007329	2	2	0	2	0	0	0	0	4	2	14	2	6	2	2	0	8	0	6
Ech complex	EchA	IPR001750	0	0	4	6	0	3	14	0	4	9	8	6	9	6	0	7	11	0	3
		IPR001516	0	0	2	2	0	1	3	0	0	1	0	2	2	2	0	1	0	0	1
	EchB	IPR001694	0	0	3	4	0	2	8	0	0	2	2	0	1	4	0	4	6	0	2
	EchC	IPR006137	0	2	6	16	2	2	19	6	12	6	12	4	8	8	4	12	22	6	9
	EchD	IPR001268	0	0	2	2	0	1	3	0	0	2	1	0	1	2	0	3	4	0	1

		IPR012179	0	0	0	0	0	0	0	0	0	0	0	0	0	0	0	0	0	0	0
	EchE	IPR001135	0	0	4	3	0	2	5	0	0	3	1	0	1	2	0	4	6	0	2
Etf alpha	-	IPR014731	3	1	4	4	6	4	2	0	10	4	7	4	7	3	3	3	3	0	1
Etf beta	-	IPR012255	3	1	4	4	7	4	2	0	10	4	5	4	7	3	3	3	2	0	1
Bcd	-	IPR006089	7	6	17	7	8	12	6	0	54	9	18	4	10	21	22	15	0	15	20
		IPR009075	18	13	28	14	20	20	6	0	*	36	64	17	36	45	44	22	0	34	30
		IPR006092	7	6	10	6	9	8	3	0	82	15	31	7	16	19	18	8	0	15	15
		IPR006091	18	13	27	14	20	18	6	0	*	36	68	17	36	45	43	22	0	36	30
		IPR013786	8	6	12	6	9	9	3	0	90	15	31	7	17	19	19	9	0	18	15
		IPR009100	9	7	14	8	11	9	3	0	*	18	34	9	19	25	23	12	0	18	15
DUF224	-	IPR003816	1	1	1	1	2	1	2	0	5	4	6	2	5	8	3	4	2	2	1
		IPR004017	6	15	10	27	13	26	17	8	58	25	54	24	34	39	18	34	33	10	31
		IPR023234	1	1	1	5	3	3	4	0	19	6	27	6	14	15	9	8	8	6	3
Cytochrome	c	IPR023155	1	1	0	6	0	0	12	0	12	4	10	4	4	20	11	1	3	2	0
		IPR024673	0	0	0	3	0	0	0	0	10	3	2	0	4	0	0	0	6	0	0
	cIII	IPR020942	0	0	0	2	0	0	4	2	10	5	11	4	10	4	2	0	0	1	0
		IPR002322	0	0	0	0	0	0	8	4	24	16	40	16	24	8	4	0	0	4	0
	b561	IPR016174	6	6	6	3	1	2	1	1	4	2	0	4	2	6	1	13	11	0	1
		IPR000516	0	0	4	2	0	0	0	0	4	2	0	0	0	0	0	10	10	0	2
	b5	IPR001199	0	3	0	3	0	0	0	0	0	3	0	4	0	3	0	0	0	0	0

¥ The ability of substrate conversion was retreived from literature [18,21,22,24-37,48-56].

**more than 99*

†These IPR numbers were unique for NiFe hydogenase alpha subunits. As the Ech complex also contains a NiFe hydrogenase alpha subunit, coresponding domains were also found in this EchE.

present. Furthermore domain co-occurrence suggests that *D. autotrophicum* HRM2, *D. tiedjei* and *D. meridiei* are able to adopt a syntrophic lifestyle.

6.2.4 Domain based functional profiling of electron transfer mechanisms

For syntrophic butyrate and propionate degradation, electron transfer mechanisms are required to transfer electrons to the terminal acceptor, which can be sulfate in a sulfidogenic lifestyle or protons and/or CO_2 in a syntrophic lifestyle. As the previous paragraph focussed on functional domains that are present in all syntrophic and not in non-syntrophic propionate and butyrate degraders, here we profile the functional domains involved in electron transfer mechanisms (Table 6.2). As can be seen from Table 6.2, cytoplasmic and extra-cytoplasmic formate dehydrogenases contain InterPro domains that are unique for each protein. "IPR006443" is only present in extra-cytoplasmic FDH's, not in cytoplasmic FDH's whereas "IPR027467", "IPR006655" and "IPR006478" of cytoplasmic FDH, are not present in extra-cytoplasmic FDH's. Domains of cytoplasmic FDH's are present in genomes of syntrophs and non-syntrophs, whereas the domain of extra-cytoplasmic FDH's is present only in syntrophs. Formate transporter linked domains are absent in genomes of non-syntrophs, whereas they are present in a number of syntrophs. These observations again point to the importance of formate as interspecies electron carrier. The membrane bound Rnf complex that can conserve energy by the reversible translocation of protons or sodium ions from ferredoxin oxidation with NAD^+ [55] was not found in non-syntrophs, but is present in several syntrophs. As syntrophs live at the limit of what is energetically possible [56-58] they contain mechanisms to conserve energy from ferredoxin oxidation with NAD^+.

Furthermore, recently the domain with unknown function "DUF224" was shown to play a role in electron transport from an electron transfer flavoprotein (ETF) towards membrane-bound electron transfer components in *S. wolfei* [34]. DUF224 is present in 18 genomes from which 17 also contain domains linked to ETF complexes. This indicates that DUF224 may also have a role in electron transfer in bacteria other than *S. wolfei*.

6.3 Energetics and metabolism of syntrophic butyrate and propionate degradation

6.3.1 Energy conservation mechanisms

For microbial maintenance and growth the energy that is released from catabolic reactions has to be converted into energy that can be used to perform anabolic reactions. Therefore, energy is conserved as ATP by substrate level phosphorylation or via a proton or sodium gradient over the cytoplasmic membrane, termed electron transport phosphorylation. Membrane bound enzyme complexes are required to build a proton gradient over the membrane while other membrane bound enzyme complexes are required to use the proton gradient. The membrane bound enzyme complex ATP synthase can either use the proton gradient for ATP synthesis or ATP hydrolysis to build the proton gradient.

In addition to substrate level phosphorylation and the proton gradient over the cytoplasmic membrane, a recently discovered process called flavin-based electron bifurcation has been considered as a third mechanism for energy conservation [68]. In the last decade, several of such cytoplasmic bifurcation complexes were determined in bacteria and archaea [68-76]. Instead of coupling two redox reactions, as is performed by commonly known redox proteins, bifurcation (and the reversed reaction termed confurcation) enzyme complexes couple three redox reactions. With this concept, energy that would otherwise have been lost can be conserved

or endergonic reactions can be coupled to exergonic reactions and reducing equivalents that are generated can be re-oxidized efficiently. For instance endergonic reduction of ferredoxin with NADH is coupled to the exergonic reduction of crotonyl-CoA to butyryl-CoA by the butyryl-CoA / electron transfer flavoprotein complex of *Clostridium kluyveri* [60]. Another example is the [FeFe]-hydrogenase complex of *Thermotoga maritima* that couples reversible ferredoxin reduction with hydrogen to NAD^+ reduction [72]. In addition to cytoplasmic bifurcating enzyme complexes, membrane bound complexes (Rnf-complexes) were recently shown to conserve energy by the reversible translocation of protons or sodium from ferredoxin oxidation with NAD^+ [66]. The energy conserving hydrogenase (Ech) has a similar function, but performs the proton or sodium translocation by ferredoxin oxidation with hydrogen production [78].

6.3.2 Syntrophic butyrate degradation

Butyrate oxidation coupled to hydrogen or formate production is endergonic under standard conditions. This is shown by the positive standard Gibbs free energy changes; + 48 kJ and + 55 kJ, respectively (Table 6.3). When butyrate oxidation is coupled to methane production the conversion is energetically feasible. To share this energy between the syntrophic butyrate oxidizer and the methanogen in such a manner that both organisms gain enough energy to grow, the hydrogen and formate concentrations have to be kept in a low range [58]. *Syntrophomonas wolfei*, *Syntrophus aciditrophicus* and *Syntrophothermus lipocalidus* can couple butyrate oxidation to syntrophic growth with methanogens and cannot grow in pure culture with any of the common inorganic electron acceptors [32,35,79].

All syntrophic butyrate degraders oxidize butyrate via the beta-oxidation pathway (Table 6.4, Figure 6.1) [8,56]. This pathway includes two reactions that generate each two electrons and two protons and one that generates ATP. This ATP partially has to be invested in the endergonic conversion of butyryl-CoA to crotonyl-CoA. The biochemical mechanism that enables investment of a fraction of ATP for the endergonic conversion of butyryl-CoA to crotonyl-CoA has recently been revealed in *S. wolfei*. Electrons that are generated by the conversion of butyryl-CoA to crotonyl-CoA travel via butyryl-CoA dehydrogenase (encoded by genes with locus tags Swol_1933 and Swol_2053), an electron transfer flavoprotein (encoded by Swol_0696-7) and a membrane anchored protein that was annotated as DUF224 (encoded by Swol_0698) to the menaquinone pool in the membrane. Oxidation of reduced menaquinone is then coupled to formate generation by a membrane anchored extra-cytoplasmic formate dehydrogenase (encoded by Swol_0797-800) [45]. For this reaction, two protons from the membrane potential are invested and simultaneously formate is produced that is used by the methanogen. This indicates the importance of formate as an electron carrier in syntrophic butyrate degradation. The second reaction that generates electrons and protons is the conversion of hydroxybutyryl-CoA to acetoacetyl-CoA which is endergonic when coupled via NAD^+ to hydrogen or formate production. Most likely in *S. wolfei* this involves the [FeFe]-hydrogenase (encoded by Swol_1017-19) that forms a cytoplasmic complex with a formate dehydrogenase (Swol_0783-6) [81].

6.3.3 Syntrophic propionate degradation

Propionate oxidation coupled to hydrogen or formate production is endergonic under standard conditions. This is shown by the positive Gibbs free energy changes; + 72 kJ and + 82 kJ

Table 6.3 Gibbs free energy changes of butyrate, propionate and formate oxidation and methane production. Values were calculated from the Gibbs free energies of formation of the reactants at a concentration of 1M, pH 7.0, T=298K and a partial pressure of gas of 1 atmosphere according to Thauer et al. 1977 [80].

Eq. no	Reaction	$\Delta G^{0'}$ (kJ/reaction)
1a	$Butyrate^- + 2\ H_2O \rightarrow 2\ Acetate^- + H^+ + 2H_2$	+ 48
1b	$Butyrate^- + 2\ H_2O + 2\ CO_2 \rightarrow 2\ Acetate^- + 3\ H^+ + 2\ Formate^-$	+ 55
2a	$Propionate^- + 2\ H_2O \rightarrow Acetate^- + CO_2 + 3\ H_2$	+ 72
2b	$Propionate^- + 2\ H_2O + 2\ CO_2 \rightarrow Acetate^- + 3\ Formate^- + 3\ H^+$	+ 82
3	$Formate^- + H^+ \rightarrow H_2 + CO_2$	-3.4
4	$4\ Formate + 4\ H^+ \rightarrow CH_4 + 3\ CO_2 + 2\ H_2O$	- 145
5	$4\ H_2 + CO_2 \rightarrow CH_4 + 2\ H_2O$	- 131
6	$Acetate^- + H^+ \rightarrow CH_4 + CO_2$	-36

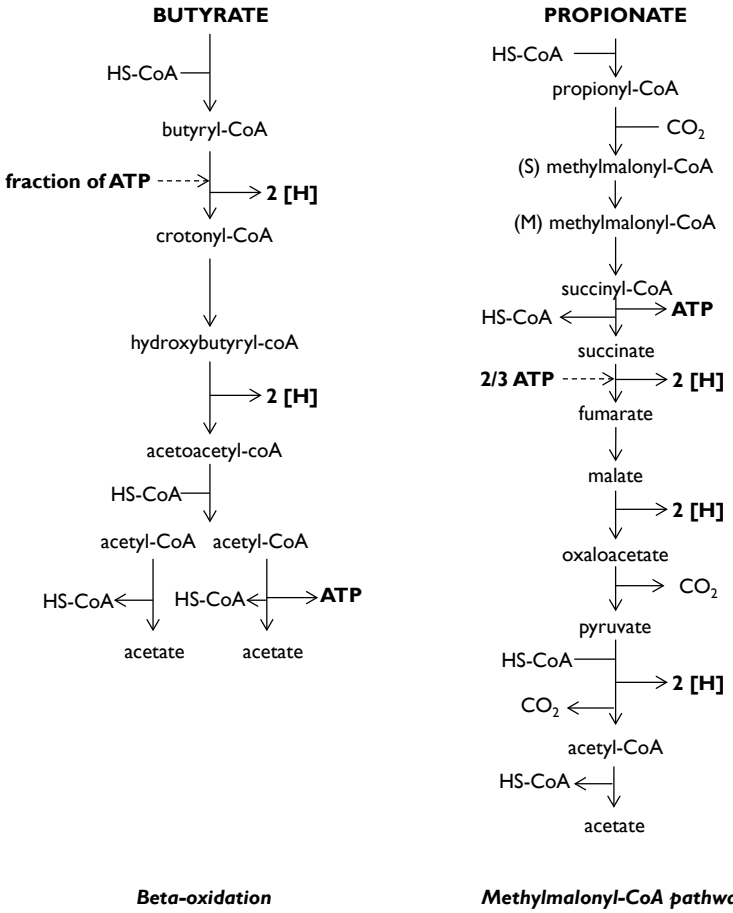

Figure 6.1: Metabolic pathways that are used for butyrate and propionate conversion by bacteria that can grow in syntrophy with methanogens.

respectively (Table 6.3). However, when propionate oxidation is coupled to methane production the conversion is energetically feasible. To share energy between the syntrophic propionate oxidizer and the methanogen in such a manner that both organisms gain enough energy to grow, the hydrogen and formate concentrations have to be kept in a low range [58]. *Smithella propionica*, *Syntrophobacter fumaroxidans* and *Pelotomaculum thermopropionicum* are able to couple propionate oxidation to syntrophic growth with methanogens [18, 47, 87, 94]. *Smithella propionica* degrades propionate via a dismutating pathway to acetate and butyrate, which is subsequently oxidized to acetate [95]. All other known syntrophic propionate-degrading bacteria use the methylmalonyl-CoA pathway to oxidize propionate to acetate and CO_2 (Figure 6.1). In this pathway one ATP is formed via substrate level phosphorylation, 2/3 ATP have to be invested and three conversions in the methylmalonyl-CoA pathway generate each two electrons and two protons.

One of the reactions that generates two electrons and two protons is the endergonic oxidation of succinate to fumarate that requires investment of 2/3 ATP [58]. Van Kuijk et al. (1998) [84] proposed that succinate oxidation could be coupled to extra-cytoplasmic hydrogen or formate formation via a menaquinone loop between a cytoplasmic oriented membrane-bound succinate dehydrogenase and a periplasmic oriented membrane bound hydrogenase or formate dehydrogenase. Genes coding for a periplasmic hydrogenase and three extra-cytoplasmic formate dehydrogenases were found in the genome of *S. fumaroxidans* [96]. Especially the gene Sfum_1273-74 that codes for one of the periplasmic formate dehydrogenase alpha subunits is highly transcribed in syntrophic conditions [97], which suggests that succinate oxidation is coupled to formate production and indicates the importance of formate as an electron carrier in syntrophic propionate degradation. Also malate oxidation to oxaloacetate generates two electrons and two protons, which in *S. fumaroxidans* are coupled to NAD^+ reduction by malate dehydrogenase [98]. To couple this to hydrogen production would require a hydrogen partial pressure of 10^{-8} atm, which is lower than can be maintained by methanogens [58]. The third reaction that generates electrons and protons is the conversion of pyruvate to acetyl-CoA and CO_2 that can be coupled to ferredoxin reduction using the pyruvate:ferredoxin oxidoreductases [99]. Genome analysis suggests that NADH generated from malate oxidation and reduced ferredoxin generated from pyruvate oxidation could be coupled to formate or hydrogen production by confurcating formate dehydrogenases and hydrogenases [96]. Such a mechanism would use the energy that remains from ferredoxin oxidation with protons to allow the endergonic coupling of NADH oxidation to proton reduction. Formate dehydrogenases from *S. fumaroxidans* were studied for subunit-composition, enzyme activity, cofactor binding and direction of conversion. Formate dehydrogenase 1 contains W, Se, four [2Fe2S], one [4Fe4S] and is a heterotrimer. Formate dehydrogenase 2 contains W, Se, two [4Fe4S] and is heterodimer. Both enzymes oxidize formate with benzyl viologen and reduce CO_2 with reduced methylviologen. The purified enzyme was not able to reduce NAD^+ [100]. Whether these formate dehydrogenases can confurcate electrons from NADH and reduced ferredoxin to CO_2 reduction, has never been tested.

6.3.4 Syntrophic formate degradation

Genome comparison pointed to the role of formate in syntrophic butyrate and propionate degradation. Interestingly, syntrophic growth with formate was described as well [14]. Formate oxidation coupled to hydrogen is endergonic under standard conditions. This is shown by the Gibbs free energy change that is close to zero; -3.4 kJ (Table 6.3). However, when formate

Table 6.4. Physiological characteristics of the butyrate and propionate degrading syntrophs and non-syntrophs: Syntrophomonas wolfei subsp. wolfei (A), Syntrophus aciditrophicus (B), Syntrophothermus lipocalidus (C), Syntrophobacter fumaroxidans (D), Pelotomaculum thermopropionicum (E), Desulfotomaculum kuznetsovii (F), Desulfobulbus propionicus (G).

	A	B	C	D	E	F	G
Gram reaction	-	-	-[a]	-	-[a]	-[a]	-
Motility	+	-	+	-	-	+	-
Spore formation	-	-	-	-	+	+	-
Growth pH (range /optimum)	ND/7.2?	ND/7.0?	5.8-7.5 (6.5-7)	6.0-8.0/7	6.5-8.0/7.0	ND	6.0-8.6 (7.1-7.5)
Growth temperature (°C) (range/optimum)	ND/35	25-42/35	45-60/55	20-40/37	45-65/55	50-85/60-65	10-43/39
Growth rate (d^{-1})	0.27 in coculture on butyrate with *Methanospirillum hungatei*	0.22 in coculture with *Desulfovibrio strain* G11	0.93 in pure culture on crotonate 1.06 in coculture on butyrate	0.17 in coculture	0.19 coculture on propionate 2.4 coculture on ethanol	ND	0.42 (propionate + sulfate)
Cytochrome b and - c Menaquinone	Cyt C MK-7	MQ	Not found	Cyt b, Cyt c MK-6, MK-7	MK	ND	Cyt b, Cyt c MK-4, MK-5
Metabolic pathway used	β-oxidation	β-oxidation	β-oxidation	Methylmalonyl-CoA	Methylmalonyl-CoA	Wood Ljungdahl Methylmalonyl-CoA β-Oxidation	Methylmalonyl-CoA
Complete/ Incomplete oxidizer	Incomplete	Incomplete	Incomplete	Incomplete	Incomplete	complete	incomplete
Electron acceptor utilization in pure culture	none	none	None	sulfate, thiosulfate, fumarate	fumarate	sulfate, sulfite, thiosulfate	sulfate, sulfite, thiosulfate, nitrate, oxygen, Fe(III)
Substrate utilization in pure culture	crotonate	crotonate	crotonate	propionate, formate, fumarate, succinate, hydrogen, malate, aspartate, pyruvate	propionate, fumarate, pyruvate, ethanol, lactate	formate, acetate, propionate, butyrate, valerate, lactate, malate, fumarate, succinate, methanol, ethanol, propanol, butanol, hydrogen, (up to 50%) CO	propionate, lactate, pyruvate, ethanol, 1-propanol + 1 butanol, H_2

Substrate utilization in co-culture	butyrate, caproate, caprylate, valerate, heptonoate, isoheptanoate	butyrate, benzoate, hexanoate, heptanoate, octanoate, palmitate, stearate, trans-2-pentenoate, trans-2-hexanoate, trans-3-hexanoate, 2-octenoate, methyl esters of butyrate and hexanoate,	butyrate, isobutyrate, straight-chain fatty acids from C4 to C10	Propionate	propionate, ethanol, lactate, 1-butanol, ethylene glycol, 1-propanol, 1-pentanol, 1,3-propanediol	None	None
Syntrophic partner used	*M. hungatei* *Desulfovibrio* G11 *M. bryantii* MoH *M. arboriphilus*	*M. hungatei* *Desulfovibrio* G11 in the presence of sulfate	*M. thermoautotrophicum*	*M. hungatei* *M. formicicum*	*M. thermoautotrophicus*	None	None
References	33, 79, 82, 83	32, 56	35	36, 84, 85	18, 86, 87	75, 88	7, 38, 89-93

[a] *Cells stain Gram-negative but the organism has a Gram-positive cell wall ultrastructure.* [b] *ND: not determined or not reported.*

oxidation is coupled to methane production the conversion is energetically feasible. To share energy between the syntrophic formate oxidizer and the methanogen in such a manner that both organisms gain enough energy to grow, the hydrogen concentrations have to be kept in a low range. The thermophilic *Moorella* sp. strain AMP and mesophilic *Desulfovibrio* sp. strain G11 are able to couple formate oxidation to syntrophic growth with methanogens that can only use hydrogen as electron donor [14]. The electron transfer mechanism that allows syntrophic formate degradation is not known. Possibly an extra-cytoplasmic formate dehydrogenase is coupled to a membrane integrated, cytoplasmic oriented hydrogenase which generates a proton motive force that can be used for ATP synthesis [14]. To what extend and in what types of anaerobic microbial environments syntrophic formate degradation can compete with formate degradation by methanogens is not widely explored.

6.4 Discussion

Recently, Sieber et al. performed a genome comparison of bacteria capable of syntrophic growth with not only butyrate or propionate, but also with acetate, amino acids, lactate, ethanol or sugars [118]. They concluded that confurcating hydrogenases and membrane associated reverse electron transport complexes are present in many syntrophic metabolizers and play a critical role in syntrophy. The domain based functional profiling analysis presented in this chapter confirms the importance of membrane associated reverse electron transport complexes, like the Rnf complex. However, possible confurcating hydrogenases can also be found in non-syntrophs, like *Desulfotomaculum kuznetsovii* [88]. This indicates that these complexes are not exclusive for syntrophs and can also be important for energy conservation in non-syntrophs. In addition, profiling domains involved in electron transfer mechanisms indicates that DUF224 may also have a role in electron transfer in bacteria other than *S. wolfei,* for both syntrophs as well as non-syntrophs.

The analysis of Sieber et al. [118] confined to the genomes of syntrophs whereas this chapter also used the genomes of non-syntrophic sulfate-reducing bacteria in order to identify key-genes in syntrophy. Unfortunately, not many sulfate-reducing bacteria were tested for syntrophic butyrate or propionate degradation. Only *Desulfotomaculum kuznetsovii* and *Desulfobulbus propionicus* are validated non-syntrophs. To strengthen the importance of the analysis, more butyrate- and propionate-degrading sulfate-reducing bacteria have to be tested for syntrophic capability.

Systematic functional profiling of genomes shed light on the question: "what are the key properties that make a butyrate- or propionate-degrading bacterium able to grow in syntrophy with methanogens and another not". The presence or absence of extra-cytoplasmic formate dehydrogenases, including their maturation proteins, is clearly a difference between syntrophic and non-syntrophic butyrate or propionate degraders. Together with transcription and proteomic studies that show an increase of extra-cytoplasmic formate dehydrogenase during syntrophic growth [34, 97], it seems evident that this enzyme is a key factor for syntrophic butyrate and propionate degradation. Moreover, this simultaneously suggests that formate is an important interspecies electron carrier in syntrophic butyrate and propionate degradation. This is supported by the presence of the formate transporter in several butyrate and propionate degrading syntrophs. Further biochemical examination and knock-out experiments of genes involved in formate transport and extra-cytoplasmic formate dehydrogenase activity and maturation would give more insight in the importance of this enzyme complexes during syntrophy. Genetic

manipulation protocols for butyrate and propionate degrading syntrophic bacteria have to be developed.

Furthermore the presence or absence of two domains, both linked to membrane integrated proteins with a currently unknown function in syntrophy, appear to make a difference as well. Both are membrane integrated proteins. One is putatively involved in capsule or biofilm formation and a second in cell division, shape-determination or sporulation. Capsule formation, cell division, shape-determination and sporulation by these bacteria during syntrophic growth could be assessed with microscopic techniques.

Sulfate-reducing bacteria such as *Desulfobacterium autotrophicum* HRM2, *Desulfomonile tiedjei* and *Desulfosporosinus meridiei* were never tested for syntrophic growth, but all crucial domains for syntrophy identified in this chapter were found in corresponding genomes, which suggests their possible ability to grow in syntrophic association with methanogens.

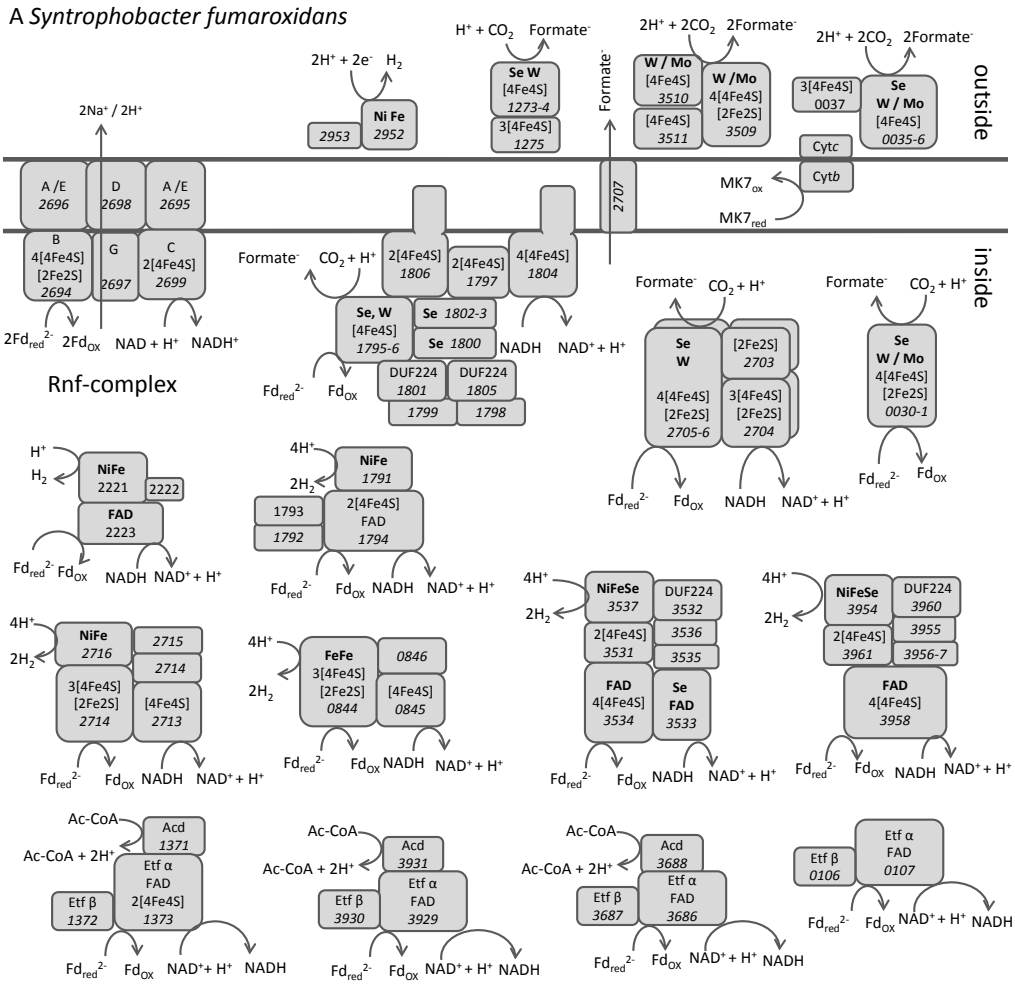

B *Syntrophomonas wolfei*

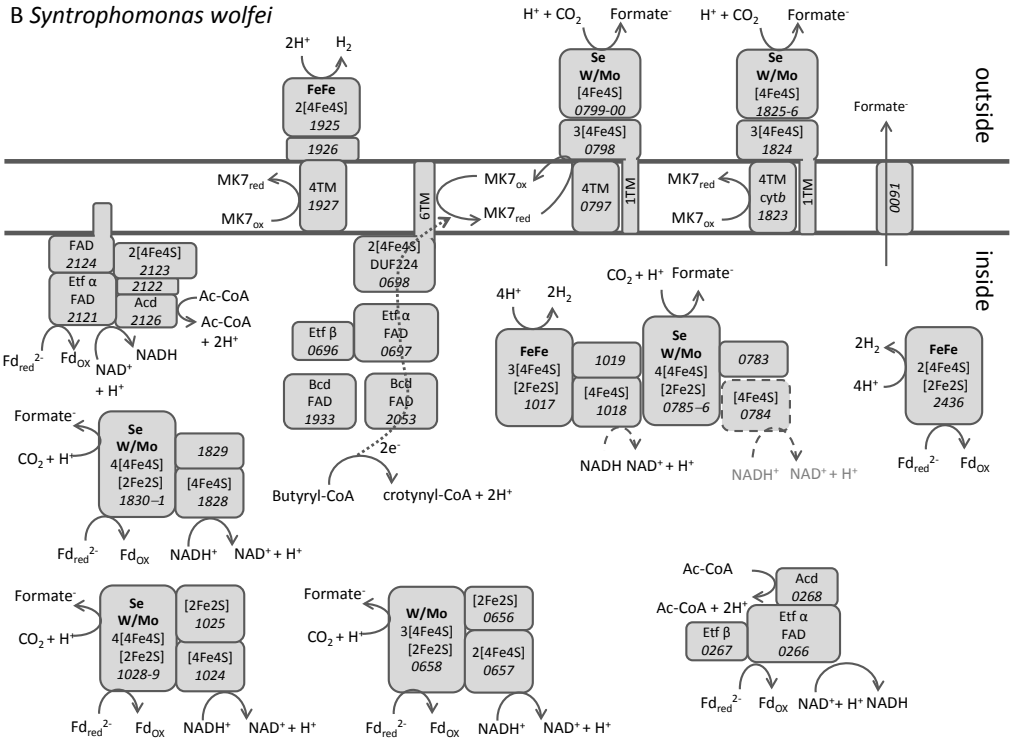

C *Syntrophothermus lipocalidus DSM 12680*

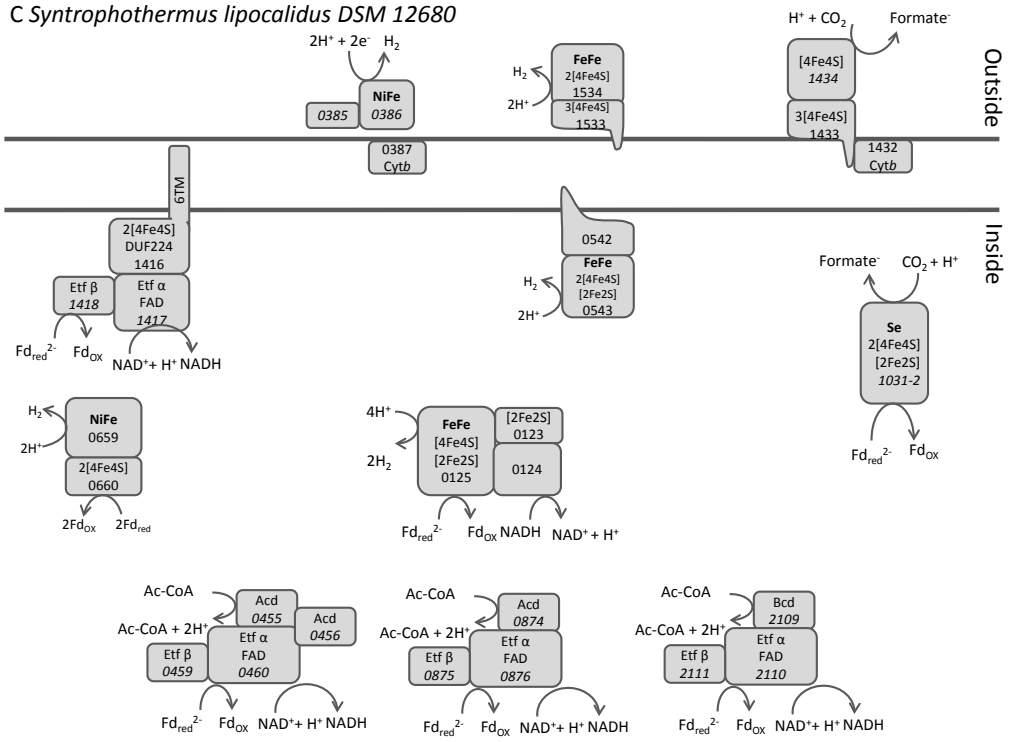

D *Syntrophus aciditrophicus*

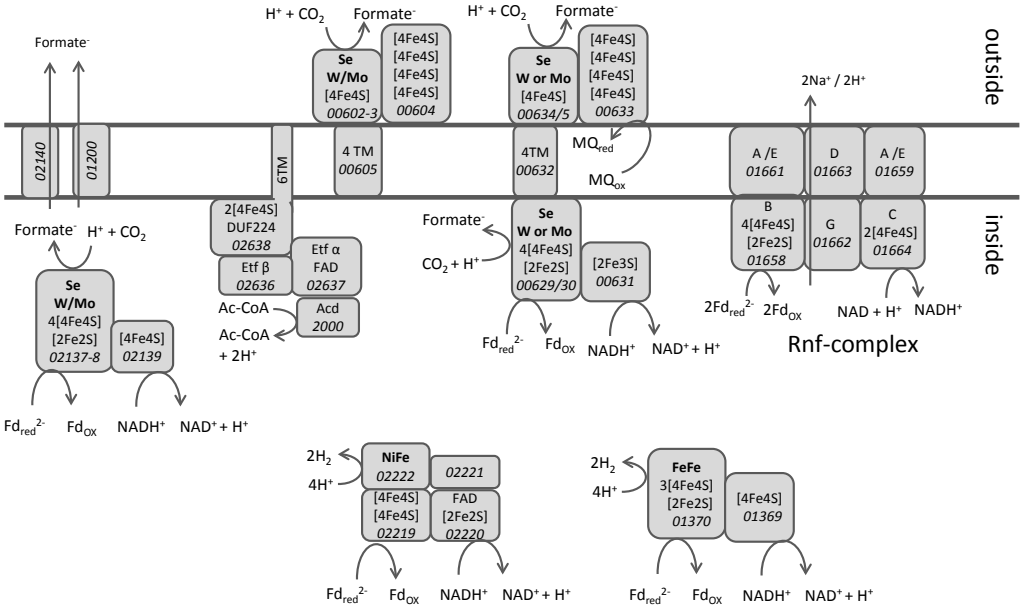

E *Pelotomaculum thermopropionicum*

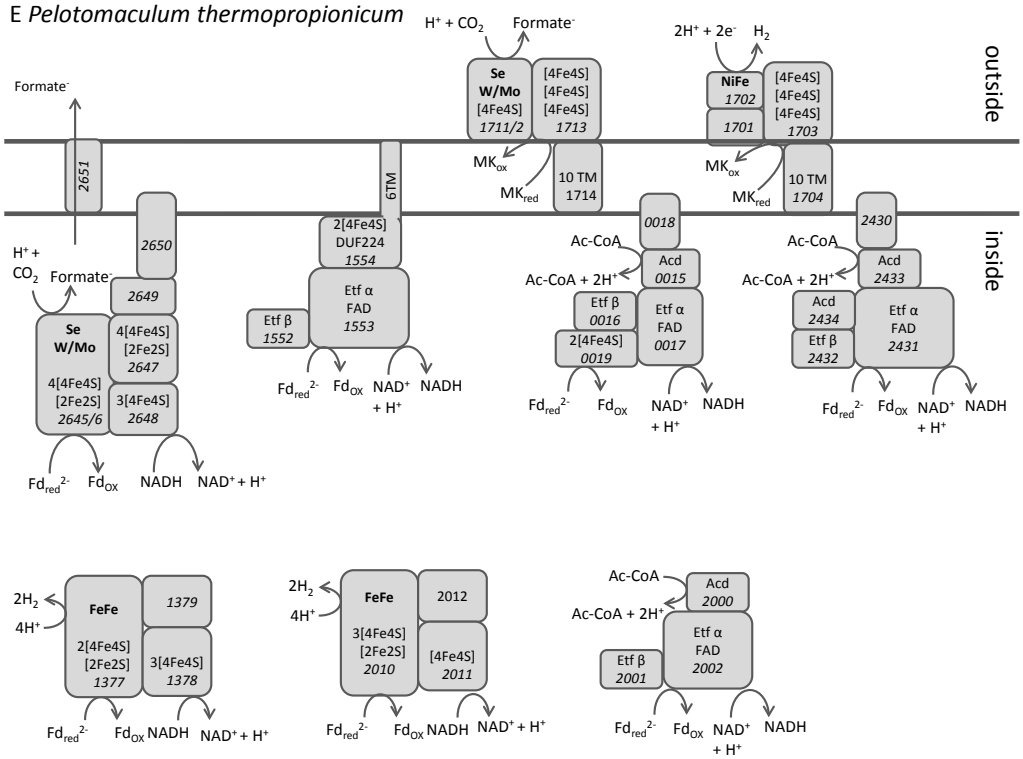

F *Desulfotomaculum kuznetsovii*

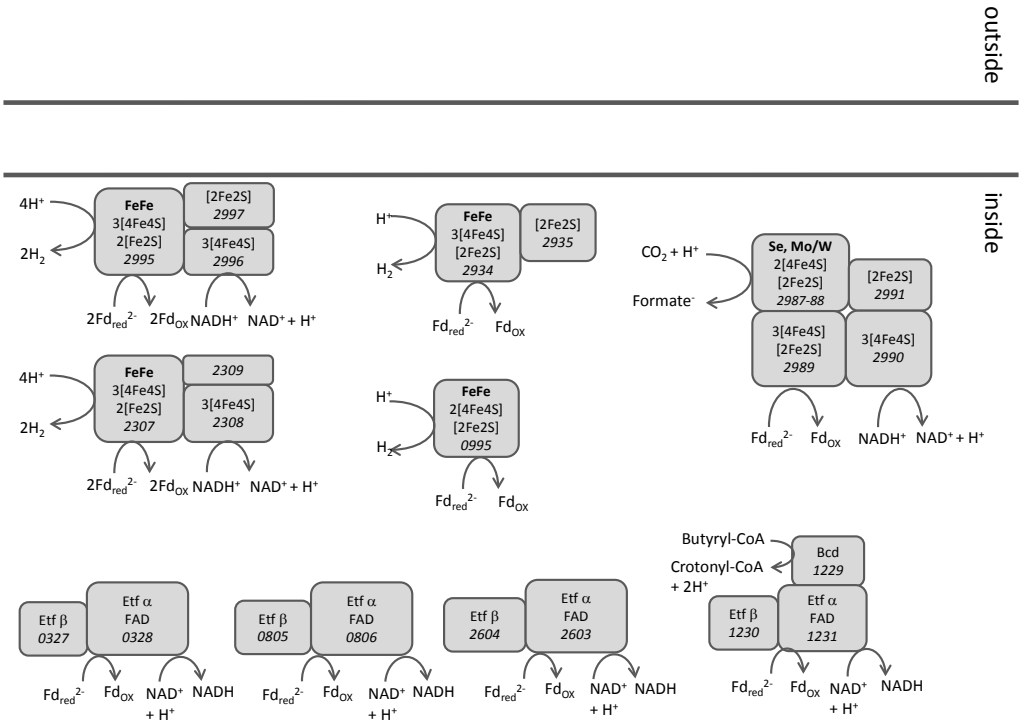

G *Desulfobulbus propionicus* DSM 2032

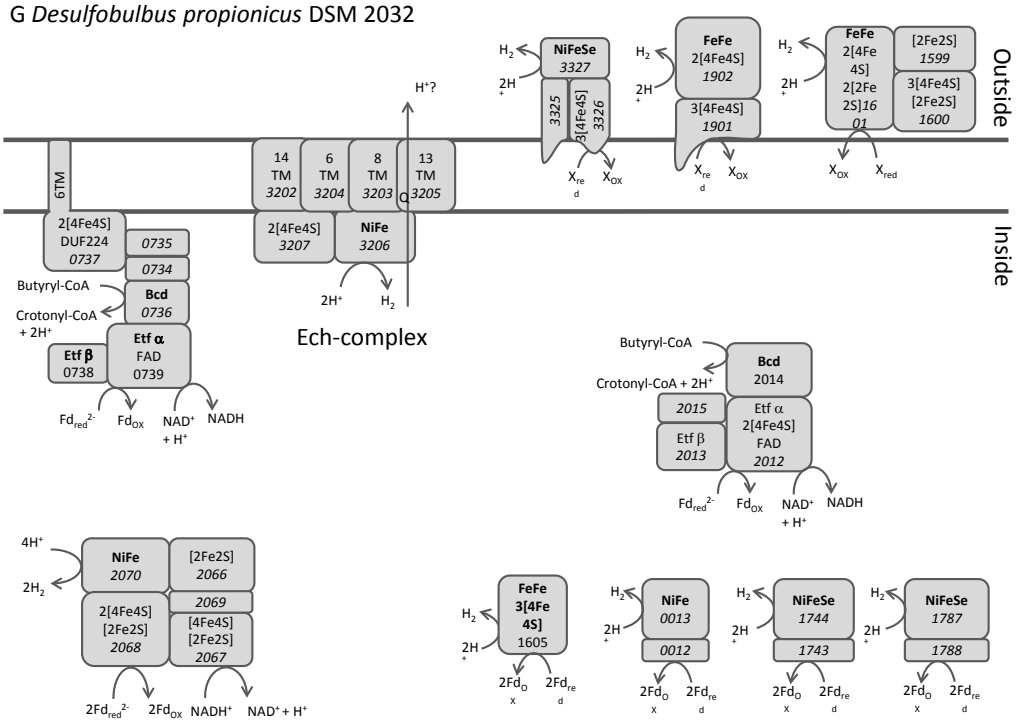

Figure 6.2: Energy converting enzyme complexes predicted from the genomes of bacteria that can degrade propionate and butyrate in syntrophic growth with methanogens; Syntrophobacter fumaroxidans (A), Syntrophomonas wolfei (B), Syntrophothermus lipocalidus (C), Syntrophus aciditrophicus (D), Pelotomaculum thermopropionicum (E), and from those that cannot grow in syntrophic growth with methanogens; Desulfotomaculum kuznetsovii (F), and Desulfobulbus propionicus (G)

6.5 References

1. Blank, C.E. Not so old Archaea - the antiquity of biogeochemical processes in the archaeal domain of life Geobiology **7,** 495-514 (2009).
2. Shao, M.F., Zhang, T., Fang, H.H. Sulfur-driven autotrophic denitrification: diversity, biochemistry, and engineering applications *Applied Microbiology and Biotechnology*. **88**, 1027-42 (2010).
3. Offre, P., Spang, A., Schleper, C. Archaea in biogeochemical cycles *Annual Review of Microbiology* **67,** 437-57 (2013).
4. Muyzer, G., Stams, A.J.M. The ecology and biotechnology of sulphate-reducing bacteria *Nature Review Microbiology* **6**, 441-54 (2008).
5. Lovley, D.R., Klug, M.J. Sulfate reducers can outcompete methanogens at freshwater sulfate concentrations *Applied Environmental Microbiology* **45**, 187-92 (1983).
6. Luther, 3rd, G.W., Findlay, A.J., Macdonald, D.J., Owings, S.M., Hanson, T.E., Beinart, R.A., Girguis, P.R. Thermodynamics and kinetics of sulfide oxidation by oxygen: a look at inorganically controlled reactions and biologically mediated processes in the environment *Frontiers in Microbiology* **2**, 62 (2011).
7. Laanbroek, H.J., Abee, T., Voogd, I.L. Alcohol conversions by *Desulfobulbus propionicus* Lindhorst in the presence and absence of sulfate and hydrogen *Archieves of Microbiology* **133**, 178-84 (1982).
8. Stams, A.J.M., Plugge, C.M. Electron transfer in syntrophic communities of anaerobic bacteria and archaea, *Nature Review Microbiology* **7,** 568-77 (2009).
9. Ferry, J.G., Lessner, D.J. Methanogenesis in marine sediments *Annual New York Academic Science* **1125,** 147-57 (2008).
10. Hansen, T.A. Metabolism of sulfate-reducing prokaryotes *Antonie Van Leeuwenhoek* **66**, 165-85 (1994).
11. Liu, Y., Whitman, W.B. Metabolic, phylogenetic, and ecological diversity of the methanogenic archaea *Annual New York Academic Science* **1125**, 171-89 (2008).
12. McInerney, M.J., Struchtemeyer, C.G., Sieber, J., Mouttaki, H., Stams, A.J.M., Schink, B., Rohlin, L., Gunsalus, R.P., Physiology, ecology, phylogeny, and genomics of microorganisms capable of syntrophic metabolism *Annual New York Academic Science* **1125**, 58-72 (2008).
13. Hattori, S. Syntrophic acetate-oxidizing microbes in methanogenic environments *Microbes and Environments* **23**, 118-27 (2008).
14. Dolfing, J., Jiang, B., Henstra, A.M., Stams, A.J.M., Plugge, C.M. Syntrophic growth on formate: a new microbial niche in anoxic environments *Applied Environmental Microbiology* **74**, 6126-31 (2008).
15. Plugge, C.M., Scholten, J.C.M., Culley, D.E., Nie, L., Brockman, F.J., Zhang, W.W. Global transcriptomics analysis of the *Desulfovibrio vulgaris* change from syntrophic growth with *Methanosarcina barkeri* to sulfidogenic metabolism *Microbiology* (UK) **156**, 2746-56 (2010).
16. C.M. Plugge, W. Zhang, J.C.M. Scholten, A.J.M. Stams, Metabolic flexibility of sulfate-reducing bacteria *Frontiers in Microbiology* **2**, 81 (2011).
17. Meyer, B., Kuehl, J.V., Deutschbauer, A.M., Arkin, A.P., Stahl, D.A. Flexibility of syntrophic enzyme systems in *Desulfovibrio* species ensures their adaptation capability to environmental changes *Journal of Bacteriology* **195**, 4900-14 (2013).
18. Imachi, H., Sekiguchi, Y., Kamagata, Y., Hanada, S., Ohashi, A., Harada, H. *Pelotomaculum thermopropionicum* gen. nov., sp. nov., an anaerobic, thermophilic, syntrophic propionate-oxidizing bacterium *International Journal of Systematic and Evolutionary Microbiology* **52**, 1729-35 (2002).
19. Markowitz, V.M., Chen, I.M.A., Palaniappan, K., Chu, K., Szeto, E., Grechkin, Y., Ratner, A., Jacob, B., Huang, J., Williams, P., Huntemann, M., Anderson, I., Mavromatis, K., Ivanova, N.N., Kyrpides, N.C. IMG: the integrated microbial genomes

database and comparative analysis system DOE-JGI Walnut Creek, USA (Version 4.2. November 2013).

20. Punta, M., Coggill, P.C., Eberhardt, R.Y., Mistry, J., Tate, J., Boursnell, C., Pang, N., Forslund, K., Ceric, G., Clements, J., Heger, A., Holm, L., Sonnhammer, E.L.L., Eddy, S.R., Bateman, A., Finn, R.D. The Pfam protein families database *Nucleic Acids Research* **40**, D290-D301 (2012).
21. Moller, S., Croning, M.D.R., Apweiler, R. Evaluation of methods for the prediction of membrane spanning regions *Bioinformatics* **17**, 646-53 (2001).
22. Bendtsen, J.D., Nielsen, H., Widdick, D., Palmer, T., Brunak, S. Prediction of twin-arginine signal peptides *BMC Bioinformatics* **6**, (2005).
23. Mathews, D.H., Sabina, J., Zuker, M., Turner, D.H. Expanded sequence dependence of thermodynamic parameters improves prediction of RNA secondary structure *Journal of Molecular Biology* **288**, 911-40 (1999).
24. Zuker, M. Mfold web server for nucleic acid folding and hybridization prediction *Nucleic Acids Research* **31**, 3406-15 (2003).
25. Zhang, Y., Gladyshev, V.N. An algorithm for identification of bacterial selenocysteine insertion sequence elements and selenoprotein genes *Bioinformatics* **21**, 2580-9 (2005).
26. Stothard, P. The sequence manipulation suite: JavaScript programs for analyzing and formatting protein and DNA sequences *Biotechniques* **28**, 1102-4 (2000).
27. Buckel, W., Thauer, R.K. Energy conservation via electron bifurcating ferredoxin reduction and proton/Na(+) translocating ferredoxin oxidation *Biochimica et Biophysica Acta* **1827**, 94-113 (2013).
28. Yano, T. The energy-transducing NADH: quinone oxidoreductase, complex I *Molecular Aspects of Medicine* **23**, 345-68 (2002).
29. Vignais, P.M., Billoud, B. Occurrence, classification, and biological function of hydrogenases: an overview *Chemical Reviews* **107,** 4206-72 (2007).
30. Schlindwein, C., Giordano, G., Santini, C.L., Mandrand, M.A. Identification and expression of the *Escherichia coli* fdhD and fdhE genes, which are involved in the formation of respiratory formate dehydrogenase *Journal of Bacteriology* **172**, 6112-21 (1990).
31. Sieber, J.R., Le, H.M., McInerney, M.J. The importance of hydrogen and formate transfer for syntrophic fatty, aromatic and alicyclic metabolism *Frontiers in Microbiology* **16**, 177-88 (2014).
32. Jackson, B.E., Bhupathiraju, V.K., Tanner, R.S., Woese, C.R., McInerney, M.J. *Syntrophus aciditrophicus* sp. nov., a new anaerobic bacterium that degrades fatty acids and benzoate in syntrophic association with hydrogen-using microorganisms *Archieves of Microbiology* **171**, 107-14 (1999).
33. McInerney, M.J., Bryant, M.P., Hespell, R.B., Costerton, J.W. *Syntrophomonas wolfei* gen. nov. sp. nov., an anaerobic, syntrophic, fatty acid-oxidizing bacterium *Applied Environmental Microbiology* **41**, 1029-39 (1981).
34. Schmidt, A., Müller, N., Schink, B., Schleheck, D. A proteomic view at the biochemistry of syntrophic butyrate oxidation in *Syntrophomonas wolfei PLoS One* **8**, (2013).
35. Sekiguchi, Y. Kamagata, Y., Nakamura, K., Ohashi, A., Harada, H. *Syntrophothermus lipocalidus* gen. nov., sp. nov., a novel thermophilic, syntrophic, fatty-acid-oxidizing anaerobe which utilizes isobutyrate *International Journal of Systematic and Evolutionary Microbiology* **50**, Pt 2, 771-9 (2000).
36. Harmsen, H.J.M., Van Kuijk, B.L.M., Plugge, C.M., Akkermans, A.D.L., De Vos, W.M., Stams, A.J.M. *Syntrophobacter fumaroxidans* sp. nov., a syntrophic propionate-degrading sulfate-reducing bacterium *International Journal of Systematic Bacteriology* **48**, Pt 4, 1383-7 (1998).
37. Nazina, T.N., Ivanova, A.E., Kanchaveli, L.P., Rozanova, E.P. A new sporeforming thermophilic methylothrophic sulfate-reducing bacterium, *Desulfotomaculum kuznetsovii* sp. nov. *Microbiology* **57**, 659-63 (1988).
38. Widdel, F. Anaerober abbau von fettsäuren und benzoesäure durch neu isolierte arten sulfatreduzierender bacterien, Thesis (1980).
39. Suzuki, D., Ueki, A., Amaishi, A., Ueki, K. *Desulfobulbus japonicus* sp. nov., a novel Gram-negative propionate-oxidizing, sulfate-reducing bacterium isolated from an estuarine sediment in Japan *International Journal of Systematic and Evolutionary Microbiology* **57**, 849-55 (2007).

40. Cravo-Laureau, C., Matheron, R., Joulian, C., Cayol, J.L., Hirschler-Rea, A. *Desulfatibacillum alkenivorans* sp. nov., a novel n-alkene-degrading, sulfate-reducing bacterium, and emended description of the genus *Desulfatibacillum International Journal of Systematic and Evolutionary Microbiology* **54**, 1639-42 (2004).
41. Balk, M., Altinbas, M., Rijpstra, W.I., Sinninghe Damste, J.S., Stams, A.J.M. *Desulfatirhabdium butyrativorans* gen. nov., sp. nov., a butyrate-oxidizing, sulfate-reducing bacterium isolated from an anaerobic bioreactor *International Journal of Systematic and Evolutionary Microbiology* **58**, 110-5 (2008).
42. Brysch, K., Schneider, C., Fuchs, G., Widdel, F. Lithoautotrophic growth of sulfate-reducing bacteria, and description of *Desulfobacterium autotrophicum* gen. nov., sp. nov. *Archieves of Microbiology* **148**, 264-74 (1987).
43. Finster, K., Liesack, W., Tindall, B. J. *Desulfospira joergensenii*, gen. nov., sp. nov., a new sulfate-reducing bacterium isolated from marine surface sediment Systametic and Applied Microbiology **20**, 201-8 (1997).
44. Ommedal, H., Torsvik, T. *Desulfotignum toluenicum* sp. nov., a novel toluene-degrading, sulphate-reducing bacterium isolated from an oil-reservoir model column *International Journal of Systematic and Evolutionary Microbiology* **57**, 2865-9 (2007).
45. Deweerd, K.A., Suflita, J.M. Anaerobic aryl reductive dehalogenation of halobenzoates by cell extracts of "*Desulfomonile tiedjei*" *Applied Environmental Microbiology* **56**, 2999-3005 (1990).
46. Robertson, W.J., Bowman, J.P., Franzmann, P.D., Mee, B.J. *Desulfosporosinus meridiei* sp. nov., a spore-forming sulfate-reducing bacterium isolated from gasolene-contaminated groundwater *International Journal of Systematic and Evolutionary Microbiology* **51**, 133-40 (2001).
47. Knoblauch, C., Sahm, K., Jorgensen, B.B. Psychrophilic sulfate-reducing bacteria isolated from permanently cold arctic marine sediments: description of *Desulfofrigus oceanense* gen. nov., sp. nov., *Desulfofrigus fragile* sp. nov., *Desulfofaba gelida* gen. nov., sp. nov., *Desulfotalea psychrophila* gen. nov., sp. nov. and *Desulfotalea arctica* sp. nov International Journal of Systematic Bacteriology **49**, Pt 4 1631-43 (1999).
48. Kuever, J., Rainey, F.A., Hippe, H. Description of *Desulfotomaculum* sp. Groll as *Desulfotomaculum gibsoniae* sp. nov *International Journal of Systematic Bacteriology* **49** Pt 4 1801-8 (1999).
49. Candela, T., Fouet, A. Poly-gamma-glutamate in bacteria, *Molecular Microbiology* **60**, 1091-8 (2006).
50. Candela, T., Moya, M., Haustant, M., Fouet, A. *Fusobacterium nucleatum*, the first Gram-negative bacterium demonstrated to produce polyglutamate in: *Canadian Journal of Microbiology* pp. 627-632 (2009).
51. Morikawa, M., Kagihiro, S., Haruki, M., Takano, K., Branda, S., Kolter, R., Kanaya, S. Biofilm formation by a *Bacillus subtilis* strain that produces gamma-polyglutamate *Microbiology* **152**, 2801-7 (2006).
52. Ikeda, M., Sato, T., Wachi, M., Jung, H.K., Ishino, F., Kobayashi, Y., Matsuhashi, M. Structural similarity among *Escherichia coli* FtsW and RodA proteins and *Bacillus subtilis* SpoVE protein, which function in cell division, cell elongation, and spore formation, respectively *Journal of Bacteriology* **171**, 6375-8 (1989).
53. Joris, B., Dive, G., Henriques, A., Piggot, P.J., Ghuysen, J.M. The life-cycle proteins RodA of *Escherichia coli* and SpoVE of *Bacillus subtilis* have very similar primary structures *Molecular Microbiology* **4**, 513-7 (1990).
54. Mohammadi, T., Sijbrandi, R., Lutters, M., Verheul, J., Martin, N., den Blaauwen, T., de Kruijff, B., Breukink, E. Specificity of the transport of Lipid II by FtsW in *Escherichia coli Journal of Biology and Chemestry* (2014).
55. Tremblay, P.L., Zhang, T., Dar, S.A., Leang, C., Lovley, D.R. The Rnf complex of *Clostridium ljungdahlii* is a proton-translocating ferredoxin:NAD+ oxidoreductase essential for autotrophic growth *MBio* **4**, e00406-12 (2012).
56. McInerney, M.J., Rohlin, L., Mouttaki, H., Kim, U., Krupp, R.S., Rios-Hernandez, L., Sieber, J., Struchtemeyer, C.G., Bhattacharyya, A., Campbell, J.W., Gunsalus, R.P. The genome of *Syntrophus aciditrophicus*: life at the thermodynamic limit of microbial growth *Proceedings of the National Academy of Sciences of the United States of America* **104**, 7600-5 (2007).
57. Scholten, J.C.M., Conrad, R. Energetics of syntrophic propionate oxidation in defined batch and chemostat cocultures *Applied Environmental Microbiology* **66**, 2934-42 (2000).
58. Schink, B. Energetics of syntrophic cooperation in methanogenic degradation *Microbiology of Molecular Biology Review* **61**, 262-80 (1997).
59. Westerholm, M., Roos, S., Schnürer, A. *Tepidanaerobacter acetatoxydans* sp. nov., an anaerobic, syntrophic acetate-

oxidizing bacterium isolated from two ammonium-enriched mesophilic methanogenic processes *Systematic Applied Microbiology* **34**, 260-6 (2011).

60. Oehler, D., Poehlein, A., Leimbach, A., Müller, N., Daniel, R., Gottschalk, G., Schink, B. Genome-guided analysis of physiological and morphological traits of the fermentative acetate oxidizer *Thermacetogenium phaeum BMC Genomics* **13**, 723 (2012).
61. Schnürer, A., Schink, B., Svensson, B.H. *Clostridium ultunense* sp. nov., a mesophilic bacterium oxidizing acetate in syntrophic association with a hydrogenotrophic methanogenic bacterium *International Journal of Systematic Bacteriology* **46**, 1145-52 (1996).
62. Widdel, F. New types of acetate-oxidizing, sulfate-reducing *Desulfobacter* species, *D. hydrogenophilus* sp. no., *D. latus* sp. nov., and *D. curvatus* sp. nov. *Archieves of Microbiology* **148**, 286-91 (1987).
63. Widdel, F., Pfennig, N. Studies on dissimilatory sulfate-reducing bacteria that decompose fatty acids. I. Isolation of new sulfate-reducing bacteria enriched with acetate from saline environments. Description of *Desulfobacter postgatei* gen. nov., sp. nov *Archieves of Microbiology* **129**, 395-400 (1981).
64. Schnell, S., Bak, F., Pfennig, N. Anaerobic degradation of aniline and dihydroxybenzenes by newly isolated sulfate-reducing bacteria and description of *Desulfobacterium anilini Archieves of Microbiology* **152**, 556-63 (1989).
65. Ollivier, B., Hatchikian, C.E., Prensier, G., Guezennec, J., Garcia, J.L. *Desulfohalobium retbaense* gen. nov., sp. nov. a halophilic sulfate-reducing bacterium from sediments of a hypersaline lake in senegal *International Journal of Systematic Bacteriology* **41**, 74-81 (1991).
66. Oude Elferink, S.J., Akkermans-van Vliet, W.M., Bogte, J.J., Stams, A.J.M. *Desulfobacca acetoxidans* gen. nov., sp. nov., a novel acetate-degrading sulfate reducer isolated from sulfidogenic granular sludge *International Journal of Systematic Bacteriology* **49**, 345-50 (1999).
67. Widdel, F., Pfennig, N. A new anaerobic, sporing, acetate-oxidizing, sulfate-reducing bacterium, *Desulfotomaculum* (emend.) *acetoxidans Archieves of Microbiology* **112**, 119-22 (1977).
68. Buckel, W., Thauer, R.K. Energy conservation via electron bifurcating ferredoxin reduction and proton/Na+ translocating ferredoxin oxidation *Biochimica et Biophysica Acta* **1827**, 94-113 (2013).
69. Wang, S., Huang, H., Kahnt, J., Mueller, A.P., Kopke, M., Thauer, R.K. NADP-specific electron-bifurcating [FeFe]-hydrogenase in a functional complex with formate dehydrogenase in *Clostridium autoethanogenum* grown on CO *Journal of Bacteriology* **195**, 4373-86 (2013).
70. Huang, H., Wang, S., Moll, J., Thauer, R.K. Electron bifurcation involved in the energy metabolism of the acetogenic bacterium *Moorella thermoacetica* growing on glucose or H_2 plus CO_2 *Journal of Bacteriology* **194**, 3689-99 (2012).
71. Li, F., Hinderberger, J., Seedorf, H., Zhang, J., Buckel, W., Thauer, R.K. Coupled ferredoxin and crotonyl coenzyme A (CoA) reduction with NADH catalyzed by the butyryl-CoA dehydrogenase/Etf complex from *Clostridium kluyveri Journal of Bacteriology* **190**, 843-50 (2008).
72. Schut, G.J., Adams, M.W. The iron-hydrogenase of *Thermotoga maritima* utilizes ferredoxin and NADH synergistically: a new perspective on anaerobic hydrogen production *Journal of Bacteriology* **191**, 4451-7 (2009).
73. Kaster, A.K., Moll, J., Parey, K., Thauer, R.K. Coupling of ferredoxin and heterodisulfide reduction via electron bifurcation in hydrogenotrophic methanogenic archaea *Proceedings of the National Academy of Sciences of the United States of America* **108**, 2981-6 (2011).
74. Wang, S., Huang, H., Moll, J., Thauer, R.K. NADP+ reduction with reduced ferredoxin and NADP+ reduction with NADH are coupled via an electron-bifurcating enzyme complex in *Clostridium kluyveri Journal of Bacteriology* **192** 5115-23 (2010).
75. Wang, S., Huang, H., Kahnt, J., Thauer, R.K. *Clostridium acidurici* electron-bifurcating formate dehydrogenase *Applied Environmental Microbiology* **79**, 6176-9 (2013).
76. Costa, K.C., Lie, T.J., Xia, Q., Leigh, J.A. VhuD facilitates electron flow from H2 or formate to heterodisulfide reductase in *Methanococcus maripaludis Journal of Bacteriology* **195**, 5160-5 (2013).
77. Biegel, E., Schmidt, S., Gonzalez, J.M., Müller, V. Biochemistry, evolution and physiological function of the Rnf complex, a novel ion-motive electron transport complex in prokaryotes *Cellular and Molecular Life Sciences* **68**, 613-34 (2011).

78. Hedderich, R., Forzi, L. Energy-converting [NiFe] hydrogenases: more than just H_2 activation, *Journal of Molecular Microbiology and Biotechnology* **10**, 92-104 (2005).
79. Beaty, P.S., McInerney, M.J. Nutritional features of *Syntrophomonas wolfei Applied Environment Microbiology* **56**, 3223-24 (1990).
80. Thauer, R.K., Jungermann, K., Decker, K. Energy conservation in chemotrophic anaerobic bacteria *Microbiology and Molecular Biology Reviews* **41**, 100-80 (1977).
81. Müller, N., Schleheck, D., Schink, B. Involvement of NADH:acceptor oxidoreductase and butyryl coenzyme A dehydrogenase in reversed electron transport during syntrophic butyrate oxidation by *Syntrophomonas wolfei Journal of Bacteriology* **191**, 6167-77 (2009).
82. McInerney, M.J., Wofford, N.Q., Enzymes involved in crotonate metabolism in *Syntrophomonas wolfei Archieves of Microbiology* **158**, 344-9 (1992).
83. Wallrabenstein, C., Schink, B. Evidence of reversed electron transport in syntrophic butyrate or benzoate oxidation by Syntrophomonas wolfei and *Syntrophus buswellii Archieves of Microbiology* **162**, 136-42 (1994).
84. van Kuijk, B.L.M., Schlösser, E., Stams, A.J.M. Investigation of the fumarate metabolism of the syntrophic propionate-oxidizing bacterium strain MPOB *Archieves of Microbiology* **169**, 346-52 (1998).
85. Dong, X., Plugge, C.M., Stams, A.J.M. Anaerobic degradation of propionate by a mesophilic acetogenic bacterium in coculture and triculture with different methanogens *Applied Environment Microbiology* **60**, 2834-38 (1994).
86. Kosaka, T., Kato, S., Shimoyama, T., Ishii, S., Abe, T., Watanabe, K. The genome of *Pelotomaculum thermopropionicum* reveals niche-associated evolution in anaerobic microbiota *Genome Research* **18**, 442-8 (2008).
87. Kosaka, T., Uchiyama, T., Ishii, S., Enoki, M., Imachi, H., Kamagata, Y., Ohashi, A., Harada, H., Ikenaga, H., Watanabe, K., Reconstruction and regulation of the central catabolic pathway in the thermophilic propionate-oxidizing syntroph *Pelotomaculum thermopropionicum Journal of Bacteriology* **188**, 202-10 (2006).
88. Visser, M., Worm, P., Muyzer, G., Pereira, I.A.C., Schaap, P.J., Plugge, C.M., Kuever, J., Parshina, S.N., Nazina, T.N., Ivanova, A.E., Bernier-Latmani, R., Goodwin, L.A., Kyrpides, N.C., Woyke, T., Chain, P., Davenport, K.W., Spring, S., Klenk, H.P., Stams, A.J.M. Genome analysis of *Desulfotomaculum kuznetsovii* strain 17T reveals a physiological similarity with *Pelotomaculum thermopropionicum* strain SI^T *Standards in Genomic Sciences* **8**, 69-87 (2013).
89. Collins, M.D., Widdel, F. Respiratory quinones of sulphate-reducing and sulfur-reducing bacteria: a systematic investigation *Systematic and Applied Microbiology* **8**, 8-18 (1986).
90. Widdel, F., Pfennig, N. Studies on dissimilatory sulfate-reducing bacteria that decompose fatty acids II. Incomplete oxidation of propionate by *Desulfobulbus propionicus* gen. nov., sp. nov. *Archieves of Microbiology* **131**, 360-5 (1982).
91. Dannenberg, S., Kroder, M., Dilling, W., Heribert, C. Oxidation of H_2, organic compounds and inorganic sulfur compounds coupled to reduction of O2 or nitrate by sulfate-reducing bacteria *Archieves of Microbiology* **158**, 93-9 (1992).
92. Stams, A.J.M., Kremer, D.R., Nicolay, K., Weenk, G.H., Hansen, T.A. Pathway of propionate formation in *Desulfobulbus propionicus Archieves of Microbiology* **139**, 167-73 (1984).
93. Collins, M.D., Widdel, F.A new respiratory quinone, 2-methyl-3-V-dihydropentaprenyl-1, 4-naphthoquinone, isolated from *Desulfobulbus propionicus Systematic and Applied Microbiology* **5**, 281-6 (1984).
94. Liu, Y., Balkwill, D.L., Aldrich, H.C., Drake, G.R., Boone, D.R. Characterization of the anaerobic propionate-degrading syntrophs *Smithella propionica* gen. nov., sp. nov. and *Syntrophobacter wolinii Internation Journal of Systematic Bacteriology* **49**, Pt 2 545-56 (1999).
95. de Bok, F.A.M., Stams, A.J.M., Dijkema, C., Boone, D.R. Pathway of propionate oxidation by a syntrophic culture of *Smithella propionica* and *Methanospirillum hungatei Applied Environmental Microbiology* **67**, 1800-4 (2001).
96. Müller, N., Worm, P., Schink, B., Stams, A.J.M., Plugge, C.M. Syntrophic butyrate and propionate oxidation processes: from genomes to reaction mechanisms *Environmental Microbiology Reports* **2**, 489-99 (2010).
97. Worm, P., Stams, A.J.M., Cheng, X., Plugge, C.M. Growth- and substrate-dependent transcription of formate dehydrogenase and hydrogenase coding genes in *Syntrophobacter fumaroxidans* and *Methanospirillum hungatei Microbiology* **157**, 280-9 (2011).

98. van Kuijk, B.L.M., Stams, A.J.M. Purification and characterization of malate dehydrogenase from the syntrophic propionate-oxidizing bacterium strain MPOB *FEMS Microbiology Letters* **144**, 141-4 (1996).
99. Chabriere, E., Charon, M.H., Volbeda, A., Pieulle, L., Hatchikian, E.C., Fontecilla-Camps, J.C. Crystal structures of the key anaerobic enzyme pyruvate:ferredoxin oxidoreductase, free and in complex with pyruvate *Nature Structural & Molecular Biology* **6**, 182-90 (1999).
100. de Bok, F.A.M., Hagedoorn, P.L., Silva, P.J., Hagen, W.R., Schiltz, E., Fritsche, K., Stams, A.J.M. Two W-containing formate dehydrogenases (CO_2-reductases) involved in syntrophic propionate oxidation by *Syntrophobacter fumaroxidans European Journal of Biochemistry* **270**, 2476-85 (2003).
101. Hattori, S., Kamagata, Y., Hanada, S., Shoun, H. *Thermacetogenium phaeum* gen. nov., sp. nov., a strictly anaerobic, thermophilic, syntrophic acetate-oxidizing bacterium International *Journal of Systematic and Evolutionary Microbiology* **50**, Pt 4 1601-9 (2000).
102. Poehlein, A., Schmidt, S., Kaster, A.K., Goenrich, M., Vollmers, J., Thurmer, A., Bertsch, J., Schuchmann, K., Voigt, B., Hecker, M., Daniel, R., Thauer, R.K., Gottschalk, G., Muller, V. An ancient pathway combining carbon dioxide fixation with the generation and utilization of a sodium ion gradient for ATP synthesis *PLoS One* **7**, e33439 (2012).
103. Manzoor, S., Bongcam-Rudloff, E., Schnurer, A., Muller, B. First genome sequence of a syntrophic acetate-oxidizing bacterium, *Tepidanaerobacter acetatoxydans* strain Re1 *Genome Announcements* **1**, (2013).
104. Barker, H. A., On the biochemistry of methane formation *Archieves of Microbiology* **7**, 404-19 (1936).
105. Zinder, S.H., Cardwell, S.C., Anguish, T., Lee, M., Koch, M. Methanogenesis in a thermophilic (58 degrees C) anaerobic digestor: *Methanothrix* sp. as an important aceticlastic methanogen *Applied Environmental Microbiology* **47**, 796-807 (1984).
106. Schnürer, A., Zellner, G., Svensson, B.H. Mesophilic syntrophic acetate oxidation during methane formation in biogas reactors *FEMS Microbiology and Ecology* **29**, 249-61 (1999).
107. Sousa, D.Z., Smidt, H., Alves, M.M., Stams, A.J.M. Ecophysiology of syntrophic communities that degrade saturated and unsaturated long-chain fatty acids *FEMS Microbiology and Ecology* **68**, 257-72 (2009).
108. Sieber, J.R., Sims, D.R., Han, C., Kim, E., Lykidis, A., Lapidus, A.L., McDonnald, E., Rohlin, L., Culley, D.E., Gunsalus, R., McInerney, M.J. The genome of *Syntrophomonas wolfei*: new insights into syntrophic metabolism and biohydrogen production *Environmental Microbiology* **12**, 2289-301 (2010).
109. Stams, A.J.M., Sousa, D.Z., Kleerebezem, R., Plugge, C.M. Role of syntrophic microbial communities in high-rate methanogenic bioreactors *Water Sciences Technology* **66**, 352-62 (2012).
110. Plugge, C.M., Henstra, A.M., Worm, P., Swarts, D.C., Paulitsch-Fuchs, A.H., Scholten, J.C., Lykidis, A., Lapidus, A.L., Goltsman, E., Kim, E., McDonald, E., Rohlin, L., Crable, B.R., Gunsalus, R.P., Stams, A.J.M., McInerney, M.J. Complete genome sequence of *Syntrophobacter fumaroxidans* strain (MPOBT) Standards in Genomic Sciences **7**, 91-106 (2012).
111. Balk, M., Weijma, J., Stams, A.J.M. *Thermotoga lettingae* sp. nov., a novel thermophilic, methanol-degrading bacterium isolated from a thermophilic anaerobic reactor *Journal of Systematic and Evolutionary Microbiology* **52**, 1361-8 (2002).
112. Westerholm, M., Roos, S., Schnurer, A. *Syntrophaceticus schinkii* gen. nov., sp nov., an anaerobic, syntrophic acetate-oxidizing bacterium isolated from a mesophilic anaerobic filter *FEMS Microbiology Letters* **309**, 100-4 (2010).
113. Sekiguchi, Y., Imachi, H., Susilorukmi, A., Muramatsu, M., Ohashi, A., Harada, H., Hanada, S., Kamagata, Y. *Tepidanaerobacter syntrophicus* gen. nov., sp. nov., an anaerobic, moderately thermophilic, syntrophic alcohol- and lactate-degrading bacterium isolated from thermophilic digested sludges *Journal of Systematic and Evolutionary Microbiology* 56 (2006) 1621-1629.
114. Sorokin, D.Y., Abbas, B., Tourova, T.P., Bumazhkin, B.K., Kolganova, T.V., Muyzer, G. Sulfate-dependent acetate oxidation under extremely natron-alkaline conditions by syntrophic associations from hypersaline soda lakes *Microbiology* **160**, 723-32 (2014).
115. Nilsen, R.K., Torsvik, T., Lien, T. *Desulfotomaculum thermocisternum* sp. nov., a sulfate reducer isolated from a hot North Sea oil reservoir *International Journal of Systematic Bacteriology* **46**, 397-402 (1996).
116. Plugge, C.M., Balk, M., Stams, A.J.M. *Desulfotomaculum thermobenzoicum* subsp. *thermosyntrophicum* subsp. nov., a thermophilic, syntrophic, propionate-oxidizing, spore-forming bacterium *Journal of Systematic and Evolutionary*

Microbiology **52**, 391-9 (2002).

117. Klein, M., Friedrich, M., Roger, A.J., Hugenholtz, P., Fishbain, S., Abicht, H., Blackall, L.L., Stahl, D.A., Wagner, M. Multiple lateral transfers of dissimilatory sulfite reductase genes between major lineages of sulfate-reducing prokaryotes *Journal of Bacteriology* **183**, 6028-35 (2001).
118. Sieber, J.R., McInerney, M.J., Gunsalus, R.P. Genomic insights into syntrophy, the paradigm for anaerobic metabolic cooperation *Annual Review of Microbiology* **66**, 429-52 (2012).

Chapter 7

General discussion

7. General discussion

The anaerobic degradation of one carbon compounds has been a subject of study for many decades. CO is an excellent electron donor for the reduction of CO_2, sulfate, fumarate, metals [1-6], and even for the reduction of protons to produce hydrogen [6-14]. Moreover, it was shown that a CODH complex is involved in coupling CO oxidation and hydrogen [3, 15-35]. Studies on anaerobic methanol metabolism lead to insight into the methanol degradation pathway in methanogens and acetogenic bacteria [36-44].

The research presented in this thesis focuses on the proteins involved in one carbon metabolism (especially CO, methanol and formate) and the genes encoding these proteins. Performing genome and proteome analysis enabled the description of: the CO metabolism of two *Desulfotomaculum nigrificans* strains (Chapter 2), the methanol metabolism of *Sporomusa ovata* An4 and *Desulfotomaculum kuznetsovii* (Chapter 3,4,5; expanding the initial description of anaerobic methanol degradation in bacteria), and the importance of formate as an interspecies electron carrier in syntrophic butyrate and propionate degradation (Chapter 4, 6).

7.1 Anaerobic CO metabolism and the different CODH complexes

By comparing the genomes of two *Desulfotomaculum nigrificans* strains, we were able to explain why they possess a different CO metabolism and we could confirm that the presence of one operon structure in strain CO-1-SRB, consisting of CODH and ECH genes, allows growth and hydrogen production with 100% CO in the gas phase (Chapter 2). In addition, we suggested that the synthesis of the two CODH complexes encoded in the genome of the type strain allows growth with 20% CO and sulfate, as energy substrates, and acetate as carbon source.

D. kuznetsovii has three *cooS* genes, Desku_1492; 2150; 2787 (Chapter 4). Desku_1492 is part of a gene complex including genes coding for proteins involved in the acetyl-CoA pathway, while Desku_2150 only has *acsB* as neighbor gene. Interestingly, the comparative proteomics data showed that both Desku_1492 and Desku_2150 and other enzymes involved in the acetyl-CoA pathway were formed during growth at all conditions (Chapter 5). Which growth condition results in formation of the gene product of Desku_2787 cannot be deduced from our analysis.

Since the description of multiple *cooS* genes in *Carboxydothermus hydrogenoformans* and the proposed function of four of the five CODH complexes [45] no extensive studies have been done on the function of the CODH II, IV and V complexes. Recently, Techtmann et al. [46] discussed that 6% of the sequenced bacterial and archaeal genomes have at least one *cooS* gene and that many (43 %) have multiple *cooS* genes. With the number of sequenced genomes increasing and the expectation that more CO-utilizing bacteria will be isolated in the near future, this percentage might even increase in the coming decade. In addition, Techtmann et al. [46] concluded that the distribution of the CODH catalytic subunit is related to function rather than to phylogeny, which means that for example the catalytic subunits of the CODH I complexes clustered together in differently constructed phylogenetic trees as a result of horizontal gene transfer.

From the neighbor genes and the *cooS* trees described by Techtmann et al. (2012) it can be derived that the CODH complexes of the *D. nigrificans* type strain, DesniDRAFT_0851-0855 and DesniDRAFT_1323-1326, are similar to CODH IV and V of *Carboxydothermus hydrogenoformans,* respectively. This indicates that in general the presence of a CODH IV and/or V complex is sufficient for CO utilization by an anaerobic microorganism. However, more research is necessary to better understand the functions of the CODH complexes, especially CODH II, IV and V

complexes.

7.2 Anaerobic methanol metabolism

7.2.1 Involvement of MtaA methyltransferase in acetogens

Anaerobic methanol metabolism is well studied in methanogenic archaea and acetogenic bacteria. A methyltransferase system consisting of three subunits, MtaA, MtaB and MtaC is thought to be involved in methylotrophic growth of these microorganisms. In *Sporomusa ovata* and *Moorella thermoacetica* a corrinoid protein (the first methyltransferase) was formed in the presence of methanol and this enzyme was purified [36, 39, 44]. However, the MtaA, the second methyltransferase thought to be involved in the methyl transfer from the corrinoid bound to MtaC to tetrahydrofolate (THF) was only shown to be present in the genome of *Moorella thermoacetica*, but was never experimentally tested to perform the reaction. We suggested that not the *mtaA* homologs of *Sporomusa ovata* strain An4 but the methyl-THF methyltransferase (c055:9957-9160) is involved in the methyl transfer from MtaC to THF. Therefore, it is possible that also in *M. thermoacetica* no MtaA is involved. Similar to the *mtaA* homologs of strain An4 no *mtaA* of *M. thermoacetica* is situated next to the *mtaB* and *mtaC* genes. Moreover, a methyltransferase gene (Moth_1207) similar to the methyl-THF methyltransferase (c055:9957-9160) of strain An4, 97% coverage and 47% identity, is situated downstream of *mtaC* (Moth_1208) and *mtaB* (Moth_1209). If this methyltransferase (Desku_1207) or one or multiple MtaAs is involved in the methanol metabolism of *Moorella thermoacetica* needs to be analyzed, by for example a comparable proteome analysis as was performed with *S. ovata* strain An4 and *Desulfotomaculum kuznetsovii* (Chapter 3 and 5, respectively). If *M. thermoacetica* uses a methyl-THF methyltransferase instead of a MtaA this could also be true for all methanol utilizing acetogenic bacteria.

7.2.2 Methanol methyltransferase and alcohol dehydrogenase, wielding two swords instead of one

Apart from the methanol methyltransferase system, *D. kuznetsovii* also has an alcohol dehydrogenase (ADH) that is part of a second methanol degrading pathway and oxidizes both methanol as ethanol (Chapter 5). This is not the first description of an ADH that besides ethanol also oxidizes methanol. Previously, ADH activity in cell free extracts of *Desulfovibrio carbinolicus* was shown with ethanol and methanol. The cell-free extracts were prepared of ethanol-grown cells and therefore the methanol activity was assigned to the ADH involved in the ethanol metabolism of *D. carbinolicus*. It was suggested that the ability of *D. carbinolicus* to grow with methanol is due to the ADH that shows activity with methanol [47]. However, this was not confirmed as the ADH was never purified. The methanol active ADH of *D. kuznetsovii* was partially purified [48], but to confirm that *D. kuznetsovii* uses two methanol degrading pathways the methanol active ADH of *D. kuznetsovii* should be completely purified.

The presence of two methanol degrading pathways, a cobalt-dependent and a cobalt-independent one, can be beneficial e.g. during cobalt limiting conditions. Anaerobic methanol degradation by methanogens and acetogens is hampered by cobalt limitation [49-51]. Furthermore, methanogens appeared to compete better for cobalt during cobalt-limiting conditions [50] and have higher affinity for methanol than acetogens. Acetogens can only outcompete methanogens when the concentrations of methanol and cobalt are high [49]. *D. kuznetsovii* can grow fastest with the methanol methyltransferase system (Chapter 5). Mixed culture experiments of the acetogen *Moorella thermoautotrophica* and *D. kuznetsovii* in methanol limiting conditions showed that *D.*

kuznetsovii has higher affinity for methanol [52]. Moreover, at cobalt limiting conditions *D. kuznetsovii* is still able to grow using the cobalt-independent methanol dehydrogenase pathway. *D. kuznetsovii* has the advantage to shift between cobalt limiting conditions to non-limiting conditions and therefore is more flexible than microorganisms with only the methyltransferase pathway. The advantage of 'wielding two swords' is most likely not restricted to *D. kuznetsovii*. It is probable that other sulfate-reducing-bacteria also have a cobalt-dependent and a cobalt-independent methanol degrading pathway. This might even extrapolate to other anaerobes, for example the acetogen *Moorella thermoacetica* strain AMP. Moreover, a cobalt-independent methanol dehydrogenase pathway could also be involved in syntrophic degradation of methanol, even though this did not seem to be true for *D. kuznetsovii*.

Moorella thermoacetica strain AMP can grow with methanol in the presence of cobalt and vitamin B12. When cobalt and vitamin B12 were omitted from the medium strain AMP grows with methanol in syntrophic association with *Methanothermobacter thermautotrophicus* strain NJ1. In this coculture methane and nearly no acetate was formed as product [53]. This suggests the presence of a cobalt-dependent and a cobalt-independent methanol-degrading pathway. Whether this is restricted to strain AMP or if the *Moorella thermoacetica* type strain can do the same is not known. Clearly, in anaerobes the methanol methyltransferase system as described in methanogens is not the sole possible pathway to degrade methanol. Additional research is therefore necessary to unravel biochemistry and bioenergetics of either pathways.

7.2.3 Methanol degrading microorganisms in the environment

Because of the widespread occurrence of methanol on earth it is interesting to know which methanol utilizers are present in which environment. A recent investigation in a North Stavropol underground gas storage facility revealed the presence of many methanol utilizers [85]. The stratum water of this underground gas storage facility contains high methanol and acetate concentrations, but low concentrations of minerals. In addition, the main gas contains carbon dioxide and hydrogen. Acetogens were dominant in most of the samples. However, high methanogenic activity could also be measured. The dominant anaerobic microorganisms isolated from these samples were acetogens, methanogens, and sulfate reducers. The isolated strains were closely related to *Eubacterium limosum*, *Sporomusa sphaeroides*, *Methanosarcina barkeri*, *Methanobacterium formicicum*, and *Desulfovibrio desulfuricans*. All strains showed resistance to high methanol concentrations and could, except for *Methanobacterium formicicum*, grow with methanol. The sulfate reducing strain however, showed only slow growth with methanol. This could indicate that a methanol dehydrogenase is involved, as growth of *Desulfotomaculum kuznetsovii* was also slower when using the alcohol dehydrogenase compared to the methanol methyltransferase system. This however needs to be studied further. Most of the methanol is degraded by the methanol utilizing acetogens and methanogens, or in other words by microorganisms that possess the methyltransferase system.

To analyze methanol utilizers in the environment molecular tools are required. Kolb and Stacheter addressed this issue [86]. To get a better understanding of the global methanol conversion, they discussed the need for suitable gene targets to analyze methanol-utilizing microorganisms. Moreover, they pointed out five potential gene markers for aerobes and one for strict anaerobes, the *mtaC* gene [86]. However, the *mtaB* gene is a better alternative as a target to develop gene-based detection of strict anaerobic methanol utilizers in the environment, because the *mtaB* codes for

the methanol specific subunit of the methyltransferase. Furthermore, the MtaC is the cobalamin binding subunit of the methyltransferase, which has high similarity with the cobalamin binding subunits of the tri-, di-, and mono-methylamine methyltransferases.
In addition to *mtaB* another gene marker is necessary to analyze methanol-utilizing microorganisms, the methanol-utilizing alcohol dehydrogenase of *D. kuznetsovii*. However, more research needs to be performed. Similar methanol-utlizing alcohol dehydrogenases need to be demonstrated in other (sulfate-reducing) bacteria. Moreover, their difference with non-methanol-utilizing alcohol dehydrogenases needs to be established.

7.3 Syntrophy

In nature syntrophic interactions play an important role in carbon cycling. The degradation process of complex organic compounds is performed by a combination of fermentation, acetogenesis, sulfidogenesis and methanogenesis at different environmental conditions. Generally, sulfate reduction is favoured over methanogenesis when sufficient sulfate is present [4,8]. However, methanogenesis can occur simultaneously with sulfate reduction as well [54]. This shows how flexible microbial communities can be. Moreover, the ability of several sulfate reducing bacteria to grow in syntrophic association with methanogens contributes to the variable process of syntrophic degradation and with them the variability of the electron carrier in interspecies electron transfer. Chapter 6 describes the important role of formate as an electron carrier in the syntrophic growth with butyrate and propionate. However, how important is interspecies formate transfer beyond syntrophic butyrate and propionate degradation?

7.3.1 The role of formate in syntrophic lactate degradation

In syntrophic lactate degradation by *Desulfovibrio alaskensis* G20 70% of the electron flow occurs via formate in syntrophic association with a methanogenic partner [55].Additional research showed that the formate concentration increases when methanogens are inhibited by 2-bromo-ethane sulfonate. Moreover, the genes coding for a periplasmic formate dehydrogenase (FDH) were up-regulated during syntrophic growth and a knockout of these genes decreased growth rates and maximum cell densities in syntrophic cultures of *D. alaskensis* G20 with either *Methanococcus maripaludis* or *Methanospirilum hungatei* [56]. The knockout did not affect growth with lactate and sulfate, indicating the importance of the periplasmic FDH and formate as an electron carrier in syntrophic growth.
By contrast, *D. vulgaris* Hildenborough exclusively uses interspecies hydrogen transfer during syntrophic growth with lactate in coculture with a methanogen [57, 58]. Moreover, transcriptional changes between sulfidogenic growth with lactate and syntrophic growth showed an up-regulation of genes encoding periplasmic hydrogenases and a cytoplasmic oriented membrane bound hydrogenase during syntrophy. By comparing the up- and down-regulated genes of *D. alaskensis* and *D. vulgaris* during syntrophic growth it was concluded that there is no conserved core of syntrophy-associated genes [55].This represents the syntrophic flexibility of the *Desulfovibrio* species and the flexibility of electron carriers in syntrophic lactate degradation.
Syntrophic lactate degradation was also described for the type strain of *Desulfotomaculum nigrificans* ([59], Chapter 2) with a hydrogen-utilizing methanogen that cannot grow with formate. However, it was never examined if formate could also play a role as electron carrier in the coculture with *D. nigrificans* by using a different methanogen. In the genome of *D. nigrificans*

genes coding for an extra-cytoplasmic membrane bound FDH are present (Chapter 2). Since in syntrophic lactate degradation of *D. alaskensis* G20 the periplasmic FDH is an important enzyme complex, this could also be the case for *D. nigrificans*. Now that the genome of multiple *Desulfotomaculum* species have been sequenced, proteome and transcriptome analyses are possible to study syntrophic lactate degradation and the involvement of the extra-cytoplasmic membrane bound FDH in e.g. *D. nigrificans* [60], *D. gibsoniae* [61] and *D. ruminis* [62].

7.3.2 Possible interspecies formate transfer in syntrophic acetate degradation

Several species have been described to degrade acetate in syntrophic association with hydrogenotrophic methanogens but also with hydrogen and formate using methanogens [63-70]. This suggests that formate is not essential as an electron carrier in these syntrophic interactions. However, it does not exclude that interspecies formate plays a role. Recently, the genomes of three syntrophic acetate degraders, *Thermacetogenium phaeum, Tepidanaerobacter acetatoxydans* strain *Re1,* and *Clostridium ultunense* strain BS, were sequenced [71-73]. These bacteria use the acetyl-coA pathway for syntrophic acetate oxidation [69]. This pathway contains four redox reactions that each generate two electrons and two protons, catalyzed by carbon monoxide dehydrogenase (CODH), methylenetetrahydrofolate reductase (methylene-THF reductase), methylene-THF dehydrogenase, and FDH. ATP synthesis is expected to be driven by a sodium or proton motive force generated by these redox reactions. However, the proton translocating step and the types of electron carriers involved are not known, but due to the sequencing of the genome an electron chain was proposed for *Moorella thermoacetica* [74, 75]. This electron transport chain involves the oxidation of CO to CO_2 coupled to the reduction of cytochrome b. Subsequently, cytochrome b reduces methylene-THF to methyl-THF and a proton motive force is generated. Moreover, a proton motive force could be generated in *M. thermoacetica* membrane vesicles by the oxidation of CO to CO_2 [76]. In addition, other protein complexes, like a cytoplasmic oriented, membrane bound NADH and formate hydrogen lyase, were hypothesized to be involved in proton translocation in *M. thermoacetica* [74, 75]. In syntrophic acetate oxidation these protein complexes probably function in the reverse reaction. However, thus far it is unclear if and how syntrophic acetate degraders can couple the intracellular redox reactions to extracellular formate production. The latter can be answered by analyzing the genome of these bacteria for the occurrence of extra-cytoplasmic FDHs.

The genomes of *T. phaeum, T. acetatoxydans* and *C. ultunense* revealed that *T. phaeum* has two extra-cytoplasmic FDHs and that both *T. acetatoxydans* and *C. ultunense* have no extra-cytoplasmic FDH. Moreover, *T. acetatoxydans* has no genes coding for any FDH. However, it does have a gene coding for a formate transporter. Syntrophic acetate oxidation by this strain generates formate from the formyl-THF synthetase, but apparently cannot oxidize formate to CO_2 by a FDH. Formate is likely transported to the environment via the formate transporter and can there be used by formate-utilizing methanogens. By focusing on the (extra-cytoplasmic) FDHs in the genomes of these three syntrophic acetate oxidizers it becomes clear that there are differences within these strains and therefore, there are most likely differences in interspecies electron transport. It can be expected that, like syntrophic lactate degradation, the importance of interspecies formate transfer will differ between syntrophic acetate degraders.

7.3.3 Hydrogen as a possible syntrophic substrate

Chapter 6 discussed syntrophic formate degradation by interspecies hydrogen transfer. The electron transfer mechanism that allows syntrophic formate degradation is not known but *Moorella* sp. strain AMP and *Desulfovibrio* sp. strain G11 are able to couple formate oxidation to syntrophic growth with methanogens that can only use hydrogen as electron donor. In theory syntrophic hydrogen degradation by interspecies formate transfer could also be possible. By coupling the reduction of CO_2 to formate (by the bacterium) with methane production (by the methanogen) the conversion is energetically feasible.

$HCO_3^- + H_2$ à $CHOO^- + H_2O$	-1.3	kJ/reaction
$4\ CHOO^- + H_2O + H^+$ à $CH_4 + 3\ HCO_3^-$	-132	kJ/reaction

A syntrophic hydrogen degrading community that uses formate as interspecies electron donor has not been found yet. However, recent experiments with *Desulfovibrio vulgaris* Hildenborough show growth with H_2 and CO_2 in the presence [77] and absence [78] of sulfate when acetate is in the medium. Without sulfate, formate accumulation was observed. Moreover, accumulation of formate was slower and decreased in mutant strains that lacked one of the periplasmic FDHs compared to the wild type. This suggests that the electron donor hydrogen is used to produce formate by the reduction of CO_2 via the FDHs [78]. In theory the formate produced by *D. vulgaris* could subsequently be used by a methanogenic partner, which will keep formate concentrations low. This would allow *D. vulgaris* to grow in a sulfate deprived environment. However, methanogens that utilize formate can also grow with hydrogen. Da Silva et al. [78] suggested that in high hydrogen concentration environments syntrophic hydrogen utilization via interspecies formate transfer might occur.

7.3.4 Syntrophs evolved from sulfate-reducing bacteria

Chapter 4 and 6 discussed possible key genes involved in syntrophy by comparing syntrophs and sulfate reducers. Syntrophs and sulfate reducers have many similarities. Moreover, several syntrophs can also respire sulfate. Interestingly, according to 16S rRNA gene phylogeny obligate syntrophs are close related to sulfate-reducing bacteria. Moreover, the genome of the obligate syntroph *Pelotomaculum thermopropionicum* contains almost the complete sulfate-respiring pathway (Chapter 4). This suggests that *P. thermopropionicum* might have evolved from a true sulfate-reducing bacterium.

A recent study showed the evolution of a sulfate reducer towards becoming an obligate syntroph [87]. 22 cocultures of a sulfate reducer (*Desulfovibrio vulgaris*) and a hydrogenotrophic methanogen (*Methanococcus maripaludis*) were grown with lactate in the absence of sulfate for 1000 generations. The cocultures evolved increased stability, higher yields, higher growth rates, and in 13 of the 22 cultures *D. vulgaris* accumulated mutations that caused loss of functions of its sulfate-respiring pathway. The authors conclude that specialization for a mutualistic interaction can evolve by natural selection. Moreover, they suggest that a sulfate-reducing bacterium can readily evolve to become a specialized syntroph [87]. However, this cannot be true for an obligate sulfate reducer, like *Desulfotomaculum kuznetsovii*. In order for a sulfate-reducing bacterium to evolve towards a specialized syntroph it needs some syntrophic capacity. Obligate syntrophs and strict sulfate reducers seem to be two specialized extremes, with a sulfate reducer with

syntrophic capacity as a common ancestor.

7.4 Future perspectives

The research described in this thesis aimed to get a better understanding of the metabolism of one carbon compounds in acetogens and sulfate-reducing bacteria. Apart from the fundamental importance, to gain more knowledge about the microorganisms and the pathways they carry that close the circle in the global carbon cycle, it is also important for application purposes to continue to study anaerobic one carbon metabolism.

Research is necessary to better understand the functions of the CODH complexes, especially the less defined CODH II, IV and V complexes. A comparative proteome analysis would be a good approach. However, the challenge is to include conditions that use the lesser defined complexes. *Desulfotomaculum* species are good candidates for such an analysis since their genome generally encode different CODH complexes. Growth of CO in low and high concentrations and with and without sulfate can be studied. Studies on CO resistance and degradation are necessary for applications of synthesis gas. Synthesis gas is comprised for 60-80% of hydrogen and CO, with CH_4, CO_2, SO_2, H_2S, and NH_3 present in smaller concentrations [80]. Industry uses the microbial conversion of synthesis gas to produce chemicals, proteins, and hydrogen [81-83]. Elucidating the function of all CODH complexes and their role in CO resistance and degradation will assist in screening cultures for their CO degrading capacity for more efficient synthesis gas use. Subsequently, manipulating growth conditions to drive CO degradation via a specific CODH complex could improve product formation. An example of the latter would be hydrogen production via induced CODH I complexes at higher CO concentration [84]. Moreover, synthesis gas can be used for the reduction of sulfate in wastewater treatment. For this, CO metabolism studies in *Desulfotomaculum* species are beneficial, since *D. nigrificans* CO-1-SRB was isolated from an anaerobic wastewater treatment facility, suggesting their involvement in wastewater treatment (Chapter 2, [8]).

In addition to synthesis gas, methanol can be used to enhance sulfate reduction in wastewater treatment. The presence of a cobalt dependent and independent methanol degradation pathway as described in *Desulfotomaculum kuznetsovii* (Chapter 5) is useful because there is no need for the addition of cobalt and vitamin B12. The depletion of cobalt and vitamin B12 in high methanol concentration environments hampers sulfate reduction in the absence of a cobalt-independent pathway. Therefore, using an sulfate reducer that can use a cobalt-independent methanol degradation pathway, like *D. kuznetsovii,* will enhance methanol degradation and sulfate reduction. Additionally, it is interesting to find more sulfate-reducing bacteria capable of degrading methanol in a cobalt-dependent and independent fashion and investigate the cobalt independent syntrophic methanol degradation as proposed for *Moorella thermoacetica* strain AMP.

Future investigation of cobalt independent methanol degradation during syntrophic methanol degradation could elucidate the syntrophic systems involved. Furthermore, comparing phylogenetically closely related species that differ in their syntrophic capacity will help to understand how syntrophs work. *Desulfotomaculum* cluster I is an appropriate phylogenetic group for this type of study.

7.5 References

1. Drake, H.L. & Daniel, S.L. Physiology of the thermophilic acetogen *Moorella thermoacetica*. *Research in Microbiology* **155**, 422-36 (2004).
2. Henstra, A.M. & Stams, A.J. Novel physiological features of *Carboxydothermus hydrogenoformans* and *Thermoterrabacterium ferrireducens*. *Applied and Environmental Microbiology* **70**, 7236-40 (2004).
3. Oelgeschlager, E. & Rother, M. Carbon monoxide-dependent energy metabolism in anaerobic bacteria and archaea. *Archives of Microbiology* **190**, 257-69 (2008).
4. Oelgeschlager, E. & Rother, M. Influence of carbon monoxide on metabolite formation in *Methanosarcina acetivorans*. *Fems Microbiology Letters* **292**, 254-60 (2009).
5. Parshina, S.N. et al. Carbon monoxide conversion by thermophilic sulfate-reducing bacteria in pure culture and in co-culture with *Carboxydothermus hydrogenoformans*. *Applied Microbiology and Biotechnology* **68**, 390-6 (2005).
6. Sokolova, T.G. et al. Thermosinus carboxydivorans gen. nov., sp. nov., a new anaerobic, thermophilic, carbon-monoxide-oxidizing, hydrogenogenic bacterium from a hot pool of Yellowstone National Park. *International Journal of Systematic and Evolutionary Microbiology* **54**, 2353-9 (2004).
7. Alves, J.I., van Gelder, A.H., Alves, M.M., Sousa, D.Z. & Plugge, C.M. *Moorella stamsii* sp. nov., a new anaerobic thermophilic hydrogenogenic carboxydotroph isolated from digester sludge. *International Journal of Systematic and Evolutionary Microbiology* **63**, 4072-6 (2013).
8. Parshina, S.N. et al. *Desulfotomaculum carboxydivorans* sp. nov., a novel sulfate-reducing bacterium capable of growth at 100% CO. *International Journal of Systematic and Evolutionary Microbiology* **55**, 2159-65 (2005).
9. Slepova, T.V., Sokolova, T.G., Kolganova, T.V., Tourova, T.P. & Bonch-Osmolovskaya, E.A. Carboxydothermus siderophilus sp. nov., a thermophilic, hydrogenogenic, carboxydotrophic, dissimilatory Fe(III)-reducing bacterium from a Kamchatka hot spring. *International Journal of Systematic and Evolutionary Microbiology* **59**, 213-7 (2009).
10. Slepova, T.V. et al. Carboxydocella sporoproducens sp. nov., a novel anaerobic CO-utilizing/H2-producing thermophilic bacterium from a Kamchatka hot spring. *International Journal of Systematic and Evolutionary Microbiology* **56**, 797-800 (2006).
11. Sokolova, T. et al. Novel chemolithotrophic, thermophilic, anaerobic bacteria *Thermolithobacter ferrireducens* gen. nov., sp. nov. and Thermolithobacter carboxydivorans sp. nov. *Extremophiles* **11**, 145-57 (2007).
12. Sokolova, T.G. et al. *Carboxydobrachium pacificum* gen. nov., sp. nov., a new anaerobic, thermophilic, CO-utilizing marine bacterium from Okinawa Trough. *Int J Syst Evol Microbiol* **51**, 141-9 (2001).
13. Sokolova, T.G. et al. The first evidence of anaerobic CO oxidation coupled with H2 production by a hyperthermophilic archaeon isolated from a deep-sea hydrothermal vent. *Extremophiles* **8**, 317-23 (2004).
14. Sokolova, T.G. et al. *Carboxydocella thermautotrophica* gen. nov., sp. nov., a novel anaerobic, CO-utilizing thermophile from a Kamchatkan hot spring. *International Journal of Systematic and Evolutionary Microbiology* **52**, 1961-7 (2002).
15. Bonam, D., Lehman, L., Roberts, G.P. & Ludden, P.W. Regulation of carbon monoxide dehydrogenase and hydrogenase in *Rhodospirillum rubrum*: effects of CO and oxygen on

synthesis and activity. *Journal of Bacteriology* **171**, 3102-7 (1989).

16. Bonam, D. & Ludden, P.W. Purification and characterization of carbon monoxide dehydrogenase, a nickel, zinc, iron-sulfur protein, from *Rhodospirillum rubrum*. *The Journal of Biological Chemistry* **262**, 2980-7 (1987).
17. Bonam, D., McKenna, M.C., Stephens, P.J. & Ludden, P.W. Nickel-deficient carbon monoxide dehydrogenase from *Rhodospirillum rubrum*: in vivo and in vitro activation by exogenous nickel. *Proceedings of the National Academy of Sciences of the United States of America* **85**, 31-5 (1988).
18. Bonam, D., Murrell, S.A. & Ludden, P.W. Carbon monoxide dehydrogenase from *Rhodospirillum rubrum*. *Journal of Bacteriology* **159**, 693-9 (1984).
19. Daniels, L., Fuchs, G., Thauer, R.K. & Zeikus, J.G. Carbon monoxide oxidation by methanogenic bacteria. *Journal of Bacteriology* **132**, 118-26 (1977).
20. Drennan, C.L., Heo, J., Sintchak, M.D., Schreiter, E. & Ludden, P.W. Life on carbon monoxide: X-ray structure of *Rhodospirillum rubrum* Ni-Fe-S carbon monoxide dehydrogenase. *Proceedings of the National Academy of Sciences of the United States of America* **98**, 11973-8 (2001).
21. Ensign, S.A., Bonam, D. & Ludden, P.W. Nickel is required for the transfer of electrons from carbon monoxide to the iron-sulfur center(s) of carbon monoxide dehydrogenase from *Rhodospirillum rubrum*. *Biochemistry* **28**, 4968-73 (1989).
22. Ensign, S.A., Campbell, M.J. & Ludden, P.W. Activation of the nickel-deficient carbon monoxide dehydrogenase from *Rhodospirillum rubrum*: kinetic characterization and reductant requirement. *Biochemistry* **29**, 2162-8 (1990).
23. Ensign, S.A., Hyman, M.R. & Ludden, P.W. Nickel-specific, slow-binding inhibition of carbon monoxide dehydrogenase from *Rhodospirillum rubrum* by cyanide. *Biochemistry* **28**, 4973-9 (1989).
24. Ensign, S.A. & Ludden, P.W. Characterization of the CO oxidation/H_2 evolution system of *Rhodospirillum rubrum*. Role of a 22-kDa iron-sulfur protein in mediating electron transfer between carbon monoxide dehydrogenase and hydrogenase. *The Journal of Biological Chemistry* **266**, 18395-403 (1991).
25. Jeon, W.B., Cheng, J. & Ludden, P.W. Purification and characterization of membrane-associated CooC protein and its functional role in the insertion of nickel into carbon monoxide dehydrogenase from *Rhodospirillum rubrum*. *The Journal of Biological Chemistry* **276**, 38602-9 (2001).
26. Jeon, W.B., Singer, S.W., Ludden, P.W. & Rubio, L.M. New insights into the mechanism of nickel insertion into carbon monoxide dehydrogenase: analysis of *Rhodospirillum rubrum* carbon monoxide dehydrogenase variants with substituted ligands to the [Fe3S4] portion of the active-site C-cluster. *Journal of Biological Inorganic Chemistry : JBIC : a publication of the Society of Biological Inorganic Chemistry* **10**, 903-12 (2005).
27. Kerby, R.L. et al. Genetic and physiological characterization of the *Rhodospirillum rubrum* carbon monoxide dehydrogenase system. *Journal of Bacteriology* **174**, 5284-94 (1992).
28. Kerby, R.L., Ludden, P.W. & Roberts, G.P. In vivo nickel insertion into the carbon monoxide dehydrogenase of *Rhodospirillum rubrum*: molecular and physiological characterization of cooCTJ. *Journal of Bacteriology* **179**, 2259-66 (1997).
29. Meuer, J., Bartoschek, S., Koch, J., Kunkel, A. & Hedderich, R. Purification and catalytic

properties of Ech hydrogenase from *Methanosarcina barkeri*. *European journal of biochemistry / FEBS* **265**, 325-35 (1999).

30. Stephens, P.J., McKenna, M.C., Ensign, S.A., Bonam, D. & Ludden, P.W. Identification of a Ni- and Fe-containing cluster in *Rhodospirillum rubrum* carbon monoxide dehydrogenase. *The Journal of Biological Chemistry* **264**, 16347-50 (1989).
31. Tan, G.O. et al. On the structure of the nickel/iron/sulfur center of the carbon monoxide dehydrogenase from *Rhodospirillum rubrum*: an x-ray absorption spectroscopy study. *Proceedings of the National Academy of Sciences of the United States of America* **89**, 4427-31 (1992).
32. Uffen, R.L. Anaerobic growth of a *Rhodopseudomonas* species in dark with carbon-monoxide as sole carbon and energy substrate. *Proceedings of the National Academy of Sciences of the United States of America* **73**, 3298-302 (1976).
33. Ferry, J.G. CO Dehydrogenase. *Annual Review of Microbiology* **49**, 305-33 (1995).
34. Fox, J.D., He, Y.P., Shelver, D., Roberts, G.P. & Ludden, P.W. Characterization of the region encoding the CO-induced hydrogenase of *Rhodospirillum rubrum*. *Journal of Bacteriology* **178**, 6200-8 (1996).
35. Fox, J.D., Kerby, R.L., Roberts, G.P. & Ludden, P.W. Characterization of the CO-induced, CO-tolerant hydrogenase from *Rhodospirillum rubrum* and the gene encoding the large subunit of the enzyme. *Journal of Bacteriology* **178**, 1515-24 (1996).
36. Das, A. et al. Characterization of a corrinoid protein involved in the C1 metabolism of strict anaerobic bacterium *Moorella thermoacetica*. *Proteins* **67**, 167-76 (2007).
37. Harms, U. & Thauer, R.K. Methylcobalamin: coenzyme M methyltransferase isoenzymes MtaA and MtbA from *Methanosarcina barkeri*. Cloning, sequencing and differential transcription of the encoding genes, and functional overexpression of the mtaA gene in *Escherichia coli*. *European Journal of Biochemistry / FEBS* **235**, 653-9 (1996).
38. Sauer, K., Harms, U. & Thauer, R.K. Methanol:coenzyme M methyltransferase from *Methanosarcina barkeri*. Purification, properties and encoding genes of the corrinoid protein MT1. *European journal of biochemistry / FEBS* **243**, 670-7 (1997).
39. Stupperich, E., Aulkemeyer, P. & Eckerskorn, C. Purification and characterization of a methanol-induced cobamide-containing protein from *Sporomusa ovata*. *Archives of Microbiology* **158**, 370-3 (1992).
40. van der Meijden, P. et al. Methyltransferases involved in methanol conversion by *Methanosarcina barkeri*. *Archives of Microbiology* **134**, 238-42 (1983).
41. van der Meijden, P. et al. Activation and inactivation of methanol: 2-mercaptoethanesulfonic acid methyltransferase from *Methanosarcina barkeri*. *Journal of Bacteriology* **153**, 6-11 (1983).
42. van der Meijden, P., te Brommelstroet, B.W., Poirot, C.M., van der Drift, C. & Vogels, G.D. Purification and properties of methanol:5-hydroxybenzimidazolylcobamide methyltransferase from *Methanosarcina barkeri*. *Journal of Bacteriology* **160**, 629-35 (1984).
43. van der Meijden, P., van der Lest, C., van der Drift, C. & Vogels, G.D. Reductive activation of methanol: 5-hydroxybenzimidazolylcobamide methyltransferase of *Methanosarcina barkeri*. *Biochemical and Biophysical Research Communications* **118**, 760-6 (1984).
44. Zhou, W. et al. Isolation, crystallization and preliminary X-ray analysis of a methanol-induced corrinoid protein from *Moorella thermoacetica*. *Acta Crystallographica. Section F, Structural Biology and Crystallization Communications* **61**, 537-40 (2005).

45. Wu, M. et al. Life in hot carbon monoxide: the complete genome sequence of *Carboxydothermus hydrogenoformans* Z-2901. *PLoS Genetics* **1**, e65 (2005).
46. Techtmann, S.M. et al. Evidence for horizontal gene transfer of anaerobic carbon monoxide dehydrogenases. *Frontiers in Microbiology* **3**, 132 (2012).
47. Kremer, D.R., Nienhuiskuiper, H.E. & Hansen, T.A. Ethanol dissimilation in *Desulfovibrio*. *Arch Microbiol* **150**, 552-57 (1988).
48. Goorissen, H.P., Stams, A.J.M. & Hansen, T.A. Methanol dissimilation in *Desulfotomaculum kuznetsovii. PhD dissertation: Thermophilic methanol utilization by sulfate reducing bacteria* **Chapter 3**, 55-61 (2002).
49. Florencio, L., Field, J.A. & Lettinga, G. Importance of cobalt for individual trophic groups in an anaerobic methanol-degrading consortium. *Applied and Environmental Microbiology* **60**, 227-34 (1994).
50. Florencio, L., Jenicek, P., Field, J.A. & Lettinga, G. Effect of cobalt on the anaerobic degradation of methanol. *Journal of Fermentation and Bioengineering* **75**, 368-74 (1993).
51. Paulo, P.L., Jiang, B., Cysneiros, D., Stams, A.J. & Lettinga, G. Effect of cobalt on the anaerobic thermophilic conversion of methanol. *Biotechnol Bioeng* **85**, 434-41 (2004).
52. Goorissen, H.P., Stams, A.J. & Hansen, T.A. Methanol utilization in defined mixed cultures of thermophilic anaerobes in the presence of sulfate. *FEMS Microbiology Ecology* **49**, 489-94 (2004).
53. Jiang, B. et al. Atypical one-carbon metabolism of an acetogenic and hydrogenogenic *Moorella thermoacetica* strain. *Archives of Microbiology* **191**, 123-31 (2009).
54. Struchtemeyer, C.G., Duncan, K.E. & McInerney, M.J. Evidence for syntrophic butyrate metabolism under sulfate-reducing conditions in a hydrocarbon-contaminated aquifer. *FEMS Microbiol Ecol* **76**, 289-300 (2011).
55. Meyer, B. et al. Variation among *Desulfovibrio* species in electron transfer systems used for syntrophic growth. *J Bacteriol* **195**, 990-1004 (2013).
56. Meyer, B., Kuehl, J.V., Deutschbauer, A.M., Arkin, A.P. & Stahl, D.A. Flexibility of syntrophic enzyme systems in *Desulfovibrio* species ensures their adaptation capability to environmental changes. *J Bacteriol* **195**, 4900-14 (2013).
57. Walker, C.B. et al. The electron transfer system of syntrophically grown Desulfovibrio vulgaris. *J Bacteriol* **191**, 5793-801 (2009).
58. Stolyar, S. et al. Metabolic modeling of a mutualistic microbial community. *Mol Syst Biol* **3**, 92 (2007).
59. Klemps, R., Cypionka, H., Widdel, F. & Pfennig, N. Growth with hydrogen, and further physiological-characteristics of *Desulfotomaculum* species. *Archives of Microbiology* **143**, 203-8 (1985).
60. Visser, M., Parshina, S.N., Alves, J.I., Sousa, D.Z., Pereira, I.A., Muyzer, G., Kuever, J., Lebedinsky, A.V., Koehorst, J.J., Worm, P., Plugge, C.M., Schaap, P., Goodwin, L., Lapidus, A., Kyrpides, N.C., Detter, J.C., Woyke, T., Chain, P., Davenport, K.W., Spring, S., Rohde, M., Klenk, H.P., Stams, A.J.M. Genome analyses of the carboxydotrophic sulfate-reducers *Desulfotomaculum nigrificans* and *Desulfotomaculum carboxydivorans* and reclassification of *Desulfotomaculum carboxydivorans* as a later synonym of *Desulfotomaculum nigrificans*. *Standards in Genomic Sciences* **9**, 655-75 (2014).
61. Kuever, J., Visser, M., Loeffler, C., Boll, M., Worm, P., Sousa, D.Z., Plugge, C.M., Schaap, P.J.,

Muyzer, G., Pereira, I.A., Parshina, S.N., Goodwin, L.A., Kyrpides, N.C., Detter, J., Woyke, T., Chain, P., Davenport, K.W., Rohde, M., Spring, S., Klenk, H.P., Stams, A.J.M. Genome analysis of *Desulfotomaculum gibsoniae* strain GroIl^T a highly versatile Gram-positive sulfate-reducing bacterium. *Standards in Genomic Sciences* **9** (2014).

62. Spring, S. Visser, M., Lu, M., Copeland, A., Lapidus, A., Lucas, S., Cheng, J.F., Han, C., Tapia, R., Goodwin, L.A., Pitluck, S., Ivanova, N., Land, M., Hauser, L., Larimer, F., Rohde, M., Göker, M., Detter, J.C., Kyrpides, N.C., Woyke, T., Schaap, P.J., Plugge, C.M., Muyzer, G., Kuever, J., Pereira, I.A., Parshina, S.N., Bernier-Latmani, R., Stams, A.J., Klenk, H.P. Complete genome sequence of the sulfate-reducing firmicute *Desulfotomaculum ruminis* type strain (DL(T)). *Stand Genomic Sci* **7**, 304-19 (2012).
63. Balk, M., Weijma, J., Goorissen, H.P., Ronteltap, M., Hansen, T.A., Stams, A.J.M. Methanol utilizing *Desulfotomaculum* species utilizes hydrogen in a methanol-fed sulfate-reducing bioreactor. *Applied Microbiology and Biotechnology* **73**, 1203-11 (2007).
64. Hattori, S., Kamagata, Y., Hanada, S. & Shoun, H. *Thermacetogenium phaeum* gen. nov., sp. nov., a strictly anaerobic, thermophilic, syntrophic acetate-oxidizing bacterium. *International Journal of Systematic and Evolutionary Microbiology* **50 Pt 4**, 1601-9 (2000).
65. Lee, M.J. & Zinder, S.H. Isolation and characterization of a thermophilic bacterium which oxidizes acetate in syntrophic association with a methanogen and which grows acetogenically on H_2-CO_2. *Applied Environmental Microbiology* **54**, 124-9 (1988).
66. Schnurer, A., Schink, B. & Svensson, B.H. Clostridium ultunense sp. nov., a mesophilic bacterium oxidizing acetate in syntrophic association with a hydrogenotrophic methanogenic bacterium. *Int J Syst Bacteriol* **46**, 1145-52 (1996).
67. Sorokin, D.Y. et al. Genome analysis of *Chitinivibrio alkaliphilus* gen. nov., sp. nov., a novel extremely haloalkaliphilic anaerobic chitinolytic bacterium from the candidate phylum Termite Group 3. *Environmental Microbiology* **16**, 1549-65 (2014).
68. Westerholm, M., Roos, S. & Schnurer, A. *Syntrophaceticus schinkii* gen. nov., sp nov., an anaerobic, syntrophic acetate-oxidizing bacterium isolated from a mesophilic anaerobic filter. *Fems Microbiology Letters* **309**, 100-4 (2010).
69. 69. Zinder, S.H. & Koch, M. Non-aceticlastic methanogenesis from acetate - acetate oxidation by a thermophilic syntrophic coculture. *Archieves of Microbiology* **138**, 263-72 (1984).
70. Balk, M., Weijma, J. & Stams, A.J. *Thermotoga lettingae* sp. nov., a novel thermophilic, methanol-degrading bacterium isolated from a thermophilic anaerobic reactor. *International Journal of Systematic and Evolutionary Microbiology* **52**, 1361-8 (2002).
71. Manzoor, S., Bongcam-Rudloff, E., Schnurer, A. & Muller, B. First genome sequence of a syntrophic acetate-oxidizing bacterium, *Tepidanaerobacter acetatoxydans* strain Re1. *Genome Announcements* **1** (2013).
72. Oehler, D. et al. Genome-guided analysis of physiological and morphological traits of the fermentative acetate oxidizer *Thermacetogenium phaeum*. *BMC Genomics* **13**, 723 (2012).
73. Wei, Y. et al. Draft genome sequence of *Clostridium ultunense* strain BS (DSMZ 10521), recovered from a mixed culture. *Genome Announcements* **2** (2014).
74. Ragsdale, S.W. & Pierce, E. Acetogenesis and the Wood-Ljungdahl pathway of CO_2 fixation. *Biochimica Et Biophysica Acta-Proteins and Proteomics* **1784**, 1873-98 (2008).
75. Pierce, E. et al. The complete genome sequence of *Moorella thermoacetica* (f. *Clostridium thermoaceticum*). *Environmental Microbiology* **10**, 2550-73 (2008).

76. Hugenholtz, J. & Ljungdahl, L.G. Electron transport and electrochemical proton gradient in membrane vesicles of Clostridium thermoautotrophicum. *J Bacteriol* **171**, 2873-5 (1989).
77. Pereira, P.M. et al. Energy metabolism in Desulfovibrio vulgaris Hildenborough: insights from transcriptome analysis. *Antonie Van Leeuwenhoek* **93**, 347-62 (2008).
78. da Silva, S.M. et al. Function of formate dehydrogenases in Desulfovibrio vulgaris Hildenborough energy metabolism. *Microbiology* **159**, 1760-9 (2013).
79. Muyzer, G. & Stams, A.J. The ecology and biotechnology of sulphate-reducing bacteria. *Nature Reviews Microbiology* **6**, 441-54 (2008).
80. Sipma, J. et al. H2 enrichment from synthesis gas by *Desulfotomaculum carboxydivorans* for potential applications in synthesis gas purification and biodesulfurization. *Applied Microbiology and Biotechnology* **76**, 339-47 (2007).
81. Henstra, A.M., Sipma, J., Rinzema, A. & Stams, A.J. Microbiology of synthesis gas fermentation for biofuel production. *Current Opinion in Biotechnology* **18**, 200-6 (2007).
82. Hussain, A., Guiot, S.R., Mehta, P., Raghavan, V. & Tartakovsky, B. Electricity generation from carbon monoxide and syngas in a microbial fuel cell. *Appl Microbiol Biotechnol* **90**, 827-36 (2011).
83. Munasinghe, P.C. and Khanal, S.K. Biomass-derived syngas fermentation into biofuels: Opportunities and challenges. *Bioresource Technology* **101**, 5013-22 (2010).
84. Techtmann, S.M. et al. Regulation of multiple carbon monoxide consumption pathways in anaerobic bacteria. *Frontiers in Microbiology* **2**, 147 (2011).
85. Tarasov, A. L., Borzenkov, I. A., Chernykh, N. A., S. S. Belyayev Isolation and investigation of anaerobic microorganisms involved in methanol transformation in an underground gas storage facility. *Microbiology* 80 (2), 172–79 (2011).
86. Kolb, S. and Stacheter, A. Prerequisites for amplicon pyrosequencing of microbial methanol utilizers in the environment. *Frontiers in Microbiology* **4**:268 (2013).
87. Hillesland, K.L., Lim, S., Flowers, J.J., Turkarslan, S., Pinel, N., Zane, G.M., Elliott, N., Qin, Y., Wu, L., Baliga, N.S., Zhou, J., Wall, J.D., Stahl, D.A. Erosion of functional independence early in the evolution of a microbial mutualism. *Proceedings of the National Academy of Sciences of the United States of America* **111**(41):14822-7 (2014).

Supplementary data

Chapter 2

S1 *To reveal genomic differences between the very closely related Desulfotomaculum nigrificans and D. carboxydivorans a bidirectional BLAST of the protein coding genes was performed. BLAST analyses were performed using standard settings and best hits were filtered for 70% sequence coverage and 40% identity. The table displays the locus tag and the function of the genes that were filtered. Colors indicate genes that are situated next to each other in the genome.*

Table can be found in: Standards in Genomic Sciences (2014) ***9****: 655-675*

Chapter 3

S1 *Proteomic data of the proteins with >9 peptide counts of Sporomusa strain An4. The table shows the predicted function of the proteins, the reference to the genome, and their related peptide abundance in the five different growth conditions: hydrogen and carbon dioxide (H_2 CO_2), methanol (MeOH), methanol and nitrate (NO_3^-), betaine (B), and fructose (F).*

Predicted function	Genome reference	H_2CO_2	MeOH	NO_3^-	B	F
CobN component of cobalt chelatase involved in B12 biosynthesis	s01:1003993-1000277	5	91	34	21	2
Ethanolamine utilization protein similar to PduL	s01:1019277-1018705	31	29	16	25	42
Aspartate aminotransferase (EC 2.6.1.1)	s01:1020847-1019684	10	7	2	7	9
S-adenosylhomocysteine deaminase (EC 3.5.4.28); Methylthioadenosine deaminase	s01:1022252-1020972	8	10	13	14	21
Adenosylhomocysteinase (EC 3.3.1.1)	s01:1023522-1022281	13	30	30	23	20
5'-methylthioadenosine phosphorylase (EC 2.4.2.28)	s01:1025386-1024595	11	18	8	18	14
Inosine-5'-monophosphate dehydrogenase (EC 1.1.1.205)	s01:1036297-1034843	68	76	78	59	74
LSU ribosomal protein L28p	s01:1045134-1045325	11	6	2	7	11
Tricarboxylate transport protein TctC	s01:1051786-1050836	13	10	17	14	2
6,7-dimethyl-8-ribityllumazine synthase (EC 2.5.1.78)	s01:1056844-1056374	1	29	12	5	10
3,4-dihydroxy-2-butanone 4-phosphate synthase (EC 4.1.99.12) / GTP cyclohydrolase II (EC 3.5.4.25)	s01:1058058-1056847	21	12	11	9	18
Serine/threonine protein kinase PrkC, regulator of stationary phase	s01:1063582-1061699	8	10	11	1	4
S-adenosylmethionine synthetase (EC 2.5.1.6)	s01:1077301-1076111	40	42	38	29	41
Protein YicC	s01:1080839-1079955	11	12	7	9	11
Isoleucyl-tRNA synthetase (EC 6.1.1.5)	s01:1094692-1091900	52	61	48	82	97
Cell division initiation protein DivIVA	s01:1095754-1095302	9	54	43	44	48
Pyrroline-5-carboxylate reductase (EC 1.5.1.2)	s01:1097382-1096570	20	41	14	39	32
FIG001960: FtsZ-interacting protein related to cell division	s01:1097865-1097413	11	19	12	0	11
Translation elongation factor G-related protein	s01:1101648-1099567	109	264	109	78	42
ATP:Cob(I)alamin adenosyltransferase	s01:1102603-1102079	10	16	17	13	17

Nucleoside diphosphate kinase (EC 2.7.4.6)	s01:1103048-1102596	6	13	5	7	10
Acetylornithine aminotransferase (EC 2.6.1.11)	s01:1106377-1105121	11	15	7	9	2
Chaperone protein HtpG	s01:1112541-1114502	92	159	101	83	55
CoA-disulfide reductase (EC 1.8.1.14) / Disulfide bond regulator	s01:111523-109055	8	9	7	10	7
RNA-binding protein Hfq	s01:1147644-1147381	12	2	2	7	7
Cytosol aminopeptidase PepA (EC 3.4.11.1)	s01:1159206-1157707	10	4	5	6	6
FIG002344: Hydrolase (HAD superfamily)	s01:1161930-1160386	5	44	34	28	33
RecA protein	s01:1163645-1162551	12	15	11	9	10
DEAD-box ATP-dependent RNA helicase CshA (EC 3.6.4.13)	s01:1165324-1163747	26	57	63	61	71
Competence/damage-inducible protein CinA	s01:1166582-1165335	9	9	6	13	14
Transcriptional regulator in cluster with unspecified monosaccharide ABC transport system	s01:1172354-1171623	3	13	3	5	7
Putative mandelate racemase STM3833	s01:134957-133767	2	4	1	0	13
Gluconate dehydratase (EC 4.2.1.39)	s01:136304-135090	56	81	59	45	67
Methyl-accepting chemotaxis protein	s01:140873-138918	41	49	38	22	18
Biosynthetic Aromatic amino acid aminotransferase alpha (EC 2.6.1.57) @ Aspartate aminotransferase (EC 2.6.1.1)	s01:142889-141696	9	14	7	16	23
Methyl-accepting chemotaxis protein	s01:146726-145668	17	44	42	39	94
Flavoprotein	s01:148850-148611	6	12	13	11	8
Alkyldihydroxyacetonephosphate synthase (EC 2.5.1.26)	s01:149914-148892	8	23	15	14	9
Rubrerythrin	s01:150407-149907	11	31	24	20	24
HtrA protease/chaperone protein	s01:155278-154157	11	10	4	7	12
diguanylate cyclase/phosphodiesterase (GGDEF & EAL domains) with PAS/PAC sensor(s)	s01:164096-161715	3	8	4	3	11
Tryptophan synthase beta chain like (EC 4.2.1.20)	s01:165860-164478	13	19	13	10	11
Aspartate/glutamate/uridylate kinase	s01:172019-171243	9	17	3	16	13
Tungsten-containing aldehyde:ferredoxin oxidoreductase (EC 1.2.7.5)	s01:177597-175870	474	606	606	453	670
Molybdopterin biosynthesis protein MoeA	s01:178195-179409	28	10	17	10	10
Outer membrane vitamin B12 receptor BtuB	s01:186270-184285	22	29	30	8	16
RNA-binding protein Hfq	s01:190997-191257	11	7	3	10	7
Methyl-accepting chemotaxis protein	s01:196729-195017	7	9	11	8	9
Aminomethyltransferase (glycine cleavage system T protein) (EC 2.1.2.10)	s01:208869-206227	41	89	88	90	43
COG1020: Non-ribosomal peptide synthetase modules and related proteins	s01:21572-6825	54	125	50	80	80
probable electron transfer protein	s01:220049-218250	0	0	0	24	1
Trimethylamine:corrinoid methyltransferase @ pyrrolysine-containing	s01:235381-233915	9	0	18	177	4

Predicted function	Genome reference	H_2CO_2	MeOH	NO_3^-	B	F
Trimethylamine:corrinoid methyltransferase @ pyrrolysine-containing	s01:236881-235415	12	2	48	159	7
5-methyltetrahydrofolate--homocysteine methyltransferase (EC 2.1.1.13)	s01:237546-236914	9	1	30	140	4
Methyl-accepting chemotaxis protein	s01:241415-239700	7	13	14	7	13
ABC-type polar amino acid transport system, ATPase component	s01:260113-259376	1	0	0	10	1
Amino acid ABC transporter, periplasmic amino acid-binding portion	s01:261606-260803	7	7	5	39	12
2-hydroxy-3-oxopropionate reductase (EC 1.1.1.60)	s01:266617-265727	70	22	20	3	25
2-keto-3-deoxy-D-arabino-heptulosonate-7-phosphate synthase I beta (EC 2.5.1.54)	s01:346639-345620	50	52	23	17	18
Siderophore biosynthesis non-ribosomal peptide synthetase modules	s01:347121-346657	70	169	153	46	35
COG1020: Non-ribosomal peptide synthetase modules and related proteins	s01:352169-347145	477	895	715	385	459
Thiazolinyl imide reductase in siderophore biosynthesis gene cluster	s01:353376-352258	42	83	64	44	35
Putative reductoisomerase in siderophore biosynthesis gene cluster	s01:354473-353373	43	23	39	24	21
predicted protein	s01:35490-35888	5	13	0	4	18
iron aquisition yersiniabactin synthesis enzyme (Irp2)	s01:362527-354578	851	1430	1103	474	589
2,3-dihydroxybenzoate-AMP ligase (EC 2.7.7.58) of siderophore biosynthesis / Isochorismate synthase (EC 5.4.4.2) of siderophore biosynthesis	s01:365552-362571	411	498	491	214	249
TonB-dependent receptor; Outer membrane receptor for ferrienterochelin and colicins	s01:371626-369686	186	198	279	111	98
Duplicated ATPase component BL0693 of energizing module of predicted ECF transporter	s01:373770-372280	18	38	40	14	26
ABC transporter ATP-binding protein	s01:376122-377927	25	88	56	27	36
ABC transporter ATP-binding protein	s01:377927-379663	38	140	95	30	82
Tungsten-containing aldehyde:ferredoxin oxidoreductase (EC 1.2.7.5)	s01:4098-5825	462	595	599	448	657
N-terminal of elongation factor Ts	s01:410283-410726	0	16	8	3	11
Glycyl-tRNA synthetase beta chain (EC 6.1.1.14)	s01:414444-416507	28	26	37	20	14
Glutamine synthetase type III, GlnN (EC 6.3.1.2)	s01:426391-428484	232	35	54	44	34
Glutamine synthetase, clostridia type (EC 6.3.1.2)	s01:429436-431346	77	252	161	97	113
Rubrerythrin	s01:431508-432017	27	109	54	60	68
Dissimilatory sulfite reductase (desulfoviridin), alpha and beta subunits	s01:432156-432827	19	43	16	38	37
Butyryl-CoA dehydrogenase (EC 1.3.99.2)	s01:440323-441456	36	41	51	50	45
Peptide chain release factor 3	s01:446410-448014	5	5	3	17	10

Threonyl-tRNA synthetase (EC 6.1.1.3)	s01:449656-451566	12	23	43	22	16
Translation initiation factor 3	s01:451899-452327	22	17	15	26	36
LSU ribosomal protein L20p	s01:452586-452942	5	25	8	37	42
Fructose-bisphosphate aldolase class II (EC 4.1.2.13)	s01:453162-454010	4	21	0	15	9
RND efflux system, membrane fusion protein CmeA	s01:45441-44371	5	5	11	5	6
Phenylalanyl-tRNA synthetase alpha chain (EC 6.1.1.20)	s01:457427-458449	10	10	4	17	15
Phenylalanyl-tRNA synthetase beta chain (EC 6.1.1.20)	s01:458546-460975	27	48	37	25	45
Recombination inhibitory protein MutS2	s01:465578-467938	10	6	10	13	11
Multimodular transpeptidase-transglycosylase (EC 2.4.1.129) (EC 3.4.-.-)	s01:472189-470024	7	13	5	2	2
Tyrosyl-tRNA synthetase (EC 6.1.1.1)	s01:472551-473768	12	15	18	16	30
Molybdenum ABC transporter ATP-binding protein	s01:478876-479628	3	3	2	12	13
FIG000859: hypothetical protein YebC	s01:479795-480535	6	12	7	22	18
5-formyltetrahydrofolate cyclo-ligase (EC 6.3.3.2)	s01:489335-489916	9	13	5	10	12
Protein-export membrane protein SecD (TC 3.A.5.1.1)	s01:490754-491983	17	29	27	29	29
Protein-export membrane protein SecF (TC 3.A.5.1.1)	s01:491973-492881	2	7	6	11	12
Histidyl-tRNA synthetase (EC 6.1.1.21)	s01:503287-504552	15	15	20	25	27
Aspartyl-tRNA synthetase (EC 6.1.1.12) @ Aspartyl-tRNA(Asn) synthetase (EC 6.1.1.23)	s01:504552-506402	36	42	74	88	73
Cysteine desulfurase (EC 2.8.1.7)	s01:511057-512265	20	26	22	21	27
Iron-sulfur cluster assembly scaffold protein IscU/ NifU-like	s01:512290-512661	10	15	4	15	19
Alanyl-tRNA synthetase (EC 6.1.1.7)	s01:516086-518704	59	67	78	86	81
hypothetical protein	s01:519785-520126	4	4	1	10	7
Stage 0 sporulation two-component response regulator (Spo0A)	s01:547413-548201	2	3	3	11	2
HlyB/MsbA family ABC transporter	s01:55294-53552	9	4	34	13	5
Tryptophanyl-tRNA synthetase (EC 6.1.1.2)	s01:565869-566846	15	20	12	21	19
HlyB/MsbA family ABC transporter	s01:57038-55314	14	14	61	32	9
Fructose-bisphosphate aldolase class II (EC 4.1.2.13)	s01:586052-585123	18	38	14	21	67
TonB-dependent receptor; Outer membrane receptor for ferrienterochelin and colicins	s01:59076-57127	16	7	53	10	2
Duplicated ATPase component BL0693 of energizing module of predicted ECF transporter	s01:62286-60802	11	8	24	9	10
Superoxide reductase (EC 1.15.1.2)	s01:648503-648895	24	41	21	20	20
Aspartokinase (EC 2.7.2.4)	s01:649619-650839	20	36	45	43	40

Predicted function	Genome reference	H_2CO_2	MeOH	NO_3^-	B	F
Biosynthetic Aromatic amino acid aminotransferase alpha (EC 2.6.1.57) @ Aspartate aminotransferase (EC 2.6.1.1)	s01:652327-653574	10	18	11	12	17
Predicted molybdate-responsive regulator YvgK in bacilli	s01:654826-653888	7	5	2	8	11
Uridine kinase (EC 2.7.1.48)	s01:655952-657613	2	11	11	10	10
Oxaloacetate decarboxylase alpha chain (EC 4.1.1.3)	s01:659018-657669	3	12	13	6	8
FIG01054622: hypothetical protein	s01:664063-665421	15	14	13	24	24
ATP-dependent RNA helicase YfmL	s01:666262-667440	10	8	3	11	7
2-keto-3-deoxy-D-arabino-heptulosonate-7-phosphate synthase I beta (EC 2.5.1.54)	s01:679274-678261	55	73	56	98	72
Molybdenum cofactor biosynthesis protein MoaC	s01:682728-683207	6	21	23	12	15
FIG060329: MOSC domain protein	s01:683211-683651	2	17	5	9	19
Molybdenum cofactor biosynthesis protein MoaB	s01:683644-684132	9	15	7	13	16
2-keto-3-deoxy-D-arabino-heptulosonate-7-phosphate synthase I beta (EC 2.5.1.54)	s01:687908-688924	23	17	13	14	5
protein of unknown function DUF964	s01:696792-697142	15	0	0	18	4
Metallo-beta-lactamase family protein, RNA-specific	s01:698280-699893	22	34	28	32	22
GTP-binding protein TypA/BipA	s01:716386-718191	2	4	9	50	16
DNA polymerase III alpha subunit (EC 2.7.7.7)	s01:742733-746158	2	0	0	2	10
Electron transfer flavoprotein, beta subunit	s01:746943-747728	1	11	7	19	9
Electron transfer flavoprotein, alpha subunit	s01:747748-748947	5	6	8	14	10
iron-sulfur flavoprotein	s01:750483-751142	8	86	24	3	5
Anthranilate phosphoribosyltransferase (EC 2.4.2.18)	s01:754359-755399	3	6	1	12	0
Tryptophan synthase alpha chain (EC 4.2.1.20)	s01:757971-758762	8	8	7	12	7
Anthranilate synthase, aminase component (EC 4.1.3.27)	s01:758759-760255	4	18	9	21	2
Pyruvate kinase (EC 2.7.1.40)	s01:768932-770686	12	32	19	20	19
hypothetical protein	s01:774538-774876	6	1	0	10	3
hypothetical protein	s01:780321-780773	6	8	3	5	17
DNA polymerase I (EC 2.7.7.7)	s01:785663-788305	22	30	29	44	30
5-Enolpyruvylshikimate-3-phosphate synthase (EC 2.5.1.19)	s01:802788-804086	27	28	29	27	19
SSU ribosomal protein S1p	s01:810074-812035	10	16	14	5	12
Homoserine dehydrogenase (EC 1.1.1.3)	s01:822106-823398	16	13	18	14	15
Glutamine ABC transporter, periplasmic glutamine-binding protein (TC 3.A.1.3.2)	s01:826819-827607	5	16	7	14	5
hypothetical protein	s01:843042-843881	37	50	36	36	53
Oligopeptide ABC transporter, periplasmic oligopeptide-binding protein OppA (TC 3.A.1.5.1)	s01:874737-873184	4	11	11	0	17

Outer membrane vitamin B12 receptor BtuB	s01:886734-884845	0	16	23	11	0
Outer membrane vitamin B12 receptor BtuB	s01:909313-904670	0	29	5	3	1
Outer membrane vitamin B12 receptor BtuB	s01:921024-918184	0	48	22	5	0
Ferric siderophore transport system, periplasmic binding protein TonB	s01:924416-923709	13	22	17	2	7
Biopolymer transport protein ExbD/TolR	s01:924832-924422	7	12	4	12	5
hypothetical protein	s01:927794-925785	2	44	31	10	0
TonB-dependent receptor; Outer membrane receptor for ferrienterochelin and colicins	s01:929903-927891	0	22	15	0	0
Cobalt-precorrin-8x methylmutase (EC 5.4.1.2)	s01:930584-929952	0	13	1	0	0
TonB-dependent receptor; Outer membrane receptor for ferrienterochelin and colicins	s01:934273-932318	0	8	10	1	0
hypothetical protein	s01:959043-957784	0	11	6	2	0
Outer membrane vitamin B12 receptor BtuB	s01:962159-959148	0	31	23	8	0
hypothetical protein	s01:965907-964606	7	125	54	10	1
TonB-dependent receptor plug	s01:971196-966076	0	115	89	18	0
ABC-type nitrate/sulfonate/bicarbonate transport systems, periplasmic components	s02:1002093-1000972	2	2	3	15	1
ABC-type nitrate/sulfonate/bicarbonate transport systems, periplasmic components	s02:1004113-1003016	0	1	1	16	0
Benzoyl-CoA reductase subunit BadG (EC 1.3.99.15)	s02:1014393-1013563	0	0	0	13	0
hypothetical protein	s02:1015554-1014397	0	2	3	42	5
Hypothetical protein Cj1505c	s02:1017549-1016959	0	0	0	12	1
Methylcobalamin:coenzyme M methyltransferase, methanol-specific	s02:1020874-1019798	0	0	0	18	0
ABC-type nitrate/sulfonate/bicarbonate transport systems, periplasmic components	s02:1022997-1021921	0	0	0	25	0
5-methyltetrahydrofolate--homocysteine methyltransferase (EC 2.1.1.13)	s02:1024844-1024197	0	1	0	229	11
Trimethylamine methyltransferase family protein	s02:1026315-1024885	2	0	3	701	24
Tetrahydromethanopterin S-methyltransferase subunit H (EC 2.1.1.86) homolog	s02:1027341-1026421	3	8	4	539	11
Arginine utilization regulatory protein RocR	s02:1028194-1029642	7	14	15	5	16
Urea ABC transporter, urea binding protein	s02:109652-108405	24	0	0	0	14
Molybdopterin converting factor, large subunit	s02:140854-140444	2	8	2	8	15
Gluconate permease	s02:146600-145200	0	16	20	10	2
Altronate dehydratase (EC 4.2.1.7)	s02:147937-146777	11	7	13	14	3
FIG00675759: hypothetical protein	s02:153267-151990	10	5	4	8	5
3'-to-5' exoribonuclease RNase R	s02:162689-160416	8	24	32	21	23
Pyrophosphate-energized proton pump (EC 3.6.1.1)	s02:166773-164767	31	71	85	65	81
Enolase (EC 4.2.1.11)	s02:168899-167613	40	53	88	84	85

Predicted function	Genome reference	H_2CO_2	MeOH	NO_3^-	B	F
Triosephosphate isomerase (EC 5.3.1.1)	s02:171258-170506	7	12	11	10	12
Phosphoglycerate kinase (EC 2.7.2.3)	s02:172467-171280	13	9	10	16	25
Predicted L-lactate dehydrogenase, Fe-S oxidoreductase subunit YkgE / Predicted L-lactate dehydrogenase, Iron-sulfur cluster-binding subunit YkgF	s02:17299-15131	1	38	0	51	12
NAD-dependent glyceraldehyde-3-phosphate dehydrogenase (EC 1.2.1.12)	s02:173554-172547	64	75	97	77	121
Predicted L-lactate dehydrogenase, hypothetical protein subunit YkgG	s02:17911-17303	1	2	1	15	7
L-lactate permease	s02:18244-19872	0	4	0	27	19
Cof-like hydrolase	s02:189277-188480	0	6	2	10	6
Excinuclease ABC subunit A	s02:196626-193789	23	8	16	16	15
Carboxyl-terminal protease (EC 3.4.21.102)	s02:201808-200672	3	2	4	12	4
Transketolase, C-terminal section (EC 2.2.1.1)	s02:206696-205749	25	37	14	35	54
Transketolase, N-terminal section (EC 2.2.1.1)	s02:207771-206929	3	17	12	24	24
FIG01165608: hypothetical protein	s02:211803-209734	2	0	11	5	7
Protein export cytoplasm protein SecA ATPase RNA helicase (TC 3.A.5.1.1)	s02:216305-213720	53	52	64	72	113
Formate dehydrogenase -O, gamma subunit (EC 1.2.1.2)	s02:217248-216550	1	5	5	11	11
Periplasmic [Fe] hydrogenase small subunit (EC 1.12.7.2)	s02:217572-217261	10	8	3	9	10
Periplasmic [Fe] hydrogenase large subunit (EC 1.12.7.2)	s02:218844-217585	103	148	108	74	141
Ribosomal subunit interface protein	s02:219946-219407	22	42	24	37	48
Cold shock protein CspA	s02:220533-220333	9	7	7	12	9
Glutamine transport ATP-binding protein GlnQ (TC 3.A.1.3.2)	s02:221338-220619	3	12	7	10	12
Glutamine ABC transporter, periplasmic glutamine-binding protein (TC 3.A.1.3.2)	s02:222908-222123	66	67	63	56	69
hypothetical protein	s02:223408-223112	24	24	4	20	23
hypothetical protein	s02:223877-224335	1	17	21	6	12
Flagellin protein FlaA	s02:248965-247733	225	27	37	32	32
flagellar protein	s02:258125-257724	6	10	5	3	13
Glucose-6-phosphate isomerase (EC 5.3.1.9)	s02:269057-267618	2	6	9	9	10
UTP--glucose-1-phosphate uridylyltransferase (EC 2.7.7.9)	s02:269994-269080	9	42	15	23	24
Phosphomannomutase (EC 5.4.2.8)	s02:271378-270017	21	22	27	27	32
hypothetical protein	s02:273620-272817	2	16	4	6	7
UDP-glucose dehydrogenase (EC 1.1.1.22)	s02:283454-282138	7	10	9	8	11
Capsule assembly protein	s02:285136-283595	57	53	79	41	51
[Citrate [pro-3S]-lyase] ligase (EC 6.2.1.22)	s02:313942-312386	1	11	11	8	9

dTDP-glucose 4,6-dehydratase (EC 4.2.1.46)	s02:322930-321848	2	4	7	11	8
Glucose-1-phosphate cytidylyltransferase (EC 2.7.7.33)	s02:323728-322952	1	12	3	21	13
UDP-glucose 4-epimerase (EC 5.1.3.2)	s02:328581-327601	0	12	12	0	0
Tyrosine-protein kinase transmembrane modulator EpsC	s02:334025-332565	1	2	14	6	5
Xaa-Pro aminopeptidase (EC 3.4.11.9)	s02:33973-32792	2	8	10	7	10
Glycosyltransferase	s02:342904-341807	8	11	13	10	16
hypothetical protein	s02:351578-350649	4	23	6	8	18
S-layer domain protein domain protein	s02:352959-351700	943	1243	1179	1273	1575
S-layer domain protein domain protein	s02:354555-353281	929	1104	1307	928	958
S-layer domain protein domain protein	s02:356218-354938	312	317	340	342	387
2-Keto-3-deoxy-D-manno-octulosonate-8-phosphate synthase (EC 2.5.1.55)	s02:366394-365570	3	25	3	12	6
Lipid A export ATP-binding/permease protein MsbA	s02:371408-369684	0	3	2	5	10
general stress protein, putative	s02:37449-37150	28	40	9	33	37
Outer membrane protein H precursor	s02:382670-382251	24	47	17	42	48
outer membrane chaperone Skp (OmpH)	s02:384311-383790	10	24	15	8	39
Outer membrane protein/protective antigen OMA87	s02:387417-385696	37	38	54	52	44
Protein of unknown function DUF490	s02:393156-388825	21	21	20	32	15
Outer membrane protein	s02:394667-393312	46	45	38	38	39
FIG01197338: hypothetical protein	s02:399685-397883	19	14	7	19	12
MreB-like protein (Mbl protein)	s02:407392-406364	28	31	30	43	47
ATP synthase epsilon chain (EC 3.6.3.14)	s02:411971-411558	9	44	25	26	33
Rubrerythrin	s02:4122-3580	5	5	5	6	13
ATP synthase beta chain (EC 3.6.3.14)	s02:413384-411975	341	494	549	378	441
ATP synthase gamma chain (EC 3.6.3.14)	s02:414268-413417	38	71	30	35	39
ATP synthase alpha chain (EC 3.6.3.14)	s02:415798-414275	136	163	165	124	170
ATP synthase delta chain (EC 3.6.3.14)	s02:416435-415881	16	33	26	27	28
ATP synthase F0 sector subunit b	s02:416932-416429	29	114	61	59	87
UDP-N-acetylglucosamine 2-epimerase (EC 5.1.3.14)	s02:420025-418859	14	12	8	13	23
Uracil phosphoribosyltransferase (EC 2.4.2.9)	s02:423147-422521	8	8	6	22	13
Serine hydroxymethyltransferase (EC 2.1.2.1)	s02:424402-423167	21	15	14	16	25
Ribose 5-phosphate isomerase B (EC 5.3.1.6)	s02:425452-425009	8	10	4	16	19
LSU ribosomal protein L31p @ LSU ribosomal protein L31p, zinc-dependent	s02:430946-430737	7	11	1	20	14
Zn-dependent peptidase, insulinase family	s02:441965-439032	50	59	57	57	38
Amino acid ABC transporter, amino acid-binding protein	s02:454960-454196	24	52	17	44	60
Peptidyl-prolyl cis-trans isomerase (EC 5.2.1.8)	s02:457495-456881	10	9	9	11	9

Predicted function	Genome reference	H_2CO_2	MeOH	NO_3^-	B	F
Putative metal chaperone, involved in Zn homeostasis, GTPase of COG0523 family	s02:47458-46865	0	20	17	0	3
Radical SAM domain heme biosynthesis protein	s02:479113-477935	6	9	3	18	9
5-methyltetrahydrofolate-homocysteine methyltransferase (EC 2.1.1.13)	s02:48497-47700	5	317	110	0	2
Methyl-accepting chemotaxis protein	s02:485682-487370	18	10	13	11	12
Nitrogen regulatory protein P-II	s02:491329-490991	11	6	2	4	5
YadA-like Haemagluttinin	s02:492939-491689	84	184	166	77	59
Methanol:corrinoid methyltransferase	s02:49951-48572	49	996	848	21	26
Corrinoid methyltransferase protein	s02:50613-49981	35	631	527	9	20
TRAP-type C4-dicarboxylate transport system, periplasmic component	s02:506988-505948	8	6	4	10	12
UPF0251 protein CTC-01373	s02:516229-515843	0	2	2	13	3
Methyl-accepting chemotaxis protein	s02:537971-540001	6	9	10	4	6
Methyl-accepting chemotaxis protein	s02:542361-544403	8	9	10	6	8
probable electron transfer protein	s02:54730-52898	37	122	106	55	75
Methyl-accepting chemotaxis protein	s02:548036-549727	10	14	18	6	15
Rubrerythrin	s02:556070-556654	28	61	33	61	57
GTP-sensing transcriptional pleiotropic repressor codY	s02:56452-55673	4	49	11	36	38
Uncharacterized protein aq-372	s02:569060-567645	6	10	4	4	3
Phosphate ABC transporter, periplasmic phosphate-binding protein PstS (TC 3.A.1.7.1)	s02:576083-575184	35	56	20	63	33
Pyridoxine biosynthesis glutamine amidotransferase, synthase subunit (EC 2.4.2.-)	s02:580088-580966	15	20	32	23	18
Methyl-accepting chemotaxis protein	s02:585177-586235	33	91	56	56	113
Ribonuclease J2 (endoribonuclease in RNA processing)	s02:590734-589073	13	19	30	19	29
Glutamate synthase [NADPH] large chain (EC 1.4.1.13)	s02:600207-598576	36	167	179	62	90
Nicotinate-nucleotide--dimethylbenzimidazole phosphoribosyltransferase (EC 2.4.2.21)	s02:603570-602518	3	66	28	89	1
Nicotinate-nucleotide--dimethylbenzimidazole phosphoribosyltransferase (EC 2.4.2.21)	s02:604762-603563	3	43	29	60	2
Branched-chain amino acid ABC transporter, amino acid-binding protein (TC 3.A.1.4.1)	s02:606224-605010	76	61	93	82	81
Tricarboxylate transport protein TctC	s02:607578-606601	16	18	24	21	2
Tricarboxylate transport protein TctC	s02:608760-607735	14	15	22	19	2
Anti-sigma F factor antagonist (spoIIAA-2); Anti-sigma B factor antagonist RsbV	s02:625005-624679	18	14	6	30	19
TonB-dependent receptor; Outer membrane receptor for ferrienterochelin and colicins	s02:626674-628617	0	3	14	0	0
Outer membrane vitamin B12 receptor BtuB	s02:630139-632250	6	13	23	0	2

ABC-type probable sulfate transporter, periplasmic binding protein	s02:641948-640992	10	28	6	17	18
Acetylornithine aminotransferase (EC 2.6.1.11)	s02:660887-659685	2	2	14	0	0
Myosin heavy chain	s02:667244-667765	3	14	13	3	3
Zinc finger domain	s02:6885-7199	16	11	6	21	30
Anaerobic dehydrogenases, typically selenocysteine-containing	s02:707446-705302	0	0	0	11	0
Acetolactate synthase small subunit (EC 2.2.1.6)	s02:728450-727953	8	21	33	20	29
Acetolactate synthase large subunit (EC 2.2.1.6)	s02:730147-728450	33	73	43	59	45
Molybdenum ABC transporter, periplasmic molybdenum-binding protein ModA (TC 3.A.1.8.1)	s02:733280-732468	24	69	44	21	49
DUF124 domain-containing protein	s02:737066-737908	12	33	17	31	24
Carboxynorspermidine dehydrogenase, putative (EC 1.1.1.-)	s02:740982-739732	4	10	4	5	14
Thiazole biosynthesis protein ThiG	s02:749564-748797	9	36	19	26	21
Branched-chain amino acid ABC transporter, amino acid-binding protein (TC 3.A.1.4.1)	s02:757341-756208	43	63	63	53	17
Creatinine amidohydrolase (EC 3.5.2.10)	s02:758164-757394	2	14	0	5	3
sporulation kinase	s02:759676-758282	4	11	17	12	4
Multimeric flavodoxin WrbA family protein	s02:778105-777476	5	31	12	18	20
Rubrerythrin	s02:801617-802165	40	41	41	43	65
4-hydroxy-tetrahydrodipicolinate synthase (EC 4.3.3.7)	s02:805984-805103	17	38	25	29	34
Methyl-accepting chemotaxis protein	s02:812535-811060	16	34	28	27	33
Hydroxyethylthiazole kinase (EC 2.7.1.50)	s02:819543-818731	6	17	4	15	14
Adenylosuccinate lyase (EC 4.3.2.2)	s02:843336-844694	8	16	20	12	14
Serine protease, DegP/HtrA, do-like (EC 3.4.21.-)	s02:863004-861883	14	17	18	8	12
Dipeptide-binding ABC transporter, periplasmic substrate-binding component (TC 3.A.1.5.2)	s02:86502-84886	14	13	19	14	12
Deoxyribose-phosphate aldolase (EC 4.1.2.4)	s02:869887-869219	22	13	4	16	17
Ferric uptake regulation protein FUR	s02:870403-869972	0	6	2	1	11
Transcription accessory protein (S1 RNA-binding domain)	s02:876478-878652	8	9	10	2	5
Glutamate-1-semialdehyde aminotransferase (EC 5.4.3.8)	s02:886921-885608	9	10	13	7	18
Porphobilinogen synthase (EC 4.2.1.24)	s02:887909-886944	18	12	2	6	14
Uroporphyrinogen-III methyltransferase (EC 2.1.1.107) / Uroporphyrinogen-III synthase (EC 4.2.1.75)	s02:889429-887912	10	21	20	24	26
Aspartate aminotransferase (EC 2.6.1.1)	s02:901987-900815	5	3	2	13	9
Urea carboxylase-related ABC transporter, periplasmic substrate-binding protein	s02:904695-903682	23	23	18	28	37
NAD-dependent formate dehydrogenase alpha	s02:917157-914470	24	22	15	19	16

Predicted function	Genome reference	H_2CO_2	MeOH	NO_3^-	B	F
Methyl-accepting chemotaxis protein	s02:946776-944728	7	11	10	16	7
Periplasmic [Fe] hydrogenase large subunit (EC 1.12.7.2)	s02:950720-948975	6	5	5	24	11
NAD-dependent formate dehydrogenase beta subunit	s02:952024-950723	0	0	0	18	0
Betaine reductase component B beta subunit (EC 1.21.4.4) @ selenocysteine-containing	s02:955063-953744	20	97	34	634	33
Betaine reductase component B alpha subunit (EC 1.21.4.4)	s02:956398-955076	29	95	41	749	46
Glycine/sarcosine/betaine reductase component C chain 2	s02:959004-957838	5	17	4	218	18
Glycine/sarcosine/betaine reductase component C chain 1	s02:960547-959009	21	85	48	612	46
Glycine/sarcosine/betaine reductase protein A @ selenocysteine-containing	s02:961292-960882	4	4	3	18	0
Selenocysteine-specific translation elongation factor	s02:964433-962559	0	0	0	15	0
Selenide,water dikinase (EC 2.7.9.3) @ selenocysteine-containing	s02:965472-964441	0	0	0	10	0
Glycine/sarcosine/betaine reductase component C chain 2	s02:969321-968155	1	3	9	67	5
Glycine/sarcosine/betaine reductase component C chain 1	s02:970864-969326	6	24	37	291	12
Glycine/sarcosine/betaine reductase protein A @ selenocysteine-containing	s02:971558-971070	4	2	3	20	0
Thioredoxin	s02:971933-971616	7	2	0	64	2
Thioredoxin reductase (EC 1.8.1.9)	s02:972899-971970	1	5	1	92	0
FIG042921: similarity to aminoacyl-tRNA editing enzymes YbaK, ProX	s02:976015-975497	0	0	3	25	1
N-methylhydantoinase (ATP-hydrolyzing) (EC 3.5.2.14)	s02:978241-976232	0	0	6	130	3
Trimethylamine:corrinoid methyltransferase @ pyrrolysine-containing	s02:979643-978258	32	0	78	505	11
Trimethylamine:corrinoid methyltransferase @ pyrrolysine-containing	s02:981223-979757	37	7	108	474	25
5-methyltetrahydrofolate--homocysteine methyltransferase (EC 2.1.1.13)	s02:981887-981255	13	2	44	239	4
Glycine reductase component B gamma subunit (EC 1.21.4.2) @ selenocysteine-containing	s02:983278-981968	12	0	48	337	13
Glycine reductase component B beta subunit (EC 1.21.4.2) / Glycine reductase component B alpha subunit (EC 1.21.4.2)	s02:984589-983303	5	0	11	105	0
5-methyltetrahydrofolate--homocysteine methyltransferase (EC 2.1.1.13)	s02:987110-986313	5	0	3	160	4

Methyl-accepting chemotaxis protein	s02:991410-989347	56	116	112	52	37
Signal transduction histidine kinase CheA (EC 2.7.3.-)	s03:105473-102753	3	6	10	6	4
Methyl-accepting chemotaxis protein	s03:107711-105504	16	13	30	12	9
Acetolactate synthase large subunit (EC 2.2.1.6)	s03:114332-112662	3	14	17	15	13
3-isopropylmalate dehydrogenase (EC 1.1.1.85)	s03:115417-114344	11	16	11	19	22
3-isopropylmalate dehydratase large subunit (EC 4.2.1.33)	s03:117252-115987	2	8	10	20	15
2-isopropylmalate synthase (EC 2.3.3.13)	s03:118801-117245	4	12	22	10	14
Ketol-acid reductoisomerase (EC 1.1.1.86)	s03:119826-118834	50	58	46	89	95
Amino acid-binding ACT	s03:121415-120963	2	13	2	8	15
Phenylacetate-coenzyme A ligase (EC 6.2.1.30)	s03:122750-121446	16	6	13	16	23
FIG000557: hypothetical protein co-occurring with RecR	s03:127014-126688	24	15	13	23	15
Ferrous iron transport protein B	s03:134585-132210	190	362	418	255	285
Methyl-accepting chemotaxis protein	s03:154427-155485	59	172	115	123	212
Positive regulator of CheA protein activity (CheW)	s03:155512-156000	2	27	22	8	31
hypothetical protein	s03:175119-175535	2	7	0	5	11
NADPH-dependent FMN reductase	s03:193021-193575	11	19	9	8	11
Nitrogen regulatory protein P-II	s03:19681-19355	10	0	0	0	1
hypothetical protein	s03:215434-214682	4	6	3	12	4
FIG00241420: hypothetical protein	s03:233266-235380	24	30	46	32	41
Outer membrane vitamin B12 receptor BtuB	s03:258598-256649	12	10	27	0	1
Zinc ABC transporter, periplasmic-binding protein ZnuA	s03:271223-272146	77	107	60	88	40
NAD-dependent 4-hydroxybutyrate dehydrogenase (EC 1.1.1.61)	s03:283278-282160	5	7	10	7	8
RND efflux system, inner membrane transporter CmeB	s03:31039-27905	12	22	20	24	23
hypothetical protein	s03:312500-310503	6	4	13	0	3
RND efflux system, membrane fusion protein CmeA	s03:32188-31052	15	27	21	19	32
Single-stranded DNA-binding protein	s03:349362-348967	9	10	10	13	21
two component transcriptional regulator, Fis family	s03:374725-372812	12	4	9	13	5
Methyl-accepting chemotaxis protein	s03:376738-374942	27	33	51	39	22
Indolepyruvate oxidoreductase subunit IorB (EC 1.2.7.8)	s03:387822-387253	12	22	17	18	22
Indolepyruvate oxidoreductase subunit IorA (EC 1.2.7.8)	s03:389603-387822	66	63	54	61	103
Lead, cadmium, zinc and mercury transporting ATPase (EC 3.6.3.3) (EC 3.6.3.5); Copper-translocating P-type ATPase (EC 3.6.3.4)	s03:390679-393411	0	0	1	4	12

Predicted function	Genome reference	H_2CO_2	MeOH	NO_3^-	B	F
Pyruvate-flavodoxin oxidoreductase (EC 1.2.7.-)	s03:397688-394182	147	263	134	196	147
Threonine dehydratase (EC 4.3.1.19)	s03:398976-397768	8	14	8	8	4
TRAP transporter solute receptor, unknown substrate 1	s03:40267-39299	150	154	109	114	127
Bipolar DNA helicase HerA	s03:450319-448067	9	23	10	3	2
FIG036446: hypothetical protein	s03:451710-450316	5	14	13	4	6
Nitrogen regulatory protein P-II	s03:50524-50895	67	43	22	25	67
Ferrous iron transport protein B	s03:52959-51112	3	1	4	11	5
Cobalt-precorrin-2 C20-methyltransferase (EC 2.1.1.130)	s03:56963-56241	1	10	6	8	6
Seryl-tRNA synthetase (EC 6.1.1.11)	s03:68813-67545	17	13	17	11	30
Uracil-DNA glycosylase, family 4	s03:69290-69961	0	4	8	11	6
Nucleoside-diphosphate-sugar epimerases	s03:71895-70888	17	26	14	22	18
TPR domain protein, putative component of TonB system	s03:72986-71910	30	31	15	25	31
Phosphoserine aminotransferase (EC 2.6.1.52)	s03:74395-73298	14	8	6	6	8
Mll1230 protein	s03:82561-81161	0	0	0	11	0
Phosphoenolpyruvate-protein phosphotransferase of PTS system (EC 2.7.3.9)	s03:92519-90783	11	24	33	25	262
PTS system, fructose-specific IIA component	s03:93272-92820	1	7	1	4	28
PTS system, fructose-specific IIB component (EC 2.7.1.69) / PTS system, fructose-specific IIC component (EC 2.7.1.69)	s03:94704-93331	2	6	2	1	24
1-phosphofructokinase (EC 2.7.1.56)	s03:95679-94741	0	0	0	0	9
Transcriptional repressor of the fructose operon, DeoR family	s03:96462-95692	0	1	0	0	16
hypothetical protein	s04:107497-106766	8	23	8	15	44
Molybdenum ABC transporter, periplasmic molybdenum-binding protein ModA (TC 3.A.1.8.1)	s04:108246-109037	4	14	3	4	11
NADP-dependent malic enzyme (EC 1.1.1.40)	s04:11423-12652	30	17	19	25	6
Conserved protein	s04:116925-117278	45	14	13	34	35
Fumarate hydratase class I, aerobic (EC 4.2.1.2); L(+)-tartrate dehydratase alpha subunit (EC 4.2.1.32)	s04:12666-13511	26	47	23	34	15
hypothetical protein	s04:135080-136132	17	23	27	32	19
Fumarate hydratase class I, aerobic (EC 4.2.1.2); L(+)-tartrate dehydratase beta subunit (EC 4.2.1.32)	s04:13525-14088	15	19	9	12	6
Probable non-ribosomal peptide synthetase	s04:136162-138246	7	15	13	0	1
Flavodoxin	s04:139586-140014	36	24	34	32	27
S-layer protein, putative	s04:171778-173058	251	321	311	247	311
Methylaspartate mutase, S subunit (EC 5.4.99.1)	s04:1750-2160	9	21	9	12	3

DNA topoisomerase III (EC 5.99.1.2)	s04:179137-181326	3	4	3	2	15
2-(5"-triphosphoribosyl)-3'-dephosphocoenzyme-A synthase (EC 2.7.8.25)	s04:183957-185357	0	2	12	6	1
ABC transporter ATP-binding protein uup	s04:185409-187028	3	3	6	16	11
Pyridine nucleotide-disulfide oxidoreductase; NADH dehydrogenase (EC 1.6.99.3)	s04:196598-198280	9	20	14	14	22
Cytosolic Fe-S cluster assembling factor NBP35	s04:203848-202634	63	55	34	80	97
Uncharacterized protein MJ0282	s04:207242-207631	1	49	8	13	25
Molybdenum ABC transporter ATP-binding protein	s04:207938-208690	4	11	5	15	9
METHYLASPARTATE MUTASE (EC 5.4.99.1)	s04:2176-3558	2	27	15	11	0
Iron-sulfur cluster assembly ATPase protein SufC	s04:220622-221389	3	13	5	16	25
Iron-sulfur cluster assembly protein SufB	s04:221386-222615	26	27	26	32	47
Cell division trigger factor (EC 5.2.1.8)	s04:225901-227190	56	120	126	186	187
ATP-dependent Clp protease proteolytic subunit (EC 3.4.21.92)	s04:227215-227820	15	24	29	31	28
ATP-dependent Clp protease ATP-binding subunit ClpX	s04:227833-229095	5	17	26	19	41
ATP-dependent protease La (EC 3.4.21.53) Type I	s04:231074-233392	32	135	94	118	121
UbiD family decarboxylase associated with menaquinone via futalosine	s04:241281-242741	2	4	3	4	14
Methenyltetrahydrofolate cyclohydrolase (EC 3.5.4.9)	s04:243851-244483	102	118	41	51	86
Branched-chain amino acid ABC transporter, amino acid-binding protein (TC 3.A.1.4.1)	s04:24439-25563	18	9	14	10	11
Methylenetetrahydrofolate dehydrogenase (NADP+) (EC 1.5.1.5)	s04:244496-245359	79	128	40	67	100
CO dehydrogenase accessory protein CooC (nickel insertion)	s04:246171-246959	1	16	3	8	13
Formate--tetrahydrofolate ligase (EC 6.3.4.3)	s04:246990-248750	2053	1769	971	944	1337
Carbon monoxide dehydrogenase CooS subunit (EC 1.2.99.2)	s04:248953-250890	718	619	232	278	353
CO dehydrogenase/acetyl-CoA synthase, acetyl-CoA synthase subunit (EC 2.3.1.169)	s04:250966-253092	564	713	252	226	307
Acetyl-CoA synthase corrinoid iron-sulfur protein, large subunit	s04:253218-254561	673	779	635	476	819
Acetyl-CoA synthase corrinoid activation protein	s04:254634-256604	130	153	77	50	71
CO dehydrogenase accessory protein CooC (nickel insertion)	s04:256651-257406	28	57	10	43	77
Acetyl-CoA synthase corrinoid iron-sulfur protein, small subunit	s04:257428-258396	312	284	173	208	323
5-methyltetrahydrofolate:corrinoid iron-sulfur protein methyltransferase	s04:258478-259269	170	196	94	139	209
CoB--CoM heterodisulfide reductase subunit C (EC 1.8.98.1)	s04:259305-259895	30	38	31	14	42

Predicted function	Genome reference	H_2CO_2	MeOH	NO_3^-	B	F
CoB--CoM heterodisulfide reductase subunit B (EC 1.8.98.1)	s04:259892-260755	59	59	19	26	40
heterodisulfide reductase, subunit A/ methylviologen reducing hydrogenase, subunit delta	s04:260877-263705	291	312	181	116	210
CoB--CoM-reducing hydrogenase (Sec) delta subunit @ selenocysteine-containing	s04:263708-264115	36	36	6	21	38
Zinc-finger protein	s04:264137-264805	64	81	46	34	76
5,10-methylenetetrahydrofolate reductase (EC 1.5.1.20)	s04:264802-265755	112	120	53	63	107
NAD-dependent formate dehydrogenase gamma subunit	s04:265929-266465	35	36	40	24	52
NAD-reducing hydrogenase subunit HoxF (EC 1.12.1.2)	s04:266455-268209	235	224	186	148	275
Formate dehydrogenase-O, major subunit (EC 1.2.1.2)	s04:268226-271744	756	751	574	501	749
NAD-dependent formate dehydrogenase alpha subunit @ selenocysteine-containing	s04:280505-277827	489	508	366	270	555
Valyl-tRNA synthetase (EC 6.1.1.9)	s04:281018-283678	17	16	21	29	28
Dihydrofolate synthase (EC 6.3.2.12) @ Folylpolyglutamate synthase (EC 6.3.2.17)	s04:283715-284998	10	11	9	9	17
NADH-ubiquinone oxidoreductase chain E (EC 1.6.5.3)	s04:289988-290497	4	39	23	16	66
NADP-reducing hydrogenase, subunit B	s04:291058-291423	36	37	7	34	105
NAD-reducing hydrogenase subunit HoxF (EC 1.12.1.2)	s04:291452-293242	374	500	317	265	780
Periplasmic [Fe] hydrogenase large subunit (EC 1.12.7.2)	s04:293308-295035	218	242	156	119	504
Methylmalonyl-CoA mutase (EC 5.4.99.2)	s04:296327-297982	33	50	44	53	48
B12 binding domain of Methylmalonyl-CoA mutase (EC 5.4.99.2)	s04:298000-298395	15	4	0	27	11
Methylmalonyl-CoA epimerase (EC 5.1.99.1)	s04:299476-299919	1	22	8	17	17
Acetyl-coenzyme A carboxyl transferase alpha chain (EC 6.4.1.2) / Acetyl-coenzyme A carboxyl transferase beta chain (EC 6.4.1.2); Propionyl-CoA carboxylase beta chain (EC 6.4.1.3)	s04:299947-301476	24	39	25	54	52
Biotin carboxyl carrier protein of oxaloacetate decarboxylase; Biotin carboxyl carrier protein	s04:301832-302227	6	25	15	22	22
Sigma factor RpoE regulatory protein RseC	s04:302995-303414	10	8	1	8	4
Electron transport complex protein RnfC	s04:303464-304789	103	166	117	69	134
Electron transport complex protein RnfD	s04:304802-305776	2	29	6	17	16
Electron transport complex protein RnfG	s04:305783-306352	20	32	20	15	30
Electron transport complex protein RnfE	s04:306364-307032	9	20	12	13	18
Electron transport complex protein RnfB	s04:307638-308492	55	97	72	48	69

Rod shape-determining protein MreB	s04:311288-312322	27	25	22	21	43
CO dehydrogenase/acetyl-CoA synthase, acetyl-CoA synthase subunit (EC 2.3.1.169)	s04:31610-32719	246	270	99	99	117
Septum site-determining protein MinD	s04:316515-317306	2	28	11	31	32
Cell division topological specificity factor MinE	s04:317333-317608	6	6	4	10	7
LSU ribosomal protein L21p	s04:325212-325523	13	13	4	18	25
LSU ribosomal protein L27p	s04:325861-326169	19	8	4	29	24
Gamma-glutamyl phosphate reductase (EC 1.2.1.41)	s04:329537-330793	14	13	18	11	14
Ribosomal silencing factor RsfA (former lojap)	s04:333855-334208	10	7	8	15	15
Carbon monoxide oxidation accessory protein CoxE	s04:343108-344484	10	8	10	13	12
Methyl-accepting chemotaxis protein	s04:34486-36183	48	137	134	90	110
Methylaspartate mutase, E subunit (EC 5.4.99.1)	s04:3581-5032	104	291	137	111	17
Endoribonuclease L-PSP	s04:359633-360013	5	4	0	15	8
Tungsten-containing aldehyde:ferredoxin oxidoreductase (EC 1.2.7.5)	s04:36804-38519	948	929	898	774	917
Leucyl-tRNA synthetase (EC 6.1.1.4)	s04:373060-375540	53	50	53	72	63
Thioredoxin	s04:375577-375894	10	1	0	8	7
Radical SAM domain heme biosynthesis protein	s04:377668-378660	4	12	0	10	9
Uptake hydrogenase small subunit precursor (EC 1.12.99.6)	s04:378765-379895	11	42	17	18	27
Uptake hydrogenase large subunit (EC 1.12.99.6)	s04:379918-381810	70	94	93	72	75
Ni,Fe-hydrogenase I cytochrome b subunit	s04:381830-382552	2	19	13	7	13
Sulfur carrier protein adenylyltransferase ThiF	s04:38599-40029	18	16	19	11	14
hypothetical protein BVU-3741	s04:399144-402872	21	34	29	23	23
Tungsten-containing aldehyde:ferredoxin oxidoreductase (EC 1.2.7.5)	s04:41740-43479	1028	1004	968	845	995
Tungsten-containing aldehyde:ferredoxin oxidoreductase (EC 1.2.7.5)	s04:43576-43947	121	96	139	100	134
Alcohol dehydrogenase (EC 1.1.1.1)	s04:46856-48016	834	270	734	538	1025
Molybdopterin biosynthesis protein MoeA / Periplasmic molybdate-binding domain	s04:49967-51907	13	5	13	7	18
Methylaspartate ammonia-lyase (EC 4.3.1.2)	s04:5139-6383	66	140	75	109	17
L-lactate permease	s04:71947-70292	33	22	20	19	6
Glycolate dehydrogenase (EC 1.1.99.14), subunit GlcD	s04:73372-74754	189	159	78	160	19
Glycolate dehydrogenase (EC 1.1.99.14), iron-sulfur subunit GlcF	s04:74757-76067	99	91	47	78	13
Citrate lyase beta chain (EC 4.1.3.6)	s04:7696-8574	33	68	29	28	5
Pyruvate-flavodoxin oxidoreductase (EC 1.2.7.-)	s04:77617-81120	733	1191	656	839	523
Alanine dehydrogenase (EC 1.4.1.1)	s04:83184-84299	860	1465	1034	417	433
D-serine/D-alanine/glycine transporter	s04:84414-85811	17	49	20	9	3

Predicted function	Genome reference	H_2CO_2	MeOH	NO_3^-	B	F
Citrate lyase alpha chain (EC 4.1.3.6)	s04:8567-10114	20	37	27	11	2
flotillin 1	s05:113675-115177	15	37	32	36	18
L,L-diaminopimelate aminotransferase (EC 2.6.1.83)	s05:11452-12684	29	49	47	79	51
Vitamin B12 ABC transporter, B12-binding component BtuF	s05:124108-125160	8	10	5	0	6
ABC transporter, ATP-binding protein	s05:126930-127493	0	3	11	0	0
Flavodoxin	s05:127991-128512	51	64	61	26	46
Radical SAM family protein HutW, similar to coproporphyrinogen III oxidase, oxygen-independent, associated with heme uptake	s05:128509-129939	16	23	51	6	21
TonB-dependent receptor; Outer membrane receptor for ferrienterochelin and colicins	s05:131194-133122	133	126	353	48	9
conserved hypothetical protein	s05:141438-140935	13	18	17	15	20
Nitrogen regulatory protein P-II	s05:143355-142990	24	1	0	0	8
Dimethylamine:corrinoid methyltransferase; pyrrolysine-containing	s05:146411-145011	15	0	0	0	4
5-methyltetrahydrofolate--homocysteine methyltransferase (EC 2.1.1.13)	s05:147091-146441	19	0	0	0	15
Nitrogen regulatory protein P-II	s05:147521-147153	31	0	1	0	9
5-methyltetrahydrofolate--homocysteine methyltransferase (EC 2.1.1.13)	s05:151396-152055	51	1	2	3	27
Monomethylamine:corrinoid methyltransferase; pyrrolysine-containing	s05:152061-153452	39	0	0	1	16
Signal peptidase-like protein	s05:182112-182924	1	10	2	14	19
Methionyl-tRNA synthetase (EC 6.1.1.10)	s05:185101-187038	21	33	32	21	24
Positive regulator of CheA protein activity (CheW)	s05:205303-205785	0	5	24	1	6
Predicted regulator PutR for proline utilization, GntR family	s05:206652-207335	5	6	9	11	12
N-acetylglucosamine-1-phosphate uridyltransferase (EC 2.7.7.23) / Glucosamine-1-phosphate N-acetyltransferase (EC 2.3.1.157)	s05:209269-210642	16	11	4	5	11
Ribose-phosphate pyrophosphokinase (EC 2.7.6.1)	s05:210643-211590	15	27	4	33	32
Biotin carboxylase of acetyl-CoA carboxylase (EC 6.3.4.14)	s05:217119-215794	46	35	39	28	59
universal stress family protein	s05:233077-233547	12	45	29	12	15
Ferredoxin 3 fused to uncharacterized domain	s05:233730-234440	14	17	23	23	11
D-3-phosphoglycerate dehydrogenase (EC 1.1.1.95)	s05:239089-240669	100	66	77	54	81
2-oxoglutarate oxidoreductase, alpha subunit (EC 1.2.7.3)	s05:244841-245971	24	18	21	24	39
2-oxoglutarate oxidoreductase, beta subunit (EC 1.2.7.3)	s05:245985-246803	8	15	2	10	13

2-oxoglutarate oxidoreductase, gamma subunit (EC 1.2.7.3)	s05:246806-247327	12	16	10	14	25
Methyl-accepting chemotaxis protein	s05:251099-250251	16	21	16	15	13
Phosphoribosylformylglycinamidine synthase, synthetase subunit (EC 6.3.5.3) / Phosphoribosylformylglycinamidine synthase, glutamine amidotransferase subunit (EC 6.3.5.3)	s05:255137-258919	122	136	116	117	153
Arginyl-tRNA synthetase (EC 6.1.1.19)	s05:266707-268374	6	15	13	16	21
DNA-directed RNA polymerase delta subunit (EC 2.7.7.6)	s05:268473-268892	5	4	3	3	10
CTP synthase (EC 6.3.4.2)	s05:268997-270610	15	23	24	43	34
Transaldolase (EC 2.2.1.2)	s05:275469-276113	8	7	4	9	10
ClpB protein	s05:27556-24971	113	132	120	103	60
Fructose-1,6-bisphosphatase, GlpX type (EC 3.1.3.11)	s05:276215-277180	23	39	34	49	69
2',3'-cyclic-nucleotide 2'-phosphodiesterase (EC 3.1.4.16)	s05:279231-278527	9	13	3	14	12
Nucleoside triphosphate pyrophosphohydrolase MazG (EC 3.6.1.8)	s05:286306-287775	1	3	4	5	12
DNA-binding protein HBsu	s05:287870-288145	21	16	6	23	18
Methyl-accepting chemotaxis protein	s05:291591-293624	44	28	25	18	28
Lysine-arginine-ornithine-binding periplasmic protein precursor (TC 3.A.1.3.1)	s05:295844-296620	0	14	5	2	8
Phosphate ABC transporter, periplasmic phosphate-binding protein PstS (TC 3.A.1.7.1)	s05:302546-303409	0	11	0	12	0
Adenylate cyclase (EC 4.6.1.1)	s05:306947-305349	7	10	5	6	6
RNA binding protein, contains ribosomal protein S1 domain	s05:311885-312334	9	10	10	12	12
Hypoxanthine-guanine phosphoribosyltransferase (EC 2.4.2.8)	s05:319636-320187	11	12	7	22	22
Cell division protein FtsH (EC 3.4.24.-)	s05:320298-322217	44	36	36	33	39
Transcription elongation factor GreA	s05:331498-331977	4	10	7	12	19
Lysyl-tRNA synthetase (class II) (EC 6.1.1.6)	s05:332010-333512	27	18	26	39	34
Glutamine ABC transporter, periplasmic glutamine-binding protein (TC 3.A.1.3.2)	s05:33379-34149	4	24	4	20	33
Exonuclease SbcC	s05:3518-6730	6	1	0	1	12
ATP-dependent nuclease, subunit A	s05:37834-41589	7	7	11	14	18
Methionine ABC transporter ATP-binding protein	s05:506-1594	11	5	6	5	11
Sodium/glycine symporter GlyP	s05:53197-54588	1	9	15	9	20
Alanine dehydrogenase (EC 1.4.1.1)	s05:54690-55805	17	20	13	8	13
Glycogen phosphorylase (EC 2.4.1.1)	s05:69518-71959	7	18	16	9	14
Methyl-accepting chemotaxis protein	s05:76175-78154	10	16	17	5	12
Cytochrome d ubiquinol oxidase subunit I (EC 1.10.3.-)	s05:85259-86644	4	12	7	3	1

Predicted function	Genome reference	H_2CO_2	MeOH	NO_3^-	B	F
ATPase of the AAA+ family protein associated with FIG137771 hypothetical protein	s05:91489-93036	8	38	37	14	16
N-acetyl-gamma-glutamyl-phosphate reductase (EC 1.2.1.38)	s06:118305-119345	13	26	37	18	26
Glutamate N-acetyltransferase (EC 2.3.1.35) / N-acetylglutamate synthase (EC 2.3.1.1)	s06:119357-120568	3	9	16	22	8
Acetylglutamate kinase (EC 2.7.2.8)	s06:120602-121507	1	47	44	15	15
Acetylornithine aminotransferase (EC 2.6.1.11)	s06:121500-122690	10	22	29	15	17
Ornithine carbamoyltransferase (EC 2.1.3.3)	s06:122715-123647	3	20	34	16	13
Argininosuccinate synthase (EC 6.3.4.5)	s06:123741-124964	33	60	133	73	66
Argininosuccinate lyase (EC 4.3.2.1)	s06:124957-126372	2	2	25	5	6
Branched-chain amino acid aminotransferase (EC 2.6.1.42)	s06:126408-127481	7	11	10	9	37
NAD(FAD)-utilizing dehydrogenase, sll0175 homolog	s06:129468-131063	7	25	3	9	1
FIG00895125: hypothetical protein	s06:13024-12626	9	11	4	4	19
Glucosamine--fructose-6-phosphate aminotransferase [isomerizing] (EC 2.6.1.16)	s06:132935-134764	15	13	21	28	22
CO dehydrogenase/acetyl-CoA synthase, acetyl-CoA synthase subunit (EC 2.3.1.169)	s06:160691-162826	137	146	76	53	93
Glutamyl-tRNA synthetase (EC 6.1.1.17) @ Glutamyl-tRNA(Gln) synthetase (EC 6.1.1.24)	s06:16214-17674	15	23	21	25	30
Protein hypA	s06:167134-170052	22	32	37	32	20
Ferredoxin-type protein NapG (periplasmic nitrate reductase)	s06:196037-196582	2	5	29	10	0
Periplasmic nitrate reductase precursor (EC 1.7.99.4)	s06:197916-200177	0	0	170	0	0
Cytochrome c heme lyase subunit CcmF	s06:202990-205176	0	0	37	0	0
Radical SAM domain heme biosynthesis protein	s06:205231-206214	0	0	10	0	0
Cytochrome c nitrite reductase, small subunit NrfH	s06:206354-206827	0	0	24	0	0
Cytochrome c552 precursor (EC 1.7.2.2)	s06:206820-208109	5	1	177	3	2
Hydroxylamine reductase (EC 1.7.-.-)	s06:208981-210624	10	18	76	11	9
Isocitrate dehydrogenase [NAD] (EC 1.1.1.41)	s06:230517-229516	11	6	17	17	11
Aconitate hydratase (EC 4.2.1.3)	s06:232450-230522	31	12	115	39	52
Anaerobic sulfite reductase subunit A	s06:234586-235608	0	0	37	0	0
Anaerobic sulfite reductase subunit C (EC 1.8.1.-)	s06:236405-237367	0	0	10	0	0
hypothetical protein	s06:246844-247149	5	4	2	8	13
6-phosphofructokinase (EC 2.7.1.11)	s06:26275-27372	14	9	11	6	13
Glycolate dehydrogenase (EC 1.1.99.14), subunit GlcD	s06:276976-278370	3	11	5	11	14
Macrolide export ATP-binding/permease protein MacB (EC 3.6.3.-)	s06:286935-287639	5	11	1	5	13

Translation elongation factor Tu	s06:29973-31016	282	541	379	565	540
Translation elongation factor Tu	s06:31019-31156	30	15	18	30	37
Transcription antitermination protein NusG	s06:31908-32450	1	4	1	6	10
LSU ribosomal protein L11p (L12e)	s06:32466-32891	30	33	21	55	39
LSU ribosomal protein L1p (L10Ae)	s06:32960-33664	53	69	54	67	110
LSU ribosomal protein L10p (P0)	s06:33886-34416	28	34	25	53	52
LSU ribosomal protein L7/L12 (P1/P2)	s06:34495-34866	41	62	29	58	61
DNA-directed RNA polymerase beta subunit (EC 2.7.7.6)	s06:35260-39060	133	256	201	256	228
DNA-directed RNA polymerase beta' subunit (EC 2.7.7.6)	s06:39094-43062	199	273	213	303	282
SSU ribosomal protein S12p (S23e)	s06:44384-44767	9	7	8	18	18
SSU ribosomal protein S7p (S5e)	s06:44810-45280	38	78	49	87	123
Translation elongation factor G	s06:45389-47464	191	167	176	250	204
Translation elongation factor Tu	s06:47529-48731	313	556	397	596	577
SSU ribosomal protein S10p (S20e)	s06:48889-49200	37	24	5	51	40
LSU ribosomal protein L3p (L3e)	s06:49217-49858	41	57	47	106	109
LSU ribosomal protein L4p (L1e)	s06:49927-50550	28	53	54	66	79
LSU ribosomal protein L23p (L23Ae)	s06:50547-50837	15	5	1	20	19
LSU ribosomal protein L2p (L8e)	s06:50867-51712	27	52	36	73	92
SSU ribosomal protein S19p (S15e)	s06:51798-52079	12	16	10	22	31
LSU ribosomal protein L22p (L17e)	s06:52127-52459	17	27	8	36	42
SSU ribosomal protein S3p (S3e)	s06:52485-53159	22	37	34	83	82
LSU ribosomal protein L16p (L10e)	s06:53162-53638	60	66	53	73	107
SSU ribosomal protein S17p (S11e)	s06:53867-54127	24	22	15	33	36
LSU ribosomal protein L14p (L23e)	s06:54211-54579	18	27	13	48	51
LSU ribosomal protein L24p (L26e)	s06:54598-54936	17	36	30	35	44
LSU ribosomal protein L5p (L11e)	s06:54967-55509	46	50	53	80	94
SSU ribosomal protein S8p (S15Ae)	s06:55771-56169	30	54	38	58	126
LSU ribosomal protein L6p (L9e)	s06:56196-56747	29	41	28	48	56
LSU ribosomal protein L18p (L5e)	s06:56786-57154	6	16	19	17	27
SSU ribosomal protein S5p (S2e)	s06:57172-57672	37	35	36	46	45
ATP-dependent Clp protease, ATP-binding subunit ClpC / Negative regulator of genetic competence clcC/mecB	s06:5788-8247	129	193	84	120	131
LSU ribosomal protein L15p (L27Ae)	s06:57919-58359	28	28	32	36	43
Adenylate kinase (EC 2.7.4.3)	s06:59629-60282	46	37	22	67	59
LSU ribosomal protein L36p	s06:61660-61773	4	6	3	20	17
SSU ribosomal protein S13p (S18e)	s06:61795-62166	9	29	38	29	42
SSU ribosomal protein S11p (S14e)	s06:62182-62574	24	27	24	35	57
SSU ribosomal protein S4p (S9e)	s06:62599-63231	68	99	87	128	134
DNA-directed RNA polymerase alpha subunit	s06:63296-64255	13	31	31	53	53

Predicted function	Genome reference	H_2CO_2	MeOH	NO_3^-	B	F
LSU ribosomal protein L17p	s06:64271-64609	26	12	5	36	39
LSU ribosomal protein L13p (L13Ae)	s06:68077-68514	33	42	48	57	72
SSU ribosomal protein S9p (S16e)	s06:68538-68930	7	22	18	11	22
Rubrerythrin	s06:692-198	50	66	36	36	36
Archaeal/vacuolar-type H+-ATPase subunit H	s07:146548-147009	0	7	12	4	12
Acetate kinase (EC 2.7.2.1)	s07:150561-151763	160	175	116	193	195
3-oxoacyl-[acyl-carrier-protein] synthase, KASIII (EC 2.3.1.180)	s07:154384-155397	7	3	2	10	5
Malonyl CoA-acyl carrier protein transacylase (EC 2.3.1.39)	s07:156357-157301	8	16	2	8	6
3-oxoacyl-[acyl-carrier protein] reductase (EC 1.1.1.100)	s07:157303-158046	17	14	7	19	19
3-oxoacyl-[acyl-carrier-protein] synthase, KASII (EC 2.3.1.179)	s07:159441-160682	12	21	18	21	25
Signal recognition particle, subunit Ffh SRP54 (TC 3.A.5.1.1)	s07:167967-169307	4	14	17	10	20
SSU ribosomal protein S16p	s07:169353-169634	22	3	0	22	17
16S rRNA processing protein RimM	s07:169920-170336	14	40	23	32	48
LSU ribosomal protein L19p	s07:172308-172649	9	28	13	14	50
Branched-chain amino acid ABC transporter, amino acid-binding protein (TC 3.A.1.4.1)	s07:186570-188948	9	9	13	3	1
3-dehydroquinate synthase (EC 4.2.3.4)	s07:19211-20293	12	8	3	9	11
LemA family protein	s07:195649-196203	30	54	47	41	47
Nicotinate phosphoribosyltransferase (EC 2.4.2.11)	s07:198105-197053	12	12	7	7	9
Dihydropteroate synthase (EC 2.5.1.15)	s07:198228-199430	16	13	22	19	28
Dihydroneopterin aldolase (EC 4.1.2.25)	s07:199442-199810	8	7	0	12	14
DNA topoisomerase I (EC 5.99.1.2)	s07:202671-204869	5	6	12	6	7
ATP-dependent protease HslV (EC 3.4.25.-)	s07:207233-207763	2	13	22	4	12
ATP-dependent hsl protease ATP-binding subunit HslU	s07:207784-209181	2	45	37	37	44
GTP-sensing transcriptional pleiotropic repressor codY	s07:209216-209995	6	33	15	31	36
Flagellar M-ring protein FliF	s07:211661-213229	8	6	11	18	8
Flagellar hook protein FlgE	s07:221361-223289	32	13	9	12	4
flagellar basal body-associated protein FliL	s07:223630-224109	5	12	26	5	8
Chemotaxis regulator - transmits chemoreceptor signals to flagelllar motor components CheY	s07:226337-226699	27	4	1	32	10
Chemotaxis response regulator protein-glutamate methylesterase CheB (EC 3.1.1.61)	s07:235070-236119	16	11	6	17	12
Signal transduction histidine kinase CheA (EC 2.7.3.-)	s07:236150-238210	142	147	137	111	87

Positive regulator of CheA protein activity (CheW)	s07:238229-238693	1	13	18	4	6
Chemotaxis protein CheC -- inhibitor of MCP methylation	s07:238728-239348	4	11	7	6	7
Chemotaxis protein CheD	s07:239348-239833	0	4	10	2	8
protein of unknown function DUF342	s07:240996-242615	14	10	17	15	23
SSU ribosomal protein S2p (SAe)	s07:243641-244486	43	62	63	100	88
Translation elongation factor Ts	s07:244559-245206	90	76	81	124	131
Uridine monophosphate kinase (EC 2.7.4.22)	s07:245306-246040	16	16	18	24	25
Ribosome recycling factor	s07:246030-246590	17	23	3	15	13
1-hydroxy-2-methyl-2-(E)-butenyl 4-diphosphate synthase (EC 1.17.7.1)	s07:250962-252035	9	4	1	4	10
Prolyl-tRNA synthetase (EC 6.1.1.15), bacterial type	s07:252035-253750	25	15	41	40	44
Transcription termination protein NusA	s07:258935-260014	7	12	6	17	22
Translation initiation factor 2	s07:260618-263230	80	95	100	98	119
SSU ribosomal protein S15p (S13e)	s07:266593-266859	13	0	0	9	2
FIG099352: hypothetical protein	s07:26689-27897	1	2	4	4	10
Polyribonucleotide nucleotidyltransferase (EC 2.7.7.8)	s07:266993-269104	85	64	73	55	51
4-hydroxy-tetrahydrodipicolinate reductase (EC 1.17.1.8)	s07:276120-276914	0	4	0	1	10
Aspartate-semialdehyde dehydrogenase (EC 1.2.1.11)	s07:276983-278014	2	3	1	9	13
Ribonuclease J2 (endoribonuclease in RNA processing)	s07:280357-282021	16	14	21	20	28
GTP cyclohydrolase I (EC 3.5.4.16) type 2	s07:29262-30089	9	13	7	14	16
Cobalt-precorrin-6y C5-methyltransferase (EC 2.1.1.-)	s07:33013-33645	3	9	7	10	4
Cobalt-precorrin-4 C11-methyltransferase (EC 2.1.1.133)	s07:34264-35019	0	14	2	12	7
Cobalt-precorrin-3b C17-methyltransferase	s07:36084-36806	1	18	1	4	1
Cobalt-precorrin-8x methylmutase (EC 5.4.1.2)	s07:37602-38228	9	18	9	18	14
Cobyrinic acid A,C-diamide synthase	s07:38379-39776	2	16	11	7	4
Transition state regulatory protein AbrB	s07:3953-4201	4	4	1	3	10
Cobyric acid synthase (EC 6.3.5.10)	s07:40356-41888	11	61	27	28	22
Peptidyl-prolyl cis-trans isomerase (EC 5.2.1.8)	s07:50033-50464	0	9	6	6	17
Thioredoxin	s07:50933-51256	12	13	1	9	3
UDP-N-acetylmuramate--alanine ligase (EC 6.3.2.8)	s07:67571-68956	2	2	2	11	7
Cell division protein FtsZ (EC 3.4.24.-)	s07:74499-75545	21	22	17	23	30
FIG011856: hypothetical protein	s07:89622-89897	5	5	6	4	3
Ribonucleotide reductase of class III (anaerobic), large subunit (EC 1.17.4.2)	s07:90557-92569	11	20	27	23	21

Predicted function	Genome reference	H_2CO_2	MeOH	NO_3^-	B	F
Aspartate transaminase (EC 2.6.1.1)	s08:120988-119696	0	9	9	3	11
[FeFe]-hydrogenase maturation protein HydE	s08:123770-124816	8	10	7	3	5
Branched-chain amino acid ABC transporter, amino acid-binding protein (TC 3.A.1.4.1)	s08:125560-126762	78	86	61	57	111
Cysteine synthase (EC 2.5.1.47)	s08:127000-127935	28	21	20	28	32
Methyl-accepting chemotaxis protein	s08:130157-128100	17	25	23	19	8
Ferredoxin domain containing protein	s08:147253-147780	12	39	26	7	21
Alcohol dehydrogenase (EC 1.1.1.1)	s08:157563-158729	22	48	33	11	50
Amino acid ABC transporter, amino acid-binding protein/permease protein	s08:159010-159861	14	70	23	38	30
hypothetical protein	s08:167474-168304	7	12	4	12	3
UDP-glucose dehydrogenase (EC 1.1.1.22)	s08:188076-189338	18	18	32	14	19
TPR domain protein, putative component of TonB system	s08:190147-193536	12	21	54	25	21
Peptidoglycan N-acetylglucosamine deacetylase (EC 3.5.1.-)	s08:194906-197557	6	11	29	16	9
Circadian clock protein KaiC	s08:238789-237362	1	12	18	12	15
molybdopterin oxidoreductase	s08:244822-242444	0	0	6	0	0
Dissimilatory sulfite reductase (desulfoviridin), alpha and beta subunits	s08:37339-36419	7	20	4	8	18
Methyl-accepting chemotaxis protein	s08:41662-43143	3	11	7	5	6
Ankyrin	s08:49368-50654	3	12	5	22	12
O-acetylhomoserine sulfhydrylase (EC 2.5.1.49) / O-succinylhomoserine sulfhydrylase (EC 2.5.1.48)	s08:50826-52112	36	27	36	18	20
Chaperone protein DnaK	s08:56023-54158	23	16	24	6	0
Methyl-accepting chemotaxis protein	s08:85095-87107	35	47	26	6	14
Methyl-accepting chemotaxis protein	s09:137445-136387	23	78	46	55	108
Hydroxylamine reductase (EC 1.7.-.-)	s09:140186-138624	117	192	126	129	72
Methyl-accepting chemotaxis protein	s09:142607-140895	9	12	12	5	8
Rubrerythrin	s09:143906-143451	3	11	3	8	16
L-lactate dehydrogenase (EC 1.1.2.3)	s09:156765-155749	14	20	17	34	24
ATP-dependent protease La (EC 3.4.21.53) Type II	s09:160736-158331	80	126	93	63	47
Aspartyl-tRNA(Asn) amidotransferase subunit B (EC 6.3.5.6) @ Glutamyl-tRNA(Gln) amidotransferase subunit B (EC 6.3.5.7)	s09:163062-161620	28	25	28	29	39
Aspartyl-tRNA(Asn) amidotransferase subunit A (EC 6.3.5.6) @ Glutamyl-tRNA(Gln) amidotransferase subunit A (EC 6.3.5.7)	s09:164526-163066	10	21	23	22	29
DNA ligase (EC 6.5.1.2)	s09:167429-165225	1	8	12	8	2
FIG001943: hypothetical protein YajQ	s09:180361-179867	11	21	11	11	22
NimC/NimA family protein	s09:186208-186603	12	22	9	0	26
Formate--tetrahydrofolate ligase (EC 6.3.4.3)	s09:188329-186662	311	364	1275	983	191

Methyl-accepting chemotaxis protein	s09:194052-192073	7	10	10	6	7
Phosphoribosyl-AMP cyclohydrolase (EC 3.5.4.19) / Phosphoribosyl-ATP pyrophosphatase (EC 3.6.1.31)	s09:201080-200427	7	6	4	12	6
Histidinol dehydrogenase (EC 1.1.1.23)	s09:206218-204878	9	14	15	23	18
ATP phosphoribosyltransferase (EC 2.4.2.17)	s09:206880-206215	2	1	2	12	3
ATP phosphoribosyltransferase regulatory subunit (EC 2.4.2.17)	s09:209750-208566	5	8	11	17	18
Methionine ABC transporter substrate-binding protein	s09:210471-211289	23	60	28	32	37
Glutaminyl-tRNA synthetase (EC 6.1.1.18)	s09:216423-214702	3	14	7	10	10
Diaminopimelate decarboxylase (EC 4.1.1.20)	s09:247626-246367	16	5	5	9	11
Anaerobic nitric oxide reductase flavorubredoxin	s09:69122-67926	11	16	15	4	5
Hydroxylamine reductase (EC 1.7.-.-)	s09:70836-69277	99	168	103	112	55
Threonine synthase (EC 4.2.3.1)	s10:14524-13025	6	10	8	12	17
2-iminoacetate synthase (ThiH) (EC 4.1.99.19)	s10:31730-30312	14	62	35	59	69
Hemolysin activation/secretion protein	s10:50090-51814	0	5	13	5	1
Zinc finger domain	s10:8070-8366	24	17	9	23	14
Tricarboxylate transport protein TctC	s11:100553-101500	17	18	21	18	2
CRISPR-associated protein, Csh2 family	s11:107861-108811	9	8	6	11	10
Xanthine dehydrogenase iron-sulfur subunit (EC 1.17.1.4) / Xanthine dehydrogenase, molybdenum binding subunit (EC 1.17.1.4)	s11:15463-12734	1	12	2	5	3
Xanthine dehydrogenase iron-sulfur subunit (EC 1.17.1.4) / Xanthine dehydrogenase, molybdenum binding subunit (EC 1.17.1.4)	s11:22054-24795	37	296	79	131	119
Glutamate synthase [NADPH] small chain (EC 1.4.1.13)	s11:24905-27229	0	40	2	13	10
hypothetical protein	s11:37343-38398	0	5	1	0	10
ABC-type tungstate transport system, periplasmic binding protein	s11:5078-5962	19	79	21	35	54
SSU ribosomal protein S20p	s11:64071-63802	21	15	9	16	26
Endopeptidase spore protease Gpr (EC 3.4.24.78)	s11:64228-65199	3	15	11	5	6
Translation elongation factor LepA	s11:66906-68702	6	10	5	11	8
Heat shock protein 60 family chaperone GroEL / Thermosome subunit	s11:71004-72587	28	30	35	43	26
Heat shock protein GrpE	s11:72605-73171	25	43	38	31	29
Chaperone protein DnaK	s11:73206-75050	154	226	185	191	116
Chaperone protein DnaJ	s11:75071-76228	23	29	22	34	22
Tungsten-containing aldehyde:ferredoxin oxidoreductase (EC 1.2.7.5)	s11:7590-9329	340	309	309	279	314
Transamidase GatB domain protein	s11:80020-80472	8	14	13	9	16
DUF1432 domain-containing protein	s11:82543-83559	190	206	185	150	177
Chaperone protein DnaK	s11:85810-87648	2	12	11	4	7

Predicted function	Genome reference	H_2CO_2	MeOH	NO_3^-	B	F
DNA gyrase subunit A (EC 5.99.1.3)	s12:105173-107626	4	41	47	63	61
Dihydroxy-acid dehydratase (EC 4.2.1.9)	s12:111406-113064	38	76	78	63	85
hypothetical protein	s12:2522-1821	1	12	18	3	14
Adenylosuccinate synthetase (EC 6.3.4.4)	s12:34011-32662	23	28	20	18	102
LSU ribosomal protein L9p	s12:41519-41073	30	39	40	32	44
SSU ribosomal protein S18p @ SSU ribosomal protein S18p, zinc-dependent	s12:45450-45214	7	12	9	31	24
Single-stranded DNA-binding protein	s12:45861-45466	13	27	26	30	42
GTP-binding and nucleic acid-binding protein YchF	s12:49414-48308	3	5	6	10	11
Hypothetical protein Cj1505c	s12:51461-50859	5	7	0	7	11
CBS domain protein	s12:54333-53689	22	16	3	37	45
Branched-chain amino acid transport ATP-binding protein LivF (TC 3.A.1.4.1)	s12:55097-54387	11	8	14	20	17
Branched-chain amino acid transport ATP-binding protein LivG (TC 3.A.1.4.1)	s12:55865-55101	1	11	3	9	27
Branched-chain amino acid ABC transporter, amino acid-binding protein (TC 3.A.1.4.1)	s12:59007-57829	52	63	37	38	48
Glutamate synthase [NADPH] small chain (EC 1.4.1.13)	s12:61657-59348	99	20	64	29	35
Glutamate synthase [NADPH] large chain (EC 1.4.1.13)	s12:63307-61670	69	16	68	37	34
FIG00583938: hypothetical protein	s12:64401-63295	25	4	8	9	8
hypothetical protein	s12:69434-69057	2	1	1	6	10
[FeFe]-hydrogenase maturation protein HydF	s12:74131-72908	3	12	9	12	14
5-methyltetrahydrofolate--homocysteine methyltransferase (EC 2.1.1.13)	s12:78248-80629	24	19	18	6	12
tRNA uridine 5-carboxymethylaminomethyl modification enzyme GidA	s12:84359-82479	3	1	7	11	11
Chemotaxis protein CheV (EC 2.7.3.-)	s12:86119-87018	6	37	7	6	7
RNA-binding protein Jag	s12:88636-87992	3	9	5	14	14
DNA polymerase III beta subunit (EC 2.7.7.7)	s12:92508-93632	5	7	6	8	20
DNA gyrase subunit B (EC 5.99.1.3)	s12:96178-98112	1	16	13	22	6
ThiJ/PfpI family protein	s13:20632-21201	13	21	26	21	22
Hydroxymethylpyrimidine phosphate synthase ThiC (EC 4.1.99.17)	s13:2497-1199	10	23	25	21	12
Phosphoribosylaminoimidazole carboxylase catalytic subunit (EC 4.1.1.21)	s13:40853-41350	0	7	4	2	10
Phosphoribosylaminoimidazole-succinocarboxamide synthase (EC 6.3.2.6)	s13:41409-42119	12	19	12	17	51
Pyruvate carboxylase (EC 6.4.1.1)	s13:4484-2685	0	0	1	79	0
IMP cyclohydrolase (EC 3.5.4.10) / Phosphoribosylaminoimidazolecarboxamide formyltransferase (EC 2.1.2.3)	s13:45273-46814	39	41	65	47	130

Outer membrane protein	s13:50480-49758	4	13	3	22	10
Spermidine synthase (EC 2.5.1.16)	s13:53356-54192	1	5	1	3	4
aminopeptidase	s13:55406-54294	6	12	10	8	12
Pyruvate carboxylase (EC 6.4.1.1)	s13:6133-4532	0	0	0	59	0
FIG01197219: hypothetical protein	s13:72452-72994	4	7	14	7	8
conserved hypothetical protein	s13:73006-73677	15	14	18	13	18
Ribonucleotide reductase of class II (coenzyme B12-dependent) (EC 1.17.4.1)	s13:81102-83327	8	2	20	0	0
Ferritin-like protein 2	s14:12903-13415	13	20	15	10	12
N-acetylmuramoyl-L-alanine amidase (EC 3.5.1.28)	s14:23962-25035	12	13	7	7	4
Spore germination protein-like protein	s14:25048-25626	20	23	15	21	17
putative signal transduction histidine kinase	s14:30249-31694	3	7	11	4	6
Response regulator receiver	s14:31696-32277	3	12	2	5	10
Heat shock protein 60 family co-chaperone GroES	s14:32493-32774	19	18	6	30	17
Heat shock protein 60 family chaperone GroEL	s14:32821-34470	1610	2495	2532	2467	1537
GMP synthase [glutamine-hydrolyzing] (EC 6.3.5.2)	s14:36607-38148	12	16	25	37	18
hypothetical protein	s14:78975-81950	0	4	11	7	7
Pyruvate,phosphate dikinase (EC 2.7.9.1)	s14:90011-92668	218	267	275	292	1147
(R)-2-hydroxyglutaryl-CoA dehydratase activator-related protein	s15:19741-18341	0	0	13	0	0
Activator of (R)-2-hydroxyglutaryl-CoA dehydratase	s15:22673-19746	0	0	98	0	0
Malonyl CoA-acyl carrier protein transacylase (EC 2.3.1.39)	s15:27128-22833	0	0	91	1	0
Methyl-accepting chemotaxis protein	s15:44275-43229	12	33	36	29	69
Dihydrolipoamide acetyltransferase component of pyruvate dehydrogenase complex (EC 2.3.1.12)	s15:57313-56117	10	7	13	15	2
Acetoin dehydrogenase E1 component beta-subunit (EC 1.2.4.-)	s15:59336-58365	9	12	0	13	0
Phosphate regulon sensor protein PhoR (SphS) (EC 2.7.13.3)	s15:6374-4344	10	7	10	9	8
Orotidine 5'-phosphate decarboxylase (EC 4.1.1.23)	s15:66214-65495	16	15	17	14	24
Carbamoyl-phosphate synthase large chain (EC 6.3.5.5)	s15:71139-67918	80	83	111	97	72
Aspartate carbamoyltransferase (EC 2.1.3.2)	s15:74444-73488	13	6	2	1	6
Aspartate aminotransferase (EC 2.6.1.1)	s16:29933-28743	7	1	6	16	10
Transcriptional regulator, GntR family	s16:39603-40226	7	8	10	13	6
NAD(FAD)-utilizing dehydrogenase	s16:41665-40283	4	21	17	6	14
Uncharacterized protein MA0381	s16:46247-45639	27	25	21	25	27
5,10-methylenetetrahydrofolate reductase	s16:4696-6210	6	10	14	7	2

Predicted function	Genome reference	H_2CO_2	MeOH	NO_3^-	B	F
long-chain-fatty-acid--CoA ligase, putative	s16:48801-46276	12	13	6	13	30
Periplasmic hemin-binding protein	s16:51856-52803	2	13	2	7	0
putative receptor	s16:54003-55982	28	116	83	48	9
Cob(I)alamin adenosyltransferase (EC 2.5.1.17)	s16:58349-58882	3	16	7	8	4
Methyl-accepting chemotaxis protein	s16:60944-62716	18	30	31	10	12

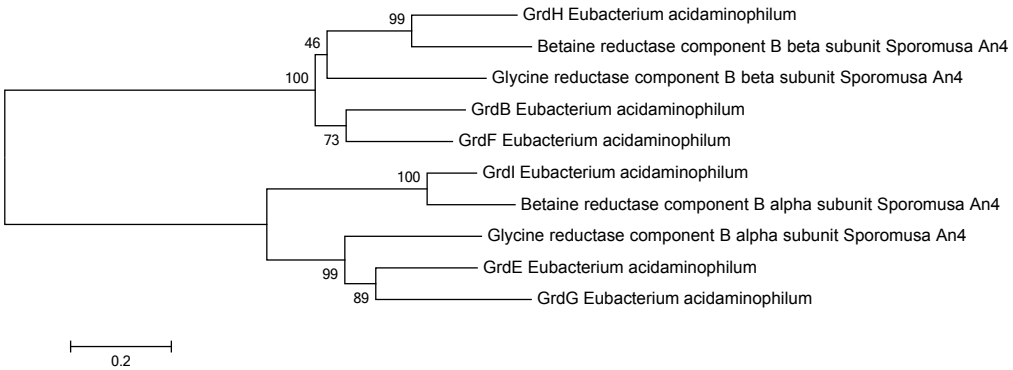

S2 *Neighbor joining tree constructed by using the amino acid sequences of the glycine/sarcosine/betaine reductase B components of Eubacterium acidaminophilum and Sporomusa strain An4.The B components have an alpha and a beta subunit.The numbers at the branches are bootstrap persentage values.The scale bar represents 20% sequence difference.*

S1 *Proteome data of the proteins 3x more abundant in one or multiple growth conditions. The table shows the predicted function of the proteins, the reference to the genome (in locus tags), and their related peptide abundance in the four different growth conditions and their independent duplicates: lactate and sulfate (L), methanol and sulfate (M), methanol and sulfate in the absence of cobalt and vitamin B12 (M -co -B12), and ethanol and sulfate (E).*

Function	locus tag	L 1	L 2	M 1	M 2	M -co -B12 1	M -co -B12 2	E 1	E 2
Pyruvate/ketoisovalerate oxidoreductase, gamma subunit	Desku_0032	36	42	7	7	8	9	10	9
Methyltransferase MtaA/CmuA family	Desku_0050	0	1	107	125	11	6	15	15
Methanol:cobalamin methyltransferase, subunit B	Desku_0051	0	1	68	77	11	1	12	14
Methyltransferase cognate corrinoid protein	Desku_0052	0	0	52	60	1	1	1	2
Cobalamin synthesis protein P47K	Desku_0053	0	0	5	7	0	0	0	0
4Fe-4S ferredoxin iron-sulfur binding domain-containing protein	Desku_0054	0	0	9	7	0	0	0	0
Methionine synthase B12-binding module cap domain protein	Desku_0056	0	0	54	49	1	1	4	6
Ferredoxin	Desku_0057	0	0	108	98	7	4	11	14
Tetrahydromethanopterin S-methyltransferase	Desku_0058	0	0	26	35	2	2	5	5
Pyridoxamine 5'-phosphate oxidase-related FMN-binding protein	Desku_0059	0	0	89	101	2	1	2	2
Methyltransferase MtaA/CmuA family	Desku_0060	0	0	62	84	3	0	7	6
Nicotinate-nucleotide- -dimethylbenzimidazole phosphoribosyltransferase	Desku_1002	93	110	60	63	10	12	58	77
DRTGG domain protein	Desku_2302	41	59	11	6	7	7	15	13
Acetyl coenzyme A synthetase (ADP forming), alpha domain protein	Desku_2303	30	45	5	3	3	5	10	12
Hydrogenase, Fe-only	Desku_2307	0	3	40	39	105	121	32	4
NADH dehydrogenase (Quinone)	Desku_2308	5	5	33	23	76	75	16	7
Ferredoxin	Desku_2309	3	2	15	13	23	19	8	1
NADH dehydrogenase (Quinone)	Desku_2311		2	5	5	20	23	3	2
Lactate utilization protein B/C	Desku_2393	38	41	1	0	0	0	0	0
Lactate utilization protein B/C	Desku_2394	12	18	0	0	0	0	0	0
L-lactate transport	Desku_2395	3	7	0	0	0	0	0	0
Acetyl-coenzyme A synthetase	Desku_2843	0	0	5	7	26	28	7	7
Acetolactate synthase	Desku_2889	2	0	2	5	20	22	7	5
Ketol-acid reductoisomerase	Desku_2890	19	21	16	21	95	110	41	26
Extracellular solute-binding protein family 1	Desku_2938	0	1	22	30	27	28	23	23

Function	locus tag	L 1	L 2	M 1	M 2	M -co -B12 1	M -co -B12 2	E 1	E 2
Aldehyde ferredoxin oxidoreductase	Desku_2951	16	20	121	125	156	166	153	126
1,3-propanediol dehydrogenase	Desku_2952	0	0	372	409	569	581	271	174
Hydrogenase, Fe-only	Desku_2995	47	70	14	13	12	23	127	151
NADH dehydrogenase (Quinone)	Desku_2996	60	86	5	8	10	16	96	101
NADH dehydrogenase (Quinone)	Desku_2997	9	9	1	1	1	2	13	17
D-lactate dehydrogenase (Cytochrome)	Desku_3009	4	9	0	0	0	0	0	0

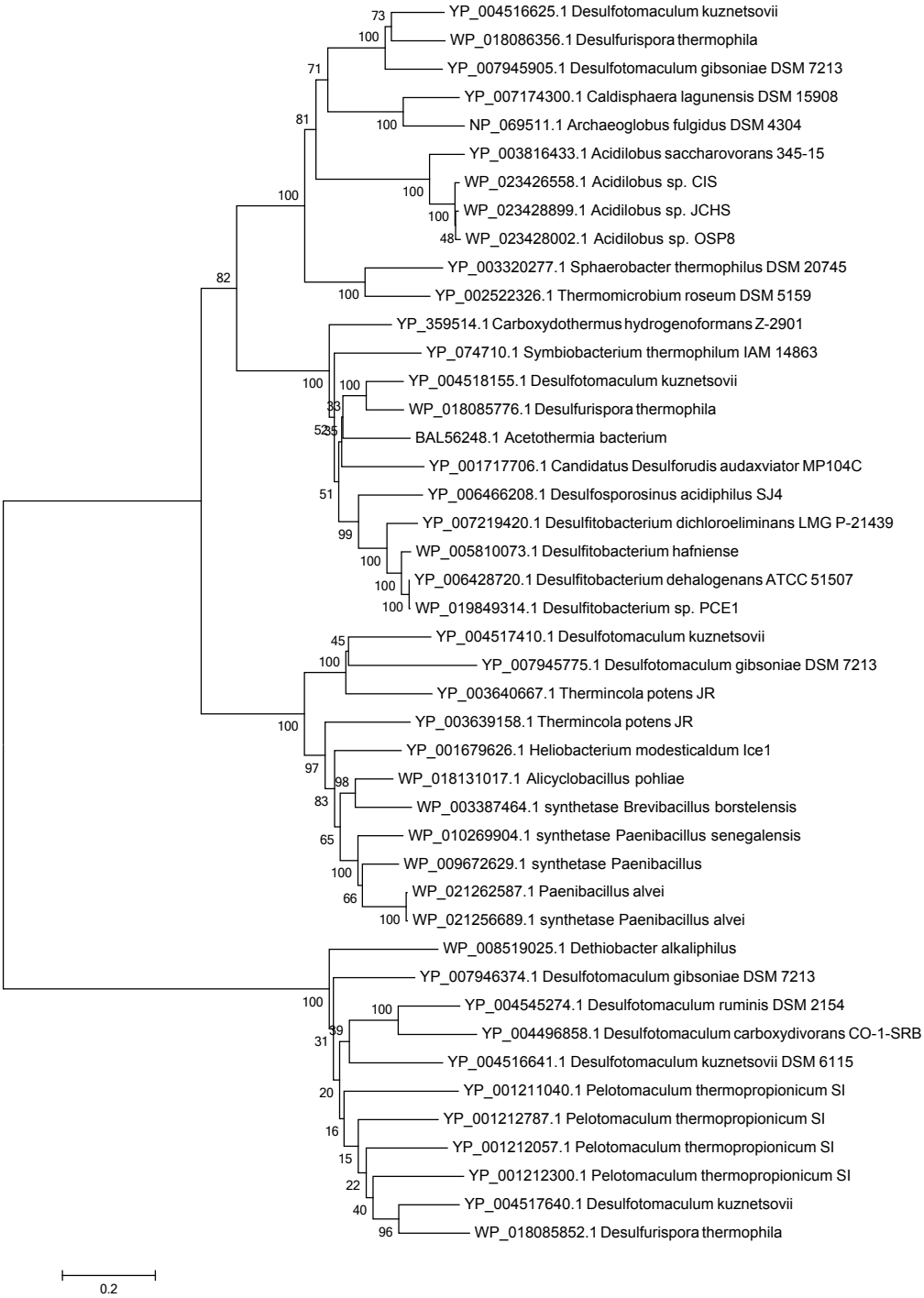

S2 *Neighbor joining tree using the ten best BLAST hits from the four ACL enzymes in D. kuznetsovii. The numbers at the branches are bootstrap persentage values.The scale bar represents 20% sequence difference.*

Appendices

Summary

Samenvatting

Acknowledgements

About the author

List of publications

Overview of completed training activities

Summary

One-carbon metabolism in acetogenic and sulfate-reducing bacteria

Life on earth is sustained by the constant cycling of six essential elements: oxygen, hydrogen, nitrogen, sulfur, phosphorous, and carbon. The continuous cycling of these elements is due to geo-chemical processes and the combined metabolism of all life on earth. Microorganisms like bacteria and archaea play a major role in this. This is also true for the carbon cycle. In this cycle carbon dioxide and methane are two important C-1 compounds present in the atmosphere. Carbon dioxide is the highest oxidative state of carbon while methane is the highest reduced form of carbon. The art to use light to produce organic compounds and conserve energy from the highest oxidative state of carbon is called photosynthesis and is performed by plants, algae and cyanobacteria. Photosynthesis is not the only system to fix carbon from carbon dioxide. Chemolithotrophs can fix carbon from carbon dioxide using inorganic electron donors, like hydrogen. Subsequently, fixed carbon can be used by other organisms, which also makes life possible for them. Microorganisms play a major role in the degradation of complex organic matter, producing smaller compounds including C-1 compounds. C-1 compounds other than carbon dioxide are e.g. carbon monoxide (CO), methanol and formate. Bacteria and archaea can utilize these relative simple compounds in the presence and absence of oxygen, alone and in cooperation with others (syntrophy). The complex and simple carbon compounds are finally oxidized to carbon dioxide, which closes the carbon cycle.

In addition to their importance to the carbon cycle, one carbon compounds like CO, methanol and formate are important for several applications. They are used as a building block for the production of chemicals. They are also used for bioremediation purposes and for wastewater treatment. Therefore, it is important to gain insight in the one carbon metabolism of microorganisms. The research described in this thesis focuses on the proteins and encoding genes involved in anaerobic degradation of C1 compounds by using genome and proteome analysis.

In Chapter 2 the genomes of two closely related sulfate-reducing bacteria, *Desulfotomaculum nigrificans* and *D. nigrificans* strain CO-1-SRB, are compared including their CO metabolism. Both the *D. nigrificans* type strain and strain CO-1-SRB can grow with CO. However, there are differences. The type strain can grow with 20% CO coupled to sulfate reduction in the presence of yeast extract, while strain CO-1-SRB can grow with 100% CO in the presence of yeast extract. Moreover, strain CO-1-SRB can grow with CO in the presence and absence of sulfate. It couples the oxidation of CO to carbon dioxide to hydrogen production. This conversion, the protein complex involved, and the genes coding for these proteins have been described before in other microorganisms. The genome of strain CO-1-SRB contains the genes coding for this protein complex while the genome of the *D. nigrificans* type strain does not. However, the genome of the type strain contains genes encoding two other CO dehydrogenases. This indicates that one or both are necessary for the type strain to grow with 20% CO. Additional research on the different CO dehydrogenases and their regulation is essential to assess if all different CO dehydrogenases can facilitate growth and how they are linked to for example creating a proton motive force for ATP production.

The methanol metabolism of anaerobic bacteria seems to differ more from that of methanogens than initially described. Methanogens use a methanol methyltransferase system that consists of

two methyltranferases, methyltransferase 1 (subunits MtaB and MtaC) and methyltransferase 2 (MtaA). The methyl group from methanol is transferred to the MtaC subunit by MtaB. Subsequently, MtaA transports the methyl group from MtaC to coenzyme M. A genome and proteome analysis of the acetogenic bacterium *Sporomusa* strain An4 suggests that instead of MtaA a methyl-tetrahydrofolate methyltransferase is involved in the transport of the methyl bound to MtaC to tetrahydrofolate (Chapter 3).

Research done on the methanol metabolism of the sulfate-reducing bacterium *Desulfotomaculum kuznetsovii* also shows differences with that of methanogens (Chapter 5). The methanol methyltransferase system is vitamin B12 and cobalt dependent. *D. kuznetsovii* grows with methanol and sulfate, but can do this in presence and absence of vitamin B12 and cobalt. In the absence of vitamin B12 and cobalt *D. kuznetsovii* grows slower and reaches a lower optical density compared to growth in the presence of vitamin B12 and cobalt. This suggests that *D. kuznetsovii* can use both a methyltransferase system and a vitamin B12 and cobalt independent system for the degradation of methanol. Proteome results confirm this and suggest that the vitamin B12 and cobalt independent system consists of an alcohol dehydrogenase and an aldehyde ferredoxin oxidoreductase. Moreover, the alcohol dehydrogenase seems to be involved in the oxidation of both methanol and ethanol (Chapter 5). The presence of two methanol degradation pathways give an ecological advantage to *D. kuznetsovii* in environments containing methanol and sulfate but limiting cobalt and vitamin B12 concentrations. Future research should elucidate if more sulfate-reducing bacteria, or perhaps even acetogenic bacteria, have two methanol degrading pathways.

Additional to the genome analysis of *D. kuznetsovii* to assess the genes coding for the proteins involved in the two methanol degradation pathways, the genome was also analyzed to assess genes encoding other degradation pathways (Chapter 4). This analysis shows many genes present in *D. kuznetsovii* are also present in *Pelotomaculum thermopropionicum*. *P. thermopropionicum* is known to degrade propionate in syntrophic interaction with a methanogen. *D. kuznetsovii* can also degrade propionate, but only coupled to sulfate reduction and not in syntrophy with methanogens. Moreover, *P. thermopropionicum* is not able to reduce sulfate. *D. kuznetsovii* is the only close related, non-syntrophic, propionate degrader of which the genome is available. Therefore, a genome comparison was performed between *D. kuznetsovii* and *P. thermopropionicum* to define the differences between a non-syntrophic and a syntrophic lifestyle. *D. kuznetsovii* misses membrane bound protein complexes like hydrogenases and an extra-cytoplasmic formate dehydrogenase. In order to expand the analysis between non-syntrophs and syntrophs, more genomes of propionate- and butyrate-degrading bacteria were included (Chapter 6). This extended analysis shows that the genomes of non-syntrophs do not contain genes coding for an extra-cytoplasmic formate dehydrogenase, in contrast to all syntrophs included in the analysis. This indicates the importance of this protein complex and the importance of formate as an interspecies electron carrier in syntrophic degradation of propionate and butyrate. Thanks to the extra cytoplasmic formate dehydrogenase the syntrophic bacteria can couple the degradation of propionate and butyrate to formate production. Subsequently, the formate is utilized by methanogens to produce methane. This keeps the formate concentration low, which is necessary for the entire process to be energetically favorable.

Samenvatting

Afbraak van één koolstof verbindingen in acetogene en sulfaatreducerende bacteriën

Het leven op aarde wordt mogelijk gemaakt door de constante cyclus van zes belangrijke elementen: zuurstof, waterstof, stikstof, zwavel, fosfor en koolstof. De cyclus van deze elementen wordt in stand gehouden door geochemische processen en door het gezamenlijke metabolisme van alle organismen op aarde. Micro-organismen zoals bacteriën en archaea spelen hier een grote rol in. Dit geldt ook voor de koolstofcyclus. Hierin zijn koolstofdioxide en methaan twee C-1 verbindingen met, respectievelijk, het meest geoxideerde en het meest gereduceerde oxidatieniveau van koolstof. De kunst om door middel van licht van de meest geoxideerde koolstof vorm organische verbindingen te vormen en energie te conserveren, heet fotosynthese, wat wordt uitgevoerd door planten, algen en cyanobacteriën. Fotosynthese is niet het enige systeem dat koolstof kan fixeren uit koolstofdioxide. Chemolithotrofe micro-organismen kunnen dit ook door anorganische elektrondonoren, zoals waterstof, te gebruiken. Gefixeerde koolstof kan op deze manier weer gebruikt worden door andere organismen, waardoor leven voor deze organismen ook mogelijk is. Micro-organismen spelen een grote rol bij de afbraak van complexe organische stoffen en produceren vaak kleinere verbindingen, waaronder andere C1 verbindingen als koolstofdioxide, als eindproduct. Andere één koolstof verbindingen zijn bijvoorbeeld koolstofmonoxide, methanol en formiaat. Bacteriën en archaea kunnen groeien op deze relatief simpele verbindingen, zowel in de aanwezigheid als afwezigheid van zuurstof en zowel alleen als in samenwerking met elkaar (syntrofie). De complexere en minder complexere koolstof verbindingen worden uiteindelijk weer geoxideerd tot koolstofdioxide en maken zo de koolstof cyclus rond.

C1 verbindingen als koolstofmonoxide, methanol en formiaat zijn niet alleen belangrijk in de koolstof cyclus, maar ook voor technologische doeleinden. Ze worden gebruikt voor de productie van chemicaliën, bij de afbraak van vervuilde stoffen in de grond en bij de zuivering van afvalwater. Daarom is het belangrijk om een goed inzicht te krijgen van de verscheidene afbraakroutes die micro-organismen gebruiken om deze stoffen af te breken. Het onderzoek in dit proefschrift focust zich voornamelijk op de eiwitten en genen betrokken bij de anaerobe afbraak van C1 verbindingen, doormiddel van genoom en proteoom analyses.

In hoofdstuk 2 worden twee sulfaatreducerende bacteriën, de type stam van *D. nigrificans* en *D. nigrificans* stam CO-1-SRB die fylogenetisch verwant zijn, op basis van hun genoom met elkaar vergeleken op onder andere het verschil in hun koolstofmonoxide metabolisme. Zowel de type stam als stam CO-1-SRB kunnen groeien met koolstofmonoxide, maar er zijn verschillen. De type stam kan groeien met 20% koolstofmonoxide gekoppeld aan sulfaat reductie en in de aanwezigheid van gistextract, terwijl *D. nigrificans* stam CO-1-SRB in de aanwezigheid van gistextract met 100% koolstofmonoxide kan groeien. De groei hoeft in dit geval niet gekoppeld te zijn aan sulfaatreductie. Stam CO-1-SRB oxideert koolstofmonoxide naar koolstofdioxide en produceert hierbij waterstof. De productie van waterstof door de oxidatie van koolstofmonoxide, het betrokken koolstofmonoxide dehydrogenase complex en de genen die coderen voor dit complex zijn al eerder beschreven in andere micro-organismen. Het genoom van stam CO-1-SRB bezit de genen die coderen voor dit eiwit complex, terwijl de *D. nigrificans* type stam deze genen mist. Wat de type stam wel heeft zijn genen die coderen

voor twee andere koolstofmonoxide dehydrogenases. Dit duidt er op dat één van de twee of allebei nodig zijn om op 20% koolstofmonoxide te kunnen groeien. Verder onderzoek naar de verschillende koolstofmonoxide dehydrogenases en de regulatie hiervan is nodig om erachter te komen of alle koolstofmonoxide dehydrogenases voor groei kunnen zorgen en hoe ze gekoppeld zijn aan bijvoorbeeld de vorming van een proton gradiënt voor ATP productie.

Het methanol metabolisme van anaerobe bacteriën lijkt niet helemaal hetzelfde te zijn als in methanogenen, waar een methanol methyltransferase systeem actief is. Dit systeem bestaat uit twee methyltransferases, methyltransferase 1 (subunits MtaB en MtaC) en methyltransferase 2 (MtaA). De methyl groep van methanol wordt door subunit MtaB overgedragen. Een genoom- en proteoomanalyse van de acetogene bacterie *Sporomusa* stam An4 suggereert dat in plaats van MtaA een methyl-tetrahydofoliumzuur methyltransferase betrokken is bij overdracht van de methyl groep gebonden aan MtaC naar tetrahydrofoliumzuur (Hoofdstuk 3).

Onderzoek naar het methanol metabolisme van de sulfaatreducerende bacterie *Desulfotomaculum kuznetsovii* laat ook verschil zien met methanogenen (Hoofdstuk 5). Het methanol methyltransferase systeem is vitamine B12 en kobalt afhankelijk. *D. kuznetsovii* groeit met methanol en sulfaat, maar doet dit zowel in de aanwezigheid als afwezigheid van vitamine B12 en kobalt. In afwezigheid van vitamine B12 en kobalt groeit *D. kuznetsovii* minder snel en tot een minder hoge dichtheid dan in de aanwezigheid van vitamine B12 en kobalt. Dit suggereert dat *D. kuznetsovii* zowel het methyltransferase systeem als een vitamine B12 en kobalt-onafhankelijk systeem kan gebruiken om methanol af te breken. De proteoomdata bevestigen dit en suggereren dat het vitamine B12 en kobalt-onafhankelijke systeem bestaat uit een alcohol dehydrogenase en een aldehyde ferredoxine oxidoreductase. Overigens lijkt het erop dat de alcohol dehydrogenase zowel betrokken is bij de oxidatie van methanol als ethanol (Hoofdstuk 5). De aanwezigheid van twee methanol afbraak routes geeft een ecologisch voordeel aan *D. kuznetsovii* in omgevingen waar methanol en sulfaat aanwezig zijn, maar weinig kobalt en vitamine B12. Toekomstig onderzoek moet aantonen of meer sulfaat-reducerende bacteriën, of misschien zelfs acetogene bacteriën, ook twee methanol afbraakroutes hebben.

Naast dat het genoom van *D. kuznetsovii* is onderzocht voor de genen die coderen voor de eiwitten van de twee methanol afbraakroutes, is het genoom ook onderzocht voor genen die coderen voor andere afbraakroutes (Hoofdstuk 4). In deze analyse komen veel genen naar voren die ook aanwezig zijn in *Pelotomaculum thermopropionicum*. Deze bacterie staat bekend om zijn afbraak van propionzuur in syntrofe interactie met een methanogeen. *D. kuznetsovii* kan ook propionzuur afbreken, maar alleen gekoppeld aan sulfaatreductie en niet in syntrofie met methanogenen. Daarentegen kan *P. thermopropionicum* geen sulfaat reduceren. Fylogenetisch is *D. kuznetsovii* de meest verwante propionzuurgebruiker die niet syntroof kan groeien, maar waarvan het genoom beschikbaar is. Daarom is een genoomvergelijking gedaan tussen *D. kuznetsovii* en *P. thermopropionicum* om de verschillen aan te tonen tussen een niet syntrofe en syntrofe levensstijl. *D. kuznetsovii* mist membraan gebonden complexen als hydrogenases en een extra-cytoplasmatische formiaatdehydrogenase. Om de analyse tussen niet-syntrofen en syntrofen uit te breiden, zijn er meer genomen vergeleken van propionzuur- en boterzuur-afbrekende bacteriën (Hoofdstuk 6). Deze uitgebreide analyse toont aan dat de genomen van de niet-syntrofen geen extra-cytoplasmatische formiaatdehydrogenase genen bezitten, terwijl dit bij alle syntrofen in de analyse wel het geval is. Dit duidt op het belang van dit complex en tegelijkertijd het belang van formiaat als intermediair in syntrofe interactie met methanogenen. Dankzij de

extra-cytoplasmatische formiaatdehydrogenase zijn de syntrofe bacteriën in staat de afbraak van propionzuur en boterzuur te koppelen aan formiaatproductie. Het geproduceerde formiaat wordt omgezet in methaan door methanogenen, die zo de formiaatconcentratie laag houden om het gehele proces energetisch mogelijk te maken.

Dankwoord / Acknowledgements

Mijn onderzoek en proefschrift zijn het resultaat van jaren enthousiast werken. Hier hebben vele mensen aan bijgedragen die ik hier graag wil bedanken.

Als eerste wil ik **Fons**, mijn begeleider en promotor, bedanken voor alle wetenschappelijke discussies en begeleiding. Jouw ideeën en professionaliteit hebben mij altijd geïnspireerd. Je hebt mij altijd aangemoedigd om samenwerkingen binnen en buiten de Wageningen Universiteit aan te gaan wat tot mooi onderzoek en resultaat heeft geleid. Ook wil ik je bedanken voor de mogelijkheid die je mij hebt gegeven om een jaar vervolg onderzoek te doen naar het methanol metabolisme van sulfaat reducerende bacteriën.

Caroline, bedankt voor al je goede ideeën en je kritische blik. Maar ook bedankt voor alle leuke gesprekken (over zowel wetenschappelijke als de alledaagse dingen) en de co-begeleiding van mijn MSc student Joseph.

I would like to thank all the people I collaborated with. **Martijn Pinkse** and **Mervin Pieterse** for performing the proteome analyses that are part of two chapters in this thesis. The *Desulfotomaculum* genome team comprising of **Gerard Muyzer**, **Inês Pereira**, **Jan Kuever**, **Sofiya Parshina**, **Rizlan Bernier-Latmani, Peter**, **Caroline** and **Fons** for the nice *Desulfotomaculum* genome papers. **Elena** and **Rizlan** for the interesting paper about sporulation genes in the *Desulfotomaculum* genus. **Peter, Jasper** and **Bart** for all bioinformatics support. **Petra**, **Joana**, **Diana**, and **Martin**, thank you for our collaborations.

My thanks also goes to the present and previous **MicFys members**. In dutch, **MicFysers**, which is pronounced like **MicVissers**… hmmm… Thanks for the years of "gezelligheid" and for all the (useful and not so useful) discussions. I would have liked to thank you all individually and write a small paragraph to each of you but that would lead to an even larger acknowledgements section then in Martin's dissertation. Just to let you know, I will not forget my evil ways ;)

I would like to thank my two students, **Robert** and **Joseph**, for their enthusiasm for and devotion to the subject. I wish them all the best for the future.

Thomas "the Viking" "the Prophet" Kruse, thank you for the help and the countless talks about.. well nothing.. Thanks for convincing the entire lab that I became fat after buying a car. Ok, I promise to cut down on the food and cycle more, but NO I will not prepare 200 bottles of medium with Viton stoppers, autoclave, and inoculate them for you! O, and stop fooling yourself; Ajax is not going to win the Dutch championship this year.

Tijdens mijn promotietijd heb ik in kantoor 0.012 gewerkt. In die tijd zijn er in dit kantoor een aantal AIO's gekomen en gegaan, soms voor een korte en soms voor een nog kortere tijd. Daarom wil ik hier een aantal woorden weiden aan kantoor 0.012 en de mensen waarmee ik dit wonderbaarlijke kantoor heb gedeeld.

Kantoor 0.012 lijkt misschien op een doodnormaal kantoor, van ongeveer 3 bij 4 met vier stoelen, vier bureaus, vier computers en zes ramen uitkijkend op het grasveld achter het Microbiologie gebouw, maar die mensen die even de tijd nemen om verder te kijken zullen beamen dat dit een wonderbaarlijke plek is. Het kantoor ligt dichtbij de lunchruimte, waardoor de gezelligheid van de leerstoelgroep altijd te horen is tijdens de koffie- en lunchpauze. Het grasveld waar het kantoor op kijkt wemelt in de lente en zomer van de konijnen, een rustgevende aanblik, en als je je blik van het grasveld afhaalt en langs de muur van het gebouw omhoog laat afdwalen zie je het valkennest, waar ieder jaar weer zo'n 5 à 6 valkenjongen geboren worden. Kantoor 0.012 is dus een kantoor vol leven. Zelfs de deur van het kantoor lijkt een eigen leven te hebben. Deze opent zichzelf namelijk op de meest rare en onverwachte tijdstippen. Kantoor 0.012 is dus echt een kantoor vol leven en het is deze plek waar mijn onderzoek het leven heeft gekregen.

Ik heb kantoor 0.012 met een aantal mensen gedeeld. Ik wil daarom graag deze mensen: **Farrakh**, **Edze**, **Rejoan Reza**, **Bryan**, **Petra**, **Nam**, **Susakul** en **Peer** bedanken voor hun gezelschap en voor alle goede gesprekken.

Farrakh, thank you for showing me around in the lab when I just started my PhD. You were finishing yours in that time and was only around for another two months. When you left you gave me some advice: *"Michael, try to avoid enzyme activity assays."* I am sorry Farrakh, I did not listen.

Bryan, you showed interest in the Netherlands, the Dutch culture, and the Dutch language. This lead to great conversations. I learned from you scientifically but also about America in general. Thanks to you I tried a peanut butter and jelly sandwich. I cannot say it changed my life or what I eat for lunch nowadays, but it was *"interesting"*. I am proud to say that I also taught you a few things, like *"gaan met die banaan!" (go with that banana!)*.

Nam, you always kept me sharp with your questions. Thanks for the many fun talks we had and the best loempias ever!

Susakul, we can also call you "Good" but honestly I do not know anyone who does that ;) Maybe your name is less difficult than you think, or we think it is less difficult than it actually is. Thanks for always being happy!

Nam and **Susakul**, I also want to thank you for just being in the same office as Peer and me without going crazy.

Peer, de persoon die het langst met mij kantoor 0.012 heeft gedeeld en een gedeelde passie heeft voor C-1 verbindingen. Als Hollander gaat er niks boven een lekker potje klagen. Jij begrijpt dat en samen hebben we wat af geklaagd, maar ook veel gelachen. Met het kantoor vlak naast de lunchruimte is het onvermijdelijk om lachende mensen te horen tijdens de koffie- en lunchpauze en daardoor soms onmogelijk te concentreren. Ik denk dat wij de meeste mensen wel kunnen benoemen door alleen hun lach te horen. Er zitten er nou eenmaal een paar heel opvallende tussen.

Er wordt dus veel gelachen in het gebouw. Dit beschrijft heel goed de sfeer en de mensen bij MIB en SSB. Dankzij jullie allemaal wordt er een wetenschappelijk kritische en behulpzame werkomgeving gecreëerd die tegelijkertijd gezellig is. Bedankt allemaal!

Verder wil ik graag mijn **familie** en **vrienden** bedanken voor alle steun. Dankzij jullie heb ik geleerd mijn onderzoek zo te verwoorden dat het ook begrijpelijk is voor niet wetenschappers. Gekoppeld hieraan wil ik meteen sorry zeggen als ik jullie soms heb verveeld met mijn bacterie praat ;)

Ik wil mijn **ouders** bedanken voor alles wat ze mij hebben geleerd en het vertrouwen die zij altijd in mij hebben gehad.

Ook wil ik mijn **schoonouders** bedanken voor alle gezelligheid en jullie jongste dochter, die ik sinds 23 mei 2014 mijn vrouw mag noemen.

Als laatste wil ik mijn vrouw bedanken. Lieve **Wendy,** met jou kan ik altijd mijn werk bespreken, maar ook even vergeten. Dit laatste is ook heel belangrijk geweest de afgelopen jaren. Samen ontspannen en leuke dingen doen heeft er altijd voor gezorgd dat ik weer vol energie en plezier aan mijn onderzoek verder ging.

About the author

Michael Visser was born on the 25th of November 1985 in Alkmaar, the Netherlands. He started his bachelor Biomedical Sciences at the VU University Amsterdam in 2004. In the last year of his bachelor he did an internship for four months at the ACTA (Academisch Centrum Tandheelkunde Amsterdam), researching oral bacterial growth in variable environments.

In September 2007 he started his master Biomedical Sciences with a specialization in immunology, also at the VU University. He did his first master internship at the Molecular Cell Biology and Immunology department under the supervision of Caroline van Stijn and Irma van Die. He researched the secretion of galectin 3 by monocyte derived cells for five months. His second master internship was at the School of Civil engineering and geosciences at Newcastle University (U.K.). This was a six month internship and was supervised by Jan Dolfing and Ian Head. He researched the stability of syntrophic communities in methanogenic degradation of propionate and benzoate as a sole carbon and energy source in four bioreactors.
During his years at the VU University he supervised students during a two week practical and worked part-time for six months as a student lab-assistant, both at the department of Molecular Cell Physiology.

In November 2009 Michael joined the Microbial Physiology group of Prof. Dr Fons Stams, starting his PhD. His research focussed on the one-carbon metabolism of acetogenic and sulfate-reducing bacteria. The results are described in this thesis.

Publications

van Stijn C.M.W., van den Broek, M., van de Weerd, R., Visser, M., Taşdelen, I., Tefsen, B., van Die, I. Regulation of expression and secretion of galectin-3 in human monocyte-derived dendritic cells. *Molecular Immunology* **46**(16): 3292–99 (2009).

Spring, S., Visser, M., Lu, M., Copeland, A., Lapidus, A., Lucas, S., Cheng, J.F., Han, C., Tapia, R., Goodwin, L.A., Pitluck, S., Ivanova, N., Land, M., Hauser, L., Larimer, F., Rohde, M., Göker, M., Detter, J.C., Kyrpides, N.C., Woyke, T., Schaap, P.J., Plugge, C.M., Muyzer, G., Kuever, J., Pereira, I.A., Parshina, S.N., Bernier-Latmani, R., Stams, A.J.M., Klenk, H.P. Complete genome sequence of the sulfate-reducing firmicute *Desulfotomaculum ruminis* type strain DL^T. *Standards in Genomic Sciences* **7**: 304-319 (2012).

Visser, M., Worm, P., Muyzer, G., Pereira, I., Schaap, P.J., Plugge, C.M., Kuever, J., Parshina, S.N., Bernier-Latmani, R., Goodwin, L.A., Kyrpides, N.C., Detter, J., Woyke, T., Chain, P., Davenport, K.W., Spring, S., Klenk, H.P., Stams, A.J.M. Genome analysis of *Desulfotomaculum kuznetsovii* strain 17^T reveals a physiological similarity with *Pelotomaculum thermopropionicum* strain SI^T. *Standards in Genomic Sciences* **8**: 69-87 (2013).

Visser, M., Parshina, S.N., Alves, J.I., Sousa, D.Z., Pereira, I., Muyzer, G., Kuever, J., Lebedinsky, A.V., Koehorst, J.J., Worm, P., Plugge, C.M. Schaap, P.J., Goodwin, L.A., Lapidus, A., Kyrpides, N.C., Detter, J.C., Woyke, T., Chain, P., Davenport, K.W., Spring, S., Rohde, M., Klenk, H.P., Stams, A.J.M. Genome analyses of the carboxydotrophic sulfate-reducers *Desulfotomaculum nigrificans* and *Desulfotomaculum carboxydivorans* and reclassification of *Desulfotomaculum caboxydivorans* as a later synonym of *Desulfotomaculum nigrificans*. *Standards in Genomic Sciences* **9**: 655-675 (2013).

Kuever, J., Visser, M., Boll, M., Worm, P., Sousa, D.Z., Plugge, C.M., Schaap, P.J., Muyzer, G., Pereira, I.A., Parshina, S.N., Goodwin, L.A., Kyrpides, N.C., Detter, J., Woyke, T., Chain, P., Davenport, K.W., Rohde, M., Spring, S., Klenk, H.P., Stams, A.J.M. Genome analysis of *Desulfotomaculum gibsoniae* strain Groll^T, a highly versatile Gram-positive sulfate-reducing bacterium. *Standards in Genomic Sciences* **9**(3): 821-39 (2014).

Worm, P., Koehorst, J.J.*, Visser, M.*, Sedano-Núñez, V.T., Schaap, P.J., Plugge, C.M., Sousa, D.Z., Stams, A.J.M. A genomic view on syntrophic versus non-syntrophic lifestyle in anaerobic fatty acid degrading communities. *Biochimica et Biophysica Acta – Bioenergetics Special Issue* **1837**(12): 2004-16 (2014).
*Both authors contributed equally

Vecchia, D.E., Visser, M., Stams, A.J.M., Bernier-Latmani, R. Investigation of sporulation in the *Desulfotomaculum* genus: a genomic comparison with the genera *Bacillus* and *Clostridium*. *Environmental Microbiology Reports* **6**(6): 756-66 (2014).

Visser, M., Pieterse, M., Pinkse, M.W. , Nijsse, B., de Vos, W.M. , Schaap, P.J., Stams, A.J.M. Genome and proteome analysis reveals novel insight of the one-carbon metabolism of the acetogen *Sporomusa* strain An4. *In preparation for publication.*

Visser, M., Pieterse, M., Pinkse, M.W. , Stams, A.J.M. Comparative proteomics reveals two methanol-degrading pathways in the sulfate-reducing bacterium *Desulfotomaculum kuznetsovii. In preparation for publication*

Netherlands Research School for the
Socio-Economic and Natural Sciences of the Environment

D I P L O M A

For specialised PhD training

The Netherlands Research School for the
Socio-Economic and Natural Sciences of the Environment
(SENSE) declares that

Michael Visser

born on 25 November 1985 in Alkmaar, The Netherlands

has successfully fulfilled all requirements of the
Educational Programme of SENSE.

Wageningen, 14 January 2015

the Chairman of the SENSE board	the SENSE Director of Education
Prof. dr. Huub Rijnaarts	Dr. Ad van Dommelen

The SENSE Research School has been accredited by the Royal Netherlands Academy of Arts and Sciences (KNAW)

K O N I N K L I J K E N E D E R L A N D S E
A K A D E M I E V A N W E T E N S C H A P P E N

The SENSE Research School declares that **Mr Michael Visser** has successfully fulfilled all requirements of the Educational PhD Programme of SENSE with a work load of 38.3 EC, including the following activities:

SENSE PhD Courses

- Biological Processes in Environmental Technology (2010)
- Environmental Research in Context (2011)
- Research Context Activity: Organising a SENSE symposium: 'Microbes for Sustainability', Wageningen (2012)

Other PhD and Advanced MSc Courses

- Bioinformation Technology (2010)
- Scientific writing (2012)
- Career orientation (2013)

Management and Didactic Skills Training

- Practical supervision BSc course 'Microbial Physiology' (2010-2012)
- Member of the Daily Board of the Laboratory of Microbiology (2010-2013)
- Supervision of BSc thesis 'Comparing *Moorella perchloratireducens* to *Sporomusa* strain An4' (2011)
- Supervision of MSc thesis 'Unravelling the methanol metabolism in *Desulfotomaculum kuznetsovii*' (2012)

Oral Presentations

- *Methanol metabolism in Sporomusa strain An4.* SENSE PhD trip 'Microbiology in China and Japan', 15 April – 1 May 2011, Peking and Shanghai, China
- *Key factors in syntrophy.* Annual Conference of the Association for General and Applied Microbiology (VAAM) in collaboration with the Royal Netherlands Society for Microbiology (KNVM), 10-13 March 2013, Bremen, Germany

SENSE Coordinator PhD Education

Dr. ing. Monique Gulickx

The research described in this thesis was performed at the Laboratory of Microbiology, Wageningen University, Wageningen, NL and funded by grants of the division of Chemical Sciences (CW-TOP 700.55.343) and Earth and Life Sciences (ALW 819.02.014) of the Netherlands Organisation for Scientific Research (NWO).

Cover design: Michael Visser

Thesis layout: Michael Visser

Printed by: Gildeprint drukkerijen, Enschede, NL

Financial support from the Laboratory of Microbiology (Wageningen University) for printing this thesis is gratefully acknowledged.